Non-Invasive Electrophysiological Assessment of the Corticospinal Tract in Health and Disease

Stephan R. Jaiser

Thesis submitted for the degree of
Doctor of Philosophy

September 2013

Institute of Neuroscience
Faculty of Medical Sciences
Newcastle University
Newcastle Upon Tyne, UK

Supervisors
Prof. Stuart N. Baker
Dr Mark R. Baker

Newcastle University

Abstract

To date, no candidate markers of upper motor neuron (UMN) function have performed sufficiently well to enter widespread clinical use, and the lack of such markers impedes both the diagnostic process and clinical trials in motor neuron disease (MND). We studied 15-30Hz intermuscular coherence (IMC), a novel marker of UMN function, and central motor conduction time (CMCT), an established marker of UMN function based on transcranial magnetic stimulation (TMS), in healthy volunteers and patients newly diagnosed with MND. To clarify the relative contributions of different parts of the motor system to IMC generation, we examined IMC in patients with longstanding diagnoses of hereditary spastic paraparesis (HSP), multifocal motor neuropathy (MMN) and inclusion body myositis (IBM).

Previous studies reported conflicting results for the relationship between CMCT and predictors such as age and height. We only found a significant correlation between lower limb CMCT and height. IMC did not vary significantly with age, allowing data from healthy subjects across all ages to be pooled into a single normative dataset. The variability of IMC between subjects was considerable, and within a given subject variability was greater between than within recording sessions; potential contributors are discussed. Anodal transcranial direct current stimulation (tDCS) caused a significant increase in IMC, but interindividual variability was substantial, which might hinder its future use as an adjunct to IMC.

To compare individual disease groups to the normal cohort, we evaluated the area under the receiver-operating characteristic curve (AUC). IMC generally matched or exceeded the performance of CMCT in discriminating patients with MND from normal, achieving AUCs of 0.83 in the upper and 0.79 in the lower limb. Previous evidence suggests that IMC abnormalities are primarily attributable to corticospinal tract (CST) dysfunction. In line with this, most patients with HSP exhibited diminished IMC. However, patients with MMN also showed decreased IMC, suggesting either that subclinical CST involvement was present or that dysfunction of lower motor neurons (LMNs) may affect IMC; clarification through computational modelling is suggested. In

IBM, IMC was generally increased, which might reflect that the altered motor unit discharge pattern makes synchronisation more readily detectable.

IMC appears to be a promising marker of CST function. It remains to be clarified how strongly it is influenced by LMN lesions, and optimisation of methods should help to minimise the variability of results. Since IMC is non-invasive and can be measured using commonly available EMG equipment, wider dissemination should prove straightforward.

Meinen Eltern.

Acknowledgements

This thesis would not have been possible without the generous help and support of many people.

Firstly, I would like to thank my supervisors, Stuart Baker and Mark Baker, for their support, encouragement and patience. Special thanks go to Tim Williams for helping me to recruit patients with motor neuron disease from his clinic, and for serving on my progress review panel along with Jenny Read. I recruited patients with hereditary spastic paraparesis through the neurogenetics service, and am indebted to Patrick Chinnery, Patrick Yu-Wai-Man, Grant Guthrie and Gail Eglon for their assistance. Similarly, I would like to thank James Miller for his help in recruiting patients with acquired neuromuscular conditions. Suzanne Pinkney, Sarah Armstrong and Jonathan Barnes found many of the healthy volunteers, and Jonathan also gave me a hand with some early experiments. I am grateful to Elizabeth Williams for creating the guided TMS system, and to Kenneth Brown for his support in using it. Felipe De Carvalho and Norman Charlton helped me build prototypes for a collaborative project from which our industrial partner ultimately withdrew. Felipe also showed me how to debug my rig on more than one occasion, and Norman was always on hand for fixing my equipment and even my bike.

My gratitude goes to everyone in the lab for their support and for making the last few years an enjoyable experience. In alphabetical order: Karen Fisher, Ferran Galán, Bonne Habekost, Thomas Hall, Andrew Jackson, Terri Jackson, Ming Lai, Kia Nazarpour, Tobias Pistohl, Claire Schofield, Ian Schofield, Harbaljit Sohal, Demetris Soteropoulos, Edina Tozser, Claire Witham, Jonas Zimmermann.

I would like to thank all the patients and volunteers who gave up their time to help with this research, which was funded by a generous fellowship from the Wellcome Trust.

Finally, I would like to thank my parents for their continued support over the years, and Lauren for her love and encouragement.

Publications 2010-2013

Abstracts

Jaiser SR, Seow H, Fisher KM, Miller JAL, Chinnery PF, Baker SN & Baker MR (2010). 15-30Hz intermuscular coherence in patients with amyotrophic lateral sclerosis/motor neuron disease mimic syndromes. *Society for Neuroscience*, San Diego.

Jaiser SR, Fisher KM, Zaaimi B, Seow H, Miller JAL, Chinnery PF, Williams TL, Baker SN & Baker MR (2011). 15-30Hz intermuscular coherence as a potential biomarker of upper motor neuron dysfunction in motor neuron disease. *Association of British Neurologists*, Newcastle upon Tyne. Abstract in *J Neurol Neurosurg Psychiatry* 2012;**83**(e1):28-9.

Jaiser SR, Soteropoulos D, Cunningham MO, Baker SN & Baker MR (2012). The effects of gyral geometry on the size of magnetic motor cortical evoked potentials. *British Society of Clinical Neurophysiology*, Stockton-on-Tees.

Jaiser SR, Barnes JD, Baker MR & Baker SN (2012). Beta-band intermuscular coherence: effects of age and anodal transcranial direct current stimulation. *Society for Neuroscience*, New Orleans.

Jaiser SR, Fisher KM, Williams TL, Baker MR & Baker SN (2012). Intermuscular coherence as a biomarker of upper motor neuron dysfunction in motor neuron disease: optimising the frequency band. *Society for Neuroscience*, New Orleans.

Ziso B, Williams TL, Walters RJL, **Jaiser SR**, Wieshmann UC & Jacob A (2013). FOSMN: Facial Onset Sensory Motor Neuronopathy. A 'benign' differential diagnosis to bulbar onset motor neuron disease. The first cohort from the United Kingdom. *Association of British Neurologists*, Glasgow.

Jaiser SR, Williams TL, Baker SN & Baker MR (2013). Beta-band intermuscular coherence in amyotrophic lateral sclerosis/motor neuron disease. *Society for Neuroscience* (forthcoming), San Diego.

Jaiser SR, Williams TL, Baker SN & Baker MR (2013). Beta-band intermuscular coherence as a biomarker of upper motor neuron dysfunction in motor neuron disease. *Motor Neuron Disease Association Symposium* (forthcoming), Milan.

Papers

Jaiser SR & Winston GP (2010). Copper deficiency myelopathy. *J Neurol* **257**:869-881.

Winston GP & **Jaiser SR** (2012). Western driving regulations for unprovoked first seizures and epilepsy. *Seizure* **21**:371-376. Editor's choice/article of the month.

Jaiser SR & Winston GP (2012). Subacute combined degeneration of the spinal cord despite prophylactic vitamin B12 treatment. *J Clin Neurosci* **19**:1607.

Winston GP & **Jaiser SR** (2013). Re: denture fixative cream and the potential for neuropathy. *Dent Update* **40**:144.

Jaiser SR, Baker MR, Whittaker RG, Birchall D & Chinnery PF (2013). Clinical reasoning: abdominal cramps. *Neurology* **81**:e5-9.

Ziso B, Williams TL, Walters RJL, **Jaiser SR**, Wieshmann UC & Jacob A (2013). Facial Onset Sensory Motor Neuronopathy – A 'benign' differential diagnosis to bulbar onset motor neuron disease: the first cohort from the United Kingdom. *Eur J Neurol* (submitted).

Table of Contents

1 Introduction and background 1

1.1 Introduction 1

1.2 Descending motor pathways 2

1.2.1 The corticospinal tract 3

1.2.2 Anatomical organisation of the corticospinal tract 4

1.2.3 Corticospinal tract lesions 5

1.2.4 Nomenclature 5

1.3 Motor neuron disease 6

1.3.1 Aetiology 6

1.3.2 Epidemiology 6

1.3.3 Pathology 6

1.3.4 Diagnosis 8

1.3.5 Management 10

1.3.6 Prognosis 10

1.4 Transcranial magnetic stimulation 10

1.4.1 Basic principles 10

1.4.2 Measures of MEP size 12

1.4.3 Central motor conduction time 13

1.4.4 Threshold 14

1.4.5 Recruitment curves 14

1.4.6 Cortical silent period 14

1.4.7 Paired-pulse measures 15

1.4.8 TMS-based measures in MND 15

1.5 Coherence analysis 17

1.5.1 Motor system oscillations 17

1.5.2 Coherence 18

1.5.3 Origin of beta-band oscillations and coherence 20

1.5.4 Function of coherence 21

1.6 Overview of this thesis 23

2 Central and peripheral motor conduction times in normal adults..... 25
2.1 Abstract..... 25
2.2 Introduction..... 26
2.3 Methods..... 30
2.3.1 Subjects..... 30
2.3.2 Recording..... 30
2.3.3 Stimulation..... 31
2.3.4 Data analysis..... 31
2.4 Results..... 32
2.4.1 CMCT..... 33
2.4.2 PMCT..... 33
2.5 Discussion..... 37
2.5.1 Methods for PMCT estimation..... 37
2.5.2 CMCT and height..... 38
2.5.3 CMCT and age..... 39
2.5.4 CMCT and sex..... 40
2.5.5 PMCT..... 40
2.5.6 Clinical application..... 41
2.6 Conclusion..... 41
3 Intermuscular coherence in normal adults: variability and changes with age..... 43
3.1 Abstract..... 43
3.2 Introduction..... 44
3.3 Methods..... 46
3.3.1 Subjects..... 46
3.3.2 Recording..... 46
3.3.3 Experiment 1: IMC..... 47
3.3.4 Experiment 2: IMC repeated after one year..... 47
3.3.5 Data analysis..... 47
3.4 Results..... 52
3.5 Discussion..... 60

3.5.1 IMC in adulthood 60
3.5.2 Variability of IMC 61
3.6 Conclusion 63
4 Effect of transcranial direct current stimulation on intermuscular coherence 64
4.1 Abstract 64
4.2 Introduction 65
4.3 Methods 68
4.3.1 Subjects 68
4.3.2 Recording 68
4.3.3 tDCS 68
4.3.4 Experiment 1: IMC 69
4.3.5 Experiment 2: MEP amplitude 69
4.3.6 Data analysis 70
4.4 Results 73
4.4.1 Experiment 1: IMC 73
4.4.2 Experiment 2: MEP amplitude 78
4.5 Discussion 80
4.5.1 Changes in IMC and power 80
4.5.2 Methodological differences from previous study 83
4.5.3 Changes in MEP amplitude 84
4.6 Conclusion 85
5 Intermuscular coherence and central motor conduction times in patients with motor neuron disease 86
5.1 Abstract 86
5.2 Introduction 87
5.3 Methods 91
5.3.1 Subjects 91
5.3.2 Recording 93
5.3.3 Experiment 1: IMC 93
5.3.4 Experiment 2: CMCT 94
5.3.5 Data analysis 95

5.4 Results 103
5.4.1 IMC 103
5.4.2 CMCT 109
5.4.3 Comparison of all individual and combined markers 112
5.4.4 Subgroup analysis 116
5.5 Discussion 118
5.5.1 Analysis 118
5.5.2 Summary of results 119
5.5.3 Potential confounders 119
5.5.4 Pathways probed by IMC 120
5.5.5 Outlook 121
5.6 Conclusion 122
6 Intermuscular coherence in patients with motor neuron disease mimic syndromes 123
6.1 Abstract 123
6.2 Introduction 124
6.3 Methods 126
6.3.1 Subjects 126
6.3.2 Recording 127
6.3.3 Experimental procedure 128
6.3.4 Data analysis 128
6.4 Results 131
6.5 Discussion 138
6.5.1 Results and their implications 138
6.5.2 Outlook 139
6.6 Conclusion 139
7 General discussion 141
7.1 Context 141
7.2 Summary and future directions 141
7.3 Conclusion 144
A Individual beta-band averages for intermuscular coherence in normal subjects .. 145

B Clinical details for patients with motor neuron disease..... 146

C Clinical details for patients with motor neuron disease mimic syndromes..... 153

References 158

List of Figures

1.1 Descending motor pathways ... 3

1.2 Age-specific incidence and macroscopic pathology for MND ... 7

1.3 Magnetic stimulation ... 11

1.4 Oscillations and coherence ... 19

2.1 Single-subject cortical and root MEPs ... 32

2.2 CMCT against age, height and sex ... 34

2.3 PMCT against age, height and sex ... 35

3.1 Single-subject power and coherence in the lower limb ... 53

3.2 Group data for coherence ... 54

3.3 Correlation between coherence and age ... 55

3.4 Coherence by decade of age ... 56

3.5 Coherence across all ages ... 57

3.6 Z-scores for intrasession differences in coherence ... 58

3.7 Difference between variances of intersession and intrasession Z-scores ... 59

4.1 Previously reported after-effects of tDCS to M1 ... 67

4.2 Single-subject power and coherence in the upper limb ... 74

4.3 Group data for power and coherence ... 75

4.4 Z-scores for differences in coherence ... 77

4.5 Single-subject and group data for MEPs ... 79

4.6 Comparison of surface measurements and TMS hotspot mapping ... 80

5.1 Subject flow ... 92

5.2 Single-subject power and coherence in the upper limb ... 103

5.3 Group data for coherence ... 104

5.4 Coherence in normal control subjects and patients with MND ... 106

5.5 Optimal linear combination of coherence data ... 108

5.6 Single-subject cortical and root MEPs ... 109

5.7 CMCT in normal control subjects and patients with MND ... 111

5.8 Optimal linear combination of CMCT data ... 114

5.9 Optimal linear combination of coherence and CMCT data..... 115

5.10 Area under the ROC curve for individual and combined markers..... 117

6.1 Single-subject power and coherence in the lower limb..... 131

6.2 Group data for coherence..... 132

6.3 Coherence in normal control subjects and patients with MND mimic syndromes 134

6.4 Optimal linear combination of coherence data..... 136

6.5 Area under the ROC curve for individual and combined markers..... 137

List of Tables

1.1 Diagnostic criteria for ALS 8

1.2 Oscillations in the motor system 18

2.1 Previously reported normal CMCT and PMCT data 27

2.2 CMCT and PMCT in this study 36

5.1 Breakdown of MND patients by phenotype 93

5.2 Area under the ROC curve for individual and combined markers, and coefficients for calculating combined markers 101

6.1 Area under the ROC curve associated with coherence markers and their linear and non-linear combinations 137

A.1 Individual averages of beta-band IMC in normal individuals 145

B.1 History for patients with MND 146

B.2 Examination findings for patients with MND 148

B.3 Blood results for patients with MND 149

B.4 CSF and MRI findings for patients with MND 150

B.5 Phenotype, handedness, affected limbs, limbs studied with TMS and IMC, and exclusion criteria for patients with MND 152

C.1 Genetic mutations of patients with HSP 153

C.2 Electrophysiological diagnostic category and key features for patients with MMN 153

C.3 Clinico-pathological diagnostic category for patients with IBM 153

C.4 History for patients with HSP, MMN and IBM 154

C.5 Blood results for patients with HSP, MMN and IBM 156

C.6 CSF and MRI findings for patients with HSP, MMN and IBM 157

List of Abbreviations

ADM	Abductor digiti minimi
AH	Abductor hallucis
ALS	Amyotrophic lateral sclerosis
ANOVA	Analysis of variance
APB	Abductor pollicis brevis
AUC	Area under the curve
CDF	Cumulative distribution function
CM	Corticomotorneuronal
CMC	Corticomuscular coherence
CMCT	Central motor conduction time
CNS	Central nervous system
CSF	Cerebrospinal fluid
CSP	Cortical silent period
CST	Corticospinal tract
DC	Direct current
ECoG	Electrocorticogram
EDB	Extensor digitorum brevis
EDC	Extensor digitorum communis
EEG	Electroencephalogram
EMG	Electromyogram
FDI	First dorsal interosseous
FDS	Flexor digitorum superficialis
FFT	Fast Fourier transform
FPR	False positive rate
GABA	Gamma-aminobutyric acid
HSP	Hereditary spastic paraparesis
IBM	Inclusion body myositis
ICF	Intracortical facilitation
IMC	Intermuscular coherence
IntraMC	Intramuscular coherence

ISI	Interstimulus interval
IVIg	Intravenous immunoglobulin
LFP	Local field potential
LICI	Long-interval intracortical inhibition
LMN	Lower motor neuron
M1	Primary motor cortex
MATS	Magnetic augmented translumbosacral stimulation
MEG	Magnetoencephalogram
MEP	Motor evoked potential
MG	Medial gastrocnemius
MMN	Multifocal motor neuropathy
MND	Motor neuron disease
MVC	Maximum voluntary contraction
NCS	Nerve conduction study
NMDA	N-methyl-D-aspartate
PBP	Progressive bulbar palsy
PDF	Probability density function
PEG	Percutaneous endoscopic gastrostomy
PLS	Primary lateral sclerosis
PMA	Progressive muscular atrophy
PMCT	Peripheral motor conduction time
QuadS	Quadruple stimulation test
RMT	Resting motor threshold
ROC	Receiver-operating characteristic
SD	Standard deviation
SEP	Somatosensory evoked potential
SICI	Short-interval intracortical inhibition
SOD1	Superoxide dismutase 1
SPG	Spastic paraplegia
TA	Tibialis anterior
tDCS	Transcranial direct current stimulation

TDP-43	Transactive response DNA binding protein 43kDa
TMS	Transcranial magnetic stimulation
TTTMS	Threshold tracking transcranial magnetic stimulation
TPR	True positive rate
TST	Triple stimulation test
UMN	Upper motor neuron

1 Introduction and background

In this chapter, I present the motivation for and discuss the scientific background of the work presented in this thesis. I review the organisation of the primary motor system, the nature and management of motor neuron disease, as well as theoretical aspects of magnetic stimulation and coherence analysis.

1.1 Introduction

More than 1,700 people in the United Kingdom are newly diagnosed with motor neuron disease (MND) per year. MND is a fatal neurodegenerative disorder of unknown cause and typically follows a relentlessly progressive trajectory, with a median survival of 30 months from symptom onset (Chancellor *et al.*, 1993). Early physical manifestations are protean, often leading to late presentation and delayed referral to a neurologist. Further delays arise through investigations and a possible need for serial follow-up. Intervals from symptom onset to diagnosis are often long, having a median of around one year (Househam & Swash, 2000; Mitchell *et al.*, 2010). These diagnostic delays are a burden for patients, their families and the health service; they are also likely to limit the survival benefits offered by neuroprotective treatment.

Common forms of MND involve the simultaneous degeneration of upper and lower motor neurons (UMNs, LMNs). UMNs project from the primary motor cortex to the brainstem and spinal cord, where they connect to LMNs which supply the peripheral musculature. The diagnosis of MND requires evidence of damage to both UMNs and LMNs in the absence of alternative causes. Initially relying on clinical examination findings alone (Brooks, 1994), the diagnostic process has been modified to incorporate electromyographic (EMG) features of LMN damage (Brooks *et al.*, 2000; De Carvalho *et al.*, 2008), thus increasing sensitivity (De Carvalho & Swash, 2009). By contrast, assessment of UMN function remains entirely clinical. If a reliable test of UMN integrity were available, it might help to decrease diagnostic delays and may also

prove useful in the longitudinal follow-up of patients, both for individual prognosis and as a surrogate marker in clinical trials.

For over two decades, the development of tests for UMN function has focussed on transcranial magnetic stimulation (TMS). TMS-based measures, such as central motor conduction time (CMCT), have shown only moderate performance (Mills, 2003) and require expensive specialist equipment. In consequence, they have not entered widespread clinical use. Our group has recently described intermuscular coherence (IMC) as a novel test for UMN function (Fisher *et al.*, 2012). IMC is non-invasive and can be performed using widely available EMG equipment. Previous work focussed on an animal model of UMN damage and rare subtypes of MND in humans, but paid little attention to commoner forms of MND (Fisher *et al.*, 2012).

In this thesis, I aim to advance the field by studying IMC and CMCT in large cohorts of healthy human volunteers and patients with suspected MND of any type, as well as in smaller groups of patients with established diagnoses of other motor conditions. My results show that IMC is a promising marker of UMN function which meets or exceeds the performance of CMCT.

Individual chapters in this thesis are self-contained but do not provide detailed background regarding descending motor pathways, MND, TMS and coherence analysis. These areas are introduced below, followed by an overview of all chapters.

1.2 Descending motor pathways

Mammals possess several descending motor pathways which vary in relative size and importance between species but retain the same overall functions (Figure 1.1; for an extensive review of descending pathways, see Porter & Lemon, 1993). The dorsolateral pathways of the corticospinal and rubrospinal tracts provide fine control of distal muscles, particularly in the hand. The ventromedial pathways, which include the reticulospinal, vestibulospinal and tectospinal tracts, are traditionally viewed as

controlling proximal limb and truncal muscles for posture and balance, although small projections to hand motor neurons also exist (Riddle & Baker, 2010; Riddle *et al.*, 2009).

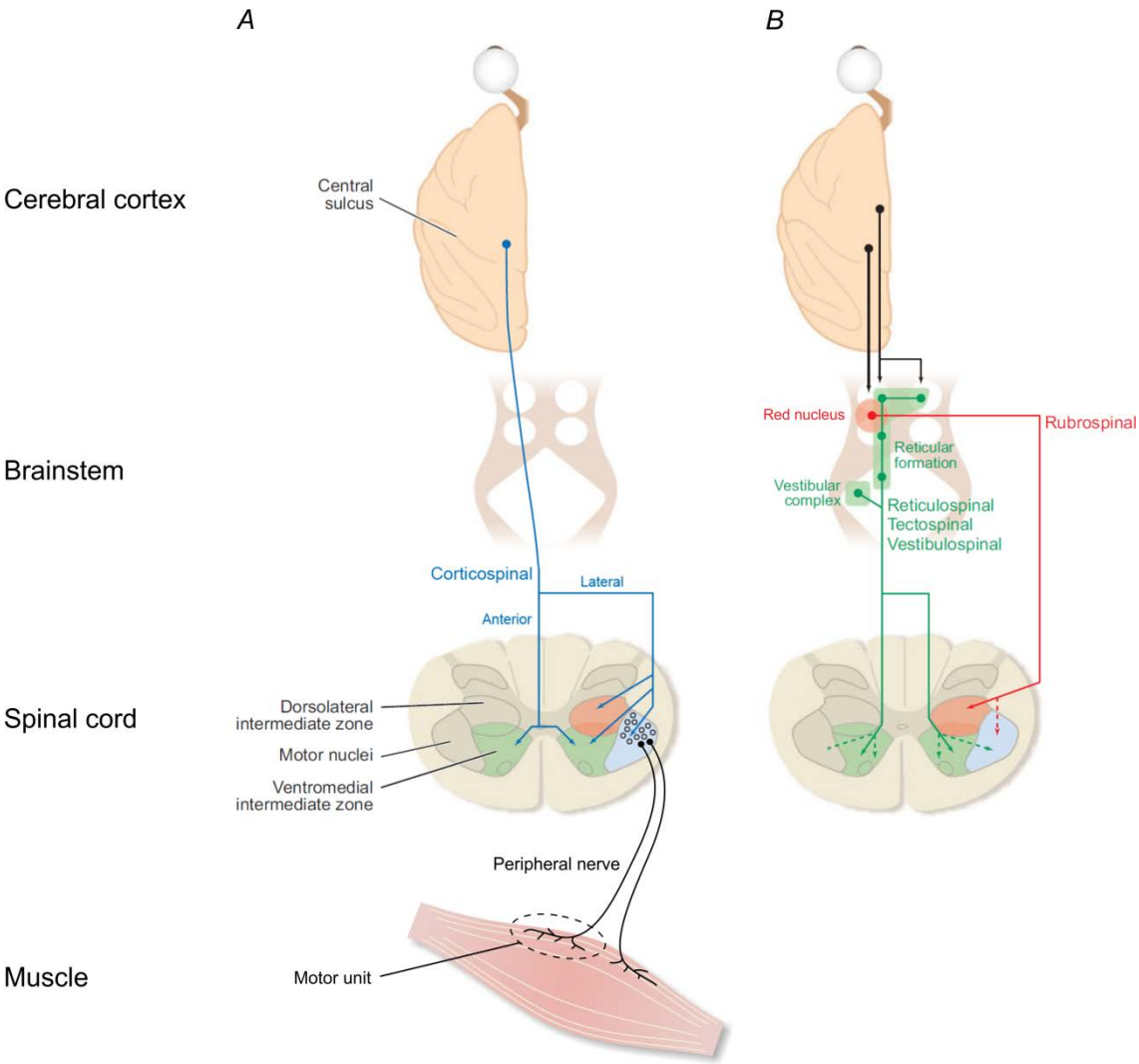

Figure 1.1: Descending motor pathways. The lateral corticospinal tract (CST) decussates at the level of the medulla and projects to the spinal motor neurons (blue area) both directly and indirectly via the dorsolateral (red area) and ventromedial interneurons (green area, A). The anterior CST partly crosses at the spinal level and projects to ventromedial interneurons only. The remaining descending tracts are either crossed or uncrossed and mostly project to spinal interneurons (B). Spinal motor neurons exit through the ventral horn and run in the peripheral nerves to supply multiple fibres in a given muscle, thus forming a motor unit (adapted from Lemon, 2008).

1.2.1 The corticospinal tract

Primates have a unique ability to perform fine, skilled movements of distal muscles. This ability has evolved in parallel with the CST, which is most prominent in the higher

apes, particularly humans. The size of the CST and the proportion of direct corticomotorneuronal (CM) connections are related to manual dexterity (Heffner & Masterton, 1983).

1.2.2 Anatomical organisation of the corticospinal tract

CST fibres arise from pyramidal cells in layer V of the cerebral cortex (Ramón y Cajal, 1893). These cells are named according to the shape of their soma; those giving rise to large axons are sometimes referred to as Betz cells. The CST originates primarily in the primary motor cortex (M1), with further contributions from the supplementary motor area, premotor cortex, somatosensory cortex and parietal lobe (Dum & Strick, 1991; Jane *et al.*, 1967; Murray & Coulter, 1981; Russell & DeMyer, 1961). M1 is arranged in a broadly somatotopic manner, epitomised by the classical homunculus in humans (Penfield & Rasmussen, 1950) and the simiusculus in monkeys (Woolsey *et al.*, 1952). Cortical representations of the lower limbs, upper limbs and the face are arranged mediolaterally, with proximal and distal muscles represented along a rostrocaudal gradient. The size of the cortical representation is related to the complexity of movements of the relevant body part; the hand, for example, has a disproportionately large representation. However, this somatotopy only involves gross representations of body parts. Representations of smaller body regions or individual muscles are more widely distributed and overlap considerably. Furthermore, there is substantial convergence and divergence within the motor system, as well as plasticity throughout life (Schieber, 2001). Hence, the homunculus and simiusculus represent useful but invariably oversimplified concepts.

In humans, the CST contains approximately one million fibres which have mostly small diameters and slow conduction velocities, with a smaller proportion being large, myelinated and fast conducting (Humphrey & Corrie, 1978). It descends through the cerebral peduncles and the brainstem to the level of the medullary pyramids, which give the tract its alternative name (pyramidal tract; its origin from pyramidal cells being coincidental). Approximately 85% of fibres decussate and descend in the lateral CST (Figure 1.1 A; Rosenzweig *et al.*, 2009). They project directly onto spinal motor neurons to form monosynaptic CM connections (Palmer & Ashby, 1992), as well as having additional indirect projections through interneurons. Uncrossed CST fibres

enter the anterior CST but only have very weak effects on ipsilateral muscles (Soteropoulos *et al.*, 2011). Recently, it has been reported that corticospinal fibres may also decussate and/or branch at a spinal level, pointing to an even greater complexity of corticospinal projections (Rosenzweig *et al.*, 2009).

1.2.3 Corticospinal tract lesions

In humans, naturally occurring lesions rarely affect the CST in isolation. Lacunar infarcts may appear to cause pure motor deficits on clinical assessment, but the infarct zone often extends beyond the CST to involve neighbouring descending outputs to the brainstem nuclei as well as ascending sensory inputs. Nonetheless, truly isolated involvement of the pyramids can occur with medial medullary infarcts (Bassetti *et al.*, 1997), and such cases help to delineate the role of the CST. Pyramidal strokes cause a unilateral motor deficit which is most pronounced for fine, distal voluntary movements. Similar to more extensive infarcts, recovery tends to be weighted towards synergistic, proximal movements, and thus appears to be driven by brainstem motor pathways (Lang *et al.*, 2006).

In monkeys, selective CST lesions result in little gross deficit post recovery, with animals being able to stand, run and climb in an apparently normal manner. However, there are substantial, persistent deficits in independent finger movements, exemplified by difficulties in grooming (Schwartzman, 1978) or retrieving food from small wells (Lawrence & Kuypers, 1968). In addition, reaction speeds are slower due to delayed EMG onset times (Hepp-Reymond *et al.*, 1974). Hence, the CST appears to superimpose speed and fractionation on movements produced by other descending motor pathways (Lawrence & Kuypers, 1968). This hypothesis is backed by more recent studies where the $GABA_A$ agonist muscimol was used to effect reversible inactivation of small areas of M1, causing transient impairment of fractionated finger movements (Brochier *et al.*, 1999; Schieber & Poliakov, 1998).

1.2.4 Nomenclature

The terms 'CST' and 'spinal motor neurons' are used mostly in the scientific community, whereas the corresponding terms 'UMNs' and 'LMNs' are preferred in a clinical setting.

Strictly speaking, UMNs include not only the CST but also brainstem motor pathways, but this distinction is rarely made in practice.

1.3 Motor neuron disease

MND is characterised by degeneration and loss of motor neurons, involving variable proportions of UMNs and LMNs. The classical form of MND, first described by Charcot in the late 19th century (Charcot, 1874), has a phenotype called amyotrophic lateral sclerosis (ALS) with signs of both UMN and LMN dysfunction. Although the term ALS is sometimes used synonymously with MND, this is misleading as MND also encompasses three related syndromes: progressive bulbar palsy (PBP), primary lateral sclerosis (PLS) and progressive muscular atrophy (PMA), respectively presenting with bulbar dysfunction, pure UMN signs and pure LMN signs. Nonetheless, ALS is the commonest subtype and accounts for more than 85% of MND.

1.3.1 Aetiology

Approximately 90% of cases are considered to be sporadic. In around 10%, there is a family history of MND, and an increasing number of pathogenic mutations have been identified across multiple genes (Al-Chalabi *et al.*, 2012; Turner *et al.*, 2013).

1.3.2 Epidemiology

MND is a rare condition occurring worldwide with an incidence of approximately 2 per 100,000 per year (McGuire & Nelson, 2006). The incidence is 20-60% higher in men than women, and peaks between 65 and 75 years of age (Figure 1.2 A). The prevalence is estimated at 6 per 100,000.

1.3.3 Pathology

Macroscopically, there are few if any abnormalities. In advanced cases, atrophy of the precentral gyrus and atrophy and discolouration of the anterior spinal nerve roots may be apparent (Figure 1.2 B, C). Microscopically, there is loss of motor neurons with secondary loss of myelin from M1, the CST, hypoglossal nucleus and ventral horn of

the spinal cord; cortical interneurons in M1 are also lost (Nihei *et al.*, 1993). Cell loss is accompanied by gliosis, and surviving motor neurons typically contain cytoplasmic inclusions of TDP-43 (transactive response DNA binding protein 43kDa; Arai *et al.*, 2006). There is mounting evidence of extra-motor pathology, highlighting that MND is only relatively selective for the motor system (Wharton & Ince, 2003), and this is exemplified by the clinical and molecular association of MND with fronto-temporal dementia (Arai *et al.*, 2006; Lomen-Hoerth & Strong, 2006).

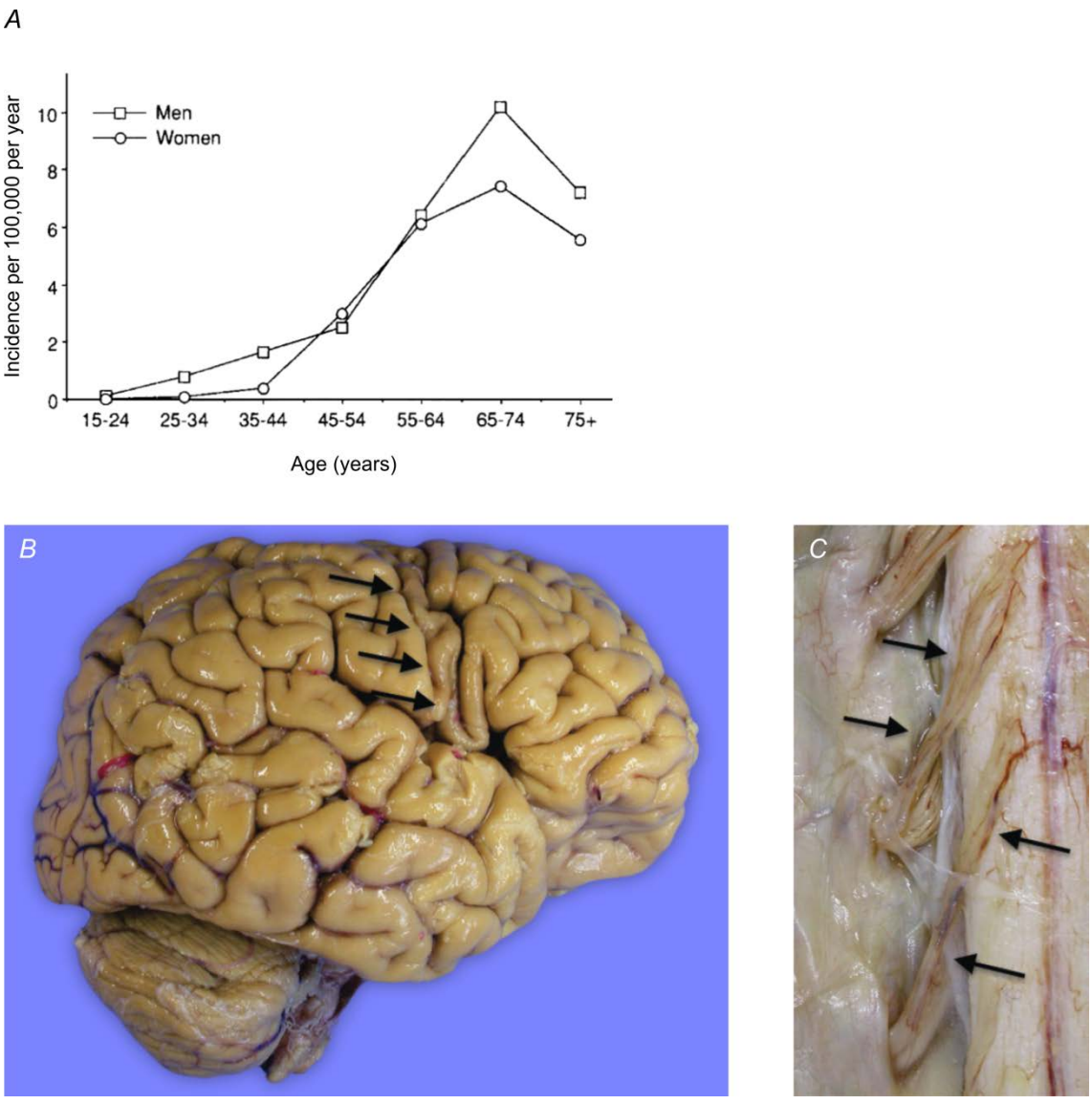

Figure 1.2: Age-specific incidence (A) and macroscopic pathology (B, C) for MND. MND presents across a wide age-range but shows a clear peak in the seventh decade (A; adapted from McGuire and Nelson, 2006). At post mortem, clear macroscopic abnormalities are infrequent but may include atrophy of the precentral gyrus (B, arrows), and atrophy and discolouration of the anterior spinal nerve roots (C, arrows; adapted from Jeans and Ansorge, 2009).

1.3.4 Diagnosis

Typically, MND is focal in onset. Initial features occur more commonly in the limbs than in the bulbar territory. The diagnosis is clinical and depends on detection of an appropriate phenotype paired with exclusion of other potential causes (Table 1.1 A).

Table 1.1: Diagnostic criteria for ALS. 'Regions' refer to the bulbar, cervical, thoracic and lumbosacral territories (adapted from Turner *et al.*, 2013).

A. The diagnosis of ALS requires:

- The presence of
    - Evidence of LMN degeneration by clinical, electrophysiological or neuropathological examination;
    - Evidence of UMN degeneration by clinical examination; and
    - Progression of motor syndrome within a region or to other regions, as determined by history or examination
- The absence of
    - Electrophysiological and pathological evidence of other disease processes that might explain the signs of LMN and UMN degeneration; and
    - Neuroimaging evidence of other disease processes that might explain the observed clinical and electrophysiological signs

B. El Escorial criteria

- *Definite ALS:* UMN and LMN signs in three regions
- *Probable ALS:* UMN and LMN signs in at least two regions with UMN signs rostral to the LMN signs
- *Possible ALS:* UMN and LMN signs in one region, UMN signs in two or more regions, or LMN signs above UMN signs
- *Suspected ALS:* LMN signs only in two or more regions

C. Revised El Escorial (Airlie House) criteria

- *Clinically definite ALS:* clinical evidence alone of UMN and LMN signs in three regions
- *Clinically probable ALS:* clinical evidence alone of UMN and LMN signs in at least two regions with some UMN signs rostral to the LMN signs
- *Clinically probable/laboratory-supported ALS:* clinical signs of UMN and LMN dysfunction in only one region, or UMN signs alone in one region, together with LMN signs defined by EMG criteria in at least two regions, together with proper application of neuroimaging and clinical laboratory protocols to exclude other causes
- *Possible ALS:* clinical signs of UMN and LMN dysfunction in only one region, or UMN signs alone in two or more regions, or LMN signs rostral to UMN signs and the diagnosis of clinically probable/laboratory-supported ALS cannot be proven
- *Suspected ALS:* category deleted

Diagnostic criteria have been formulated to aid research by standardising patient groups (Belsh, 2000). The first widely used criteria were defined in El Escorial, and classify cases as definite, probable, possible or suspected ALS depending on the nature and extent of clinical and electrophysiological findings (Table 1.1 B; Brooks, 1994). For the assessment of LMN function, EMG is regarded as an extension of the clinical examination and serves to confirm clinical signs, to detect clinically occult abnormalities and to exclude other pathological processes. By contrast, UMN integrity is assessed by clinical means only.

The revised El Escorial criteria abolished the category of suspected ALS and introduced a new category of clinically probable/laboratory-supported ALS, thus giving more weight to EMG findings in certain scenarios (Table 1.1 C; Brooks *et al.*, 2000). In addition, the list of relevant EMG features was streamlined to make them more user-friendly. The Awaji-Shima criteria marked a further strengthening of the role of EMG (De Carvalho *et al.*, 2008). By allowing clinical and EMG findings to be used additively when grading a limb, the category of clinically probable/laboratory-supported ALS was rendered obsolete. Moreover, additional EMG features of LMN dysfunction were introduced.

These changes have boosted sensitivity, with one report describing an increase from 53% for the revised El Escorial criteria to 95% for the Awaji criteria (De Carvalho & Swash, 2009). However, the study employed a cohort with an established clinical diagnosis of MND; sensitivity is likely to be lower when the disease is at an earlier stage, a clinical diagnosis has not been made yet, and greater diagnostic uncertainties remain. Advances have been limited to improved detection of LMN dysfunction, with assessment of UMN integrity remaining entirely clinical. In a study applying the revised El Escorial criteria to almost 400 patients, 41% were classified as possible ALS at the point of clinical diagnosis, with 10% remaining in this category at their death (Traynor *et al.*, 2000b). Patients with possible ALS show the same clinical progression as those with definite ALS, but have too few demonstrable UMN signs to attain a higher diagnostic category. This has caused frustration with the current diagnostic framework (Turner *et al.*, 2013) and highlights the need for biomarkers of UMN function (Turner *et al.*, 2009).

1.3.5 Management

Management is principally supportive and focuses on regular, individualised, multidisciplinary follow-up to assess the rate of progression and maintain well-being where possible (Miller *et al.*, 2009b). In selected patients, non-invasive ventilation and percutaneous endoscopic gastrostomy (PEG) can prolong survival (Miller *et al.*, 2009a).

The only disease-modifying drug licensed for the treatment of MND is riluzole, an agent thought to ameliorate glutamatergic excitotoxicity. Treatment with 100mg of riluzole per day is reasonably safe and prolongs survival by approximately two to three months (Miller *et al.*, 2012), though the evidence base only pertains to patients with an ALS phenotype (Talbot, 2009). It is plausible that earlier introduction of riluzole could delay the onset of disability and extend survival further (Swash, 1998). Any future neuroprotective agents should also be administered as early as possible to maximise impact.

1.3.6 Prognosis

Although the median survival is 30 months from symptom onset (Chancellor *et al.*, 1993) the survival curve tapers out to 20 years or more. Death usually results from respiratory failure. Older age at onset, bulbar onset and early respiratory involvement are predictors of reduced survival (Talbot, 2009).

1.4 Transcranial magnetic stimulation

1.4.1 Basic principles

Unlike an electric current, a time-varying magnetic field traverses bone with little attenuation. Such a field induces a current in conductive tissue in accordance with Faraday's Law (Barker, 2002), and can therefore be used to deliver stimulating currents to many areas of the nervous system where bony structures make direct electrical stimulation difficult, including the brain and the spinal nerve roots (Lemon, 2002; Maccabee, 2002). Magnetic stimulation of the spinal cord (Tomberg, 1995) or the cauda equina within the spinal canal (Maccabee *et al.*, 1996) has been achieved only rarely unless special stimulation coils are used (Matsumoto *et al.*, 2009b), and this may

be attributable to the depth of stimulation required, focussing of the induced current by bony structures, and shielding of the current by cerebrospinal fluid (Efthimiadis *et al.*, 2010; Maccabee *et al.*, 1991; Ugawa *et al.*, 1989). When applied to M1 or the peripheral motor pathways, suprathreshold magnetic stimulation leads to motor evoked potentials (MEPs) recordable from the surface of the corresponding muscles (Figure 1.3 A; Barker *et al.*, 1985).

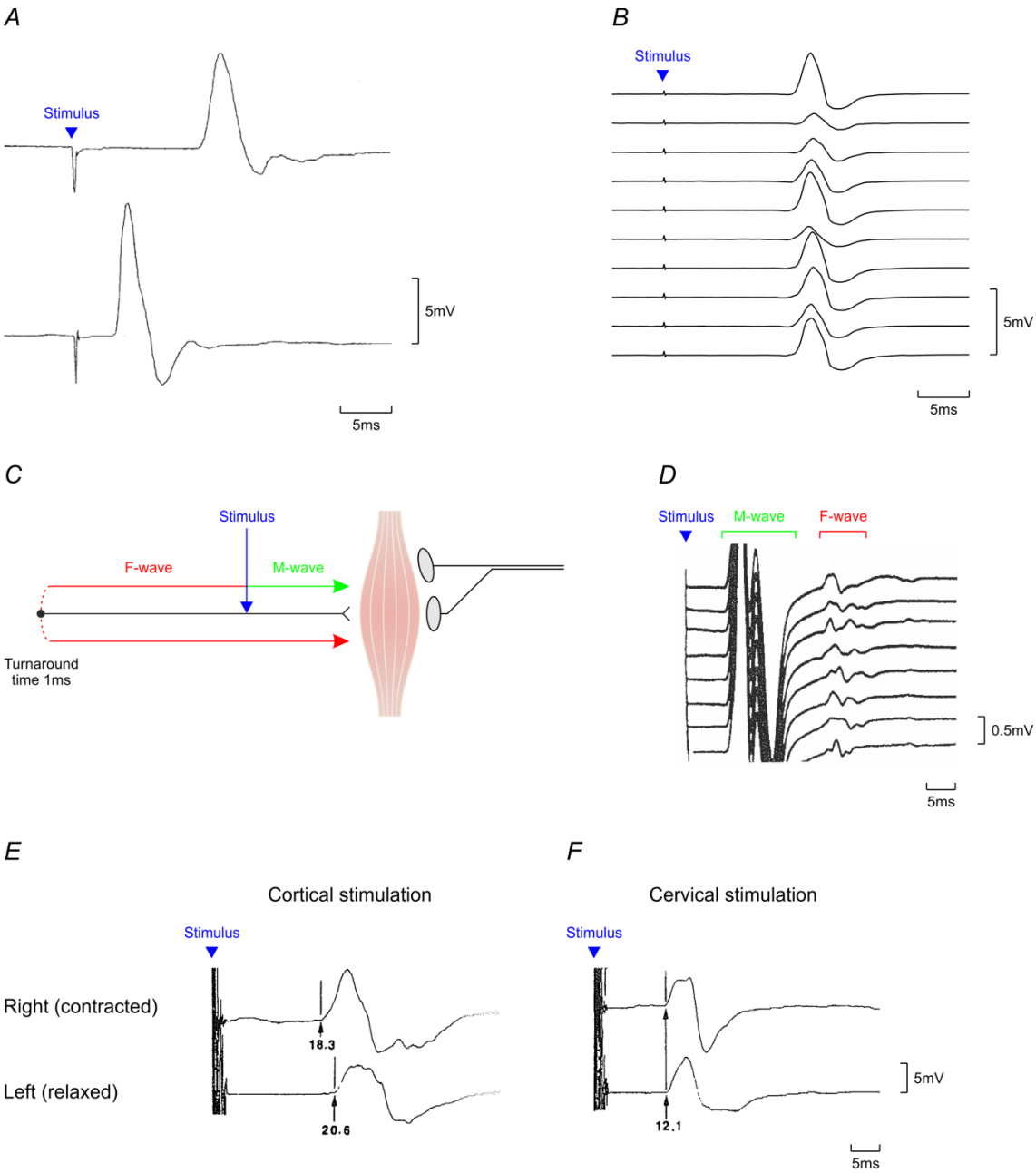

Figure 1.3: Magnetic stimulation. MEPs recorded from abductor digiti minimi (ADM) after magnetic stimulation to the contralateral M1 (A, top) and to the ulnar nerve at the elbow (A, bottom; adapted from Barker *et al.*, 1985). Variability of MEPs recorded from first dorsal interosseous (FDI) after magnetic stimulation to the contralateral M1

under constant experimental conditions (B). Generation of M-wave and F-wave after electrical stimulation of a peripheral motor nerve (C). Consecutive recordings from the thenar muscles showing M-waves and F-waves after ulnar nerve stimulation at the elbow (D; adapted from Kimura, 2001). MEPs evoked by magnetic stimulation over the cervical spine and over the contralateral M1, during voluntary contraction and at rest. Voluntary contraction decreases the latency of cortical but not spinal MEPs (E, F; adapted from Kimura, 2001).

1.4.2 Measures of MEP size

MEPs resulting from TMS to M1 reflect sequential activity of UMNs, LMNs and muscle fibres. They show considerable intertrial variability (Figure 1.3 B; Ellaway *et al.*, 1998; Kiers *et al.*, 1993) which appears to be attributable to multiple factors. Firstly, the descending volley in the CST varies between trials (Burke *et al.*, 1995), potentially due to background oscillatory activity in the motor system (Mitchell *et al.*, 2007). Errors in coil positioning do not appear to contribute (Gugino *et al.*, 2001). Secondly, LMNs may fire repetitively (Day *et al.*, 1987; Hess *et al.*, 1987). Thirdly, surface EMG reflects the summed activity of many muscle fibres, with low-pass filtering by conduction through soft tissue (Merletti & Parker, 2004). Since the descending volley is desynchronised (Magistris *et al.*, 1998), the surface EMG response involves a variable amount of phase cancellation.

Although widely used, averages of multiple MEPs do not truly address the issues underlying MEP variability, and measures of average MEP size such as amplitude, duration and area must be interpreted with caution. At sufficiently high stimulation intensities, MEPs can be detected in the distal muscles of virtually all normal subjects, and consistent absence of a response is likely to be abnormal.

The triple and quadruple stimulation techniques (TST, QuadS) use collision of action potentials to circumvent the issues of desynchronisation and repetitive discharges (Magistris *et al.*, 1998; Z'Graggen *et al.*, 2005) but have several drawbacks. Firstly, they are time-consuming. Secondly, protocols exist only for three muscles in the upper limb (Humm *et al.*, 2004; Magistris *et al.*, 1998) and one muscle in the lower limb (Bühler *et al.*, 2001). Thirdly, they require supramaximal electrical stimulation of proximal

peripheral nerves, which is uncomfortable and, in the lower limb, involves use of a needle electrode. These downsides have prevented widespread adoption.

1.4.3 Central motor conduction time

Central motor conduction time (CMCT) estimates the conduction delay from M1 to LMNs. Magnetic stimulation is performed over M1 to measure cortical latency to the target muscle; CMCT is then calculated by subtracting an estimate of peripheral motor conduction time (PMCT).

PMCT may be estimated by two main methods. In the first method, magnetic stimulation over the spinal column activates LMNs at the level of the exit foramina (Chokroverty *et al.*, 1993; Chokroverty *et al.*, 1991; Maccabee *et al.*, 1991; Ugawa *et al.*, 1989), and the corresponding MEP latency provides an estimate of PMCT. Conduction delays along proximal nerve roots are not included in such PMCTs and remain part of CMCT.

The second method involves electrical stimulation of a distal motor nerve. The orthodromic volley travels to the muscles to elicit an M-wave (Figure 1.3 C, D). The antidromic volley runs to the LMN cell bodies; a fraction of the LMNs fire regeneratively and an orthodromic volley travels back to the muscles, giving rise to a second, smaller wave of activity called an F-wave (Kimura, 2001). If the point of stimulation is moved along the length of the nerve, there are equal but opposite changes in the latencies of M-waves and F-waves; the sum of their latencies remains constant. Assuming a turnaround time of 1ms at the cell body (Kimura, 2001), the PMCT may be calculated as

$$PMCT = \frac{(F\ latency) + (M\ latency) - 1ms}{2} \tag{1.1}$$

Although the F-wave method results in PMCT estimates which include the proximal root segment (Cros *et al.*, 1990; Mills & Murray, 1986), it has other weaknesses which are discussed in Chapter 2.

Cortical MEPs for CMCT estimation are routinely recorded during a weak background contraction, which shortens MEP latency by approximately 2-3ms and facilitates the MEP response (Figure 1.3 E; Hess *et al.*, 1986), allowing lower stimulus intensities to be used. Although spinal MEPs are also facilitated by voluntary activity (Shafiq & Macdonell, 1994), their latency does not appear to be affected (Figure 1.3 F) and they are usually recorded at rest.

1.4.4 Threshold

MEP threshold is defined as the stimulus intensity at which the response probability is 50%, and is usually measured at rest (resting motor threshold, RMT). RMT is thought to reflect neuronal membrane excitability (Chen *et al.*, 2008), and is also inversely related to the strength of the corticospinal projection, being lower in intrinsic hand muscles than in the proximal upper limb, lower limb or trunk. A range of methods for threshold estimation have been described (Awiszus, 2003; Mills & Nithi, 1997b; Rossini *et al.*, 1994; Rothwell *et al.*, 1999; Tranulis *et al.*, 2006), and there is no universal agreement how threshold should be determined. Considerable variability within subjects has been reported (Tranulis *et al.*, 2006), and owing to the extent of intrasubject and intersubject variability the clinical utility of RMT has been called into question (Wassermann, 2002).

1.4.5 Recruitment curves

Recruitment curves, also known as input-output or stimulus-response curves, plot MEP amplitude against stimulus intensity. The slope of such curves is thought to provide a further measure of cortical excitability (Currà *et al.*, 2002), and tends to be greater in muscles with low RMT (Chen *et al.*, 2008).

1.4.6 Cortical silent period

The cortical silent period (CSP) refers to a period of post-stimulus EMG silence occurring when TMS is applied during sustained contraction. CSP is deemed to have intracortical and intrinsic spinal components (Chen *et al.*, 2008). As a marker of disease, CSP has several weaknesses. Interindividual variability of CSP is high (Orth & Rothwell, 2004), measurements of CSP are only comparable between subjects if acquired at a stimulus intensity defined relative to threshold, and CSP might no longer be reliable

once threshold is affected by a disease process (Attarian *et al.*, 2005). In addition, CSP has been shown to be abnormal in a wide range of neurological conditions including non-motor conditions (Chen *et al.*, 2008), implying poor specificity for individual conditions and for involvement of the motor system.

1.4.7 Paired-pulse measures

Corticospinal output results from the interplay of multiple excitatory and inhibitory systems in the motor cortex, and these can be investigated using paired-pulse TMS to M1 (Chen *et al.*, 2008). Paradigms involve a conditioning stimulus and a test stimulus separated by a specified interstimulus interval (ISI). Depending on the stimulation intensities and the ISI, several phenomena including short-interval intracortical inhibition (SICI), long-interval intracortical inhibition (LICI) and intracortical facilitation (ICF) can be observed via the resultant MEPs. SICI, LICI and ICF are thought to be intracortical rather than corticospinal effects, but the neural substrates probed by these techniques are less well defined than those involved in single-pulse MEPs. Similar to the situation for CSP, anomalies of intracortical inhibition and facilitation have been described in a wide range of neurological disorders (Berardelli *et al.*, 2008; Chen *et al.*, 2008).

1.4.8 TMS-based measures in MND

TMS-based measures may capture two pathophysiological changes occurring in MND: loss of UMNs and cortical hyperexcitability (Gooch *et al.*, 2006).

MEP amplitude In cross-sectional studies, MEPs were often absent (Berardelli *et al.*, 1991; Caramia *et al.*, 1988; De Carvalho *et al.*, 2003; Eisen & Shtybel, 1990; Eisen *et al.*, 1990; Miscio *et al.*, 1999; Osei-Lah & Mills, 2004; Pohl *et al.*, 2001; Schriefer *et al.*, 1989; Uozumi *et al.*, 1991; Urban *et al.*, 2001) or diminished in size, either in absolute terms (Eisen & Shtybel, 1990; Eisen *et al.*, 1990) or relative to a response evoked by supramaximal peripheral nerve stimulation (Attarian *et al.*, 2005; De Carvalho *et al.*, 1999; De Carvalho *et al.*, 2003; Schriefer *et al.*, 1989; Uozumi *et al.*, 1991; Urban *et al.*, 2001). They were also frequently dispersed (Eisen & Shtybel, 1990). Longitudinal studies report MEP amplitude to decrease gradually (Floyd *et al.*, 2009) or to remain unchanged (De Carvalho *et al.*, 1999).

CMCT Although CST damage in MND is axonal rather than demyelinating, CMCT prolongation is sometimes seen. Several potential mechanisms have been invoked (Sandbrink, 2009): preferential loss of fast-conducting fibres in the CST early on in the disease (Kohara *et al.*, 1999; Sobue *et al.*, 1987), transmission through brainstem motor pathways (Weber *et al.*, 2000), and reduced size and synchrony of the descending volley increasing the time required for temporal summation at the LMN. CMCT in MND was variably reported to be either normal or prolonged (Attarian *et al.*, 2005; Barker *et al.*, 1986, 1987; Berardelli *et al.*, 1991; Caramia *et al.*, 1991; Claus *et al.*, 1995; Cruz Martínez & Trejo, 1999; De Carvalho *et al.*, 1999; De Carvalho *et al.*, 2003; Desiato & Caramia, 1997; Eisen & Shtybel, 1990; Floyd *et al.*, 2009; Mills & Nithi, 1998; Miscio *et al.*, 1999; Osei-Lah & Mills, 2004; Pohl *et al.*, 2001; Schriefer *et al.*, 1989; Schulte-Mattler *et al.*, 1999; Triggs *et al.*, 1999; Truffert *et al.*, 2000; Urban *et al.*, 2001). Four of these studies were longitudinal and found that CMCT remained unchanged or increased only slightly over time (Claus *et al.*, 1995; De Carvalho *et al.*, 1999; Floyd *et al.*, 2009; Triggs *et al.*, 1999).

Threshold RMT varies considerably in MND (De Carvalho *et al.*, 2002; Eisen *et al.*, 1993). Several cross-sectional studies reported that thresholds are reduced early on in the disease before gradually rising (Desiato & Caramia, 1997; Eisen *et al.*, 1993; Mills & Nithi, 1997a; Vucic & Kiernan, 2006; Zanette *et al.*, 2002). However, other reports disagree. Two cross-sectional (Attarian *et al.*, 2005; De Carvalho *et al.*, 2002) and one longitudinal study (De Carvalho *et al.*, 1999) described no change in threshold, whilst other longitudinal studies reported a monotonic increase in threshold with disease progression (Floyd *et al.*, 2009; Triggs *et al.*, 1999), limited in one study to a subgroup of patients with mixed UMN and LMN signs (Mills, 2003).

Recruitment curves One cross-sectional study found that recruitment curves become steeper in early MND before flattening off again later in the course of the disease (Zanette *et al.*, 2002). Two other cross-sectional reports describe that recruitment curves in MND were steeper than normal but did not perform an analysis by disease duration (Vucic & Kiernan, 2006; Vucic *et al.*, 2008).

Cortical silent period CSP was variably reported as being decreased (Attarian *et al.*, 2006; Schelhaas *et al.*, 2007; Vucic *et al.*, 2011; Vucic & Kiernan, 2006; Zanette *et al.*, 2002) or unchanged in MND (Karandreas *et al.*, 2007; Prout & Eisen, 1994; Ziemann *et al.*, 1997).

Paired-pulse measures SICI, whilst being described as normal in one report (Hanajima *et al.*, 1996), was found to be reduced in most studies (Salerno & Georgesco, 1998; Sommer *et al.*, 1999; Stefan *et al.*, 2001; Vucic *et al.*, 2011; Vucic & Kiernan, 2006; Vucic *et al.*, 2008; Yokota *et al.*, 1996; Zanette *et al.*, 2002; Ziemann *et al.*, 1997). Threshold tracking TMS (TTTMS) constitutes a recent refinement of SICI, and has been reported to discriminate between groups of normal subjects, patients with MND and patients with MND mimic disorders (Vucic *et al.*, 2011; Vucic & Kiernan, 2006). ICF was variably reported as being reduced (Hanajima *et al.*, 1996; Salerno & Georgesco, 1998; Stefan *et al.*, 2001), unchanged (Ziemann *et al.*, 1997) or increased (Vucic *et al.*, 2011; Vucic & Kiernan, 2006; Vucic *et al.*, 2008).

In summary, the literature yields mixed information and interpretation regarding the presence and evolution of abnormalities in TMS-based measures in MND. The variable nature of study results is probably partly attributable to differences in study populations, methods and gold standards for determining normal ranges and diagnostic success. Despite TMS-based measures being explored in MND as early as 1986 (Barker *et al.*, 1986), they have not entered routine clinical use, and their future diagnostic utility remains questionable. Nonetheless, they remain the best available electrophysiological biomarker of CST function. In our study, we decided to measure CMCT as it is the only TMS-based marker which aims to assess UMN function in isolation, and its neural substrates are relatively well defined.

1.5 Coherence analysis

1.5.1 Motor system oscillations

In the motor system, oscillations are widespread and occur across a broad range of frequencies (Table 1.2). Beta-band oscillations have been observed in M1 local field

potentials (LFPs) in monkeys (Figure 1.4 A; Baker *et al.*, 1997; Murthy & Fetz, 1992; Sanes & Donoghue, 1993), and on electrocorticogram (ECoG; Ohara *et al.*, 2000), electroencephalogram (EEG) (Halliday *et al.*, 1998; Pfurtscheller, 1981; Pfurtscheller *et al.*, 1996) and magnetoencephalogram (MEG; Conway *et al.*, 1995; Salenius *et al.*, 1997; Salmelin & Hari, 1994) in humans. They are also detectable on EMG in distal limb muscles (Figure 1.4 B). In all instances, they are task-dependent, being prominent during delay or hold phases and diminished during movement (Baker *et al.*, 1997; Kilner *et al.*, 1999; Sanes & Donoghue, 1993).

Table 1.2: Oscillations in the motor system (adapted from Grosse *et al.*, 2002, with additional input from Williams *et al.*, 2010).

Frequency	Name(s)	Origin	Seen in
2Hz	Common drive	Unknown	Isometric contractions, slow movements
5-12Hz	Alpha	Probably reticular formation, cerebellum and spinal cord	Isometric contractions, slow movements, physiological tremor
15-30Hz	Beta	Probably M1	Submaximal voluntary contractions
30-60Hz	Low gamma, Piper rhythm	Probably M1	Strong voluntary contractions, slow movements
60-100Hz	High gamma	Probably brainstem	Eye movements, respiration

1.5.2 Coherence

Coupling of oscillations between the motor cortex and contralateral muscles can be quantified by coherence analysis. Coherence is a measure of linear correlation between two signals at a given frequency. It ranges from 0 to 1, indicating absolute linear independence and a perfect linear relationship respectively. As such, coherence is analogous to the correlation coefficient r^2, except that it is interpreted as a function of frequency.

Beta-band coherence between M1 and contralateral limb muscles (corticomuscular coherence, CMC) has been demonstrated in monkeys using LFPs (Figure 1.4 C; Baker *et al.*, 1997) and in humans using ECoG (Ohara *et al.*, 2000), EEG (Halliday *et al.*, 1998;

Mima & Hallett, 1999) and MEG (Conway *et al.*, 1995; Salenius *et al.*, 1997). ECoG is invasive, MEG is only available in selected centres and EEG is suboptimal due to its low focality, modest signal-to-noise ratio and the low-pass characteristics of the skull and scalp, which might explain why beta-band coherence between EEG and EMG is not universally detectable in humans (Fisher *et al.*, 2012; Ushiyama *et al.*, 2011b). By contrast, beta-band coherence can be reliably found between pairs of muscles co-activated in a task (Figure 1.4 D) or even between pairs of motor units in the same muscle (Farmer *et al.*, 1993; Kilner *et al.*, 1999), and such intermuscular or intramuscular coherence (IMC, IntraMC) is thought to reflect the same drive as CMC.

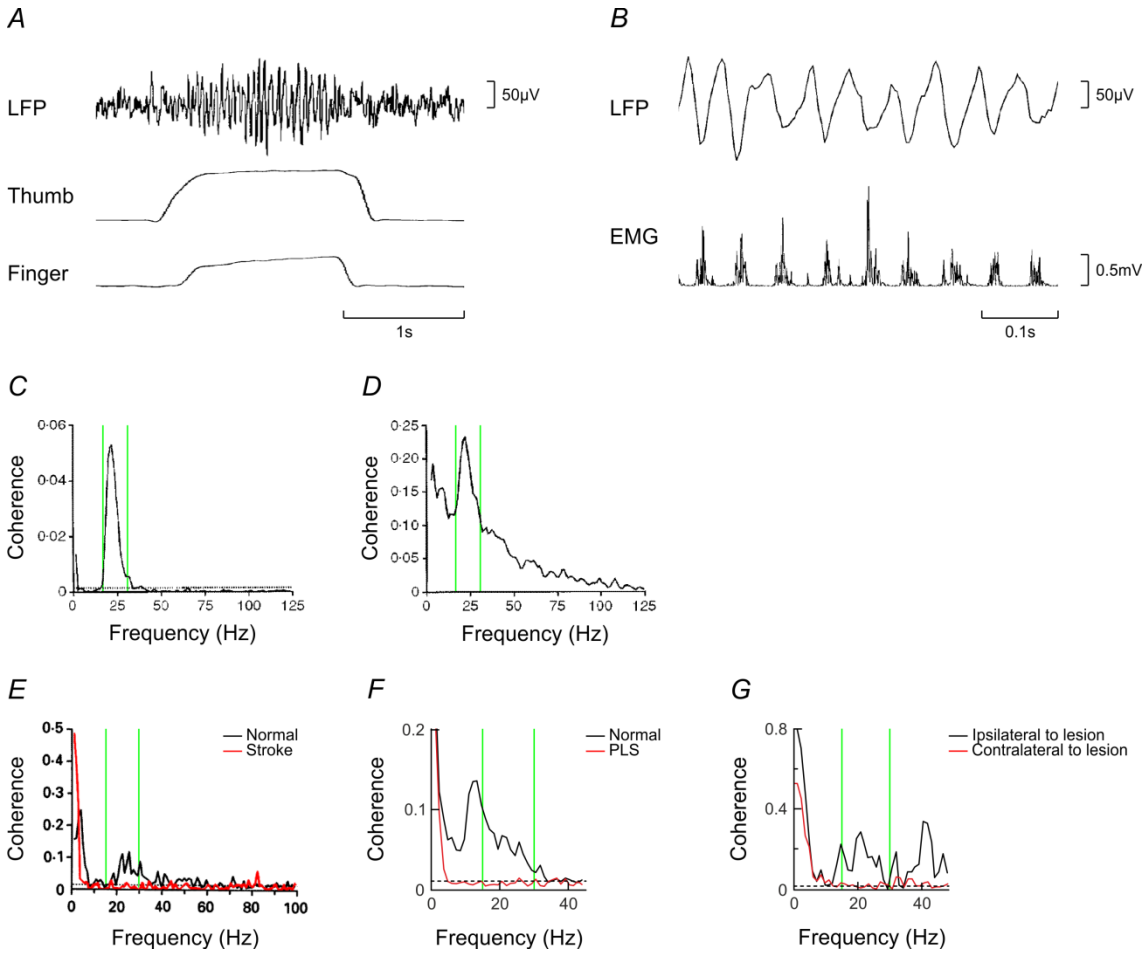

Figure 1.4: Oscillations and coherence. LFP recorded from M1 of a monkey carrying out a precision grip task, along with position of the thumb and finger levers (A). Oscillations appear during the hold phase. LFP and rectified EMG from contralateral adductor pollicis on an expanded timebase (B). Bursts of EMG activity appear to be in phase with the cortical oscillations. Coherence between cortical LFP and EMG (C). A single peak is present at ca. 20Hz. The 15-30Hz beta-band is demarcated by the vertical green lines, and the dotted horizontal line indicates the significance level for coherence. Coherence between EMGs from adductor pollicis and FDI (D). A peak is visible at ca. 20Hz, although coherence lies above the significance level at all

frequencies shown, presumably due to electrical cross-talk between the muscles (adapted from Baker *et al.*, 1997). Coherence between two motor units in FDI of a normal subject and a patient who suffered a contralateral capsular stroke four months before the recording (E; adapted from Farmer *et al.*, 1993). Average coherence between EMGs from FDS and FDI in 16 normal control subjects and eight patients with PLS (F). Coherence between EMGs from biceps and FDI in a monkey three months after unilateral pyramidotomy above the medullary decussation, ipsilateral and contralateral to the lesion (G; adapted from Fisher *et al.*, 2012).

1.5.3 Origin of beta-band oscillations and coherence

Primary motor cortex Beta-band oscillations reverse in phase as the cortex is traversed (Murthy & Fetz, 1992, 1996) and diminish once the white matter is entered (Steriade *et al.*, 1996). In brain slices, similar oscillations are observed in layer V pyramidal cells, and are unaffected by a cut through layer IV, thus demonstrating their independence from apical dendritic electrogenesis (Roopun *et al.*, 2006). These results suggest that beta-band oscillations are generated by neuronal networks in layer V which involve pyramidal cells.

Corticospinal tract A variety of evidence suggests that beta-band oscillations are transmitted to the peripheries via the CST. Firstly, beta-band oscillations have been shown to be present in M1 pyramidal tract neurons (Baker *et al.*, 2003). Secondly, beta-band coherence is abolished after damage to the descending motor tracts through capsular strokes (Figure 1.4 E; Farmer *et al.*, 1993) and spinal cord lesions (Hansen *et al.*, 2005; Norton *et al.*, 2003). More selective damage to the CST, for example through primary lateral sclerosis in humans (Figure 1.4 F; Fisher *et al.*, 2012) or experimental lesioning in monkeys (Figure 1.4 F; Fisher *et al.*, 2012; Nishimura *et al.*, 2009), is similarly associated with absence of beta-band coherence. Thirdly, pyramidal tract stimulation resets the phase of cortical beta-band oscillations in monkeys (Jackson *et al.*, 2002), implying that the CST is involved not only in the transmission but also in the generation of the beta rhythm.

Afferent pathways If a cortical generator drives peripheral oscillations with a fixed conduction delay, the phase difference between oscillations in cortex and muscle should vary linearly with frequency, with a slope related to the delay (Rosenberg *et al.*, 1989). However, in some reports the phase difference was constant across a range of

frequencies (Halliday *et al.*, 1998; Riddle & Baker, 2005; Witham *et al.*, 2011) or the phase changed in a way which implied that oscillations in muscle lead those in the cortex (Grosse *et al.*, 2003; Witham *et al.*, 2011). These results are explicable in terms of bidirectional coupling between cortex and muscle.

Three lines of evidence suggest that coherence is mediated by an efferent-afferent feedback loop. Firstly, beta-band coherence is markedly reduced by deafferentation, whether permanently through severe sensory neuropathy (Kilner *et al.*, 2004), or reversibly through ischaemia of the forearm (Pohja & Salenius, 2003) or anaesthesia of the digital nerves, which are purely afferent (Fisher *et al.*, 2002). Cooling of the upper limb slows conduction in both motor and sensory pathways, and the increase in conduction delay estimated from the phase-frequency slope is around twice the increase in motor conduction time, thus pointing towards the existence of a sensorimotor loop (Riddle & Baker, 2005). Secondly, beta-band oscillations can be observed in muscle spindle afferents (Baker *et al.*, 2006) as well as in somatosensory and posterior parietal cortex (Graziadio *et al.*, 2010; Murthy & Fetz, 1992, 1996; Witham *et al.*, 2011; Witham *et al.*, 2010; Witham *et al.*, 2007), and these are coherent with similar oscillations in EMG and/or M1. Finally, coherence as a correlational measure does not allow determination of the direction of the interaction between two signals. By contrast, directed coherence (Granger causality) can do so, and suggests bidirectional corticomuscular coupling in monkeys (Witham *et al.*, 2010) and humans (Witham *et al.*, 2011).

1.5.4 Function of coherence

The function of beta-band oscillations and coherence has been controversial.

A role analogous to sensory binding has been proposed. Oscillations might bind together either neuronal ensembles in the motor cortex that are involved in the same task (Conway *et al.*, 1995), or areas of motor and somatosensory cortex to enable sensorimotor integration (Murthy & Fetz, 1992), but there is little evidence to support these hypotheses. Oscillations are abolished during movement, when binding would be expected to be most critical, but are prominent before and after.

In light of this, it has been suggested that oscillations could represent an 'idling' rhythm that occurs when the motor cortex is 'resting' before and after the demands of task execution. However, cortical oscillations depend on neuronal activity, which is metabolically demanding and would be a surprising feature of a resting state. The activity of pyramidal tract neurons remains elevated above baseline during the hold phase (Lemon *et al.*, 1986), militating against a decrease in cortical activity. Finally, this theory would imply that oscillations in the somatosensory system are merely an epiphenomenon.

A further hypothesis states that oscillations are an efficient mechanism for recruiting motor neurons with minimal corticospinal activity during sustained contractions (Baker *et al.*, 1997). Again, this explanation does not encompass oscillations in the sensory pathways.

Most recently, it has been suggested that oscillations might act as a 'test pulse' which drives peripheral feedback to allow recalibration of the sensorimotor system (Witham *et al.*, 2011). This would plausibly explain the involvement of both motor and sensory pathways. In keeping with this hypothesis, coherence during a steady contraction increases with the degree of recalibration required after a preceding task. For example, larger displacements during the ramp phase of a precision grip task are associated with larger potential errors and greater coherence in a subsequent hold phase (Riddle & Baker, 2006). Similarly, a period of dynamic rather than static force matching is associated with increased coherence during a subsequent steady contraction, particularly if the pattern of the dynamic force is unpredictable (Omlor *et al.*, 2011). Beta-band oscillations and coherence fluctuate during a prolonged steady contraction, and epochs of elevated coherence are associated with increases in beta-band tremor and reaction times (Gilbertson *et al.*, 2005; Matsuya *et al.*, 2013). Hence, brief bursts of beta-band oscillations would help to maintain sensorimotor precision whilst minimising the transient deterioration in motor performance that accompanies the calibration process.

1.6 Overview of this thesis

MND presents across a broad age range. Potential markers of disease might be subject to age-related changes, and to investigate this possibility I recruited a large, age-stratified cohort of healthy volunteers, which formed the basis for the experiments described in Chapters 2, 3 and 4.

Many previous reports have considered how CMCT and PMCT vary with age, height or sex using single-variable regression models. In Chapter 2, I re-investigate these relationships using multiple regression modelling, and reconcile some past discrepancies. The resulting model allows a degree of individualisation of normal ranges.

In Chapter 3, I demonstrate that the amplitude of beta-band IMC does not vary with age. However, IMC varies substantially between individuals; within a given individual, variability is greater in the long than in the short term. Possible strategies for dissecting the causes of variability are considered.

It has been suggested that transcranial direct current stimulation (tDCS) might help to make IMC a more sensitive marker of CST dysfunction. In Chapter 4, I reproduce previously described effects of tDCS on IMC. Noting marked variability between subjects, I discuss how the size of the effect could be increased. The classically described effects of tDCS on MEPs remain elusive, and potential reasons are discussed.

In Chapters 5 and 6, IMC and/or CMCT are measured in patients with neurological conditions and compared to the normal data gathered in Chapters 2 and 3.

Chapter 5 describes that, in MND, IMC matches or exceeds the performance of CMCT as a potential marker of CST dysfunction. I consider further steps required to translate IMC into a clinical test.

In Chapter 6, IMC is measured in other neurological conditions affecting different parts of the motor system in order to illuminate the relative contribution of these parts to

IMC generation. One issue is that individual conditions may have affected more than one part of the motor system, and computational modelling of coherence is suggested as a complementary approach.

2 Central and peripheral motor conduction times in normal adults

For almost three decades, magnetic stimulation has been used to examine central and peripheral motor conduction times. Many studies have reported simple regression models involving predictors such as age, height and sex, often arriving at conflicting results. Here, I formulate a multiple regression model based on data from a large normal cohort, and attempt to reconcile previous contradictions.

2.1 Abstract

Objective: To analyse the effects of age, height and sex on central and peripheral motor conduction times (CMCT, PMCT) by means of a multiple regression model.

Methods: Motor evoked potentials were recorded from upper and lower limb muscles in 91 healthy volunteers stratified by age. Magnetic stimulation was performed over the primary motor cortex (cortical latency) and over the cervical and lumbar spine (spinal latency). The spinal latency was taken as an estimate of PMCT, and was subtracted from cortical latency to yield CMCT.

Results: Lower limb CMCT significantly correlated with height only; there were no significant predictors for upper limb CMCT. Upper and lower limb PMCT correlated with both age and height.

Conclusions: To our knowledge, this is the first study applying a multiple regression model to CMCT data. Our results are in keeping with reported simple regression models, and condense their hitherto separate findings into a unified model. The model presented allows normal ranges to be individualised, thereby potentially improving the diagnostic performance of clinical central motor conduction studies.

2.2 Introduction

The function of the corticospinal tract (CST) can be assessed non-invasively using magnetic stimulation. Central motor conduction time (CMCT) has emerged as the most reliable parameter (Chen *et al.*, 2008; Claus, 1990; Di Lazzaro *et al.*, 1999), and estimates the conduction time from the primary motor cortex (M1) to spinal motor neurons. Magnetic stimulation is performed over M1 to measure the cortical latency for the target muscle; CMCT is then calculated by subtracting an estimate of the peripheral motor conduction time (PMCT). Clinical CMCT studies commonly estimate PMCT using magnetic stimulation of the spinal roots as this is well tolerated and avoids the use of a further stimulation modality. We therefore adopted this method for the present study.

Normal ranges of CMCT have been described in several past reports (Table 2.1). The set of muscles examined was usually small and varied between studies, and results are only in partial agreement where comparisons are possible. Contributing factors may include small study populations and methodological discrepancies, particularly regarding the type of stimulator and coil used. Additionally, the lower limb representation of M1 was stimulated with a circular coil, whereas a double cone coil is probably better suited to this task, especially for distal muscles (Groppa *et al.*, 2012; Terao *et al.*, 1994).

Previous studies have also considered the effect of age, height and sex on CMCT. Statistical methods ranged from comparisons between discrete groups (Dvorak *et al.*, 1991; Eisen & Shtybel, 1990; Kloten *et al.*, 1992; Mano *et al.*, 1992; Mills & Nithi, 1997b; Rossini *et al.*, 1992) to correlation and regression analysis with individual predictors (Chu, 1989; Claus, 1990; Dvorak *et al.*, 1990; Furby *et al.*, 1992; Garassus *et al.*, 1993). Multiple regression modelling is required to take into account any cross-correlations between the predictors age, height and sex (e.g. young male subjects being taller on average than older female ones). This approach has been applied to somatosensory evoked potentials (SEP; Allison *et al.*, 1983; Chu, 1986; Dorfman & Bosley, 1979) but not, to our knowledge, to CMCT.

Table 2.1: Previously reported normal CMCT and PMCT data (mean±SD). Studies have only been included if a facilitatory background contraction was maintained during cortical stimulation and if PMCT was estimated using magnetic root stimulation. All used circular coils in conjunction with the stimulators listed, but other methods – including coil size – were described in variable detail and cannot be compared easily. Results are limited to the set of muscles considered in the present study; we did not find any reported data for FDS. Where comparisons are possible, results often agree only partially; potential causes include small study populations and methodological differences. Two studies categorised some results by age or height without giving pooled data so results are listed separately for each group (Dvorak *et al.*, 1991; Kloten *et al.*, 1992). One report provided an upper limit of normal as mean+3SD without individually stating the mean or SD (Di Lazzaro *et al.*, 1999), and another one specified only CMCT but not PMCT (Eisen & Shtybel, 1990). (NS=not specified)

	Muscle	CMCT (ms)	PMCT (ms)	Stimulator	n	Reference
Upper limb	APB	6.88±0.56	13.12±1.35	Magstim 200	30	Abbruzzese *et al.* (1993)
		8.0±1.2	13.1±1.0	Own design	27	Barker *et al.* (1987)
		5.2±0.6	15.6±1.2	Dantec or Magstim 200	53	Dvorak *et al.* (1990)
		6.7±1.2	NS	Dantec	95	Eisen and Shtybel (1990)
		6.73±1.01	13.58±0.98	Magstim 200	30	Garassus *et al.* (1993)
		6.7±1.7 (age 31.2±16.8) 6.3±1.0 (age 78.7±4.8)	11.1±0.7 (age 31.2±16.8) 11.7±0.9 (age 78.7±4.8)	Own design	14 26	Mano *et al.* (1992)
		8.0±1.2	11.8±1.0	Own design	30	Ugawa *et al.* (1990)
	FDI	6.0±1.0	14.6±1.3	Magstim 200	57	Bischoff *et al.* (1993)
		5.8±1.0 (age ≤29) 6.0±0.9 (age 30-59) 6.5±1.1 (age ≥60)	14.0±1.3 14.6±1.3 14.9±1.4	Magstim 200	57	Kloten *et al.* (1992)
	EDC	5.6±0.9	9.1±0.8	Magstim 200	57	Bischoff *et al.* (1993)
		6.4±1.2	NS	Dantec	42	Eisen and Shtybel (1990)

	Muscle	CMCT (ms)	PMCT (ms)	Stimulator	n	Reference
Lower limb	EDB	13.4±1.7 (pooled)	23.9±2.0 (height 150-174cm) 25.4±1.9 (height 175-191cm)	Dantec or Magstim 200	46	Dvorak *et al.* (1991)
		14.53±1.50	21.71±1.92	Magstim 200	30	Garassus *et al.* (1993)
		15.7±2.4 (age ≤29) 15.9±2.0 (age 30-59) 18.2±3.9 (age ≥60)	24.8±1.8 23.3±2.6 23.9±2.8	Magstim 200	57	Kloten *et al.* (1992)
	AH	16.7±2.4	24.5±2.1	Own design	27	Barker *et al.* (1987)
		15.9±2.0	24.3±2.6	Magstim 200	57	Bischoff *et al.* (1993)
		18.2 (mean+3SD)	30.1 (mean+3SD)	Magstim 200	30	Di Lazzaro *et al.* (1999)
		16.9±0.9	23.3±2.5	Magstim 200	15	Di Lazzaro *et al.* (2004)

Muscle	CMCT (ms)	PMCT (ms)	Stimulator	n	Reference
TA	14.35±0.85	11.73±1.37	Magstim 200	30	Abbruzzese *et al.* (1993)
	14.3±1.7	14.7±1.8	Magstim 200	57	Bischoff *et al.* (1993)
	14.8±1.1	11.7±1.1	Magstim 200	52	Chu (1989)
	17.1 (mean+3SD)	16.1 (mean+3SD)	Magstim 200	30	Di Lazzaro *et al.* (1999)
	12.8±1.4 (height 150-174cm) 14.0±1.3 (height 175-191cm)	16.1±2.3 (pooled)	Dantec or Magstim 200	46	Dvorak *et al.* (1991)
	13.8±1.5	12.3±1.2	Magstim 200	50	Furby *et al.* (1992)
	14.23±1.71	13.22±1.19	Magstim 200	30	Garassus *et al.* (1993)
	13.4±1.9 (age ≤29) 14.3±1.7 (age 30-59) 16.1±1.9 (age ≥60)	14.7±1.3 14.7±2.1 15.5±2.0	Magstim 200	57	Kloten *et al.* (1992)
	14.6±1.2	11.5±0.9	Magstim 200	51	Matsumoto *et al.* (2010)
	14.7±1.3	11.5±1.1	Magstim 200	100	Matsumoto *et al.* (2012)
	15.3±1.0	12.7±1.6	Own design	30	Ugawa *et al.* (1990)
MG	14.2±1.5	13.4±1.0	Magstim 200	57	Bischoff *et al.* (1993)

Here, we sought to clarify the effects of age, height and sex on CMCT using a stepwise multiple regression model in a large study population stratified by age. PMCT data were modelled likewise. We employed modern equipment and routine clinical methods, including the use of standard circular and double cone coils to stimulate the upper and lower limb representations of M1 respectively. Lower limb CMCT was correlated significantly with height, whereas there were no significant predictors for upper limb CMCT. Upper and lower limb PMCT correlated significantly with age and height but not sex. Regression models and normal ranges are described.

2.3 Methods

2.3.1 Subjects

At least 15 volunteers were recruited for each decade of age between 20 and 80 (50 men and 41 women). Age and height averaged 48.9±17.3 years (SD; range 22-77) and 171.0±9.6cm (range 155.0-188.0) respectively. Eighty-two subjects were right-handed and 9 left-handed as assessed by self-reporting. None had any history of neurological disorders or diabetes mellitus, or any contraindications to magnetic stimulation, and none took any neurotropic medication. All subjects provided written informed consent. The study was approved by the research ethics committee of Newcastle University's Medical Faculty, and conformed to the Declaration of Helsinki.

2.3.2 Recording

Every effort was made to maintain subjects at a constant level of alertness, and all assessments were carried out on the dominant side. Subjects were seated in a comfortable chair with their arm resting on a cushion. Surface EMG was recorded from abductor pollicis brevis (APB), first dorsal interosseous (FDI), flexor digitorum superficialis (FDS) and extensor digitorum communis (EDC) in the upper limb, and extensor digitorum brevis (EDB), abductor hallucis (AH), tibialis anterior (TA) and medial gastrocnemius (MG) in the lower limb. Adhesive electrodes (Bio-Logic M0476; Natus Medical, Mundelein, IL) were placed in a belly-tendon montage over the intrinsic muscles of the hand or foot; for the long muscles of the forearm or calf, the electrodes were placed 4cm apart, one third along the muscle from its proximal origin. Signals

were amplified, band-pass filtered (30Hz-2kHz; Digitimer D360, Digitimer, Welwyn Garden City, UK) and digitised at 5kHz (Micro1401, Cambridge Electronic Devices, Cambridge, UK).

2.3.3 Stimulation

Magnetic stimulation was delivered using a Magstim 200 stimulator (Magstim Company, Whitland, UK) at a frequency of 0.2Hz. For upper limb cortical motor evoked potentials (MEPs), a circular coil (13cm outer diameter) was held over the vertex, with its orientation optimised for stimulation of the dominant hemisphere (A side up: left hemisphere, B side up: right hemisphere). For lower limb cortical MEPs, a double cone coil was used in an analogous manner (posterior coil current: left hemisphere, anterior coil current: right hemisphere). Stimulation intensity was set at 10% of maximum stimulator output above the resting motor threshold as defined by the Rossini-Rothwell method (Rossini *et al.*, 1994). Cortical MEPs are facilitated and their onset latencies minimised by a weak background contraction of the target muscle, with no requirement for strictly controlling the force of the contraction (Chen *et al.*, 2008; Kimura, 2001). Ten MEPs were recorded in the upper limb during opposition of index finger and thumb, and in the lower limb during either dorsiflexion (EDB, TA) or plantarflexion (AH, MG) of ankle and toes. Upper and lower limb root MEPs were recorded at rest with the circular coil centred over the spinous processes of C7 and L1. The range of stimulation intensities used was 35-80% and 40-100% for cortical MEPs of the upper and lower limbs respectively, and 40-90% and 40-100% for corresponding root MEPs.

2.3.4 Data analysis

Analysis was performed in Matlab (Mathworks, Natick, MA) using custom scripts. The shortest onset latency for each set of ten MEPs was assigned interactively. In the presence of a background contraction, the earliest deflection of the MEP with the shortest latency was often ambiguous on superimposed raw traces because of background EMG activity, but could be easily identified on averages of rectified MEPs (Figure 2.1). Hence, such averages were used for assigning latencies throughout.

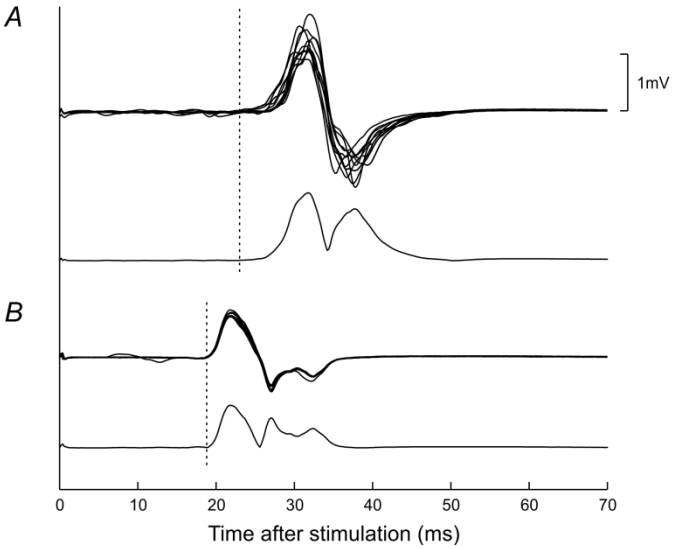

Figure 2.1: Single-subject cortical (A) and root MEPs (B) in APB. For each site of stimulation, two types of trace are shown: ten superimposed raw sweeps (top) and an average of rectified sweeps (bottom). For cortical MEPs, which were recorded in the presence of a background contraction, the earliest deflection of the MEP with the shortest latency was frequently ambiguous on superimposed raw traces, but could be easily identified on the average of rectified MEPs. All latencies (dashed lines) were assigned using such averages.

Stepwise multiple regression models were constructed for all CMCT and PMCT using age, height and sex as potential predictors ('stepwise' command in Matlab). Each step involved evaluating the residuals of the model and the associated probability for each predictor, and moving a single predictor into or out of the model as recommended by the interactive tool. Significance thresholds were set at ≤0.05 for a predictor to enter the model and at ≥0.10 for it to be removed. The model was deemed complete when no further movement of predictors was recommended.

2.4 Results

One subject did not tolerate lower limb cortical MEPs, but all remaining subjects completed all parts of the protocol.

Means, standard deviations and regression models are presented numerically in Table 2.2. For a given latency measurement (CMCT or PMCT) and within a given limb, the

same predictors were found to be significant across all muscles. Figures 2.2 and 2.3 display results for APB and EDB as examples of upper and lower limb muscles.

2.4.1 CMCT

Upper limb CMCT was not significantly related to any of the potential predictors (Table 2.2, Figure 2.2 A-C).

Lower limb CMCT showed a significant positive relationship with height; there was no significant relationship with age or sex. The regression models accounted for approximately 5-12% of the variance observed (r^2, Table 2.2). The model for EDB is shown in Figure 2.2 E along with 95% confidence and prediction intervals.

2.4.2 PMCT

Upper and lower limb PMCT was significantly and positively related to age and height. There was no significant relationship with sex. The regression models explained approximately 19-53% of the variance observed (Table 2.2). Figures 2.3 A and 2.3 C illustrate the regression model on a plot of PMCT against age and height. The shaded plane represents the model prediction, with the vertical lines showing the residuals of individual data points above (black) and below the plane (red). In order to keep the plot easily interpretable, 95% confidence and prediction intervals are only shown for the upper extremes of age and height.

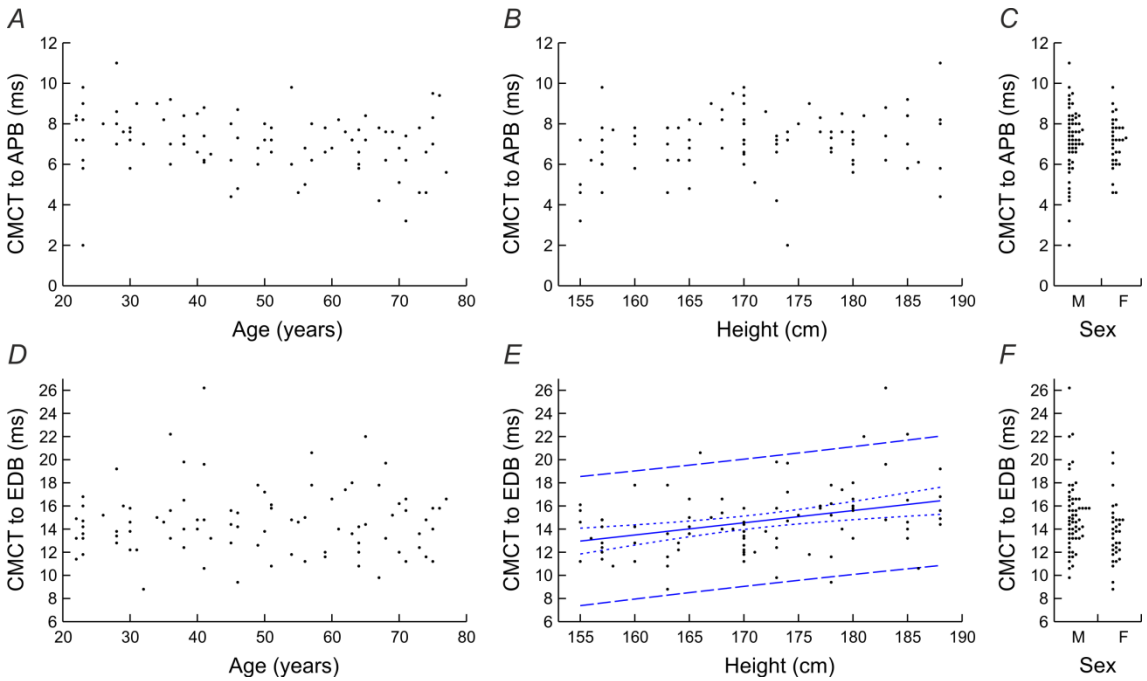

Figure 2.2: Scatterplots of CMCT to APB (A-C) and EDB (D-F) against age (A, D) and height (B, E), and dot plots of CMCT against sex (C, F). CMCT to APB was not significantly related to any of the predictors. CMCT to EDB was significantly related to height but not age or sex; the corresponding regression model is shown (CMCT to EDB=0.1055*height - 3.40, r^2=0.1225, p<0.001) together with 95% confidence (dotted lines) and prediction intervals (dashed lines).

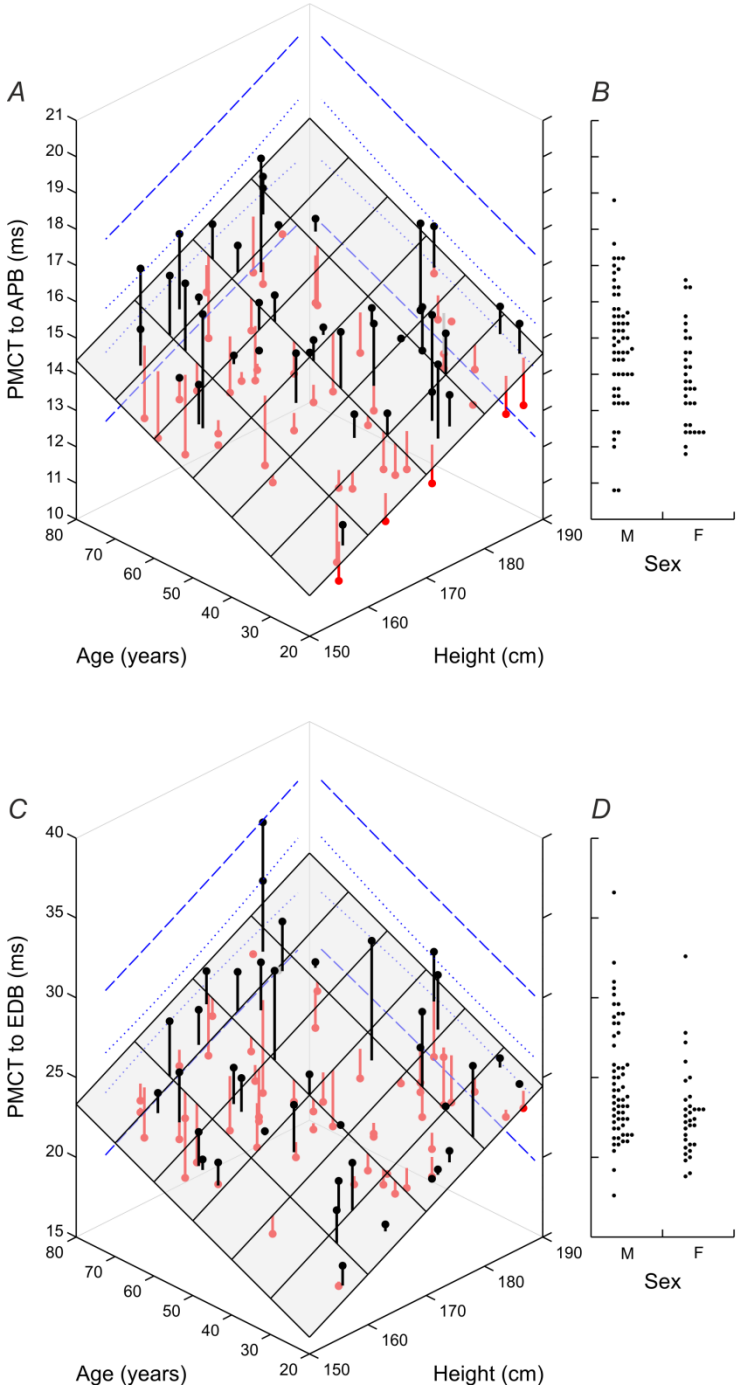

Figure 2.3: 3D scatterplots of PMCT to APB and EDB against age and height (A, C), and dot plots of PMCT against sex (B, D). PMCT in both muscles was significantly related to age and height but not sex. The shaded plane shows the regression model (PMCT to APB=0.0560*age + 0.0881*height - 3.28, r^2=0.4318, p<0.001; PMCT to EDB= 0.1214*age + 0.2106*height - 17.97, r^2=0.4819, p<0.001). Vertical lines indicate the residuals of individual data points above (black) and below the plane (red). Examples of 95% confidence (dotted lines) and prediction intervals (dashed lines) are shown for the upper extremes of age and height.

Table 2.2: Means, standard deviations (SD) and regression models for CMCT and PMCT in muscles of upper and lower limbs in this study (A=age, H=height). For upper limb CMCT, no significant regression model could be formulated (NA=not applicable). The proportion of variance explained by the model (r^2) was 5-12% for lower limb CMCT, 19-48% for lower limb PMCT, and 25-53% for upper limb PMCT.

	Muscle	**CMCT**					**PMCT**				
		Mean±SD (ms)	Regression model	SD of residuals (ms)	r^2	p	Mean±SD (ms)	Regression model	SD of residuals (ms)	r^2	p
Upper limb	APB	7.2±1.6	NA	NA	NA	NA	14.5±1.6	0.0560*A + 0.0881*H - 3.28	1.10	0.432	<0.001
	FDI	7.2±1.4	NA	NA	NA	NA	15.2±1.6	0.0549*A + 0.1082*H - 6.03	1.21	0.526	<0.001
	FDS	7.7±2.0	NA	NA	NA	NA	8.7±1.2	0.0373*A + 0.0412*H - 0.18	1.00	0.291	<0.001
	EDC	6.7±1.7	NA	NA	NA	NA	9.3±1.2	0.0340*A + 0.0483*H - 0.62	1.08	0.250	<0.001
Lower limb	EDB	14.6±2.9	0.1055*H - 3.40	2.74	0.123	<0.001	23.9±3.5	0.1214*A + 0.2106*H - 17.97	2.49	0.482	<0.001
	AH	16.0±3.3	0.0801*H + 2.29	3.16	0.057	0.024	25.8±4.0	0.0938*A + 0.2133*H - 15.22	3.37	0.293	<0.001
	TA	14.5±2.7	0.0919*H - 1.23	2.57	0.107	0.002	13.7±2.4	0.0648*A + 0.0769*H - 2.63	2.07	0.227	<0.001
	MG	15.3±3.7	0.0813*H + 1.43	3.62	0.045	0.044	15.1±3.3	0.0856*A + 0.0964*H - 5.56	2.99	0.194	<0.001

2.5 Discussion

In this study, we investigated the relationship of CMCT and PMCT with three potential predictors chosen for their ready availability. We found that lower limb CMCT depended on height only and that upper limb CMCT was not significantly related to any of the predictors. By contrast, upper and lower limb PMCT both depended on age and height. For each type of latency, the same predictors were consistently significant across all muscles of a given limb, which increases confidence in the individual findings.

2.5.1 Methods for PMCT estimation

Several methods are available for estimating PMCT, and the approach used must be borne in mind when comparing the corresponding CMCT readings between studies. Magnetic (Maccabee *et al.*, 1991; Ugawa *et al.*, 1989) or electrical stimulation (Mills & Murray, 1986) over the vertebral column excites spinal roots near the exit foramina and the MEP latency provides an estimate of PMCT. The conduction time along the proximal root segments is not included in PMCT and remains part of CMCT (often called CMCT-M). This peripheral component of CMCT is particularly pronounced in the lower limbs where a greater length of the roots is located within the spinal canal.

Alternatively, PMCT can be estimated using F-wave latencies from electrical stimulation of peripheral nerves (Kimura, 2001). Such PMCT values include the conduction time along the proximal root segments; corresponding CMCT readings (often called CMCT-F) are shorter and reflect a purer measure of CST conduction than those obtained using root stimulation. Drawbacks of F-wave latencies include a high intertrial variability and the assumption of a fixed turnaround time of 1ms, which does not take into account that the regenerative volley might be slowed by travelling along a partially refractory axon (Rossini & Pauri, 2002). In addition, a different population of motor neurons, at different ends of the conduction velocity spectrum, may be recruited by the F-wave and cortical MEPs (Olivier *et al.*, 2002).

Using a special (magnetic augmented translumbosacral stimulation, MATS) coil, one group has selectively stimulated either the lumbosacral nerve roots near the exit foramina – akin to conventional magnetic root stimulation – or the conus medullaris

within the spinal canal (Matsumoto *et al.*, 2009a; Matsumoto *et al.*, 2009b). This makes it possible to estimate the latency from cortex to conus (cortico-conus conduction time) and the peripheral component of CMCT-M (cauda equina conduction time). However, two lines of evidence suggest that the MATS coil excites spinal roots at a more distal point than standard coils, thus increasing the peripheral component of CMCT-M. Firstly, MATS-based root latencies are relatively low and corresponding CMCT-M readings relatively high compared to results obtained with conventional coils (Table 2.1; Matsumoto *et al.*, 2010; Matsumoto *et al.*, 2012). Secondly, root latencies are 0.9ms shorter than for electrical root stimulation, equivalent to a distance of about 4.5cm if a nerve conduction velocity of 50m/s is assumed (Matsumoto *et al.*, 2009a). In the same study, root stimulation was also performed with standard coils but latencies were unfortunately not compared between different coil types. Hence, CMCT-M determined using MATS-based root latencies cannot easily be compared to data obtained using conventional coils.

2.5.2 CMCT and height

Our finding of a significant relationship between lower limb CMCT-M and height is in agreement with several previous studies which described similar results in some (Dvorak *et al.*, 1991) or all muscles under investigation (Chu, 1989; Claus, 1990; Furby *et al.*, 1992); one study reported a trend which did not reach significance (Garassus *et al.*, 1993). Furthermore, our regression model for TA (CMCT=0.0919*height - 1.23) concurs with those previously published, particularly regarding the coefficient for height (CMCT=0.08*height - 0.73, $p<0.001$, Claus *et al.*, 1990; CMCT=0.083*height - 0.47, $p<0.0001$, Furby *et al.*, 1992).

It has been suggested that this relationship might be attributable to the peripheral component of CMCT-M. If this were the case, no such relationship should exist for CMCT-F. Whilst several studies have reported both CMCT-M and CMCT-F, few have considered how both types of CMCT might differ in their relationship with height. In one report, CMCT-M was related to height in one of three muscles whereas CMCT-F was not (Dvorak *et al.*, 1991); another study described a significant correlation of CMCT-M with height without commenting on CMCT-F data (Furby *et al.*, 1992); and a further one did not make it clear whether both types of CMCT were analysed in a

separate or pooled fashion (Garassus *et al.*, 1993). Recently, a study described height to be uncorrelated to lower limb cortico-conus conduction time whilst being significantly correlated to CMCT-M and cauda equina conduction time (Matsumoto *et al.*, 2010). However, the use of a MATS coil for root stimulation would have exaggerated the peripheral component of CMCT-M. It therefore remains unclear to what extent the peripheral component underlies the correlation of height and conventional lower limb CMCT-M. This could be addressed with a study in which the conus is stimulated with a MATS coil and the roots with a standard coil, thus allowing measurement of cortico-conus conduction time as well as true conventional CMCT-M and its peripheral component.

There is consensus that upper limb CMCT does not correlate with height (Chu, 1989; Claus, 1990; Dvorak *et al.*, 1990; Furby *et al.*, 1992; Garassus *et al.*, 1993). This may be because of the shorter proximal root segments in the cervical spine, because height relates less strongly to the length of the CST to the upper limb (Chu, 1989; Claus, 1990), or both.

2.5.3 CMCT and age

The effect of age on CMCT is controversial. We observed no correlation between age and CMCT-M, and this concurs with six past reports which each measured both CMCT-M and CMCT-F and found neither of them to be significantly related to age (Claus, 1990; Dvorak *et al.*, 1990; Dvorak *et al.*, 1991; Garassus *et al.*, 1993; Mano *et al.*, 1992; Rossini *et al.*, 1992). However, three other studies reported a significant positive relationship. The first employed a MATS coil, and whilst cortico-conus conduction time did not correlate with age, CMCT-M and cauda equina conduction time did. The reported correlation of CMCT-M with age is explicable in terms of an exaggerated peripheral component (Matsumoto *et al.*, 2012). A second investigation calculated PMCT from F-wave latencies in such a way that a peripheral component of unclear magnitude remained part of the CMCT-F (Eisen & Shtybel, 1990; Matsumoto *et al.*, 2012). The final study compared CMCT-M in two muscles between three groups of different ages which had been matched for height, but did not make any adjustment for multiple comparisons (Kloten *et al.*, 1992). Thus, where a significant relationship between CMCT and age was reported, this could usually be attributed to an increased

peripheral component. By contrast, the peripheral component of conventional CMCT-M appears to be sufficiently small to avoid giving rise to a significant relationship.

2.5.4 CMCT and sex

Similar to our findings, previous investigations found CMCT to be unaffected by sex (Dvorak *et al.*, 1990; Kloten *et al.*, 1992), or any differences between males and females were attributed to height differences between the sexes (Chu, 1989; Dvorak *et al.*, 1991; Furby *et al.*, 1992; Mills & Nithi, 1997b).

2.5.5 PMCT

It is well known that age and height are negatively correlated with peripheral nerve conduction velocities and positively correlated with distal motor and F-wave latencies, whereas sex is generally not thought to be a significant predictor (Kong *et al.*, 2010; Rivner *et al.*, 2001). Similarly, PMCT is related to age (Dvorak *et al.*, 1991; Kloten *et al.*, 1992; Mano *et al.*, 1992; Matsumoto *et al.*, 2012) and height (Chu, 1989; Dvorak *et al.*, 1991; Furby *et al.*, 1992). The proportion of variance explained by our model (r^2) was greater for PMCT than for CMCT. We are not aware of any previous multiple regression models for PMCT, but the proportion of variance explained by our model for PMCT is in broad agreement with values reported for multiple regression models of related peripheral conduction parameters (Kong *et al.*, 2010; Rivner *et al.*, 2001).

The relationship between PMCT and height is readily explained by the strong correlation between height and limb length and thus length of the peripheral nerves (Chu & Hong, 1985). The observation that PMCT but not CMCT correlates with age might be attributable to the greater exposure of peripheral nerves to minor trauma and injuries (Matsumoto *et al.*, 2012). Indeed, ageing is not only known to cause subclinical peripheral nerve lesions at common entrapment sites (Cruz Martinez *et al.*, 1978), but also leads to progressive loss of motor units, particularly affecting the largest and fastest units (Wang *et al.*, 1999).

2.5.6 Clinical application

In clinical practice, numerical results are typically compared to normal ranges or cut-off values, which constitutes fixed-level testing at a pre-determined significance level. Here, an appropriate cut-off would be the upper bound of a chosen prediction interval. The bound can be approximated by evaluating the regression model with the parameters of the patient and adding $q_{1-\alpha/2}$ standard deviations, where α is the desired significance level and q is the inverse of the normal cumulative distribution function. For example, a 95% prediction interval has $\alpha=0.05$ and $q_{1-\alpha/2}=q_{0.975}=1.960$; this upper bound would be exceeded by $\alpha/2=0.025=2.5\%$ of normal readings.

Alternatively, we can evaluate the probability of observing a latency at least as high as that of the patient, under the null hypothesis that the latency of the patient is normal. The regression model is evaluated with the parameters of the patient, and a Z-score calculated as Z=(actual result - regression result)/(standard deviation of residuals). The corresponding probability is then computed as $\varphi(-|Z|)$, where φ is the cumulative normal distribution.

The data provided allow either approach to be implemented easily; we have deliberately not provided prescribed cut-off values as they would force the reader into fixed-level testing with a chosen significance level.

2.6 Conclusion

This is one of the largest studies of CMCT-M in normals and, to our knowledge, the only one to employ multiple regression modelling. Such an approach was applied to somatosensory evoked potentials more than three decades ago. Its application to MEP data was long overdue and has shed some light on longstanding controversies surrounding the effects of age and height on CMCT. In addition, the model is able to account for 5-12% (CMCT) or 19-53% (PMCT) of variance. Paired with side-to-side comparisons within a given subject, this should boost the diagnostic accuracy and precision of CMCT-M. MATS coils constitute a promising development in CST assessment, and cortico-conus conduction time might ultimately replace CMCT-M in

CST assessment. However, when using a MATS coil for root stimulation, the resultant CMCT-M are not wholly comparable to results obtained using conventional coils. Previously reported inferences about conventional CMCT-M must therefore be viewed with caution.

3 Intermuscular coherence in normal adults: variability and changes with age

The effect of aging on coherence is controversial, and previous studies suggest that coherence can vary considerably between and within subjects. In this chapter, I seek to clarify whether intermuscular coherence changes across adulthood, and consider its short- and long-term variability.

3.1 Abstract

Objective: To examine changes in beta-band intermuscular coherence (IMC) across adulthood, and to analyse variability between and within subjects.

Methods: 92 healthy volunteers were recruited, stratified by decade of age. In the dominant upper limb, IMC was estimated between extensor digitorum communis (EDC) and first dorsal interosseous (FDI) as well as between flexor digitorum superficialis (FDS) and FDI. In the ipsilateral lower limb, IMC was measured between medial gastrocnemius (MG) and extensor digitorum brevis (EDB) as well as between tibialis anterior (TA) and EDB. Age-related changes in IMC were analysed with age as a continuous variable or binned by decade. We analysed intrasession variance of IMC by dividing sessions into pairs of epochs and comparing coherence estimates between these pairs. Eight volunteers returned for a further session after one year, allowing us to compare intrasession and intersession variance.

Results: We found no age-related changes in IMC amplitude across almost six decades of age. Interindividual variability ranged over two orders of magnitude. Intrasession variance was significantly greater than expected from statistical variability alone, and intersession variance was even larger.

Conclusion: The lack of age-related variability allowed us to pool results across all ages into an aggregate normative dataset. Variability between and within individuals was considerable, and we propose potential causes. With variability being critical to future

applications of IMC as a biomarker, we propose several experiments that should help to define the causes of variability so that it potentially can be minimised.

3.2 Introduction

Oscillations in the beta-band (15-30Hz) have been demonstrated in the motor systems of monkeys (Murthy & Fetz, 1992) and humans (Ohara *et al.*, 2000; Pfurtscheller, 1981; Salmelin & Hari, 1994). During sustained contractions, these oscillations are coherent between sensorimotor cortex and contralateral muscles (corticomuscular coherence, CMC; Baker *et al.*, 1997; Conway *et al.*, 1995; Halliday *et al.*, 1998; Ohara *et al.*, 2000). Coherence is also demonstrable between different co-contracting muscles within the same limb (intermuscular coherence, IMC; Baker *et al.*, 1997) and between different single motor units in a given muscle (intramuscular coherence, IntraMC; Farmer *et al.*, 1993). Whilst measured between different pairs of signals, CMC, IMC and IntraMC are thought to reflect the same central coupling mechanism. Initially hypothesised to be a purely efferent, corticofugal phenomenon mediated by the corticospinal tract (CST; Baker *et al.*, 2003), beta-band coherence has been increasingly documented to depend on afferent pathways, leading to the current concept of an underlying efferent-afferent feedback loop (Witham *et al.*, 2011; Witham *et al.*, 2010).

Several recent studies have investigated the development of coherence during childhood and its potential alteration in old age. There is agreement that beta-band CMC (Graziadio *et al.*, 2010; James *et al.*, 2008) and IMC (Farmer *et al.*, 2007) are absent in infancy and develop during the early teenage years, probably in parallel to the rising capacity for fractionated movement (Gibbs *et al.*, 1997). Although the CST establishes functional monosynaptic projections onto spinal motor neurons before birth (Eyre *et al.*, 2000) and becomes fully myelinated by two years of age (Eyre *et al.*, 1991), the patterning of the corticospinal drive only completes during adolescence (Farmer *et al.*, 2007) when maturation of GABAergic systems leads to increased intracortical inhibition (Mall *et al.*, 2004). Computational models suggest that inhibitory mechanisms are critical to oscillatory activity (Pauluis *et al.*, 1999) and thus to the emergence of coherence.

The extent and nature of senescent changes in coherence are controversial. One study reported that beta-band CMC shows a single peak at 23Hz in young adults which is replaced by multiple peaks at lower or higher frequencies in the elderly (Graziadio *et al.*, 2010). Other reports described age-related decreases but not increases in the peak frequency of CMC (Kamp *et al.*, 2013) or IntraMC (Semmler *et al.*, 2003). A similar lack of agreement applies to peak coherence amplitude, which was reported either to remain unchanged (Graziadio *et al.*, 2010; Semmler *et al.*, 2003) or to increase with age (Kamp *et al.*, 2013). These divergent results are not easily reconciled. Motor function is known to deteriorate in old age (Incel *et al.*, 2009; Krampe, 2002; Seidler *et al.*, 2010). Several potential substrates have been proposed, including decreases in neuronal size (Haug & Eggers, 1991), dendritic arborisation (Anderson & Rutledge, 1996) and synaptic density (Huttenlocher, 1979) in the cortical grey matter, reduced intracortical inhibition (Peinemann *et al.*, 2001), diminished white matter volume (Raz & Rodrigue, 2006) with accumulation of leukoaraiosis on MRI (Moscufo *et al.*, 2011), a decline in peripheral motor and sensory conduction velocities (Kong *et al.*, 2010; Rivner *et al.*, 2001) and remodelling of motor units (Rods *et al.*, 1997). It is unclear whether coherence is sensitive to these morphological and functional changes; indeed, CMCT proved surprisingly robust to them (Chapter 2). However, two factors which might plausibly affect coherence in old age are decreased intracortical inhibition and prolonged conduction delays in the efferent-afferent loop.

We are aware of only two studies which have investigated the variability of coherence within subjects. One study compared pairs of CMC measurements from either the same session ('intrasession') or two sessions separated by one year ('intersession') in ten subjects (Pohja *et al.*, 2005). In the intrasession comparison, frequency and amplitude of the 15-30Hz CMC peak were each strongly correlated between both measurements. Equivalent correlations were weaker for the intersession condition, with the amplitude of coherence varying by 17-220% in individual subjects. In one subject, CMC was estimated eight times over a 20 month interval, demonstrating relative constancy of the frequency of the CMC peak but marked variation in its amplitude. Unfortunately, correlation analysis constitutes a suboptimal approach as it fails to exploit known distributional properties of intraindividual differences in coherence. The second study assessed CMC three times in a single subject over the

course of two years (Witham *et al.*, 2011). Peak amplitude of CMC showed substantial variability, accompanied by changes in the directionality of CMC within the efferent-afferent loop.

Here, we aimed to define age-related changes in beta-band IMC in a large, age-stratified sample of adults. In a subset, we analysed the variability of IMC within and between sessions using dedicated statistical methods. IMC requires only a single recording modality and is present more consistently than CMC in healthy subjects (Ushiyama *et al.*, 2011b). Our task involved minimal instrumentation and weak, phasic contractions, optimising applicability of IMC as a biomarker of CST function in patients with neurological deficits (Fisher *et al.*, 2012). We found that IMC did not change significantly over almost six decades of adulthood. There was considerable between-subject variability; within a given subject and session, variability was larger than statistically expected, and between sessions variability was even greater. We propose experimental approaches for dissecting the causes of variability.

3.3 Methods

3.3.1 Subjects

At least 15 volunteers were recruited for each decade of age between 20 and 80 (51 men and 41 women); age averaged 48.6±17.2 years (SD; range 22-77). Eighty-three subjects were right-handed and nine left-handed as assessed by self-reporting. None had any history of neurological disorders or diabetes mellitus, and none took any neurotropic medication. All subjects provided written informed consent. The study was approved by the research ethics committee of Newcastle University's Medical Faculty, and conformed to the Declaration of Helsinki.

3.3.2 Recording

Every effort was made to maintain subjects at a constant level of alertness, and all assessments were carried out on the dominant side. Subjects were seated in a comfortable chair with their arm resting semi-pronated on a cushion. Surface EMG was recorded from first dorsal interosseous (FDI), flexor digitorum superficialis (FDS) and

extensor digitorum communis (EDC) in the upper limb, and extensor digitorum brevis (EDB), tibialis anterior (TA) and medial gastrocnemius (MG) in the lower limb. Adhesive electrodes (Bio-Logic M0476; Natus Medical, Mundelein, IL) were placed in a belly-tendon montage over the intrinsic muscles of the hand or foot; for the long muscles of the forearm or calf, the electrodes were placed 4cm apart, one third along the muscle from its proximal origin. Signals were amplified, band-pass filtered (30Hz-2kHz; Digitimer D360, Digitimer, Welwyn Garden City, UK) and digitised at 5kHz (Micro1401, Cambridge Electronic Devices, Cambridge, UK).

3.3.3 Experiment 1: IMC

In the upper limb, subjects were asked to perform a repetitive precision grip task. A length of compliant plastic tubing (length 19cm, Portex translucent PVC tubing 800/010/455/800; Smith Medical, Ashford, UK) was attached to the index finger and thumb with Micropore tape (3M Health Care, Neuss, Germany), and subjects were asked to oppose both ends of the tubing when prompted by visual and auditory cues. This auxotonic task – so-called because force increases with displacement in a spring-like fashion – required a minimum force of 1N (Fisher *et al.*, 2012) and was similar to a precision grip task used in our previous studies, albeit without measuring digit displacement (Kilner *et al.*, 2000; Riddle & Baker, 2006). In the lower limb, subjects were asked to dorsiflex ankle and toes in the air while resting the heel on the ground. Subjects produced 4s of contraction alternating with 2s of relaxation, and at least 100 repetitions. Visual feedback of raw EMG traces was provided to facilitate consistent task performance.

3.3.4 Experiment 2: IMC repeated after one year

After a period of at least one year, eight subjects were asked to repeat the above experiment (six men and two women). The average age was 33.5±8.9 years (range 24-52). All subjects were right-handed.

3.3.5 Data analysis

Analysis was performed in Matlab (Mathworks, Natick, MA) using custom scripts.

Raw data were visually inspected and the first 100 adequately performed trials examined further. Analysis focussed on the early hold phase of the contraction where beta-band oscillations are known to be maximal (Baker *et al.*, 1997; Sanes & Donoghue, 1993). EMG signals were full-wave rectified. Starting 0.8s after the cue prompting contraction, two contiguous 0.82s-long sections of data from each trial were subjected to a 4096-point fast Fourier transform (FFT), giving a frequency resolution of 1.22Hz. Many subjects showed a drop-off in EMG activity so the last 1.56s of the 4s active phase did not enter the analysis. Denoting the Fourier transform of the lth section of the first EMG signal as $F_{1,l}(\lambda)$, the auto-spectrum is given by

$$f_{11}(\lambda) = \frac{1}{L}\sum_{l=1}^{L} F_{1,l}(\lambda)\,\overline{F_{1,l}(\lambda)} \tag{3.1}$$

where λ is the frequency (Hz), L is the total number of sections and where the overbar denotes the complex conjugate. The cross-spectrum for two EMG signals with Fourier transforms $F_{1,l}(\lambda)$ and $F_{2,l}(\lambda)$ was calculated as

$$f_{12}(\lambda) = \frac{1}{L}\sum_{l=1}^{L} F_{1,l}(\lambda)\,\overline{F_{2,l}(\lambda)} \tag{3.2}$$

Coherence was computed as the cross-spectrum normalised by the auto-spectra

$$C(\lambda) = \frac{|f_{12}(\lambda)|^2}{f_{11}(\lambda)f_{22}(\lambda)} \tag{3.3}$$

Coherence was calculated for the muscle pairs EDC-FDI, FDS-FDI, MG-EDB and TA-EDB. The wide anatomical spacing between the paired muscles minimised the risk of volume conduction causing inflated coherence values (Grosse *et al.*, 2002).

Under the null hypothesis of linear independence between the signals, a level of significant coherence was determined as (Rosenberg *et al.*, 1989)

$$Z = 1 - \alpha^{1/(L-1)} \tag{3.4}$$

where the significance level α was set at 0.05.

Analyses of coherence described below were conducted separately for each muscle pair.

To provide a group summary, coherence spectra were averaged across all subjects. The significance level for averaged coherence was determined using the method described by Evans and Baker (2003).

In each subject, coherence was averaged across the 15-30Hz window. Log-transformed 15-30Hz coherence was plausibly normally distributed within each decade of age (Shapiro-Wilk test, p≥0.013 for all groups, Bonferroni-corrected significance level α/n=0.05/(4*6)=0.002). However, for the lower limb there was an indication that a normal distribution was not an ideal fit since 8 out of 12 groups had an uncorrected significance level of <0.1, a result which itself has a probability of <0.001 as calculated using the binomial distribution (p=1-F(7), where F is the cumulative distribution function of B(12,0.1)). In addition, larger samples derived by pooling coherence across all ages (see below) or obtained from cohorts with neurological conditions (Chapters 5 and 6) could not be modelled adequately with a normal distribution (Shapiro-Wilk test, p<0.001 in at least one muscle pair for pooled normal data, Bonferroni-corrected significance level α/n=0.05/4=0.0125). Therefore, we chose to model coherence distributions non-parametrically. The variable kernel method adapts the amount of smoothing to the local density of the data (Silverman, 1986) and estimates the probability density function (PDF) as

$$\hat{f}(x) = \frac{1}{N}\sum_{n=1}^{N}\left[\frac{1}{hd_{n,k}} \cdot \phi\left(\frac{x - X_n}{hd_{n,k}}\right)\right] \tag{3.5}$$

where x denotes the log-transformed independent variable, X_n the n^{th} log-transformed observation out of a total N observations, $d_{n,k}$ the distance from X_n to its

k^{th} nearest neighbour, h the global smoothing parameter and ϕ the standard normal PDF. To understand this intuitively: each observation X_n was convolved with a Gaussian kernel with unit AUC as specified inside the square brackets, and the sum of these kernels was normalised by N to yield $\hat{f}(x)$. The window width of the kernel centred on a given observation X_n was proportional to $d_{n,k}$ so that broader kernels were associated with observations in regions with sparse data; for any fixed k, the amount of smoothing depended on the global smoothing parameter h. k was set as $\sqrt{n}$ rounded to the nearest integer as suggested by Silverman (1986). Theoretically optimal methods for calculating h have been described but, for our data, resulted in overfitting. Therefore, h was optimised by eye for several datasets; the resulting values of h were empirically fitted with simple algebraic expressions and the approximation $\sqrt[12]{n-5}$ was chosen to determine h subsequently. It should be emphasised that this expression has no theoretical value, but merely provided a convenient shorthand way of determining h objectively for each dataset.

Log-transformed coherence has a bounded domain of $(-\infty,0]$. To ensure that the PDF was zero for $x>0$, $\hat{f}(x)$ was modified by reflection in the boundary (Silverman, 1986):

$$\hat{g}(x) = \begin{cases} \hat{f}(x) + \hat{f}(-x), & x \leq 0 \\ 0, & x > 0 \end{cases} \tag{3.6}$$

The resulting PDF still integrated to unity and observations near the boundary retained the same magnitude of contribution to the PDF. The estimated cumulative distribution function (CDF) was calculated as

$$\hat{G}(y) = \int_{-\infty}^{y} \hat{g}(x)dx \tag{3.7}$$

where y is the log-transformed independent variable.

Log-transformed coherence was compared between all decades of age using a Kruskal-Wallis test, and between individual muscle pairs or limbs using a paired t-test.

To measure changes in coherence occurring during experiment 1 ('intrasession'), the recording session from each subject was split into two epochs of 50 trials. Coherence spectra were estimated separately for each epoch, and the significance of changes between both epochs was determined by calculating single-subject Z-scores as

$$Z_{n_s} = \sqrt{\frac{L}{N_\lambda}} \sum_{\lambda=\lambda_1}^{\lambda_2} \left(\operatorname{atanh}\left(\sqrt{C_{n_s}^{second}(\lambda)} \right) - \operatorname{atanh}\left(\sqrt{C_{n_s}^{first}(\lambda)} \right) \right) \tag{3.8}$$

where $C_{n_s}^{first}(\lambda)$ and $C_{n_s}^{second}(\lambda)$ denote the coherence at frequency λ for subject n_s during the first and second epoch. Z_{n_s} was summed over all N_λ frequency bins in the 15-30Hz window (N_λ=bin number(λ_2)-bin number(λ_1)+1=12), and normalised so that it should be normally distributed with zero mean and unit variance under the null hypothesis of no change in coherence between epochs (Baker & Baker, 2003; Rosenberg *et al.*, 1989).

The mean compound Z-score across all N_S subjects was calculated as

$$\bar{Z} = \sqrt{\frac{1}{N_S}} \sum_{n_S=1}^{N_S} Z_{n_s} \tag{3.9}$$

The associated two-tailed probability (p_Z) was computed with reference to the standard normal distribution.

The significance of the variance of single-subject Z-scores was estimated using Monte-Carlo simulations. Each simulation involved drawing N_S random samples from a standard normal distribution and calculating their variance. This procedure was repeated 10^6 times, allowing the distribution of the variance to be estimated under the null hypothesis that coherence did not change between epochs. The two-tailed probability for the observed variance (p_{MC}) was calculated from this estimated null distribution.

For experiment 2, we calculated both intersession and intrasession variances. Coherence spectra were estimated separately for two epochs per session as described above. Intrasession changes were quantified in each subject by calculating one Z-score, comparing both epochs of session 1, and a second Z-score, comparing both epochs of session 2. The intrasession variance was computed as the variance of all resulting Z-scores, i.e. two Z-scores from each subject. Similarly, intersession changes were measured in each subject by calculating one Z-score, comparing the first epochs of both sessions, and a second Z-score, comparing the second epochs; intersession variance was calculated from all resultant Z-scores.

The significance of the difference between intersession and intrasession variance was estimated by means of Monte-Carlo simulations. For each subject, coherence spectra were shuffled across epochs and sessions, and the difference between intersession and intrasession variance was recalculated. This process was repeated 10^6 times, allowing the null distribution of the difference in variances to be estimated. The two-tailed probability for the observed difference was computed with reference to the estimated null distribution.

3.4 Results

Single-subject data are shown in Figure 3.1 for the lower limb and in Figure 4.2 for the upper limb. In most subjects, power and coherence peaked in the 15-30Hz band. On group averages, coherence in all muscle pairs was significant across the 15-30Hz window and showed either a peak or an inflexion inside this frequency band (Figure 3.2).

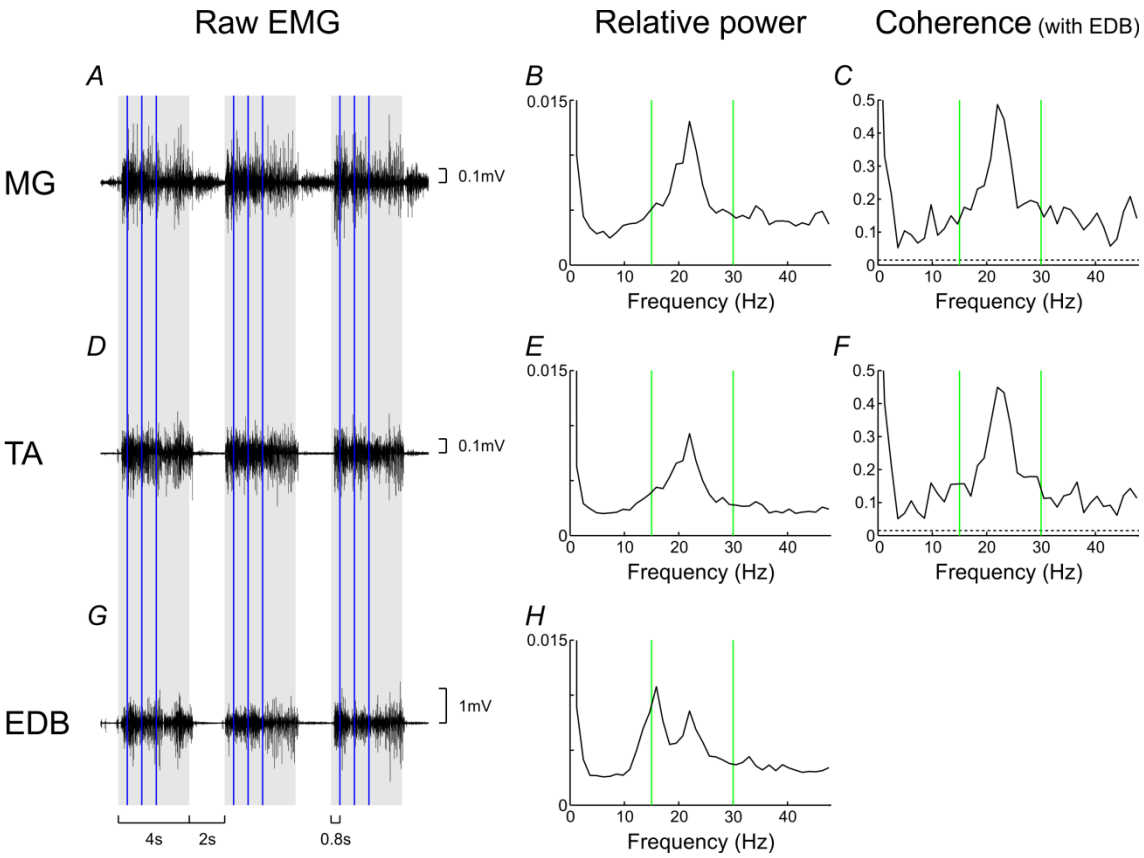

Figure 3.1: Single-subject power and coherence in the lower limb. Raw EMG is shown for three sample trials (A, D, G). The grey boxes indicate the cued contraction phase of the task, and the vertical blue lines represent the two FFT windows during the hold phase. The spectral plots show relative power (B, E, H) and coherence with EDB (C, F). The 15-30Hz beta-band is designated by the vertical green lines, and the dotted horizontal lines indicate the significance level for coherence. In most subjects, power and coherence spectra peaked in the 15-30Hz band.

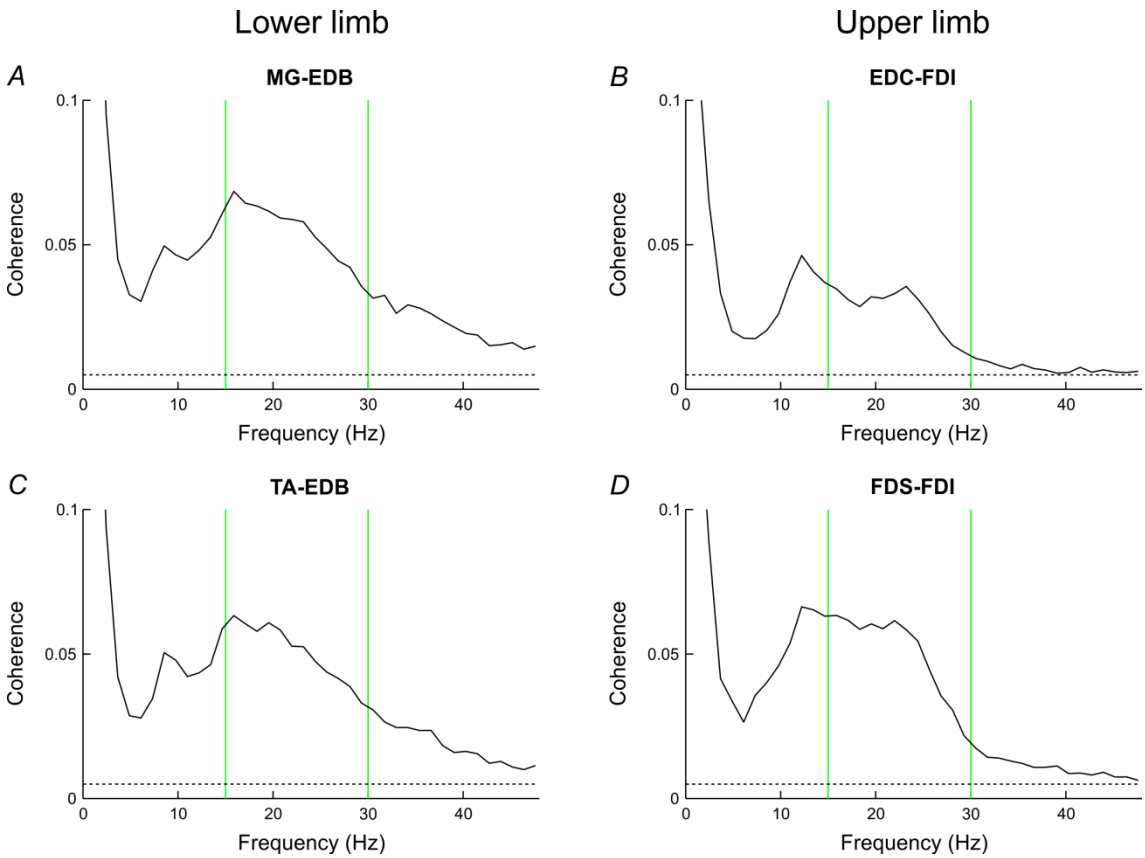

Figure 3.2: Group data for coherence. Average coherence spectra are shown for MG-EDB and TA-EDB in the lower limb (A, C) and for EDC-FDI and FDS-FDI in the upper limb (B, D). The dotted horizontal lines represent the significance level for average coherence, and the vertical green lines indicate the 15-30Hz beta-band. Significant average coherence was present in the 15-30Hz band for each muscle pair. Typically, coherence demonstrated a peak or an inflexion within this window and a further one around 9-12Hz whilst dropping off at higher frequencies.

Coherence was averaged across the 15-30Hz window in each subject; individual averages are listed in Appendix A. There was no significant correlation between coherence and age in any muscle pair (Spearman's $\varrho \leq 0.104$, $p \geq 0.325$; Figure 3.3), with interindividual variability spanning up to two orders of magnitude. The distribution of coherence was similar for all decades of age as illustrated by the stairstep curves in Figure 3.4 A, B, E, F. The smooth curves show the corresponding variable kernel density models. Summary statistics derived from these models are illustrated by the boxplots in Figure 3.4 C, D, G, H, superimposed on dot plots of individual coherence values. Coherence did not vary significantly between decades (Kruskal-Wallis $p \geq 0.531$).

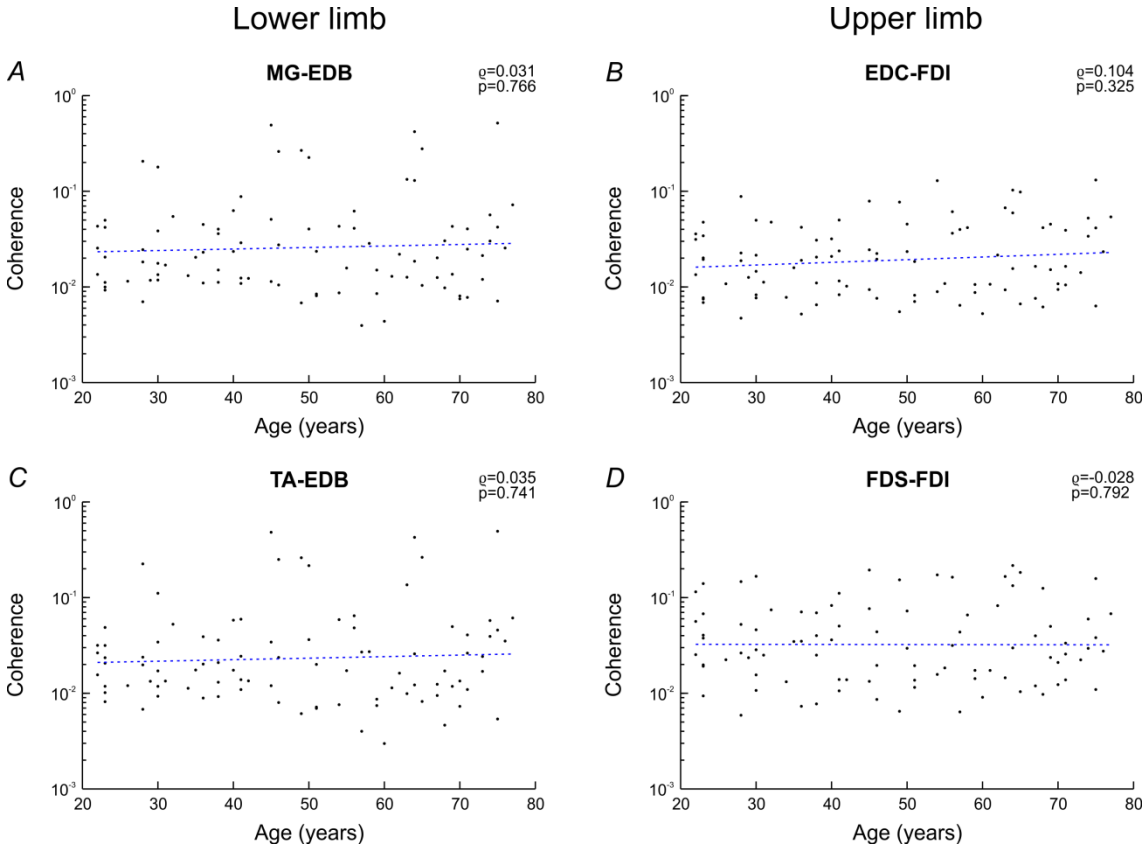

Figure 3.3: Correlation between coherence and age. For each muscle pair, average 15-30Hz coherence is plotted against age. There was no significant correlation between coherence and age in any muscle pair (Spearman's ϱ).

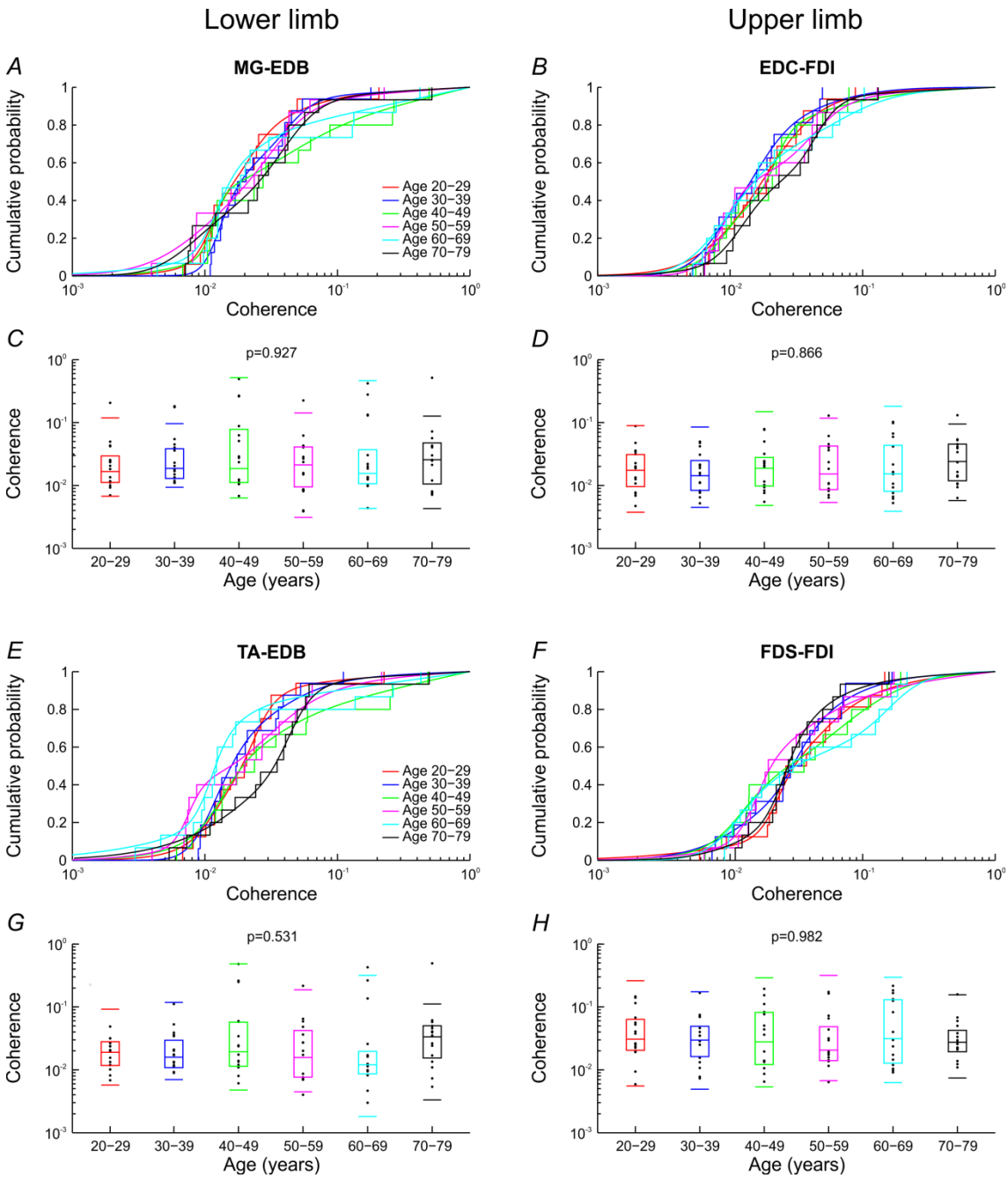

Figure 3.4: Coherence by decade of age with corresponding variable kernel density estimates and summary statistics. Each decade is illustrated in a different colour. The stairstep curves show the distribution of average 15-30Hz coherence for subjects within a given decade, with the smooth curves showing corresponding density estimates (A, B, E, F). Quartiles derived from density estimates are shown by the box plots with additional horizontal lines indicating 5th and 95th centiles, overlain on a dot plot of individual coherence values (C, D, G, H). Coherence did not vary significantly with age (Kruskal-Wallis test).

Because there was no dependence on age, we pooled coherence values across all ages into a single dataset (Figure 3.5). The combined dataset was modelled empirically with a normal distribution (blue) and a variable kernel density estimate (red). The latter

achieved a closer fit throughout whilst still smoothing out much of the small-scale variability of the data. We propose this cumulative distribution as a normative dataset for healthy subjects, against which future experimental findings can be compared.

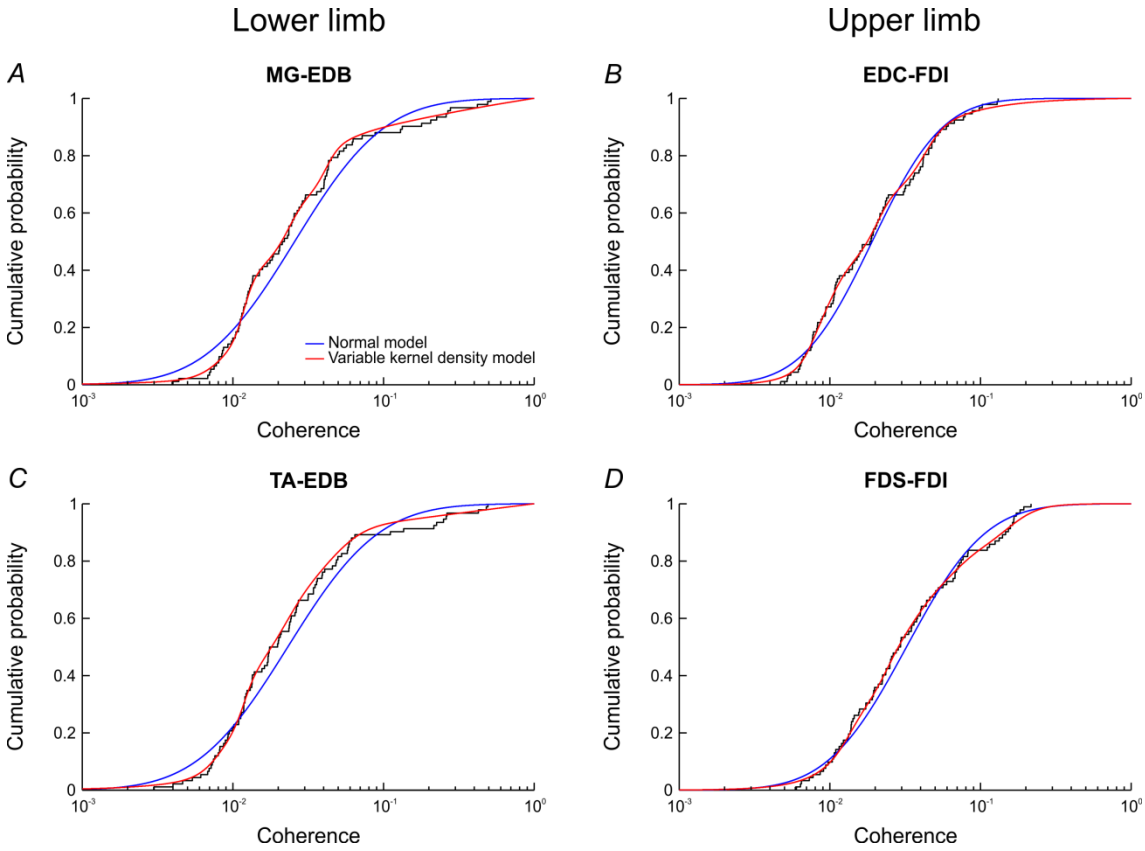

Figure 3.5: Coherence across all ages with normal and variable kernel density models. Since coherence did not vary with age, we pooled coherence readings across all ages into a single dataset. The stairstep curves illustrate the distribution of average 15-30Hz coherence for subjects of all ages. The data were modelled with a normal distribution (blue) and variable kernel density estimation (red). The density estimation model achieved a closer fit throughout, whilst still smoothing out some of the variability of the data.

Log-transformed coherence was significantly greater in FDS-FDI than in EDC-FDI (paired t-test, $p<0.001$) and in MG-EDB than in TA-EDB ($p<0.001$). By contrast, there was no significant difference in log-transformed coherence between upper and lower limbs ($p=0.596$).

In order to assess the stability of coherence within a recording session ('intrasession'), we determined single-subject Z-scores for differences in coherence between two halves of the same session (Figure 3.6). For all muscle pairs, the mean compound

Z-scores were not significantly different from zero ($p_Z \geq 0.274$) but the variances of single-subject Z-scores were significantly greater than unity ($p_{MC} < 0.001$). Thus, coherence showed greater variability within a recording session than would be statistically expected.

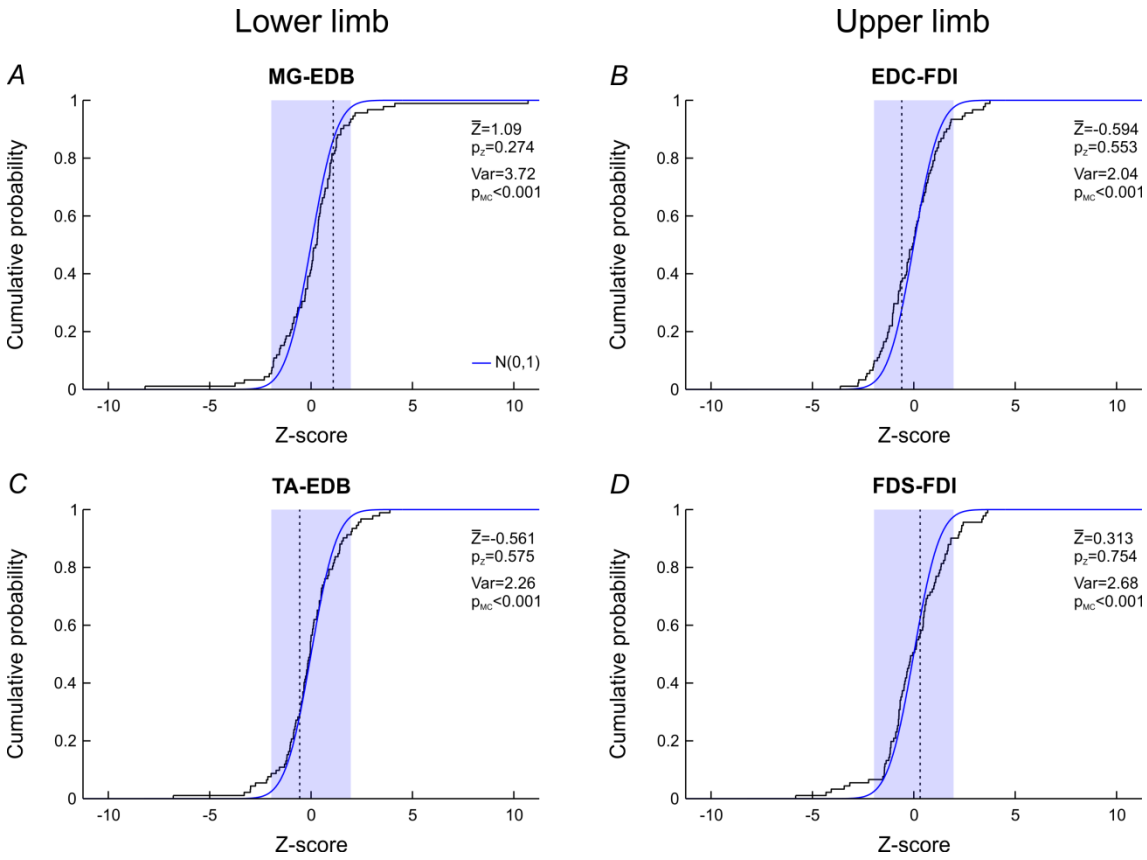

Figure 3.6: Z-scores for intrasession differences in coherence. In each subject, the recording session was divided into two epochs for which separate 15-30Hz coherence values were calculated. Single-subject Z-scores quantify the difference between both coherence values in each individual and their distribution is shown by the stairstep curves; under the null hypothesis, they should follow a standard normal distribution (blue curve). The mean compound Z-score for all subjects ($\bar{Z}$; vertical dotted lines) was not significant in any muscle pair (p_Z; blue box showing range of ±1.96). However, in all muscle pairs the variance of individual Z-scores (Var) was significantly greater than unity as estimated by Monte-Carlo simulations (p_{MC}).

A subset of the cohort returned after one year for a second recording session, allowing us to investigate whether coherence exhibited greater variability between than within sessions. We calculated single-subject Z-scores for differences in coherence between both halves of the same session ('intrasession') and for differences in coherence between corresponding halves of both sessions ('intersession'). In all muscle pairs, the

intersession variance of single-subject Z-scores was greater than the intrasession variance (Figure 3.7), with the differences reaching significance in TA-EDB (p_{MC}=0.009) and EDC-FDI (p_{MC}=0.029).

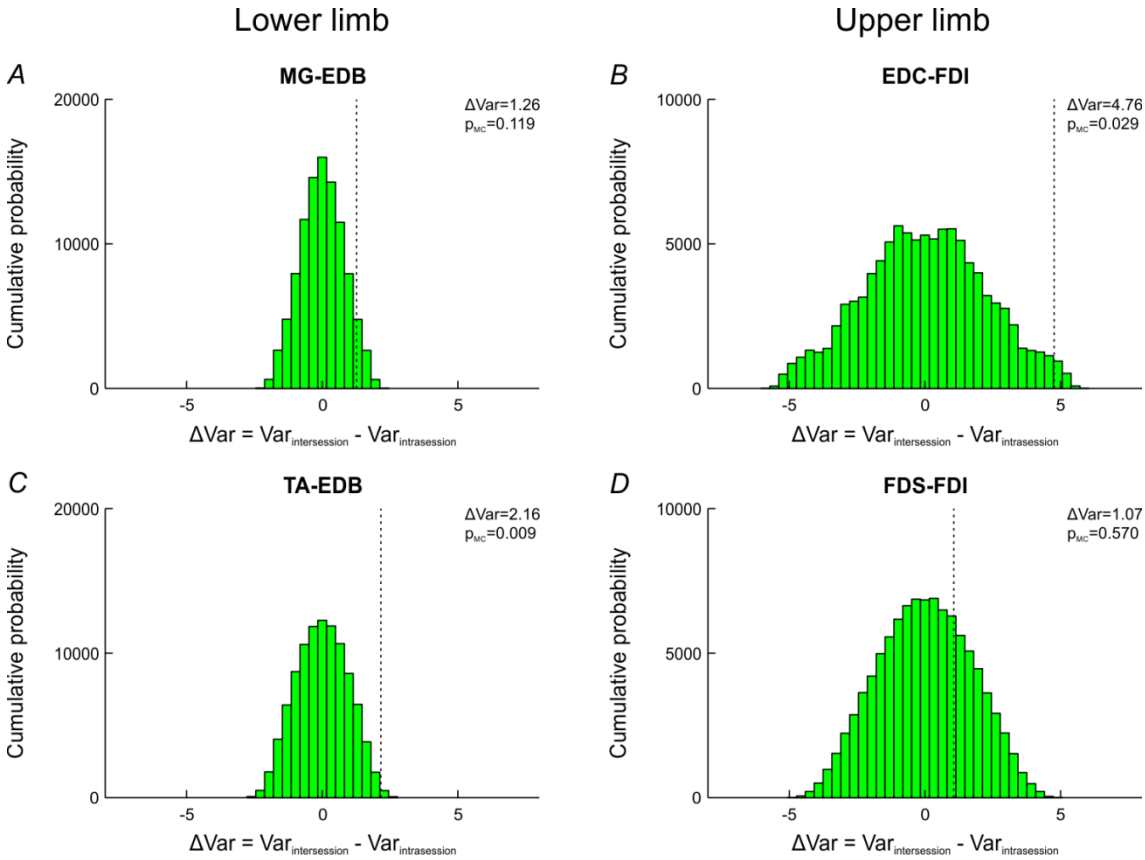

Figure 3.7: Difference between variances of intersession and intrasession Z-scores. Each recording session from experiment 2 was split into two epochs for which separate 15-30Hz coherence values were computed. Single-subject Z-scores were calculated for differences in coherence between both halves of the same session ('intrasession') and for differences in coherence between corresponding halves of both sessions ('intersession'). The difference of the variances of intersession and intrasession Z-scores was then computed (ΔVar; vertical dotted lines). For each muscle pair, the null distribution was estimated using Monte-Carlo simulations (green histograms). The probability of the observed value occurring under the null hypothesis was calculated with reference to the estimated null distribution (p_{MC}). Intersession variance exceeded intrasession variance in all muscle pairs, with the differences reaching significance in TA-EDB and EDC-FDI.

3.5 Discussion

3.5.1 IMC in adulthood

We found no significant age-related changes in beta-band IMC amplitude across almost six decades of adulthood. This agrees with two previous studies describing no significant differences in CMC (Graziadio *et al.*, 2010) or IntraMC amplitude (Semmler *et al.*, 2003) between young and old adults. Whilst another study reported an increase in CMC with age, significance levels were borderline (p=0.04; Kamp *et al.*, 2013). The weight of the evidence therefore suggests that coherence amplitude remains unchanged throughout adult age.

Senescent alterations in the efferent-afferent feedback loop might be expected to disrupt beta-band coherence. There is strong evidence that peripheral nerve conduction velocities decline with age (Kong *et al.*, 2010; Rivner *et al.*, 2001). Whilst central conduction velocities appear to remain constant (Chapter 2), ageing is associated with morphological changes in the central sensorimotor pathways (Moscufo *et al.*, 2011; Raz & Rodrigue, 2006) and may alter transmission in a manner which is not detectable on motor or sensory evoked potentials. Beta-band coherence is thus surprisingly robust to alterations in conduction pathways, and this is supported by two observations unrelated to old age: IMC reaches adult values in early teenage although peripheral conduction times continue to increase with limb length for several years (Farmer *et al.*, 2007); and beta-band coherence is present in primates of different sizes despite marked size-related differences in conduction delays (Baker *et al.*, 1997).

Reduced intracortical inhibition in old age (Peinemann *et al.*, 2001) might be expected to lead to diminished coherence, but no such change was observed. It is possible that intracortical inhibition is critical to the initial patterning of the corticospinal drive but has a less prominent role in maintaining oscillatory activity in the efferent-afferent feedback loop. One study boosted intracortical inhibition in adults using diazepam, a GABAergic agent. The power of 15-30Hz oscillations on EEG increased yet CMC amplitude decreased (Baker & Baker, 2003). These results highlight that coherence can be dissociated from alterations in cortical oscillatory activity, suggesting that that the

relationship between intracortical inhibition and coherence might not be straightforward.

One aim of this study was to gather a normative dataset for use of IMC as a biomarker of CST function. Since IMC across the 15-30Hz band appears to be related to the integrity of the CST, we focussed on average 15-30Hz IMC as our summary measure, thus also ensuring comparability with our previous study (Fisher *et al.*, 2012). By contrast, most past reports analysed the amplitude and frequency of peak coherence in the 15-30Hz window (Graziadio *et al.*, 2010; James *et al.*, 2008; Kamp *et al.*, 2013; Pohja *et al.*, 2005). Coherence estimates include a noise component and do not always show a clear single peak. Our approach of averaging across N_λ=12 frequency bins sidestepped any difficulties in quantifying single or multiple peaks and boosted signal-to-noise ratio by $\sqrt{12}$≈3.5. We did not analyse coherence outside the 15-30Hz window as it is less clearly associated with the CST. At lower frequencies, potential generators of coherence include the reticular formation, cerebellum and local spinal circuits (Williams *et al.*, 2010). At higher frequencies, coherence may involve neural substrates other than the CST and only becomes prominent during tasks involving strong (Mima *et al.*, 1999) or dynamically modulated contractions (Omlor *et al.*, 2007).

The lack of age-related changes allowed us to pool results, thus maximising the effective size of the control group for studies of IMC in neurological conditions (Chapters 5 and 6). The aggregate dataset could not be fitted adequately by a normal distribution or simple empirical formulae. Whilst variable kernel density estimation provided a good fit, it did not allow the data to be summarised using a small number of numerical parameters.

3.5.2 Variability of IMC

Interindividual variability of IMC ranged over two orders of magnitude. The degree of variability did not appear to change with age, militating against the possibility that undiagnosed neurological issues in older subjects could have caused a greater spread of coherence readings. Other than genuine differences between subjects, sources of variability within individuals may also have played a role.

Intrasession variance of IMC was significantly greater than predicted by statistical variation alone. Two potential causes are fluctuations in task performance and random moment-to-moment variation of coherence. Previous studies employed tasks which can be readily standardised but require prolonged activity or a high level of dexterity and thus are not suitable for use in patients with neurological deficits (Chapters 5 and 6). Our task involved weak, phasic contractions and a minimum of instrumentation. Inherent disadvantages were a greater freedom of movement and less precisely defined targets, making it more difficult to ensure consistent performance. It would be helpful to carry out an experiment where normal subjects perform different tasks in the same session so that resulting coherence estimates can be compared. Random moment-to-moment variation of coherence is seen during sustained contractions in normal subjects. Periods of increased coherence are thought to promote sensorimotor recalibration at the expense of increased 15-30Hz tremor and delayed reaction times (Gilbertson *et al.*, 2005; Matsuya *et al.*, 2013). Such variation contributes to the overall variability of coherence and appears to be neither consciously controlled nor related to specific features of the task.

Intersession variance was greater than intrasession variance, reaching significance in two muscle pairs. Two aspects may have contributed in addition to the above factors. Firstly, it is not possible to achieve an identical electrode montage after one year. In a previous study, electrode position significantly influenced coherence between two intrinsic hand muscles (Keenan *et al.*, 2011), but the proximity of the two muscles means that electrical cross-talk may have confounded the results. It would be useful to study this issue in a more widely spaced muscle pair. Secondly, coherence amplitude and directionality can change substantially within an individual over a timeframe of one or two years, even with a highly instrumented task (Witham *et al.*, 2011). The timeframe of these changes should be clarified by obtaining multiple coherence estimates at shorter intervals.

3.6 Conclusion

This is one of the largest studies of beta-band coherence in healthy adults to date. IMC showed no significant age-related changes across almost six decades of age; therefore results were pooled across all ages into a combined normative dataset.

Interindividual variability of IMC spanned two orders of magnitude. Intrasession variance was significantly greater than statistically expected; potential reasons include moment-to-moment variability of coherence and changes in task performance. In a smaller cohort, we examined intersession variance for two sessions separated by one year and found even greater variability. Additional causes include longer-term changes in coherence within individuals and differences in electrode montage. Variability of IMC in normal subjects is critical to future applications as a biomarker, and we proposed a number of control experiments to delineate the origins of variability so that it potentially can be minimised.

4 Effect of transcranial direct current stimulation on intermuscular coherence

A small study reported that transcranial direct current stimulation (tDCS) modulates coherence in healthy subjects. Here, I re-examine this effect in a larger cohort.

4.1 Abstract

Objective: To measure the effect of anodal transcranial direct current stimulation (tDCS) on beta-band intermuscular coherence (IMC).

Methods: 91 healthy volunteers were recruited. IMC was estimated between extensor digitorum communis (EDC) and first dorsal interosseous (FDI) as well as between flexor digitorum superficialis (FDS) and FDI in the dominant upper limb, both before and after 10min of 1mA anodal tDCS to the contralateral M1. tDCS electrode positions were determined by surface measurements relative to bony landmarks. Six volunteers also participated in a second experiment where we sought to reproduce the classical effects of anodal tDCS on motor evoked potentials (MEPs). Here, we determined tDCS electrode positions using TMS hotspot mapping, and compared them to those resulting from surface measurements.

Results: IMC increased very significantly in both muscle pairs (EDC-FDI: 12.9±12.1% (change in geometric mean of post/pre-tDCS ratios±1.96*SE), $p<0.001$; FDS-FDI: 11.3±11.5%, $p<0.001$). In the second experiment, only one subject showed the classical rise of MEP amplitude, and group effects were not significant. The discrepancy in electrode position resulting from the two positioning methods was small and probably insignificant.

Conclusion: The magnitude of the observed effects on beta-band IMC was similar to previously reported results. The duration of the effects was in keeping with classical MEP results but exceeded that previously reported for IMC. Notably, we did not observe the classical effects on MEPs in most subjects. Our study highlights that tDCS-

associated effects are subject to a substantial degree of interindividual variability. Future work should assess IMC at multiple time points after tDCS until all results have returned to baseline, and include a control condition with sham tDCS.

4.2 Introduction

Transcranial direct current stimulation (tDCS) is a subthreshold neuromodulatory technique which alters cortical excitability in a non-invasive, focal and reversible manner. A weak direct current (0.5-2mA) is applied to the scalp through two plate electrodes (3.5-35cm^2), both of which are usually placed on the head (bicephalic montage). Excitability is typically enhanced under the anode and diminished under the cathode (Figure 4.1 A; Nitsche & Paulus, 2000). Such excitability changes occur during ongoing stimulation ('acute effects') and, if stimulation is applied for a sufficiently long period and with a sufficiently strong current, they can outlast the period of stimulation by one hour or more ('after-effects', Figure 4.1 B; Nitsche & Paulus, 2001). Acute effects are thought to arise through subthreshold, tonic membrane polarisation of cortical neurons. Blockade of voltage-gated sodium or calcium channels abolishes anodal but not cathodal acute effects (Liebetanz *et al.*, 2002; Nitsche *et al.*, 2003), suggesting that anodal acute effects are mediated by inward sodium and calcium currents, whilst cathodal ones might be attributable to outward flow of potassium. After-effects of both polarities are contingent on preceding acute effects and are abolished by NMDA receptor antagonists (Liebetanz *et al.*, 2002; Nitsche *et al.*, 2003), indicating mechanisms akin to long-term potentiation and depression.

The excitability of the primary motor cortex is usually probed through TMS-evoked motor responses (Figure 4.1 A, B). However, tDCS affects not only evoked activity but also spontaneous oscillations of cortical neurons, as shown by extracellular recordings and EEG in animals (Creutzfeldt *et al.*, 1962) as well as EEG in humans (Ardolino *et al.*, 2005). Beta-band (15-30Hz) oscillations propagate from the motor cortex through the corticospinal tract (CST) to the muscles (Baker *et al.*, 1997; Baker *et al.*, 2003; Fisher *et al.*, 2012). Synchronisation of beta-band oscillations between muscles in the same limb is demonstrable as intermuscular coherence (IMC) and indicates a shared cortical drive.

A small previous study showed that anodal or cathodal tDCS to M1 respectively increases or decreases beta-band IMC in the contralateral upper limb with a time course paralleling the changes in motor evoked potential (MEP) amplitude (Figure 4.1 D, E; Power *et al.*, 2006). This finding is of potential relevance to the use of beta-band IMC as a biomarker of CST dysfunction. In some subjects with known CST damage from motor neuron disease (MND), beta-band IMC remains significant at baseline but fails to increase after anodal tDCS (J. A. Norton, personal communication, 16 November 2010). Similarly, TMS-evoked motor responses fail to be modulated by tDCS in patients with MND (Munneke *et al.*, 2011; Quartarone *et al.*, 2007). The sensitivity of beta-band IMC to detect subclinical CST dysfunction might therefore be boosted by measuring IMC before and after adjunctive anodal tDCS, and analysing both the baseline value and any change after tDCS. In a broader context, this might help to extend the remit of tDCS from basic neuroscience and exploratory therapeutic studies (Nitsche *et al.*, 2008; Nitsche & Paulus, 2011) into novel diagnostic approaches.

The previous study of tDCS and IMC was based on ten subjects (Power *et al.*, 2006). We set out to corroborate the reported effect of anodal tDCS on beta-band IMC in a larger cohort, allowing more precise quantification. A limiting factor of the present study was that most subjects were only able to attend once. In order to maximise the amount of data gathered for anodal tDCS, we performed a study without a control (sham stimulus) group. The position of the electrode over the motor cortex was determined by surface measurements relative to bony landmarks (Ardolino *et al.*, 2005) rather than TMS hotspot mapping (Nitsche & Paulus, 2000; Power *et al.*, 2006) to ensure applicability in the absence of TMS facilities. Beta-band IMC increased very significantly after tDCS; the changes were similar in amplitude but longer in duration compared to those reported by Power *et al.* (2006). To exclude the possibility that this discrepancy was due to differences in electrode positioning, we carried out a second, smaller study comparing both positioning methods and aiming to reproduce the classical effect of anodal tDCS on MEP amplitude.

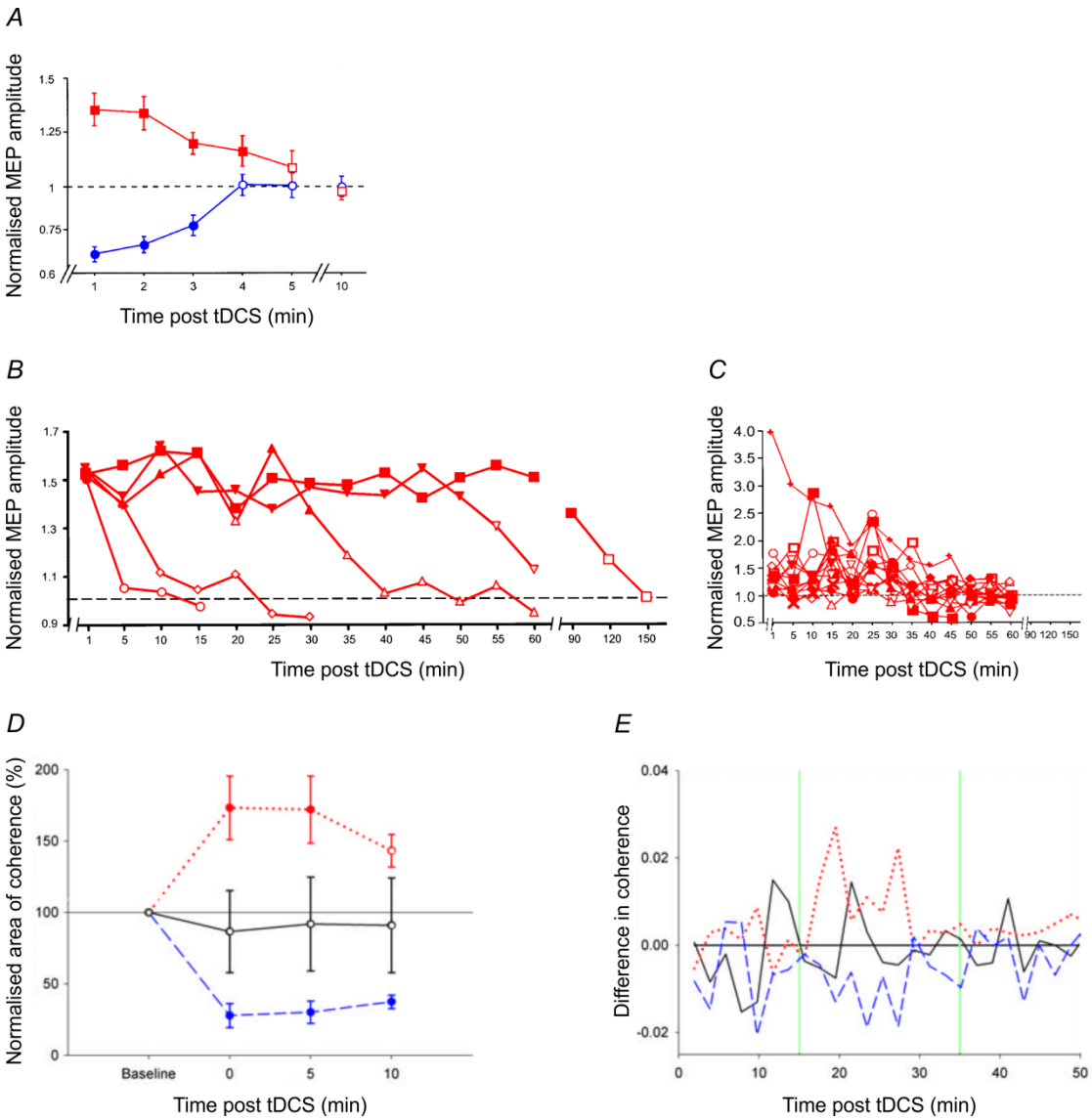

Figure 4.1: Previously reported after-effects of 1mA tDCS to M1. 5min of anodal or cathodal stimulation cause MEP amplitude to increase (red) or decrease (blue), respectively, for several minutes after the end of stimulation before returning to baseline (A; n=19; adapted from Nitsche & Paulus, 2000). Filled symbols indicate a statistically significant difference from baseline ($p<0.05$, paired t-test). If the duration of anodal stimulation is increased, MEP amplitudes remain raised for longer intervals (B; circles=5min, diamonds=7min, upward-pointing triangles=9min, downward-pointing triangles=11min, squares=13min; n=12; adapted from Nitsche & Paulus, 2001). Filled symbols designate a statistically significant difference from baseline ($p<0.05$, Fisher's protected least significant difference *post hoc* test). Single-subject data show considerable inter- and intra-subject variability (C; 9min); each point is an average of the amplitudes of 15 MEPs. Outline and filled symbols are used to differentiate subjects only and do not imply statistical significance. 10min of anodal or cathodal stimulation leads to an increase (red) or decrease (blue) in 15-35Hz intermuscular coherence respectively, with sham stimulation (black) having no significant effect (D; n=10; adapted from Power *et al.*, 2006). Filled symbols denote a statistically significant difference from baseline ($p<0.05$, paired t-test). This is also evident when plotting the difference in coherence before and after tDCS, averaged across all subjects (E).

4.3 Methods

4.3.1 Subjects

At least 15 volunteers were recruited for each decade of age between 20 and 80 (50 men and 41 women); age averaged 48.9±17.3 years (SD; range 22-77). Eighty-two subjects were right-handed and nine left-handed as assessed by self-reporting. None had any history of neurological disorders or diabetes mellitus, or any contraindications to magnetic stimulation, and none took any neurotropic medication. All subjects provided written informed consent. The study was approved by the research ethics committee of Newcastle University's Medical Faculty, and conformed to the Declaration of Helsinki.

4.3.2 Recording

Every effort was made to maintain subjects at a constant level of alertness. All assessments were carried out on the dominant arm, with tDCS and TMS targeting the contralateral M1. Subjects were seated in a comfortable chair with their arm resting semi-pronated on a cushion. Surface EMG was recorded from first dorsal interosseous (FDI), flexor digitorum superficialis (FDS) and extensor digitorum communis (EDC) in experiment 1, and from abductor digiti minimi (ADM) in experiment 2. Adhesive electrodes (Bio-Logic M0476; Natus Medical, Mundelein, IL) were placed in a belly-tendon montage over FDI and ADM; for FDS and EDC, the electrodes were placed 4cm apart, one third along the muscle from its proximal origin. Signals were amplified, band-pass filtered (30Hz-2kHz; Digitimer D360, Digitimer, Welwyn Garden City, UK) and digitised at 5kHz (Micro1401, Cambridge Electronic Devices, Cambridge, UK).

4.3.3 tDCS

tDCS was delivered by a battery-powered constant current stimulator (custom-built by the Medical Physics Department, Newcastle upon Tyne Hospitals) through a pair of 5x7cm conductive rubber electrodes covered in saline-soaked sponges (neuroConn, Ilmenau, Germany). The anode was centred on a point 7cm lateral to the vertex in experiment 1, and on the TMS hotspot for ADM in experiment 2; the cathode was placed over the contralateral forehead. The long axis of both electrodes was orientated in a coronal plane. Direct current stimulation at 1mA was administered for

10min; similar paradigms have been shown to increase MEP amplitude for at least 40min after the end of stimulation (Nitsche & Paulus, 2001). The current was ramped up or down over 5s at the start and end of stimulation respectively. Subjects reported no side-effects other than a mild tingling or burning sensation under the electrodes during stimulation.

4.3.4 Experiment 1: IMC

Subjects were asked to perform a repetitive precision grip task, both before and immediately after tDCS. A length of compliant plastic tubing (length 19cm, Portex translucent PVC tubing 800/010/455/800; Smith Medical, Ashford, UK) was attached to the index finger and thumb with Micropore tape (3M Health Care, Neuss, Germany), and subjects were asked to oppose both ends of the tubing when prompted by visual and auditory cues. This auxotonic task – so-called because force increases with displacement in a spring-like fashion – required a minimum force of 1N (Fisher *et al.*, 2012) and was similar to a precision grip task used in our previous studies, albeit without measuring digit displacement (Kilner *et al.*, 2000; Riddle & Baker, 2006). Subjects produced 4s of contraction alternating with 2s of relaxation, and at least 100 repetitions. Visual feedback of raw EMG traces was provided to facilitate consistent task performance.

4.3.5 Experiment 2: MEP amplitude

Six subjects were asked to return for experiment 2; at least one week had elapsed since the previous experiment to prevent carry-over effects. Subjects maintained a constant head position in a HeadSpot frame (UHCOtech, Houston, TX), placing their chin in a cup and their forehead against a bar. Auditory feedback of surface EMG was provided to aid the subject in maintaining complete relaxation of ADM.

Magnetic stimulation was then delivered at a frequency of 0.2Hz using a Magstim 200 stimulator (Magstim Company, Whitland, UK) and a figure-of-eight coil (70mm outer diameter). The coil was placed tangentially to the scalp with the handle pointing posterolaterally at 45 degrees from the sagittal plane. The TMS hotspot was determined as the position that evoked the largest MEP in ADM and stimulation intensity adjusted to yield a MEP amplitude of approximately 1mV. The range of final

stimulation intensities was 42-68%. The hotspot was marked on the scalp and registered relative to the head frame using a Liberty motion tracking system with six degrees of freedom (Polhemus, Colchester, VT). Positional data were sampled at 240Hz and deviations from the hotspot were displayed using a custom interface written in Delphi (Borland, Austin, TX). Typically, this allowed the experimenter to maintain coil position within ±1mm (x/y/z) and ±1 degree (roll/bank/yaw) of the registered position.

20 baseline MEPs were recorded. The subject then sat back from the frame to receive tDCS. Immediately after tDCS, the subject resumed their position in the frame. The TMS coil was repositioned over the hotspot and a further 20 MEPs were recorded. This was repeated 5, 10, 15, 25, 35 and 45min after tDCS.

4.3.6 Data analysis

Analysis was performed in Matlab (Mathworks, Natick, MA) using custom scripts.

For experiment 1, raw data were visually inspected and the first 100 adequately performed trials examined further. Analysis focussed on the early hold phase of the contraction where beta-band oscillations are known to be maximal (Baker *et al.*, 1997; Sanes & Donoghue, 1993). EMG signals were full-wave rectified. Starting 0.8s after the cue prompting contraction, two contiguous 0.82s-long sections of data from each trial were subjected to a 4096-point fast Fourier transform (FFT), giving a frequency resolution of 1.22Hz. Many subjects showed a drop-off in EMG activity so the last 1.56s of the 4s active phase did not enter the analysis. Denoting the Fourier transform of the lth section of the first EMG signal as $F_{1,l}(\lambda)$, the auto-spectrum is given by

$$f_{11}(\lambda) = \frac{1}{L}\sum_{l=1}^{L} F_{1,l}(\lambda)\,\overline{F_{1,l}(\lambda)} \tag{4.1}$$

where λ is the frequency (Hz), L is the total number of sections and where the overbar denotes the complex conjugate. The cross-spectrum for two EMG signals with Fourier transforms $F_{1,l}(\lambda)$ and $F_{2,l}(\lambda)$ was calculated as

$$f_{12}(\lambda) = \frac{1}{L}\sum_{l=1}^{L} F_{1,l}(\lambda)\,\overline{F_{2,l}(\lambda)} \tag{4.2}$$

Coherence was computed as the cross-spectrum normalised by the auto-spectra

$$C(\lambda) = \frac{|f_{12}(\lambda)|^2}{f_{11}(\lambda)f_{22}(\lambda)} \tag{4.3}$$

Coherence was calculated for the muscle pairs EDC-FDI and FDS-FDI. The wide anatomical spacing between the paired muscles minimised the risk of volume conduction causing inflated coherence values (Grosse *et al.*, 2002).

Under the null hypothesis of linear independence between the signals, a level of significant coherence was determined as (Rosenberg *et al.*, 1989)

$$Z = 1 - \alpha^{1/(L-1)} \tag{4.4}$$

where the significance level α was set at 0.05.

Analyses of power and coherence described below were conducted separately for each muscle or muscle pair respectively.

The significance of changes in coherence after tDCS was determined by calculating single-subject Z-scores as

$$Z_{n_s} = \sqrt{\frac{L}{N_\lambda}}\sum_{\lambda=\lambda_1}^{\lambda_2}\left(\operatorname{atanh}\left(\sqrt{C_{n_s}^{after}(\lambda)}\right) - \operatorname{atanh}\left(\sqrt{C_{n_s}^{before}(\lambda)}\right)\right) \tag{4.5}$$

where $C_{n_s}^{before}(\lambda)$ and $C_{n_s}^{after}(\lambda)$ denote the coherence at frequency λ for subject n_s before and after tDCS. Z_{n_s} was summed over all N_λ frequency bins in the 15-30Hz window (N_λ=bin number(λ_2)-bin number(λ_1)+1=12), and normalised so that it should

be normally distributed with zero mean and unit variance under the null hypothesis of no change in coherence after tDCS (Baker & Baker, 2003; Rosenberg *et al.*, 1989).

The mean compound Z-score across all N_S subjects was calculated as

$$\bar{Z} = \sqrt{\frac{1}{N_s}} \sum_{n_s=1}^{N_s} Z_{n_s} \tag{4.6}$$

The associated two-tailed probability (p_Z) was computed with reference to the standard normal distribution.

The assumption that single-subject Z-scores should be normally distributed under the null hypothesis could not be tested, and to allay potential concerns about its validity we also performed distribution-free testing using Monte-Carlo simulations. Arithmetic means of coherence in the 15-30Hz window were calculated before and after tDCS ('paired means') for each subject. The ratio of paired means summarised any change on a single-subject level, and the geometric mean of the ratios for all subjects encapsulated any change on a group level. For each subject, paired means were shuffled, randomly reassigning each member of the pair to the 'before' or 'after' condition, before recalculating the geometric mean. The shuffling procedure was repeated 10^6 times, allowing the distribution of the geometric mean to be estimated under the null hypothesis that tDCS did not alter mean 15-30Hz coherence. The two-tailed probability for the observed geometric mean (p_{MC}) was calculated with reference to the estimated null distribution.

Raw auto-spectra represent absolute power, which has little meaning as it is influenced by uncontrolled factors such as electrode position relative to the muscle generators. They were therefore normalised to the average total power in the 0-48Hz band before tDCS to yield relative power spectra. For each subject, arithmetic means of relative power in the 15-30Hz band were calculated before and after tDCS ('paired means'). The sample distributions of these means were right-skewed and could not be modelled adequately by a normal distribution even after applying logarithmic or

inverse transforms (Shapiro-Wilk test, $p<0.001$ in at least one muscle, Bonferroni-corrected significance level $\alpha/n=0.05/3=0.017$). Therefore, paired means were compared using a two-sided Wilcoxon signed rank test (p_W). In addition, we performed Monte-Carlo simulations similar to those outlined above.

To test for changes in power and coherence during task performance, each session before or after tDCS was divided into two epochs. Power and coherence were analysed separately for each epoch, and results compared between both epochs of a given session using the above statistical procedures.

For experiment 2, MEPs from each time point were averaged. The peak-to-peak amplitude of each average was normalised to the baseline (pre-tDCS) value, and normalised amplitudes were analysed using one-way analysis of variance (ANOVA) (Nitsche & Paulus, 2000).

4.4 Results

4.4.1 Experiment 1: IMC

Single-subject data are illustrated in Figure 4.2. Raw EMG recordings were very similar before and after tDCS. In most subjects, power and coherence spectra showed a peak in the 15-30Hz band, which often appeared to increase in amplitude after tDCS.

Relative power and coherence were averaged across the 15-30Hz band. Figure 4.3 plots the ratio of post-tDCS to pre-tDCS values for each subject (grey histograms; Figure 4.3 A, B, E, F, I) and their geometric mean across all subjects as a group summary (dotted red lines). The distribution of geometric means under the null hypothesis of no change after tDCS was estimated using Monte-Carlo simulations (green histograms, with dotted red lines indicating the observed value; Figure 4.3 C, D, G, H, J). Power increased in all muscles after tDCS but these changes did not reach significance on the primary test (EDC: 14.5±27.7% (change in geometric mean±1.96*SE), $p_W=0.106$; FDS: 17.7±39.2%, $p_W=0.148$; FDI: 2.5±25.8%, $p_W=0.558$). Monte-Carlo analysis showed borderline significance for changes in EDC and

significance for changes in FDS (EDC: p_{MC}=0.052; FDS: p_{MC}=0.022; FDI: p_{MC}=0.729). Coherence increased very significantly in both muscle pairs (EDC-FDI: 12.9±12.1%, p_Z<0.001; FDS-FDI: 11.3±11.5%, p_Z<0.001; also see Figure 4.4 A, C), with Monte-Carlo analysis also demonstrating significance (EDC-FDI: p_{MC}=0.011; FDS-FDI: p_{MC}=0.027). The coefficients of variation for within-subject increases in coherence were 52.3% (EDC-FDI) and 50.1% (FDS-FDI).

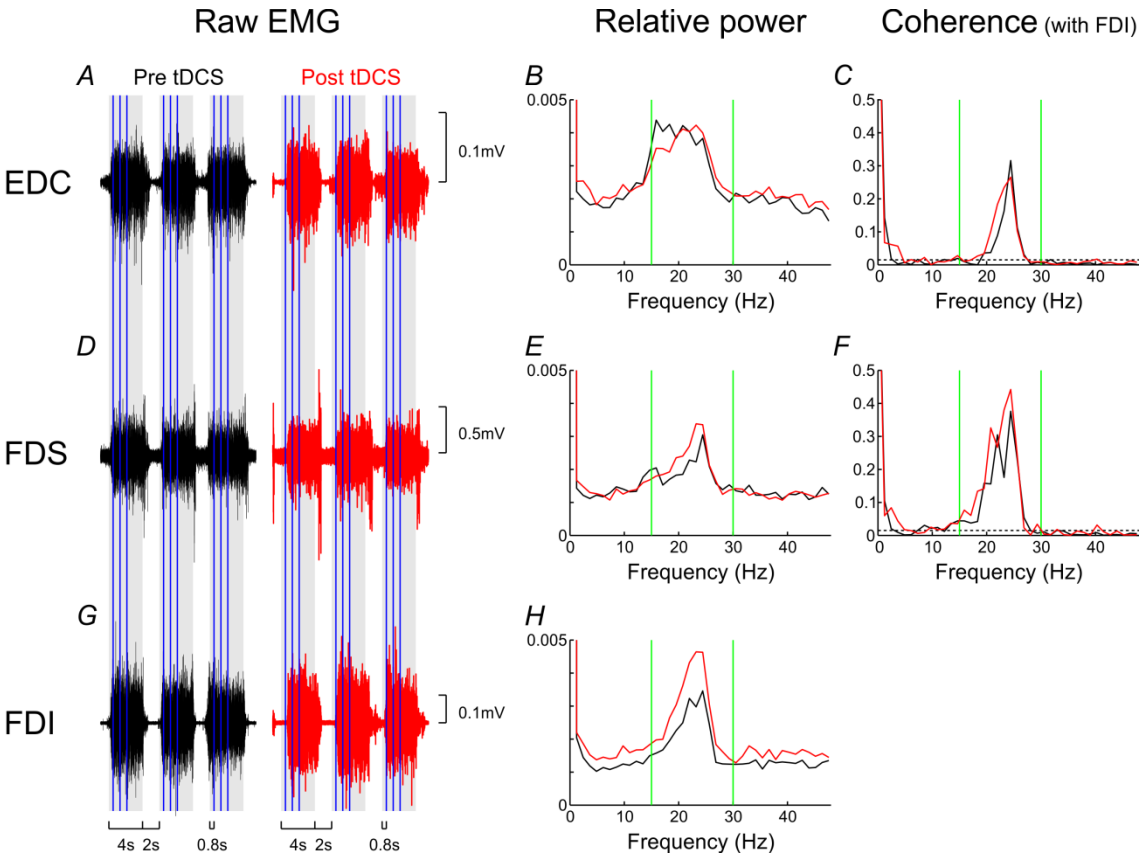

Figure 4.2: Single-subject power and coherence in the upper limb. Raw EMG is shown for three sample trials before and after tDCS (A, D, G). The cued contraction phase of the task is designated by the grey boxes, and the two FFT windows during the hold phase of the contraction are shown by the vertical blue lines. Spectra of relative power (B, E, H) and coherence with FDI (C, F) are plotted for data recorded before (black) and after tDCS (red). The 15-30Hz beta-band is flanked by the green lines, and the dotted horizontal lines indicate the significance level for coherence. In most subjects, power and coherence spectra demonstrated a peak in the 15-30Hz band, which often appeared to increase in amplitude after tDCS.

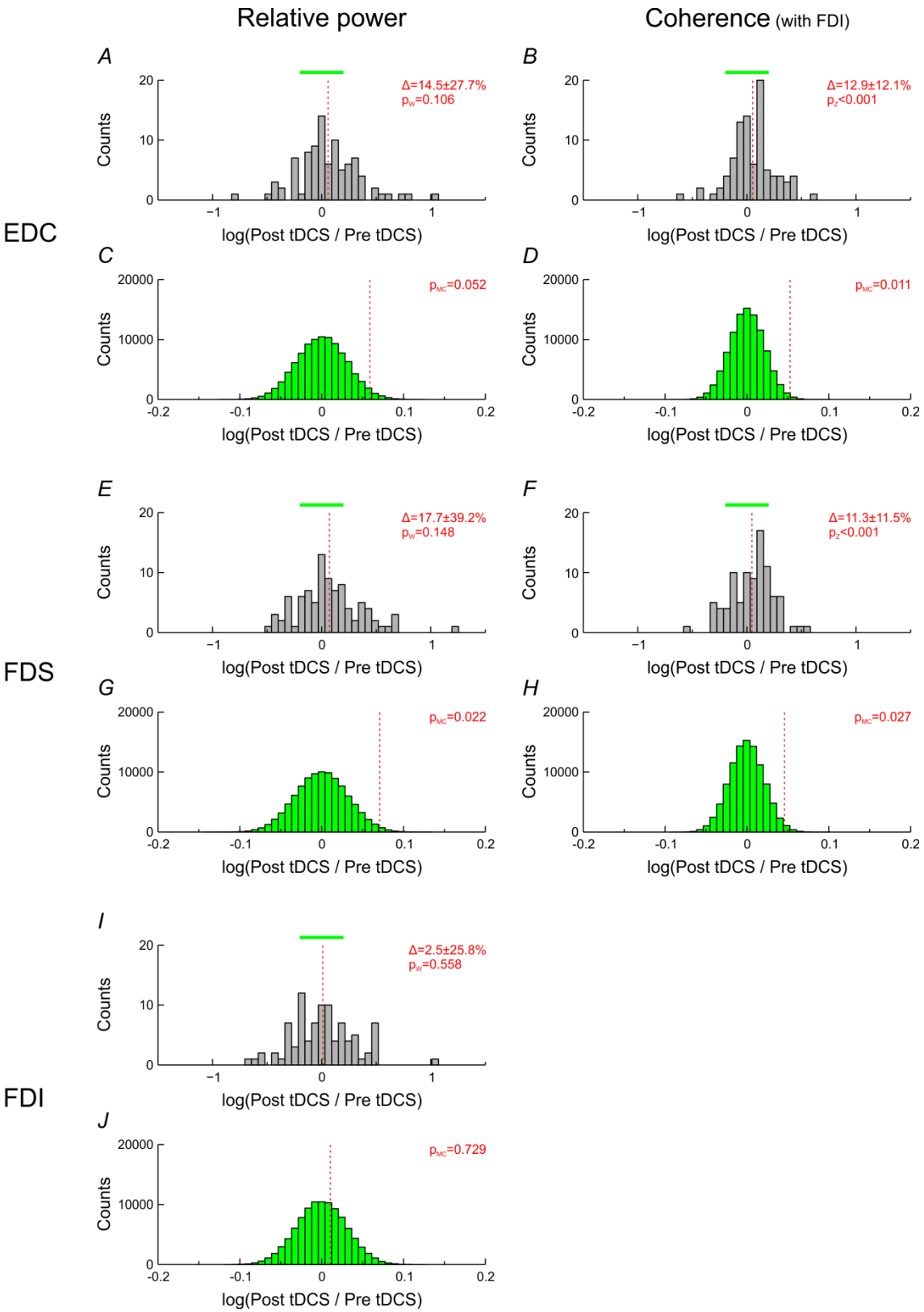

Figure 4.3: Group data for power and coherence. Relative power (left; A, C, E, G, I, J) and coherence with FDI (right; B, D, F, H) were averaged across the 15-30Hz band, and the ratio of post-tDCS and pre-tDCS averages was calculated for each subject (grey histograms; A, B, E, F, I). The geometric mean of these ratios summarised the data on a group level (vertical dotted red lines; Δ denotes change from unity±1.96SE). For each geometric mean, the null distribution was estimated using Monte-Carlo simulations (green histograms; C, D, G, H, J). The probability of the observed value occurring under

the null hypothesis was calculated with reference to the estimated null distribution. Power increased slightly in all muscles after tDCS without these changes reaching significance on the primary test (p_W). On Monte-Carlo analysis (p_{MC}), the changes were significant in FDS and borderline in EDC. Coherence increased in both muscle pairs, with both the primary test (p_Z; also see Figure 4.4) and Monte-Carlo analysis (p_{MC}) demonstrating significance in each case.

Power increased in 52.8% (EDC), 61.5% (FDS) and 51.7% (FDI) of all subjects. A rise in coherence was seen in 62.6% (EDC-FDI) and 63.7% (FDS-FDI) of subjects, with 80.2% showing an increase in at least one muscle pair.

Figure 4.4 shows Z-scores for differences in coherence. In the intersession comparison between pre-tDCS and post-tDCS sessions (Figure 4.4 A, C), the compound mean Z-scores (dotted red lines) indicated a significant increase in coherence for each muscle pair as mentioned above (EDC-FDI: $\bar{Z}$=5.86, p_Z<0.001; FDS-FDI: $\bar{Z}$=6.67, p_Z<0.001). In the intrasession analysis (Figure 4.4 B, D), data from the pre-tDCS and post-tDCS sessions were each split into two epochs; both epochs of a given session were then compared to each other. The pre-tDCS comparison yielded compound mean Z-scores (dotted black lines) which were not significantly different from zero (EDC-FDI: $\bar{Z}$=-0.594, p_Z=0.553; FDS-FDI: $\bar{Z}$=0.313, p_Z=0.754); Monte-Carlo analysis likewise showed no significant difference between epochs (EDC-FDI: -1.0±13.9%, p_Z=0.538; FDS-FDI: 2.1±13.1%, p_{MC}=0.663; see also Chapter 3 and Figure 3.6 B, D). In the post-tDCS comparison, the compound mean Z-score from FDS-FDI but not EDC-FDI (dotted red lines) was significantly increased (EDC-FDI: $\bar{Z}$=0.911, p_Z=0.362; FDS-FDI: $\bar{Z}$=3.113, p_Z=0.002). This suggested a further increase in coherence in FDS-FDI during the post-tDCS session, though Monte-Carlo analysis did not reach significance (EDC-FDI: 5.1±14.4%, p_{MC}=0.298; FDS-FDI: 6.3±10.6%, p_{MC}=0.157).

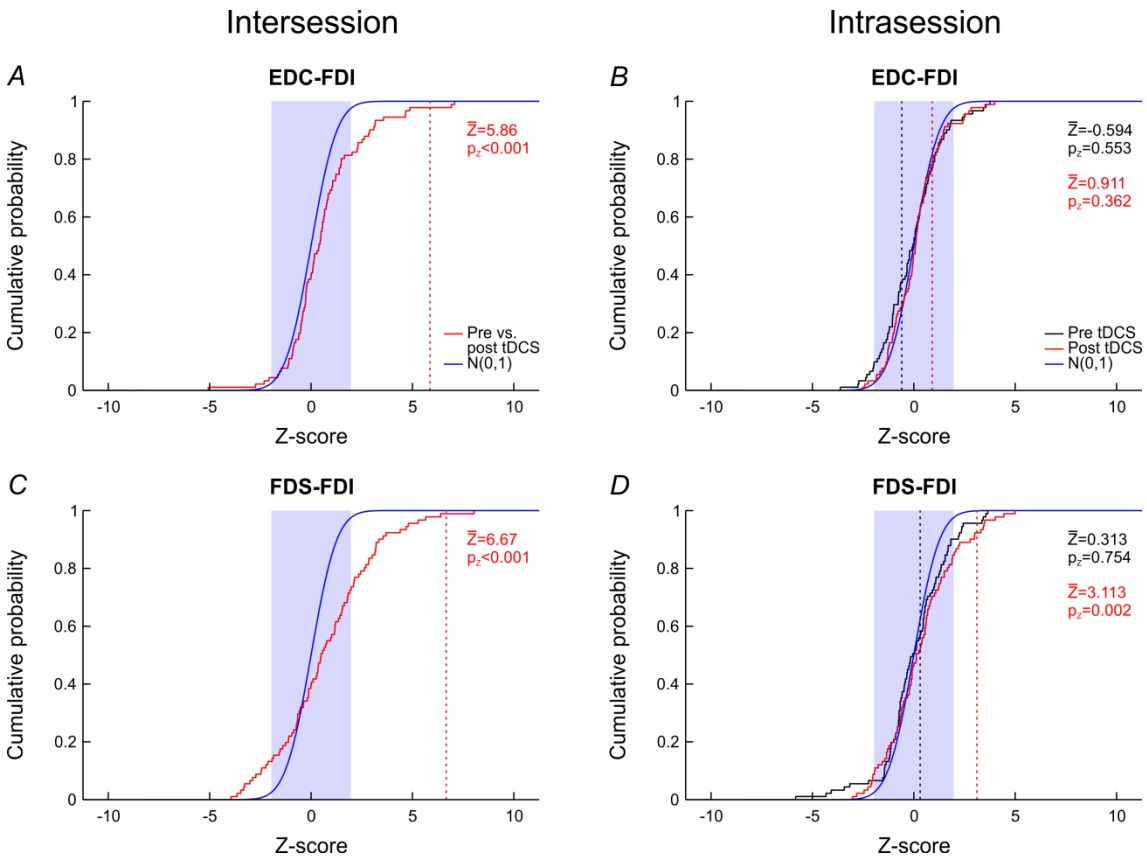

Figure 4.4: Z-scores for differences in coherence. In the intersession analysis (A, C), single-subject Z-scores quantified the difference between post-tDCS and pre-tDCS coherence. Their distribution is plotted by the stairstep curves (red); under the null hypothesis, they should follow a standard normal distribution (blue curve). The mean compound Z-score for all subjects ($\bar{Z}$; vertical dotted lines) was significantly increased in both muscle pairs (p_Z; blue box indicating range of ±1.96), demonstrating a group increase in coherence after tDCS. In the intrasession analysis (B, D), data from the pre-tDCS and the post-tDCS sessions were each divided into two epochs. Both epochs from the same session were compared to each other as outlined above. In the pre-tDCS comparison (black), the mean compound Z-score for all subjects was not significantly different from zero for either muscle pair; in the post-tDCS comparison (red), it was significantly increased in FDS-FDI (p_Z), indicating a further increase in coherence during the post-tDCS session. Note that the intrasession pre-tDCS data are identical to those presented in Figure 3.6.

Intrasession analysis of power for pre-tDCS data showed no significant changes on the primary test (EDC: -1.8±14.8%, p_W=0.689; FDS: -2.2±18.4%, p_W=0.698; FDI: -18.5±13.7%, p_W=0.207) although Monte-Carlo analysis suggested that power in FDI had declined significantly (EDC: p_{MC}=0.807; FDS: p_{MC}=0.755; FDI: p_{MC}=0.007). In the post-tDCS session, power decreased between both epochs, reaching significance in EDC and FDS on both the primary test (EDC: -18.0±18.0%, p_W=0.020; FDS: -18.9±11.3%, p_W=0.001;

FDI: -10.8±17.8%, p_W=0.256) and Monte-Carlo analysis (EDC: p_{MC}=0.006; FDS: p_{MC}<0.001; FDI: p_{MC}=0.063).

4.4.2 Experiment 2: MEP amplitude

Figure 4.5 A displays averages of 20 MEPs at baseline and at several time points after tDCS for one subject. Peak-to-peak amplitudes were measured for each average, normalised to the baseline value and plotted against time for each subject (Figure 4.5 B). In one subject, MEP amplitude increased immediately after tDCS, reaching a broad peak between 5 and 15min with amplitudes of up to 4.2x baseline before gradually decreasing towards baseline from 25min onwards. In all other subjects, MEP amplitudes after tDCS mostly remained below or around baseline.

The average of all subjects (Figure 4.5 C) showed an initial decrease in MEP amplitude followed by a sustained increase between 5 and 35min, with a return to baseline at 45min after tDCS. However, changes of MEP amplitude over time were not statistically significant (p=0.995).

Figure 4.6 compares the tDCS montages used in experiments 1 and 2. In experiment 1, the anode was centred on a point 7cm lateral to the vertex (‘measured position’, Figure 4.6 A). In experiment 2, the anode was centred on the TMS hotspot of ADM (Figure 4.6 B; striped yellow box). In four subjects participating in experiment 2, the measured position was also determined at the end of the session (Figure 4.6 B; solid coloured boxes). In each case, the measured position was no further than 30mm from the hotspot, and an electrode centred on the measured position would still have overlapped the hotspot.

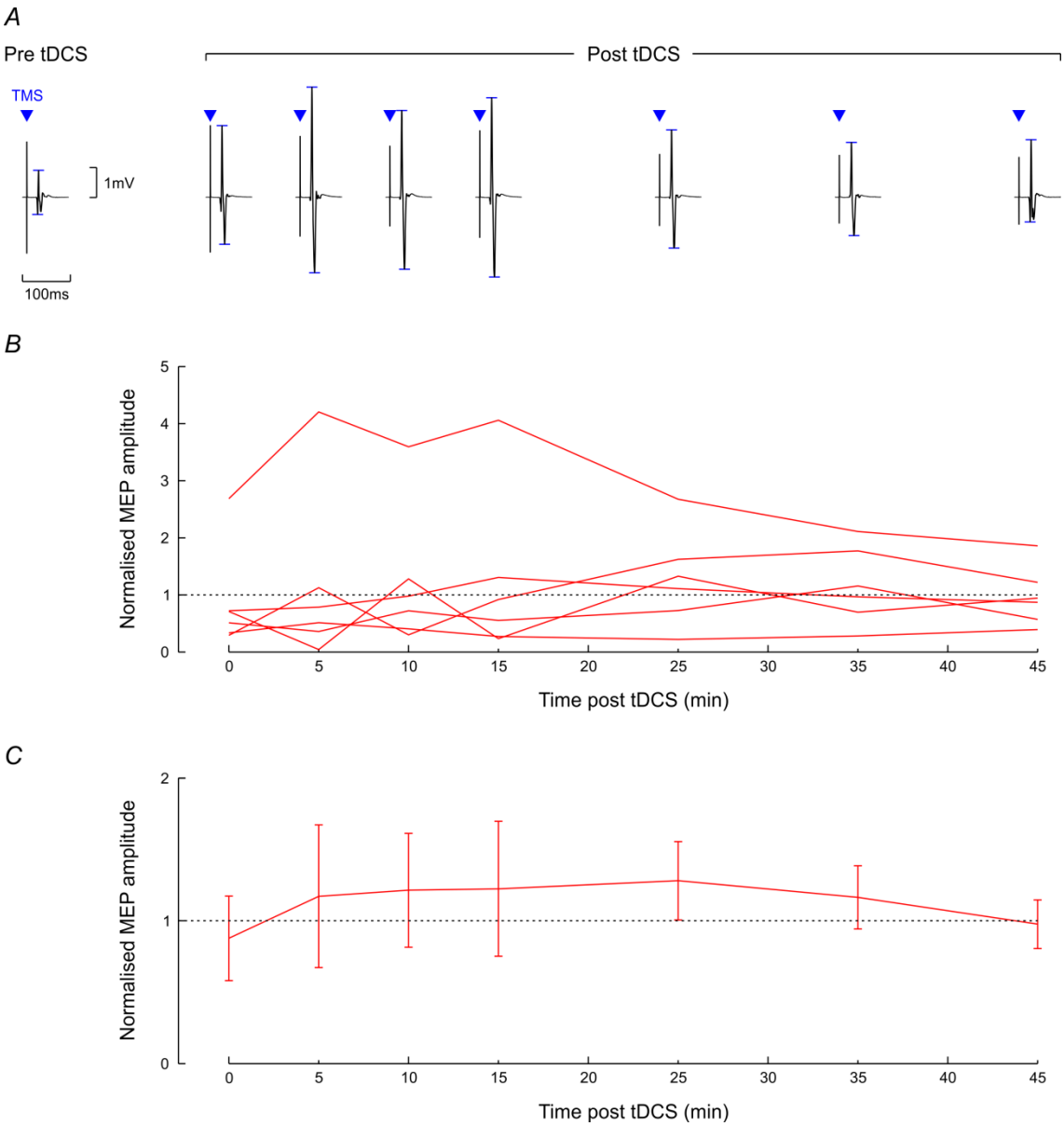

Figure 4.5: Single-subject and group data for MEPs. Averages of 20 MEPs are shown before tDCS and at multiple time points after tDCS for a single subject (A). The blue arrowheads indicate the time of the TMS pulse. Peak-to-peak amplitudes were measured between the blue bars, normalised to the pre-tDCS value and plotted against time after tDCS for all subjects (B). Error bars were omitted for clarity; the dotted horizontal line indicates no change. Normalised MEP amplitudes were averaged across all subjects (C). Error bars indicate 1.96*SE; no significant change was seen post-tDCS (p=0.995).

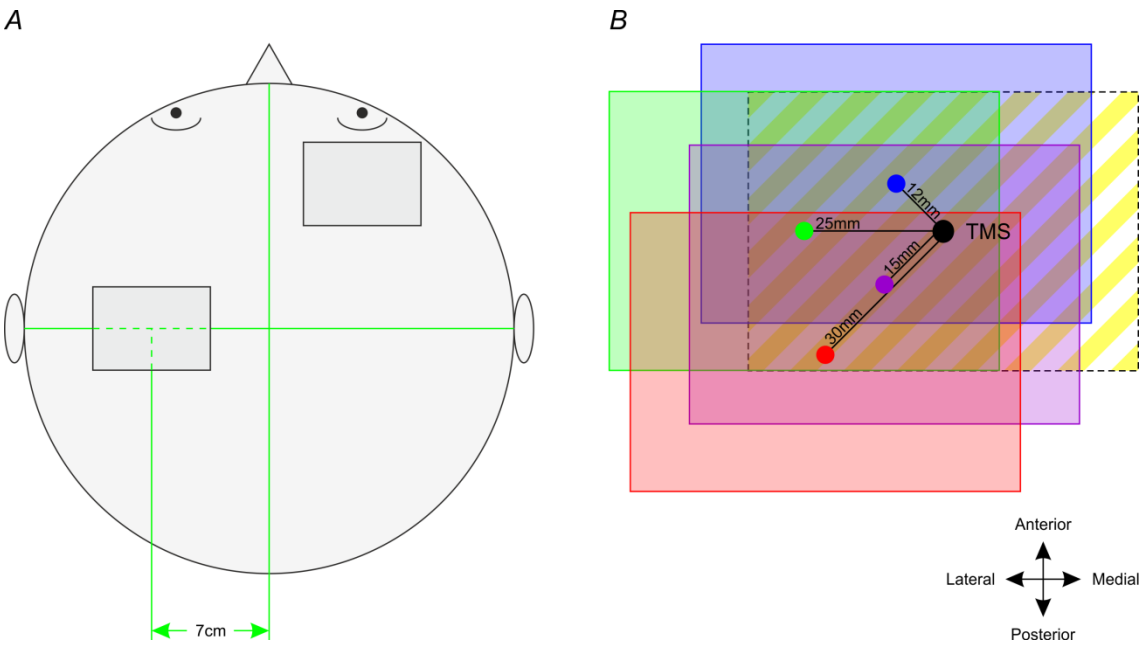

Figure 4.6: Comparison of surface measurements and TMS hotspot mapping. In the coherence experiment, the tDCS electrode over M1 was centred on a point 7cm lateral to the vertex ('measured position'), determined as the intersection of the nasion-inion and interaural lines. The reference electrode was placed over the contralateral forehead (A). In the TMS experiment, the electrode over M1 was centred on the TMS hotspot of ADM (B; different scale; striped yellow box). In four subjects, the measured position was also determined, and was found to be located no further than 30mm from the TMS hotspot. If the tDCS electrode had been centred on the measured position it would still have overlapped the TMS hotspot in each case.

4.5 Discussion

4.5.1 Changes in IMC and power

The observed elevation in beta-band IMC after anodal tDCS (EDC-FDI: 12.9%; FDS-FDI: 11.3%) was comparable in magnitude to that reported in the previous study (EDC-FDI: 18%; Power *et al.*, 2006). Notably the value of 18%, stated on p. 797 of Power *et al.* (2006), disagrees with their diagram which is reproduced in Figure 4.1 D. It also appears to be an arithmetic mean, which tends to overestimate the magnitude of any change compared to the geometric means reported in the present study.

In addition to the increases in IMC being highly significant on a group level, around 80% of individuals showed an increase in at least one muscle pair, suggesting that anodal tDCS is a potentially useful adjunct to beta-band IMC for individual diagnostics.

However, the coefficients of variation were over 50%, highlighting that within-subject increases in coherence were small relative to between-subject variability.

Use of tDCS for individual diagnostics will require increases in coherence which are sufficiently large to be reliably distinguished from random variability. Increases in current density (current per unit area of electrode) and/or duration of stimulation enhance the effects of tDCS on MEPs (Nitsche *et al.*, 2007; Nitsche & Paulus, 2000, 2001), and similar augmentation of the effects on IMC ought to be pursued. The most intense tDCS protocol to date delivered a current of 2mA through 5x5cm electrodes for 20min without adverse effects (Iyer *et al.*, 2005). This is equivalent to a current density of 0.8A/m^2 and a charge density (total charge delivered per unit area of electrode) of 960C/m^2, respectively around three and five times greater than those used in the present study (0.286A/m^2, 171C/m^2). A histological study of rat brains exposed to epicranial DC stimulation reported that no damage was evident unless current density exceeded 28.6A/m^2 and charge density exceeded 52400C/m^2 (Liebetanz *et al.*, 2009). It is therefore likely that even more powerful tDCS protocols than that applied by Iyer *et al.* (2005) will prove safe in humans (Bikson *et al.*, 2009).

Besides the rise in IMC, there was a trend to increases in beta-band power after tDCS. Although Power *et al.* (2006) reported no change in beta-band power as assessed by ANOVA, the underlying assumption of normality may have been invalid. There are several potential explanations for the increase in beta-band power we observed. Firstly, a pure learning effect is unlikely as there was no significant increase during task performance before tDCS. Secondly, power may have increased due to a subtle change in task performance, such as using greater force on average after tDCS. Such a change was not evident during the experiment but cannot be excluded as force and displacement were not measured. Finally, power may have increased as a consequence of anodal tDCS, and it would be helpful to perform a control experiment with sham tDCS to investigate this possibility.

The primary statistical test indicated that power and coherence were stable between the two epochs before tDCS, though Monte-Carlo analysis suggested that the decline in beta-band power in FDI was significant. One possible explanation is that subjects

might have altered their performance of the task to minimise use of FDI, which might be more readily fatigable than the long forearm muscles. Nonetheless, coherence remained almost constant. As a correlational measure normalised to power (Equation 4.3), one might expect that coherence should be relatively insensitive to changes in power. However, it must be kept in mind that the nervous system often shows non-linear response characteristics and therefore concomitant changes in coherence and power may not be related to each other in a straightforward manner (Baker & Baker, 2003).

Between the two epochs after tDCS, power decreased in all muscles, reaching significance in EDC and FDS on the primary test and Monte-Carlo analysis. Again, this could be attributable to subtle alterations in task performance. However, coherence continued to increase, reaching significance in one of the muscle pairs on the primary test only. This might reflect ongoing consolidation of tDCS-induced plasticity. A similar, ongoing increase in tDCS-induced effects has not been described for MEP amplitudes in humans (Figure 4.1 A, B; Nitsche & Paulus, 2000, 2001). However, a study in mouse slices designed to mimic human tDCS reported that excitatory post-synaptic potentials continued to increase in amplitude for over an hour after 15min of DC stimulation (Fritsch *et al.*, 2010). Although species and methodological differences must be taken into account, this might suggest that changes in MEPs capture only part of the plastic changes, with ongoing further changes beyond the period of stimulation which can be detected on invasive recordings and potentially through IMC analysis.

Monte-Carlo analyses were principally employed to back up the results of testing for changes in coherence using Z-transformed data (Equation 4.5), as the latter involved an assumption of normality under the null hypothesis which could not be tested. The freedom from distributional assumptions offered by Monte-Carlo approaches comes at the price of lower statistical power, and this is reflected in p_{MC} values usually being higher than corresponding p_Z values. The reverse situation applies when comparing results from Monte-Carlo analysis with those of the Wilcoxon signed-rank test (p_W). The latter is not only distribution-free but also discards much information by comparing ranks rather than numerical values, and would therefore be expected to be less powerful than Monte-Carlo analysis.

4.5.2 Methodological differences from previous study

We used a topographical method for determining the location of the motor cortical tDCS electrode. This location differed slightly from the TMS hotspot for ADM, which was the target in most classical tDCS studies and is located adjacent to the hotspot for FDI (Wilson *et al.*, 1993) over which Power *et al.* (2006) centred the electrode. Nonetheless, the tDCS montage proved effective at modulating IMC, probably because the electrode area still overlapped the M1 representation of the relevant muscles (Nitsche *et al.*, 2007) or the stimulation current was sufficiently dispersed by the extracerebral structures (Datta *et al.*, 2009; Miranda *et al.*, 2006). Combined with the results of the previous study, this makes it unlikely that a montage based on TMS or neuronavigation would substantially increase the effect of anodal tDCS on IMC. Such measures would also markedly increase cost and restrict availability.

There were several other methodological differences between the present study and Power *et al.* (2006). Firstly, our task involved phasic rather than sustained contraction as coherence is known to be maximal during the early hold phase (Baker *et al.*, 1997; Sanes & Donoghue, 1993). Absolute results before tDCS were not reported by Power *et al.* (2006) so no direct comparison can be made. Secondly, we used a slightly narrower beta-band (15-30Hz cf. 15-35Hz). This is unlikely to have had a significant effect as coherence tended to peak within our 15-30Hz window and was low or absent above the upper 30Hz boundary (also see Figure 3.2 B, D). Thirdly, we summed total coherence within the beta-band window, whereas Power *et al.* (2006) only included coherence above the significance level. As our significance level was markedly lower than in Power *et al.* (2006; 0.015 cf. 0.04), a substantial effect is improbable. Finally, our study did not include a control group. Subjects were blind to the intended effects of tDCS, there is no evidence that IMC can be consciously manipulated, and no practice effects were evident when IMC data were compared between two epochs before tDCS. Nonetheless, a sham condition would help to rule out any spurious effects.

Muscle activity in the target limb is a prerequisite for IMC analysis yet might interfere with tDCS-induced modifications of cortical plasticity. Similar to de-potentiation and de-depression observed in animal experiments, the effects of tDCS on MEPs and measures of intracortical excitability can be attenuated or abolished if the period of DC

stimulation is succeeded by voluntary muscle contraction (Thirugnanasambandam *et al.*, 2011). The effect was demonstrated using a sustained contraction of FDI at 20% maximum voluntary contraction (MVC) for two minutes, a task not unlike that used by Power *et al.* (2006) for coherence estimation. Whilst Power *et al.* (2006) described significant alterations of IMC and MEPs after tDCS, the time course of the MEP changes was much more short-lived than expected from previous work in which the subject was at rest throughout (0-5min vs. 40min; Nitsche & Paulus, 2001). This difference could be explained in terms of modification of plasticity by voluntary activity. The coherence alterations described by Power *et al.* (2006) were also brief (5-10min), contrasting with our study where changes in coherence prevailed for at least 10min and appeared to increase rather than decrease during this period. It has been suggested that activity influences the effects of neuromodulation in a task-specific manner (Thirugnanasambandam *et al.*, 2011) and our phasic task might have interfered less with tDCS-induced plasticity than a sustained contraction. The task-dependence of these effects has not been systematically characterised, and needs to be regarded as a caveat when studying the effect of tDCS on coherence.

4.5.3 Changes in MEP amplitude

We failed to reproduce clearly the classical effects of tDCS on TMS-evoked motor responses. The trend in the group data principally resulted from one subject showing an unusually large increase in MEP amplitude after tDCS, whereas MEP amplitude in the remaining subjects remained largely unchanged or even decreased. Previous studies reported a high degree of interindividual and intraindividual variability, but even in individual subjects most MEP amplitudes at relevant time points after anodal tDCS exceeded baseline (Figure 4.1 B; Nitsche & Paulus, 2001).

The reasons for not observing the classical effects on MEPs in this investigation are obscure. Our protocol closely paralleled previously reported methods (Nitsche *et al.*, 2008; Nitsche & Paulus, 2000, 2001). With few exceptions (Ardolino *et al.*, 2005), past studies used a figure-of-eight coil for evoking motor responses. The focality of this coil ensures that the cortical area effectively stimulated by TMS is no larger than that affected by tDCS (M. A. Nitsche, personal communication, 16 October 2012), but also makes TMS exquisitely sensitive to positional changes. All classical studies used hand-

held coils without positioning aids. The risk of positioning errors is high, particularly when replacing the coil after tDCS, and we attempted to mitigate this problem by use of a motion tracking system and all TMS being performed by the same experienced operator. However, the head was not fully immobilised by the frame so small positioning errors might still have occurred. This could be addressed by use of a bite-bar or automated robotic head tracking. Our previous approach of using a modified motorcycle helmet to keep the coil in a constant position relative to the head (Mitchell *et al.*, 2007) would not have been workable as the application of the tDCS electrode over the motor cortex required the coil to be removed.

4.6 Conclusion

In summary, the magnitude of the observed effects of anodal tDCS on beta-band IMC is in keeping with previously reported results. The duration of the increase in beta-band IMC agrees with the timecourse of classical MEP data but not the previous report of tDCS-associated changes in IMC. It would be useful to measure power and coherence at multiple time points after tDCS until all results have returned to baseline, and to perform a control experiment with sham tDCS. Additionally, the effects of more powerful tDCS protocols on IMC ought to be studied.

Thus far, most investigations of tDCS have targeted the M1 representation of the hand. Only a small number of studies have considered the effects of tDCS on the representation of the lower limb (Jeffery *et al.*, 2007; Madhavan & Stinear, 2010; Roche *et al.*, 2011; Tanaka *et al.*, 2009). It would be of interest to explore any impact of tDCS on lower limb IMC, but the scope of our study should only be extended in this manner once the aforementioned issues have been addressed.

5 Intermuscular coherence and central motor conduction times in patients with motor neuron disease

Having investigated central motor conduction times (CMCT) and intermuscular coherence (IMC) in normal individuals, we now turn our attention to CMCT and IMC in motor neuron disease.

5.1 Abstract

Objective: To investigate beta-band intermuscular coherence (IMC) and central motor conduction times (CMCT) as biomarkers of corticospinal tract (CST) integrity in patients with motor neuron disease (MND).

Methods: 61 patients with MND, recruited at first presentation to a tertiary MND service, and 92 healthy control subjects were included. In the upper limb, IMC was estimated between extensor digitorum communis (EDC) and first dorsal interosseous (FDI) as well as between flexor digitorum superficialis (FDS) and FDI. In the lower limb, IMC was measured between medial gastrocnemius (MG) and extensor digitorum brevis (EDB) as well as between tibialis anterior (TA) and EDB. Magnetic stimulation was performed over the primary motor cortex (cortical latency) and over the cervical and lumbar spine (spinal latency). The spinal latency was taken as an estimate of peripheral motor conduction time (PMCT), and was subtracted from cortical latency to yield CMCT. The performance of individual and combined IMC and CMCT markers was analysed using the area under the receiver-operating characteristic curve (AUC).

Results: Within a given limb, IMC in the best muscle pair was as good a classifier as combinations of IMC from both muscle pairs (AUC upper limb 0.83, lower limb 0.79). In the upper limb, IMC performed better than all CMCT markers, including combinations of CMCT. In the lower limb, performance of IMC was very similar to that of CMCT in individual muscles, but lagged behind combined CMCT markers (AUC 0.90-0.91). Non-linear combinations of markers performed at best marginally better than their linear counterparts, suggesting that linear combinations are sufficient.

Conclusion: IMC has potential as a quantitative test for CST involvement in MND. It exceeded the performance of CMCT in the upper limb and matched that of individual CMCT markers in the lower limb. Unlike CMCT, IMC requires no dedicated equipment, and thus its deployment as a clinical test would be relatively inexpensive.

5.2 Introduction

Motor neuron disease (MND) is an inexorably progressive, fatal neurodegenerative disorder. It is rare, with an estimated incidence of 2 per 100,000 per year (McGuire & Nelson, 2006), and encompasses a spectrum of phenotypes; the commonest one, amyotrophic lateral sclerosis (ALS), involves loss of pyramidal neurons in the primary motor cortex as well as motor neurons in the brainstem and spinal cord. ALS typically runs an aggressive course with a median survival of 30 months from symptom onset (Chancellor *et al.*, 1993). Diagnosis is primarily clinical and requires evidence of upper and lower motor neuron (UMN, LMN) pathology in a defined topography after excluding alternative causes, as specified by the El Escorial criteria (Brooks, 1994). Subsequent revisions of these diagnostic criteria have placed increasing emphasis on EMG features of LMN dysfunction in regions without clinical LMN signs (Brooks *et al.*, 2000; De Carvalho *et al.*, 2008), thus increasing sensitivity (De Carvalho & Swash, 2009).

One focus of therapy is to slow neuronal degeneration with neuroprotective drugs, and early diagnosis is therefore paramount. At symptom onset, fewer than 5% of motor units remain in muscles with clinical LMN signs, and up to 50% of motor units have been lost in asymptomatic muscles (Aggarwal & Nicholson, 2002). This limits the number of potentially salvageable motor neurons. Against this backdrop it is remarkable that riluzole, the only neuroprotective agent currently licensed in MND, has been shown to extend survival by a median 2-3 months (Bensimon *et al.*, 1994; Lacomblez *et al.*, 1996; Miller *et al.*, 2012). It is plausible that earlier introduction of riluzole could delay the onset of disability and extend survival further (Swash, 1998). For at least two decades, the median time from symptom onset to diagnosis has remained constant at around one year (Househam & Swash, 2000; Mitchell *et al.*, 2010). This interval is unacceptably long in relation to the typical life expectancy in

MND, and shortening it would not only maximise the impact of neuroprotective agents but also be helpful for arranging best management, providing opportunities for entering clinical trials (De Carvalho *et al.*, 2008) and serving the psychological interests of the patient (Johnston *et al.*, 1996).

The lack of a reliable test for corticospinal tract (CST) integrity constitutes one impediment to early diagnosis (Turner *et al.*, 2009). Clinical signs such as clonus, hyperreflexia and extensor plantar responses are useful pointers but may not exclusively reflect pathology in the CST (Brown, 1994). In addition, autopsy studies suggest that clinical assessment has a low sensitivity, as most cases without clinical UMN signs show histological evidence of CST degeneration (Kaufmann *et al.*, 2004). Several markers based on transcranial magnetic stimulation (TMS) have been explored, particularly lengthening of central motor conduction time (CMCT) and diminution or absence of cortical motor evoked potentials (MEPs). Despite initial enthusiasm (Di Lazzaro *et al.*, 1999) there have been continued reservations about the diagnostic utility of these parameters (Mills, 2003). The triple stimulation technique (TST) has boosted diagnostic sensitivity for CST dysfunction (Magistris *et al.*, 1999; Magistris *et al.*, 1998), but not only shares the practical disadvantages of other TMS-based measures – a requirement for specialist expertise and expensive equipment – but is also uncomfortable and time-consuming. MRI approaches for assessing CST integrity have included spectroscopy, diffusion-tensor imaging and voxel-based morphometry (Turner *et al.*, 2009). However, patients may be unable to tolerate the required period of recumbency; adequate performance in early MND at single-subject level is unproven (Filippi *et al.*, 2010); and the requisite expertise and high-field MRI facilities are not universally available. It is therefore unsurprising that diagnostic criteria have not incorporated any TMS- or MRI-based markers of CST function to date, but rather continue to bemoan the need 'for a reliable and sensitive method for assessing UMN disorder' (De Carvalho *et al.*, 2008).

A recently proposed mode of assessment leverages the role of the CST in the transmission of oscillatory activity (Fisher *et al.*, 2012). 15-30Hz beta-band oscillations can be recorded from the primary motor cortex in animals (Baker *et al.*, 1997; Murthy & Fetz, 1992; Sanes & Donoghue, 1993) and humans (Conway *et al.*, 1995; Halliday *et*

al., 1998; Ohara *et al.*, 2000; Pfurtscheller, 1981). They are task-dependent, being prominent during hold phases and diminished during movement (Baker *et al.*, 1997; Sanes & Donoghue, 1993). Coherence analysis demonstrates that beta-band oscillations are synchronised between the cortex and contralateral muscles (corticomuscular coherence, CMC; Baker *et al.*, 1997; Conway *et al.*, 1995; Halliday *et al.*, 1998; Ohara *et al.*, 2000), suggesting that they are transmitted from cortex to muscle. Similarly, coherence is demonstrable between individual muscles in a given limb (Baker *et al.*, 1997; Farmer *et al.*, 1993), and such intermuscular coherence (IMC) is thought to reflect a shared cortical drive. In practice, IMC is often preferred to CMC as no cortical recording is required and significant 15-30Hz IMC is present in most normal individuals, whereas CMC is a less consistent phenomenon (Fisher *et al.*, 2012; Ushiyama *et al.*, 2011b).

IMC depends on supraspinal pathways, as it is absent after capsular strokes (Farmer *et al.*, 1993) and spinal cord lesions (Hansen *et al.*, 2005; Norton *et al.*, 2003). Several lines of evidence suggest a critical role for the CST in particular. Firstly, beta-band IMC is absent in patients with primary lateral sclerosis (PLS), a pure UMN variant of MND, whereas significant beta-band IMC is detectable in patients with progressive muscular atrophy (PMA), a pure LMN variant of MND (Fisher *et al.*, 2012). Secondly, selective lesioning of the CST in macaques abolishes beta-band IMC (Fisher *et al.*, 2012; Nishimura *et al.*, 2009). Thirdly, stimulation of the CST resets the phase of cortical 15-30Hz oscillations in macaques, suggesting that the CST does not merely act as a conduit but forms part of a rhythm-generating network (Jackson *et al.*, 2002). Indeed, there is increasing evidence that afferent pathways contribute to 15-30Hz coherence, leading to the suggestion that coherence is mediated by an efferent-afferent feedback loop (Witham *et al.*, 2011; Witham *et al.*, 2010).

Here, we examine whether IMC is a useful biomarker of UMN function in MND. Unlike the previous study from our group, which focussed on patients with selected variants which had been followed up for many years (Fisher *et al.*, 2012), we recruited patients with all phenotypes of MND as early as possible after referral to the local tertiary service. This shifted the emphasis from the rare subtypes of PLS and PMA to the commoner ones of amyotrophic lateral sclerosis (ALS) and progressive bulbar palsy

(PBP). In addition to IMC, we measured CMCT for comparison. Magnetic stimulation was performed over the primary motor cortex (cortical latency) and over the cervical and lumbar spine (spinal latency). The spinal latency was taken as an estimate of peripheral motor conduction time (PMCT), and was subtracted from cortical latency to yield CMCT. Control data for IMC and CMCT were gathered from a large number of healthy volunteers (Chapters 2 and 3).

IMC and CMCT were treated as binary classifiers discriminating between diseased and normal states, and their performance was assessed using receiver-operating characteristic (ROC) curves. These are monotonically increasing functions from (0,0) to (1,1) and plot the true positive rate (TPR, the fraction of true positives out of all actual positives; equivalent to sensitivity) against the false positive rate (FPR, the fraction of false positives out of all actual negatives; equivalent to 1-specificity) for all possible discrimination thresholds. Hence, ROC curves illustrate the trade-off between increasing TPR and increasing FPR (Pepe & Thompson, 2000). A random guess would have a ROC curve running along a diagonal line from (0,0) to (1,1), the so-called line of no discrimination. The best possible marker would yield a point at (0,1), referred to as a perfect classification, representing 100% TPR and 0% FPR. Generally, points above and below the diagonal represent good (better than random) and poor (worse than random) discrimination respectively. A consistently poor predictor can be inverted to obtain a good predictor, equivalent to reflecting the ROC curve about the diagonal. We summarised each ROC curve by calculating the area under the curve (AUC), which ranged from 0 for a perfect but inverted classification to 1 for a perfect classification, with 0.5 corresponding to a random guess. An AUC of less than 0.5 in the overall analysis prompted inversion of the predictor. In addition to IMC and CMCT *per se*, we explored the performance of their optimal linear and non-linear combinations.

We found that IMC performed better than CMCT in the upper limb, and performed similarly to CMCT in the lower limb. Unlike CMCT, IMC does not require dedicated equipment beyond pre-existing EMG facilities, and this could ease its adoption for future studies and potential clinical use.

5.3 Methods

5.3.1 Subjects

Between February 2011 and February 2013, patients were recruited from the tertiary Motor Neuron Disease Service at Newcastle Upon Tyne Hospitals, serving a catchment population of approx. 2.6 million in the North East of England (Office for National Statistics, 2011). Recruitment took place as soon as possible after referral to the Service, either in the new patient clinic or during scheduled admission for investigation. Successfully recruited subjects were studied in the laboratory within four weeks. Out of 101 subjects assessed by the Service, 79 were recruited to the study (Figure 5.1). After clinical assessment, investigation and – if necessary – serial follow-up, 63 of these were diagnosed with MND. Two subjects were excluded due to sensory neuropathy on nerve conduction studies (NCS), leaving 61 subjects to be included in the analysis. A breakdown by phenotype is shown in Table 5.1, and clinical features including drug histories are summarised in Appendix B.

Control data were obtained from 92 healthy subjects (51 men, 41 women; age range 22-77 years, mean±SD 48.6±17.2). None had any history of neurological disorders or diabetes mellitus, and none took any neurotropic medication.

All subjects provided written informed consent. The studies on patients and control subjects were approved by the National Research Ethics Service (County Durham and Tees Valley Research Ethics Committee, reference number 08/H0908/3) and Newcastle University's Medical Faculty respectively. Both studies conformed to the Declaration of Helsinki.

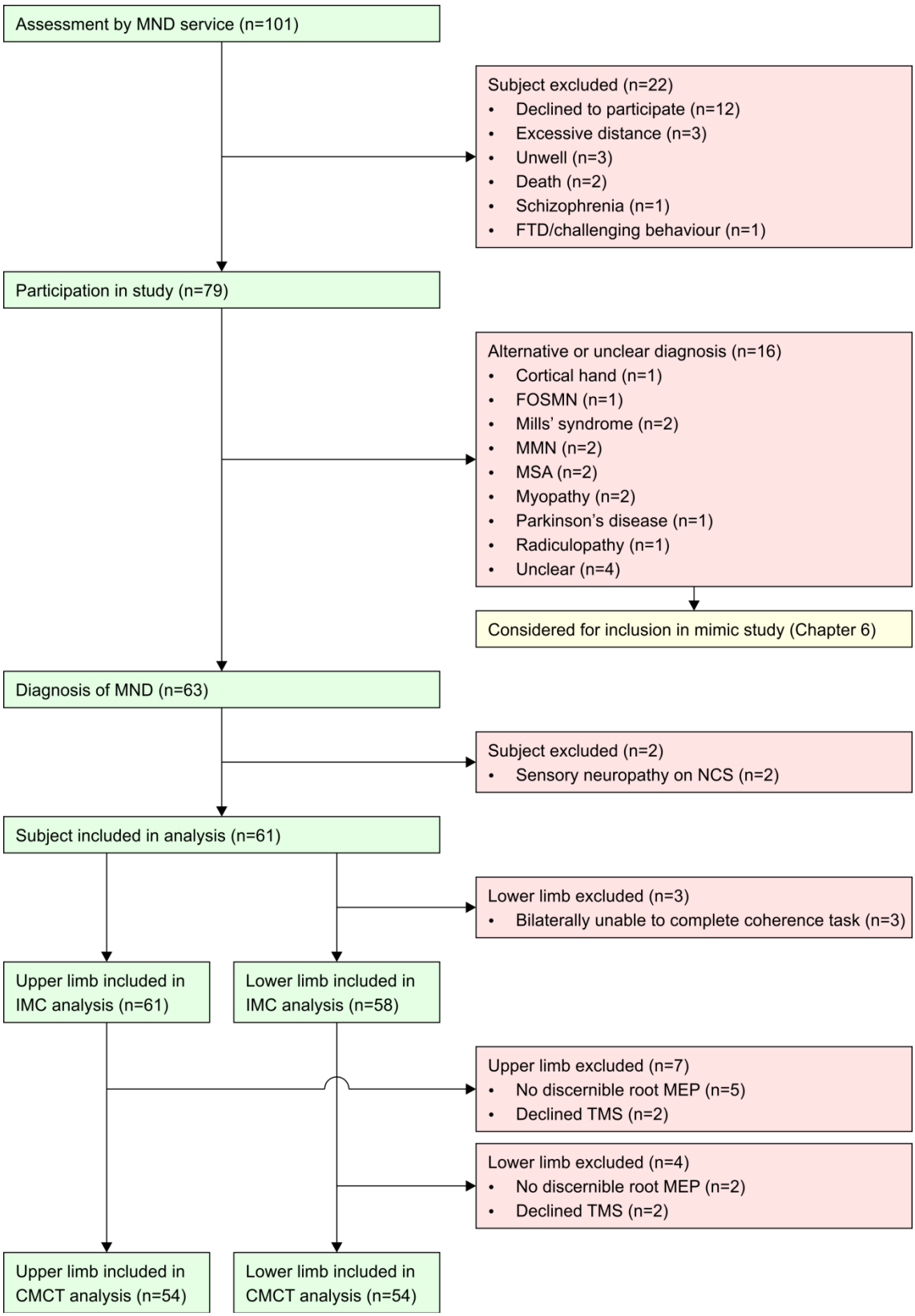

Figure 5.1: Subject flow. Numbers of subjects assessed by the MND service, participating in the study, diagnosed with MND and included in the analyses are shown along with the reasons for drop-out at each stage. (FOSMN=facial-onset sensory and motor neuronopathy, FTD=fronto-temporal dementia, MMN=multifocal motor neuropathy, MSA=multi-system atrophy, NCS=nerve conduction studies)

Table 5.1: Breakdown of MND patients by phenotype. (SOD1=superoxide dismutase 1; TDP43=transactive response DNA binding protein 43kDa; *c.229G>T, p.Asp77Tyr in exon 3)

Phenotype	Subgroup	Genetics	n
ALS			39
	Flail arm		8
	Flail leg		1
	Familial		3
		No known pathogenic mutation in SOD1 or TDP43	2
		Familial pathogenic mutation in SOD1*	1
PBP			10
ALS/PBP overlap			2
PLS			7
PMA			3
	Familial		1
		No genetic testing performed	1
Total			**61**

5.3.2 Recording

Every effort was made to maintain subjects at a constant level of alertness. Subjects were seated in a comfortable chair with their arm resting on a cushion. Surface EMG was recorded from abductor pollicis brevis (APB), first dorsal interosseous (FDI), flexor digitorum superficialis (FDS) and extensor digitorum communis (EDC) in the upper limb, and extensor digitorum brevis (EDB), abductor hallucis (AH), tibialis anterior (TA) and medial gastrocnemius (MG) in the lower limb. Adhesive electrodes (Bio-Logic M0476; Natus Medical, Mundelein, IL) were placed in a belly-tendon montage over the intrinsic muscles of the hand or foot; for the long muscles of the forearm or calf, the electrodes were placed 4cm apart, one third along the muscle from its proximal origin. Signals were amplified, band-pass filtered (30Hz-2kHz; Digitimer D360, Digitimer, Welwyn Garden City, UK) and digitised at 5kHz (Micro1401, Cambridge Electronic Devices, Cambridge, UK).

5.3.3 Experiment 1: IMC

In the upper limb, subjects were asked to perform a repetitive precision grip task. A length of compliant plastic tubing (length 19cm, Portex translucent PVC tubing

800/010/455/800; Smith Medical, Ashford, UK) was attached to the index finger and thumb with Micropore tape (3M Health Care, Neuss, Germany), and subjects were asked to oppose both ends of the tubing when prompted by visual and auditory cues. This auxotonic task – so-called because force increases with displacement in a spring-like fashion – required a minimum force of 1N (Fisher *et al.*, 2012) and was similar to a precision grip task used in our previous studies, albeit without measuring digit displacement (Kilner *et al.*, 2000; Riddle & Baker, 2006). In the lower limb, subjects were asked to dorsiflex ankle and toes in the air while resting the heel on the ground. Subjects produced 4s of contraction alternating with 2s of relaxation, and at least 100 repetitions. Where necessary, the recording was divided into a number of sections separated by rest to prevent fatigue. Visual feedback of raw EMG traces was provided to facilitate consistent task performance.

One upper limb and one lower limb were assessed in each subject. In patients with MND, we studied the most affected upper and lower limb as reported by the subject. If the subject was unable to perform the coherence task using the most affected limb, we assessed the contralateral limb instead; in three cases, the subject was unable to perform the lower limb coherence task on either side and the lower limb was excluded from IMC and CMCT analyses (Figure 5.1). Where both sides were unaffected or equally affected, the limb on the dominant side was assessed. All assessments in control subjects were carried out on the dominant side.

5.3.4 Experiment 2: CMCT

CMCT was always measured on the same side as IMC. As CMCT is known to be highly correlated between both sides in MND, studying the less affected side where necessitated by the coherence task should not have compromised CMCT performance (Mills, 2003). Two patients declined TMS; one control subject did not tolerate upper limb TMS and two control subjects did not tolerate lower limb TMS beyond 30% of maximum stimulator output. These individuals were excluded from CMCT analysis (Figure 5.1).

Magnetic stimulation was delivered using a Magstim 200 stimulator (Magstim Company, Whitland, UK) at a frequency of 0.2Hz. For upper limb cortical motor evoked

potentials (MEPs), a circular coil (13cm outer diameter) was held over the vertex, with its orientation optimised for stimulation of the contralateral hemisphere (A side up: left hemisphere, B side up: right hemisphere). For lower limb cortical MEPs, a double cone coil was used in an analogous manner (posterior coil current: left hemisphere, anterior coil current: right hemisphere). If, at a stimulation intensity of at least 40%, resting motor threshold had not been reached and the subject declined further escalation, the cortical MEP and thus CMCT was assigned as absent. Otherwise, stimulation intensity was set at 10% above the resting motor threshold as defined by the Rossini-Rothwell method (Rossini *et al.*, 1994). Cortical MEPs are facilitated and their onset latencies minimised by a weak background contraction of the target muscle, with no requirement for strictly controlling the force of the contraction (Chen *et al.*, 2008; Kimura, 2001). Ten MEPs were recorded in the upper limb during opposition of index finger and thumb, and in the lower limb during either dorsiflexion (EDB, TA) or plantarflexion (AH, MG) of ankle and toes. Upper and lower limb root MEPs were recorded at rest with the circular coil centred over the spinous processes of C7 and L1. If no clear root MEPs were obtained, the limb was excluded from CMCT analysis (Figure 5.1).

In normal subjects, the range of stimulation intensities used was 35-80% and 40-100% for cortical MEPs of the upper and lower limbs respectively, and 40-90% and 40-100% for corresponding root MEPs. In patients with MND, the equivalent ranges were all 40-100%.

5.3.5 Data analysis

Analysis was performed in Matlab (Mathworks, Natick, MA) using custom scripts.

Raw IMC data were visually inspected and the first 100 adequately performed trials examined further. Analysis focussed on the early hold phase of the contraction where beta-band oscillations are known to be maximal (Baker *et al.*, 1997; Sanes & Donoghue, 1993). EMG signals were full-wave rectified. Starting 0.8s after the cue prompting contraction, two contiguous 0.82s-long sections of data from each trial were subjected to a 4096-point fast Fourier transform (FFT), giving a frequency resolution of 1.22Hz. Many subjects showed a drop-off in EMG activity so the last 1.56s of the 4s active

phase did not enter the analysis. Denoting the Fourier transform of the lth section of the first EMG signal as $F_{1,l}(\lambda)$, the auto-spectrum is given by

$$f_{11}(\lambda) = \frac{1}{L}\sum_{l=1}^{L} F_{1,l}(\lambda)\,\overline{F_{1,l}(\lambda)} \tag{5.1}$$

where λ is the frequency (Hz), L is the total number of sections and where the overbar denotes the complex conjugate. The cross-spectrum for two EMG signals with Fourier transforms $F_{1,l}(\lambda)$ and $F_{2,l}(\lambda)$ was calculated as

$$f_{12}(\lambda) = \frac{1}{L}\sum_{l=1}^{L} F_{1,l}(\lambda)\,\overline{F_{2,l}(\lambda)} \tag{5.2}$$

Coherence was computed as the cross-spectrum normalised by the auto-spectra

$$C(\lambda) = \frac{|f_{12}(\lambda)|^2}{f_{11}(\lambda)f_{22}(\lambda)} \tag{5.3}$$

Coherence was calculated for the muscle pairs EDC-FDI, FDS-FDI, MG-EDB and TA-EDB. The wide anatomical spacing between the paired muscles minimised the risk of volume conduction causing inflated coherence values (Grosse *et al.*, 2002).

Under the null hypothesis of linear independence between the signals, a level of significant coherence was determined as (Rosenberg *et al.*, 1989)

$$Z = 1 - \alpha^{1/(L-1)} \tag{5.4}$$

where the significance level α was set at 0.05.

Analyses of coherence described below were conducted separately for each muscle pair.

To provide a group summary, coherence spectra were averaged across all patients with MND and all control subjects respectively. The significance level for averaged coherence was determined using the method described by Evans and Baker (2003).

In each subject, coherence was averaged across the 15-30Hz window. Log-transformed 15-30Hz coherence could not be modelled adequately with a normal distribution in either the MND or the control group (Shapiro-Wilk test, $p<0.001$ in at least two muscle pairs per group, Bonferroni-corrected significance level $\alpha/n=0.05/4=0.0125$). Therefore, we chose to model coherence distributions non-parametrically. The variable kernel method adapts the amount of smoothing to the local density of the data (Silverman, 1986) and estimates the probability density function (PDF) as

$$\hat{f}(x) = \frac{1}{N}\sum_{n=1}^{N}\left[\frac{1}{hd_{n,k}}\cdot\phi\left(\frac{x-X_n}{hd_{n,k}}\right)\right] \tag{5.5}$$

where x denotes the log-transformed independent variable, X_n the n^{th} log-transformed observation out of a total N observations, $d_{n,k}$ the distance from X_n to its k^{th} nearest neighbour, h the global smoothing parameter and ϕ the standard normal PDF. To understand this intuitively: each observation X_n was convolved with a Gaussian kernel with unit AUC as specified inside the square brackets, and the sum of these kernels was normalised by N to yield $\hat{f}(x)$. The window width of the kernel centred on a given observation X_n was proportional to $d_{n,k}$ so that broader kernels were associated with observations in regions with sparse data; for any fixed k, the amount of smoothing depended on the global smoothing parameter h. k was set as $\sqrt{n}$ rounded to the nearest integer as suggested by Silverman (1986). Theoretically optimal methods for calculating h have been described but, for our data, resulted in overfitting. Therefore, h was optimised by eye for several datasets; the resulting values of h were empirically fitted with simple algebraic functions and the approximation $h = \sqrt[12]{n-5}$ was chosen to determine h subsequently. It should be emphasised that this expression has no theoretical value, but merely provided a convenient shorthand way of determining h objectively for each dataset.

Log-transformed coherence has a bounded domain of $(-\infty,0]$. To ensure that the PDF was zero for $x>0$, $\hat{f}(x)$ was modified by reflection in the boundary (Silverman, 1986):

$$\hat{g}(x) = \begin{cases} \hat{f}(x) + \hat{f}(-x) , & x \leq 0 \\ 0 , & x > 0 \end{cases} \tag{5.6}$$

The resulting PDF still integrated to unity and observations near the boundary retained the same magnitude of contribution to the PDF. The estimated cumulative distribution function (CDF) was calculated as

$$\hat{G}(y) = \int_{-\infty}^{y} \hat{g}(x)dx \tag{5.7}$$

where y is the log-transformed independent variable.

The odds of a subject having MND at a given level of log-transformed coherence x were calculated as the ratio of the PDFs for the MND and control groups:

$$\widehat{OD}(x) = \frac{\hat{g}_{MND}(x)}{\hat{g}_{control}(x)} \tag{5.8}$$

For MEP data, onset latencies were assigned interactively. In the presence of a background contraction, the earliest deflection of the MEP with the shortest latency was often ambiguous on superimposed raw traces because of background EMG activity, but could be easily identified on averages of rectified MEPs (Figure 5.6). Hence, such averages were used for assigning latencies throughout. CMCT was calculated as the difference between cortical and spinal latencies. Lower limb CMCT was corrected for height using the regression model described in Chapter 2.

The group analyses of CMCT and IMC data differed in three respects. Firstly, CMCT readings were analysed on a linear rather than a logarithmic scale. Secondly, as a measure of time CMCT has a bounded domain of $[0,\infty)$, which was taken into account by inverting the inequalities in Equation 5.6. Thirdly, where the cortical MEP was absent, the CMCT was assigned an arbitrary value of 50ms which substantially

exceeded the range of CMCTs observed in this study. This allowed the data to be processed without alterations to the density estimation algorithm, and did not affect the density estimates over the plotted range of 0-30ms.

In each limb, coherence readings from both muscle pairs and CMCT readings from all four muscles were treated as separate markers M_i. The diagnostic accuracy of these markers as tests for MND was quantified using the area under the ROC curve. The ROC curve for each marker M_i was defined as the set of points {FPR(d), TPR(d)} where TPR(d) and FPR(d) are the true and false positive rates associated with the positivity criterion $M_i \geq d$ for a discrimination threshold d in the range (–∞,0). Where the area under the ROC curve (AUC) was less than 0.5, the positivity criterion was inverted, equivalent to reflecting the ROC curve about the diagonal. The AUC thus had an effective range of [0.5,1], with 0.5 indicating no discrimination capacity and 1 indicating perfect discrimination capacity.

We sought linear combinations of markers which maximised the AUC associated with the composite marker, entering either both coherence markers, all four CMCT markers or all six coherence and CMCT markers into the analysis. Each marker was transformed to standardised Z-scores. For a set of n markers M_i, $n-1$ raw coefficients α_i were assigned random values in the range [-1,1]. The first coefficient did not require transformation, so $\gamma_1 = \alpha_1$; subsequent coefficients were transformed according to the formula:

$$\gamma_i = \alpha_i \sqrt{1 - \sum_{j=1}^{i-1} \alpha_j^2} \quad , \qquad i > 1 \tag{5.9}$$

The linear combination of markers was then computed as:

$$N(\gamma) = \sum_{i=1}^{n-1} \gamma_i M_i + \sqrt{1 - \sum_{i=1}^{n-1} \gamma_i^2} \cdot M_n \tag{5.10}$$

From this starting condition, we used the GlobalSearch solver (Matlab global optimization toolbox) to find the set of coefficients α_i associated with the maximal AUC. GlobalSearch combines a random scatter search with a local gradient-based solver. We permitted up to 10^4 random trial points seeded from the starting condition and up to 10^4 iterations of the local solver per trial point. For each set of markers, we ran GlobalSearch 100 times. Most runs converged to near-identical solutions, and we chose the best overall result (Table 5.2).

Using a similar method, we investigated non-linear combinations involving all possible first-order products of markers, thus extending the number of coefficients to $\binom{n}{2} + n - 1$. The non-linear combination of markers was calculated as:

$$N(\gamma) = \sum_{i=1}^{n} \gamma_i M_i + \sum_{i=1}^{n-2} \sum_{j=i+1}^{n} \gamma_{i,j} M_i M_j + \sqrt{1 - \sum_{i=1}^{n} \gamma_i^2 - \sum_{i=1}^{n-2} \sum_{j=i+1}^{n} \gamma_{i,j}^2} \cdot M_{n-1} M_n \quad (5.11)$$

For each marker or combination of markers, the AUC was also evaluated in the ALS and PBP subgroups (Table 5.2), with the positivity criteria and any coefficients having previously been determined in the whole MND group. Since no further inversion of the positivity criteria was permitted, the AUCs for these subgroups had a range of [0,1]. Other phenotypes including ALS/PBP overlap, primary lateral sclerosis (PLS) and progressive muscular atrophy (PMA) were not evaluated separately due to the low number of subjects in each of these groups (Table 5.1). Confidence intervals for AUCs were estimated using bootstrapping. Owing to the substantial number of potential comparisons, we did not use formal statistical tests when comparing AUCs between markers and subgroups.

Table 5.2: Area under the ROC curve (AUC) associated with coherence and CMCT markers and their optimal linear and non-linear combinations, and coefficients used for deriving these combinations. The AUC was calculated in the entire MND cohort for each individual marker, and coefficients were sought which maximised the AUC for the combination of a given number of markers. These combinations were either linear, using coefficients α_i, or non-linear, referring to the additional inclusion of first-order products of all possible combinations of markers and using coefficients α_i and $\alpha_{i,j}$. Combining a given number of markers n involved $n-1$ explicitly defined coefficients, with the coefficient for the last marker given implicitly by the square root term (SRT) as defined in Equations 5.10 and 5.11. AUCs were also calculated for the subgroups of ALS and PBP; any combined markers employed coefficients previously determined in the entire MND cohort. (comb'n=combination)

	Parameter		**Coherence**				**CMCT**						**Both**	
			EDC-FDI	FDS-FDI	Linear comb'n	Non-linear comb'n	FDI	APB	FDS	EDC	Linear comb'n	Non-linear comb'n	Linear comb'n	Non-linear comb'n
Upper limb	AUC	All phenotypes	0.786	0.831	0.832	0.839	0.659	0.698	0.568	0.707	0.758	0.791	0.891	0.895
		ALS	0.806	0.848	0.848	0.849	0.675	0.704	0.589	0.705	0.747	0.772	0.890	0.895
		PBP	0.701	0.793	0.796	0.767	0.207	0.603	0.353	0.555	0.566	0.557	0.804	0.698
	Linear coefficients α_i	EDC-FDI			0.047	0.457							0.538	-0.483
		FDS-FDI			SRT	0.643							SRT	-0.510
		FDI									0.343	0.326	-0.220	-0.014
		APB									0.458	0.248	-0.325	0.310
		FDS									-0.479	-0.115	0.383	-0.192
		EDC									SRT	0.555	-0.375	0.368
	Non-linear coefficients $\alpha_{i.j}$	EDC-FDI	FDS-FDI			SRT								SRT
		EDC-FDI	FDI											-0.873
		EDC-FDI	APB											0.412
		EDC-FDI	FDS											0.980
		EDC-FDI	EDC											0.907
		FDS-FDI	FDI											-0.776
		FDS-FDI	APB											-0.320
		FDS-FDI	FDS											0.370
		FDS-FDI	EDC											-0.380
		FDI	APB									0.489		0.282
		FDI	FDS									0.430		0.155
		FDI	EDC									0.614		0.667
		APB	FDS									-0.132		0.196
		APB	EDC									0.297		-0.464
		FDS	EDC									SRT		0.849

	Parameter		Coherence				CMCT						Both	
			MG-EDB	TA-EDB	Linear comb'n	Non-linear comb'n	EDB	AH	TA	MG	Linear comb'n	Non-linear comb'n	Linear comb'n	Non-linear comb'n
Lower limb	AUC	All phenotypes	0.793	0.769	0.796	0.796	0.795	0.790	0.819	0.777	0.896	0.908	0.927	0.939
		ALS	0.739	0.715	0.743	0.743	0.814	0.761	0.835	0.772	0.885	0.908	0.911	0.935
		PBP	0.842	0.850	0.848	0.848	0.842	0.860	0.783	0.773	0.930	0.860	0.956	0.879
	Linear coefficients α_i	MG-EDB			0.948	0.949							-0.281	-0.167
		TA-EDB			SRT	1.000							SRT	0.480
		EDB									0.324	-0.372	-0.235	-0.276
		AH									0.482	-0.418	-0.469	-0.335
		TA									0.901	-0.511	-0.612	-0.479
		MG									SRT	-0.172	-0.373	-0.167
	Non-linear coefficients $\alpha_{i.j}$	MG-EDB	TA-EDB			SRT								SRT
		MG-EDB	EDB											-0.999
		MG-EDB	AH											0.719
		MG-EDB	TA											0.017
		MG-EDB	MG											-0.790
		TA-EDB	EDB											0.255
		TA-EDB	AH											0.873
		TA-EDB	TA											-0.430
		TA-EDB	MG											-0.034
		EDB	AH									-0.275		-0.176
		EDB	TA									-0.741		-0.784
		EDB	MG									0.995		0.855
		AH	TA									0.629		0.208
		AH	MG									-0.598		0.302
		TA	MG									SRT		-0.323

5.4 Results

5.4.1 IMC

Single-subject power and coherence data for a control subject and a patient with MND are shown in Figure 5.2. In subjects from either group, power usually peaked in the 15-30Hz band. In control subjects, coherence typically also peaked in the 15-30Hz band, whereas in patients with MND 15-30Hz coherence was often less pronounced or absent.

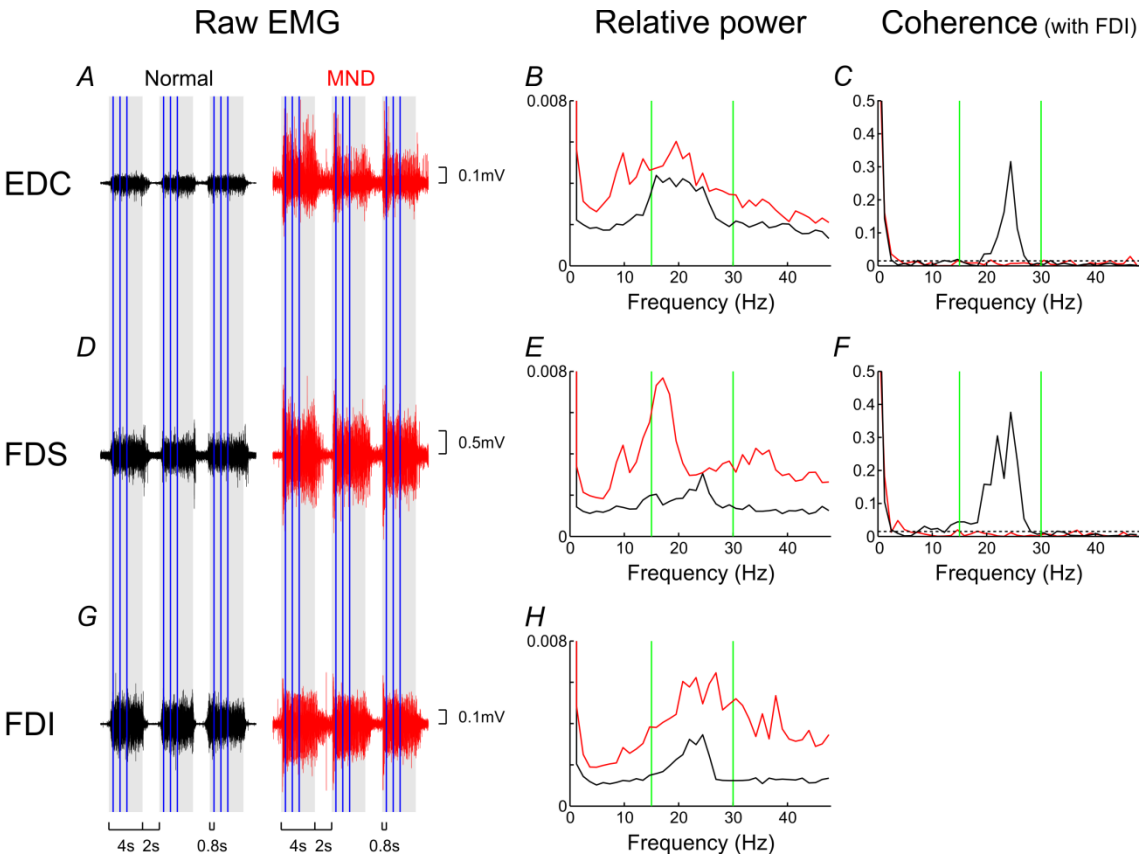

Figure 5.2: Single-subject power and coherence in the upper limb. Raw EMG is shown for three sample trials in a normal control subject (black) and in a patient with MND (red; A, D, G). The grey rectangles represent the cued contraction phase of the task, and the vertical blue lines indicate the two FFT windows during the hold phase. The spectra show relative power (B, E, H) and coherence with FDI (C, F) for each subject. The 15-30Hz beta-band is designated by the green lines, and the dotted horizontal lines indicate the significance level for coherence. In both subjects, the power spectra peaked in the 15-30Hz band, but only the control subject showed significant 15-30Hz coherence.

In order to illustrate the difference in coherence between both groups, we calculated group averages (Figure 5.3). 15-30Hz coherence in all muscle pairs was significant in

the control group and lower but still significant in the MND group. Notably, this does not imply that individual subjects in each group necessarily possessed significant 15-30Hz coherence (e.g. subject with MND in Figure 5.2).

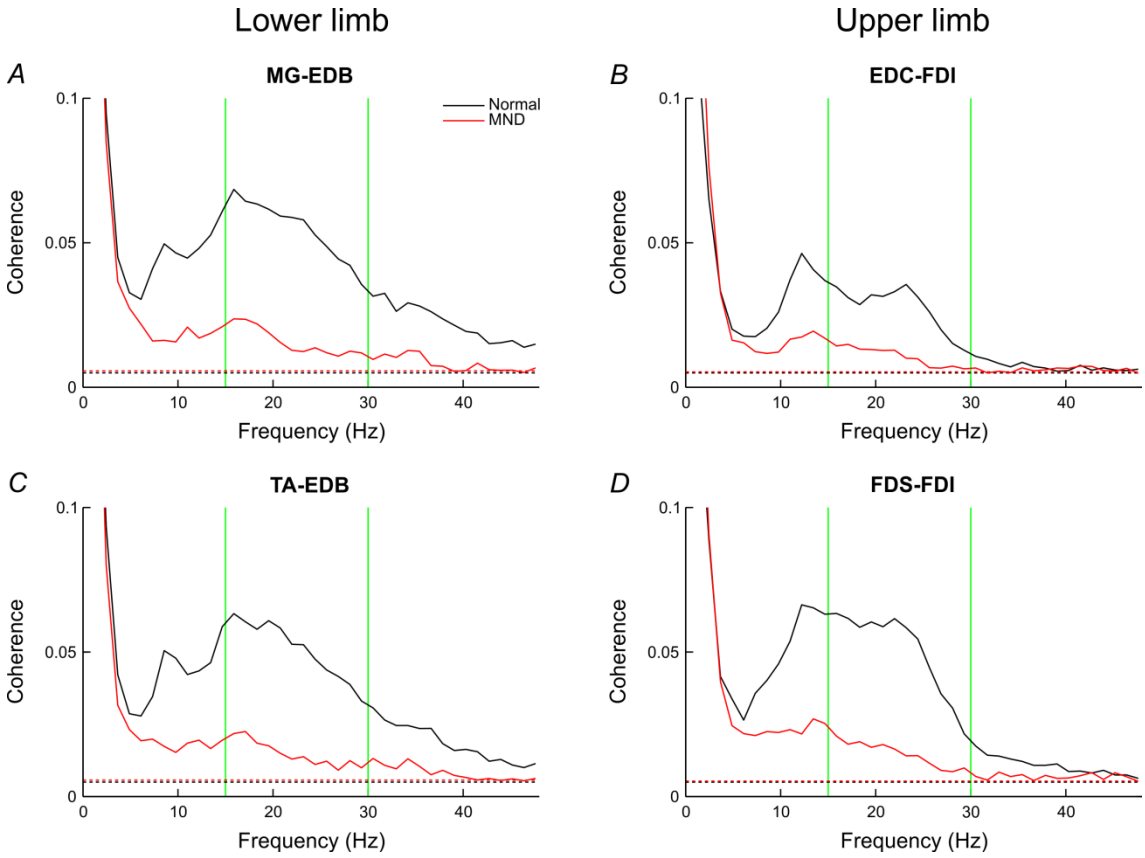

Figure 5.3: Group data for coherence. Average coherence spectra in normal control subjects (black) and patients with MND (red) are shown for MG-EDB and TA-EDB in the lower limb (A, C) and for EDC-FDI and FDS-FDI in the upper limb (B, D). The dotted horizontal lines indicate the significance level for average coherence, with the vertical green lines representing the 15-30Hz beta-band. In normal subjects (black), significant average coherence was present in the 15-30Hz band for each muscle pair. In patients with MND (red), average 15-30Hz coherence was lower but remained significant. Note that significant average coherence on a group level does not imply that individual subjects within each group necessarily possessed significant 15-30Hz coherence.

These group averages describe general trends but do not allow us to visualise the variation within each group. To achieve this, we compared the distributions of individual coherence measurements between both groups. Coherence was averaged across the 15-30Hz window in each subject, and log-transformed averages were compared between MND and control groups for all muscle pairs (Figure 5.4). The cumulative distributions of coherence are shown by the stairstep curves in Figure 5.4 A,

B, G, H. Coherence was generally lower in MND though the ranges of coherence in the MND and control groups largely overlapped. Group distributions were not adequately fitted by a normal model, shown as the smooth dotted curves, and were therefore modelled using variable kernel density estimation, shown by the smooth unbroken curves. PDFs estimated using this model are shown in Figure 5.4 C, D, I, J. The ratios of the PDFs for MND and control groups, equivalent to the odds of a subject having MND at a given level of coherence, are plotted in Figure 5.4 E, F, K, L. The odds peaked at over 10:1 at low coherence values in each muscle pair, and dropped off to less than unity at higher coherence readings.

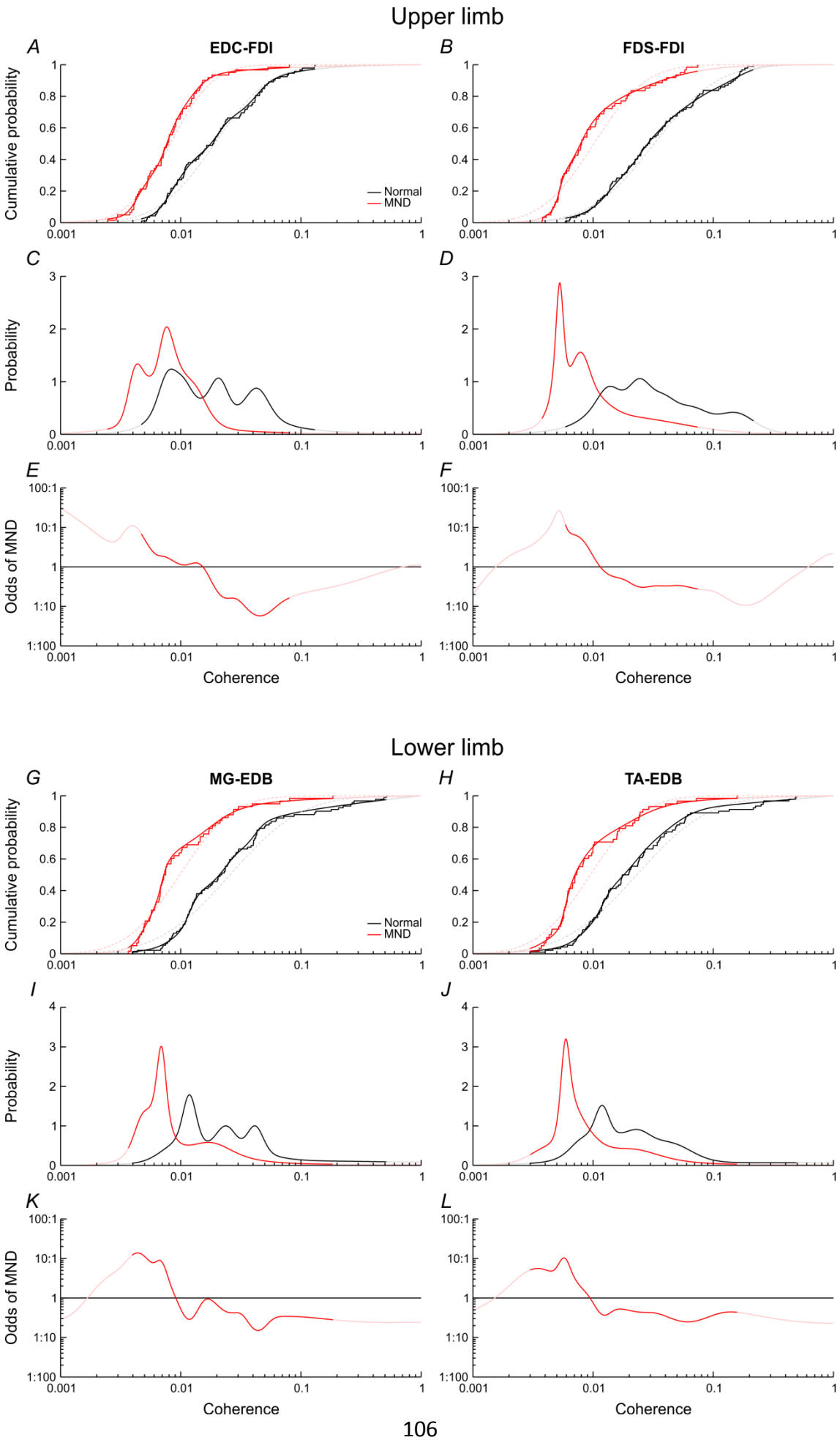
Upper limb
A
EDC-FDI
B
FDS-FDI
Cumulative probability
Normal
MND
C
D
Probability
E
F
Odds of MND
100:1
10:1
1
1:10
1:100
0.001
0.01
0.1
1
Coherence
Lower limb
G
MG-EDB
H
TA-EDB
I
J
K
L

Figure 5.4: Coherence in normal control subjects (black) and patients with MND (red) with corresponding variable kernel density estimates. The stairstep curves show the cumulative probability distribution of average 15-30Hz coherence within each group (A, B, G, H). The corresponding density estimation and normal models are represented by the smooth unbroken and dotted curves respectively. Non-cumulative probability distributions were calculated from the density estimation model (C, D, I, J). The odds of a subject having MND at a given level of coherence were computed as the ratio of the probability distributions (E, F, K, L). Curves derived from density estimation models use a fainter colour where the model was extrapolated outside the range of the measured values. Patients with MND generally had lower coherence values than normal control subjects. This is reflected in the odds of MND being greater than unity at low coherence readings.

Thus far, coherence has been investigated in individual muscle pairs. We extended this analysis by linearly combining coherence measurements from both muscle pairs in a given limb, and by employing the area under the ROC curve (AUC) as a summary measure of performance (Figure 5.5). The AUC for the optimal combination (black) was very similar to that for FDS-FDI in the upper limb (red) and for MG-EDB in the lower limb (blue), suggesting that single muscle pairs performed as well as the best linear combination.

The side panels of the ROC curves allow discrimination thresholds to be read off for any chosen TPR or FPR (Figure 5.5 B, D). For example, if one were to accept a FPR of 10% in FDS-FDI, the corresponding coherence threshold would be 0.0097 and the TPR, equivalent to sensitivity, would be 60.7% (Figure 5.5 B, dashed arrows).

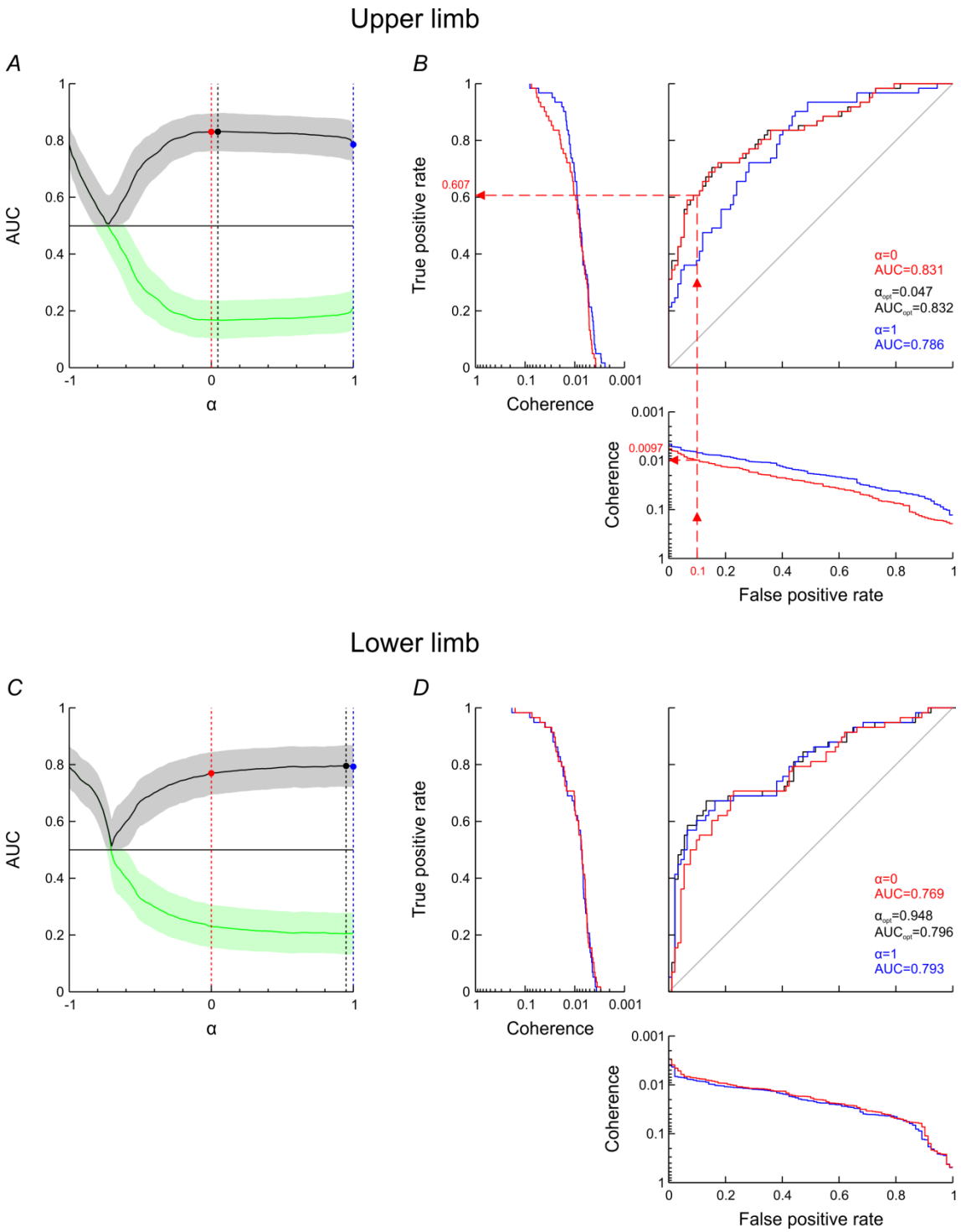

Figure 5.5: Optimal linear combination of coherence data. Standardised coherence readings from both muscle pairs in a given limb were combined using a parameter α in the range [-1,1], where values of 0 and ±1 correspond to exclusive use of one muscle pair and other values represent graded combinations. For each value of α, the combined measure was evaluated as a binary classifier for MND by determining the area under the ROC curve (AUC; A, C). Where the AUC was less than 0.5 (green curve), the ROC curve was inverted, thus yielding an effective AUC ranging from 0.5 to 1 (black curve); corresponding bootstrapped 95% confidence intervals are shown (shaded areas). The dotted lines indicate α values of 0 (red), 1 (blue) and α_{opt}, the value yielding the maximal effective AUC (black). α_{opt} was close to 0 in the upper limb (equivalent to

use of FDS-FDI coherence alone) and close to 1 in the lower limb (equivalent to use of MG-EDB coherence alone), suggesting that coherence readings from a single muscle pair performed as well as the best linear combination of both pairs in a given limb. ROC curves are illustrated for individual muscle pairs (red, blue) and the optimal combination (black; B, D). Side panels indicate coherence at a given level of true or false positives; these are only shown for individual muscle pairs as the optimal combination is a score measured on an arbitrary scale. The dashed arrows (B) demonstrate how, for a given false positive rate (0.1=10%) in FDS-FDI, the diagram can be used to find the corresponding coherence threshold (0.0097) and true positive rate (0.607=60.7%).

5.4.2 CMCT

Single-subject MEP data for a control subject and a patient with MND are displayed in Figure 5.6. All control subjects exhibited clear cortical and root MEPs. In MND, cortical responses were usually small and delayed or, in some cases, absent. Root responses were often diminished in amplitude but had normal or near-normal latencies; again, they were absent in some patients.

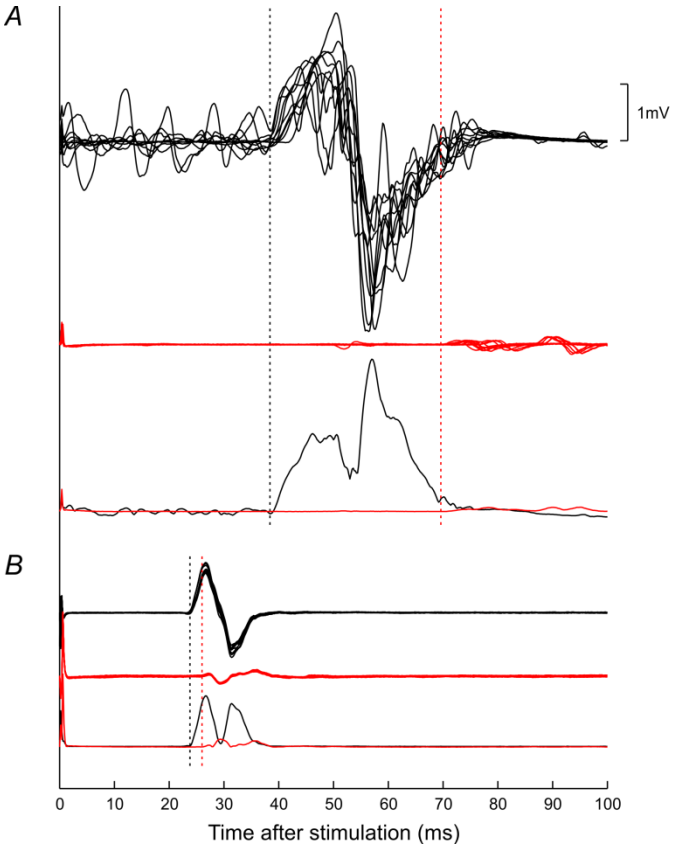

Figure 5.6: Single-subject cortical (A) and root (B) MEPs in EDB. For each site of stimulation, three types of trace are shown: ten superimposed raw sweeps for a normal control subject (black, top) and a patient with MND (red, middle), and averages

of rectified sweeps for both subjects (bottom). Latencies (dashed lines) were assigned using the average of the rectified sweeps. In the subject with MND, the cortical MEP was markedly delayed and reduced in amplitude; the root MEP had a latency which was comparable to that in the normal subject but amplitude was greatly reduced.

One could argue that cortical or root MEP responses might have been absent in some patients because they did not tolerate sufficiently strong stimulation. However, mean cortical stimulation intensities in patients who did not show clear cortical MEP responses (upper limb: 80.6±12.5%, mean±1.96SE; lower limb: 66.4±10.3%) were at least as high as those in patients who did (upper limb: 61.6±4.8%, p=0.003, unpaired t-test; lower limb: 62.4±4.3%, p=0.434) as well as those in control subjects (upper limb: 51.4±1.8%, p<0.001; lower limb 56.6±2.0%, p=0.006). Similarly, mean root stimulation intensities in patients with MND who lacked root MEP responses (upper limb: 60.0±6.2%; lower limb: 95±9.8%) were at least as high as those in patients with clear root MEP responses (upper limb: 62.2±3.2%, p=0.687; lower limb: 73.6±3.8%, p=0.039) as well as those in control subjects (upper limb: 56.3±2.0%, p=0.395; lower limb: 64.1±3.1%, p=0.004).

The group distributions of individual CMCT measurements were compared using an approach similar to that applied to the IMC data. Cumulative distributions of CMCTs are shown as the stairstep curves in Figure 5.7 A-D and M-P. In the upper limb, the MND and control distributions overlapped at low CMCTs. However, the MND distributions featured longer right-hand tails, and between 5.6 and 14.8% of cortical MEPs were absent. In the lower limb, CMCTs were generally longer in MND with 11.1 to 16.7% of cortical MEPs being absent. Nonetheless, the ranges of CMCTs in MND and control groups overlapped considerably. Distributions were modelled with variable kernel density estimates, represented by the smooth curves. This model gave rise to estimated PDFs (Figure 5.7 E-H and Q-T) and odds functions (Figure 5.7 I-L and U-X). In the upper limb, the close similarity of the distributions at low CMCTs resulted in the odds functions having complex shapes with multiple crossings of unity, whereas in the lower limb the greater separation of distributions led to more simply shaped odds functions.

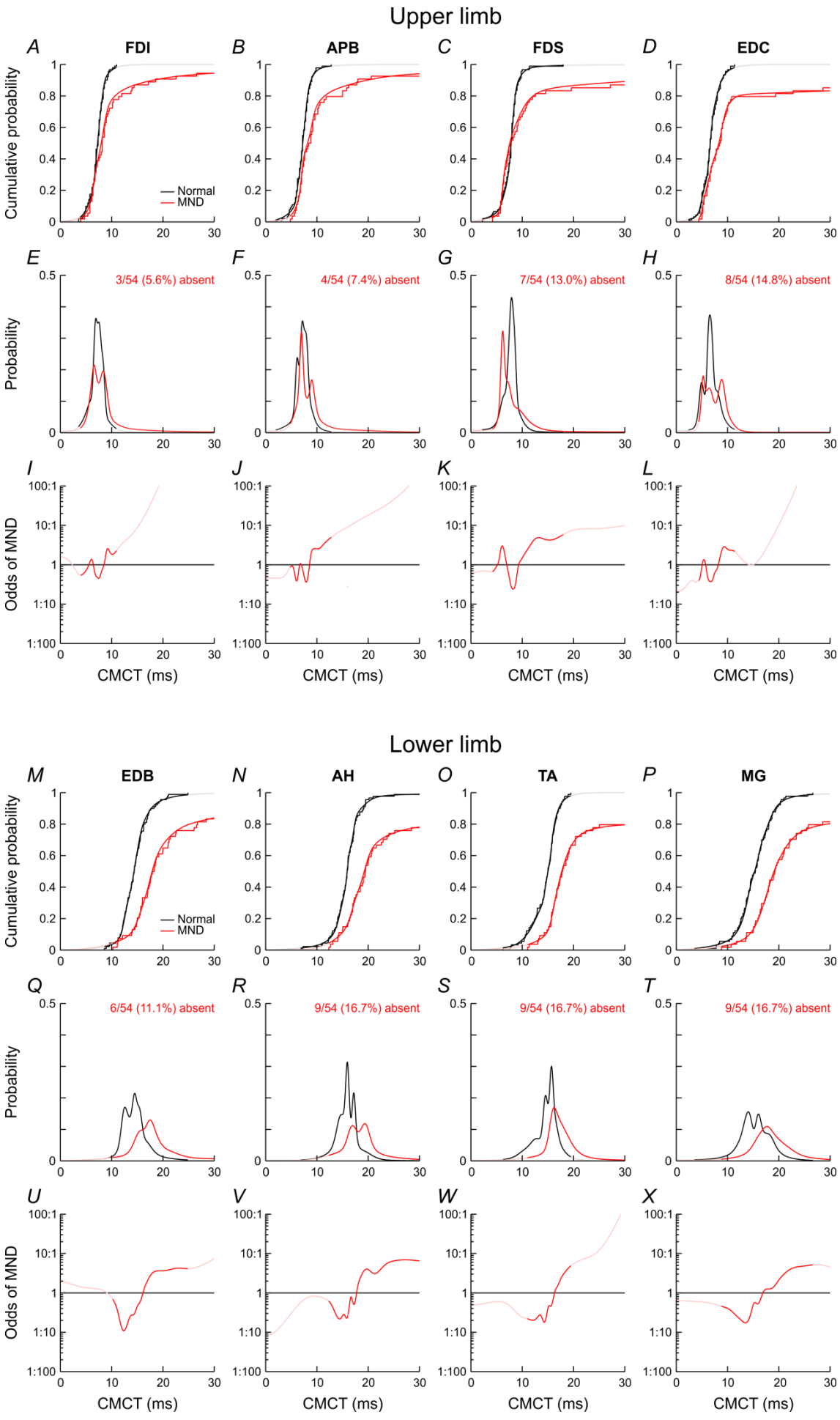
Upper limb
A
FDI
B
APB
C
FDS
D
EDC
Cumulative probability
Normal
MND
E
3/54 (5.6%) absent
F
4/54 (7.4%) absent
G
7/54 (13.0%) absent
H
8/54 (14.8%) absent
Probability
I
J
K
L
Odds of MND
100:1
10:1
1
1:10
1:100
CMCT (ms)
Lower limb
M
EDB
N
AH
O
TA
P
MG
Q
6/54 (11.1%) absent
R
9/54 (16.7%) absent
S
9/54 (16.7%) absent
T
9/54 (16.7%) absent
U
V
W
X

Figure 5.7: CMCT in normal control subjects (black) and patients with MND (red) with corresponding variable kernel density estimates. The stairstep curves represent the cumulative probability distribution of CMCTs within each group (A-D, M-P), with the smooth curves showing corresponding density estimation models. These models were also used to calculate non-cumulative probability distributions (E-H, Q-T). The proportion of absent cortical responses in the MND group is indicated; responses were present in all normal subjects. The odds of a subject having MND at a given CMCT were calculated as the ratio of the probability distributions (I-L, U-X). Curves derived from density estimation models use a fainter colour where the model was extrapolated outside the range of the measured values. Patients with MND generally had higher CMCT readings than normal control subjects, particularly in the lower limb. Although the odds of MND were mostly greater than unity at higher CMCT readings, the shape of the odds functions was often complex.

Where limb involvement was asymmetrical, we aimed to study the most affected limb. If the subject was unable to perform the coherence task on the most affected side, we assessed the contralateral limb instead. It could be argued that CMCT would have performed better if the most affected side had been studied throughout. To investigate this possibility, we compared linear combinations of CMCT from limbs on the less affected side and from all other limbs. Bootstrapped samples of AUC values were obtained for both groups using the coefficients determined in the whole MND dataset. The differences between all possible pairs of AUC values across both groups were calculated, allowing the distribution of the difference in AUC to be estimated. The difference in AUC was not significantly different from zero (upper limb $p=0.101$, lower limb $p=0.354$; two-tailed probabilities), thus negating the argument that CMCT would have performed better on the most affected side.

5.4.3 Comparison of all individual and combined markers

The ROC curves associated with the optimal linear combinations of CMCT in upper and lower limbs are illustrated in Figure 5.8, and those for the optimal linear combination of both CMCT and IMC are shown in Figure 5.9. The AUCs for all individual and combined markers are summarised in Figure 5.10 A and D. In the upper limb, coherence in FDS-FDI performed as well as linear or non-linear combinations of both coherence markers (Figure 5.10 A, black). CMCT to individual target muscles was associated with slightly lower AUCs (Figure 5.10 A, red); whilst the AUC was increased by combining all CMCT markers, such combinations still did not reach the AUC

associated with coherence in FDS-FDI. Combinations of both CMCT and coherence markers (Figure 5.10 A, blue) resulted in AUCs which were only slightly higher than the AUC for coherence in FDS-FDI. In the lower limb, coherence in MG-EDB had an AUC comparable to linear and non-linear combinations of both coherence markers (Figure 5.10 D, black). AUCs associated with individual CMCT markers (Figure 5.10 D, red) reached similar levels compared to MG-EDB; combinations of CMCT markers provided a further increase in AUC which was only increased marginally by additional inclusion of the coherence markers (Figure 5.10 D, blue). Generally, non-linear combinations were not associated with substantially greater AUCs than linear combinations, and in some instances performed worse.

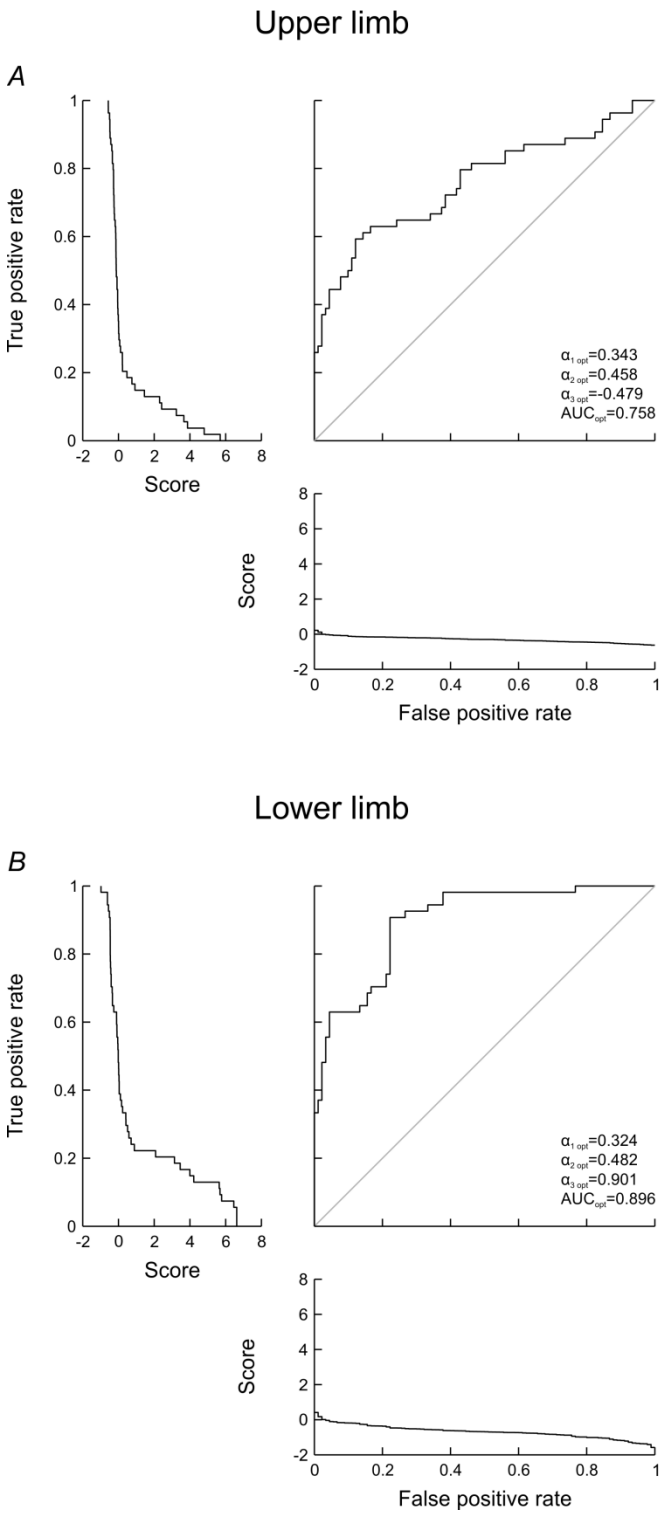

Figure 5.8: Optimal linear combination of CMCT data. Standardised CMCT readings from each muscle in a given limb were combined using three parameters $\alpha_{1\text{-}3}$, allowing all relative linear combinations. The combined measure was evaluated as a binary classifier for MND by determining the area under the ROC curve (AUC). The ROC curves and parameter values shown represent the linear combination with the maximal effective area under the curve. Side panels indicate the combined measure at a given level of true or false positives. The best linear combination of CMCT performed slightly better than CMCT from the best individual muscle, particularly in the lower limb (also see Figure 5.10).

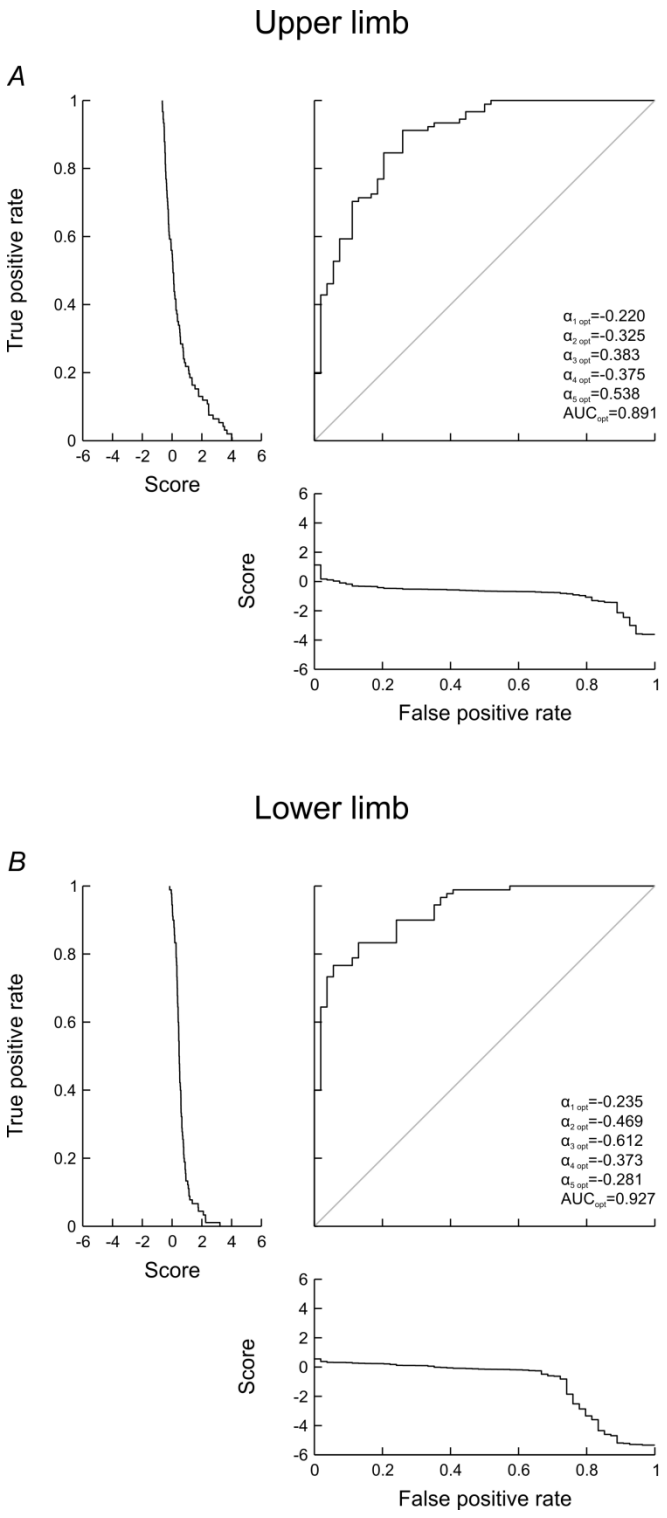

Figure 5.9: Optimal linear combination of coherence and CMCT data. Standardised coherence readings from each muscle pair and CMCT readings from each muscle in a given limb were combined using five parameters $\alpha_{1\text{-}5}$, allowing all relative linear combinations. The combined measure was evaluated as a binary classifier for MND by determining the area under the ROC curve (AUC). The ROC curves and parameter values shown represent the linear combination with the maximal effective area under the curve. Side panels indicate the combined measure at a given level of true or false positives. The best linear combination of coherence and CMCT data performed slightly

better than the best linear combination of either coherence or CMCT, particularly in the upper limb (also see Figure 5.10).

5.4.4 Subgroup analysis

Subgroup analyses of AUC by MND phenotype are shown for ALS (Figure 5.10 B and E) and PBP (Figure 5.10 C and F). In ALS, AUCs in the upper limb were very similar to those in the main analysis. In the lower limb, AUCs associated with coherence markers or their combinations dropped slightly, whilst those associated with CMCT markers or their combinations remained largely unchanged. In consequence, individual CMCT markers had a higher AUC than any coherence-based marker, and this lead was slightly greater for combinations of CMCT markers. In PBP, upper limb AUCs were slightly lower for coherence-based markers but substantially lower for CMCT-based markers when compared to the main analysis. Thus any markers incorporating coherence outperformed those based purely on CMCT. Notably, CMCT in FDI and FDS was less than 0.5 as the positivity criterion was not permitted to be inverted relative to the main analysis, and few subjects entered the CMCT analysis in PBP (n=6). In the lower limb, AUCs were very similar to those found in the main analysis.

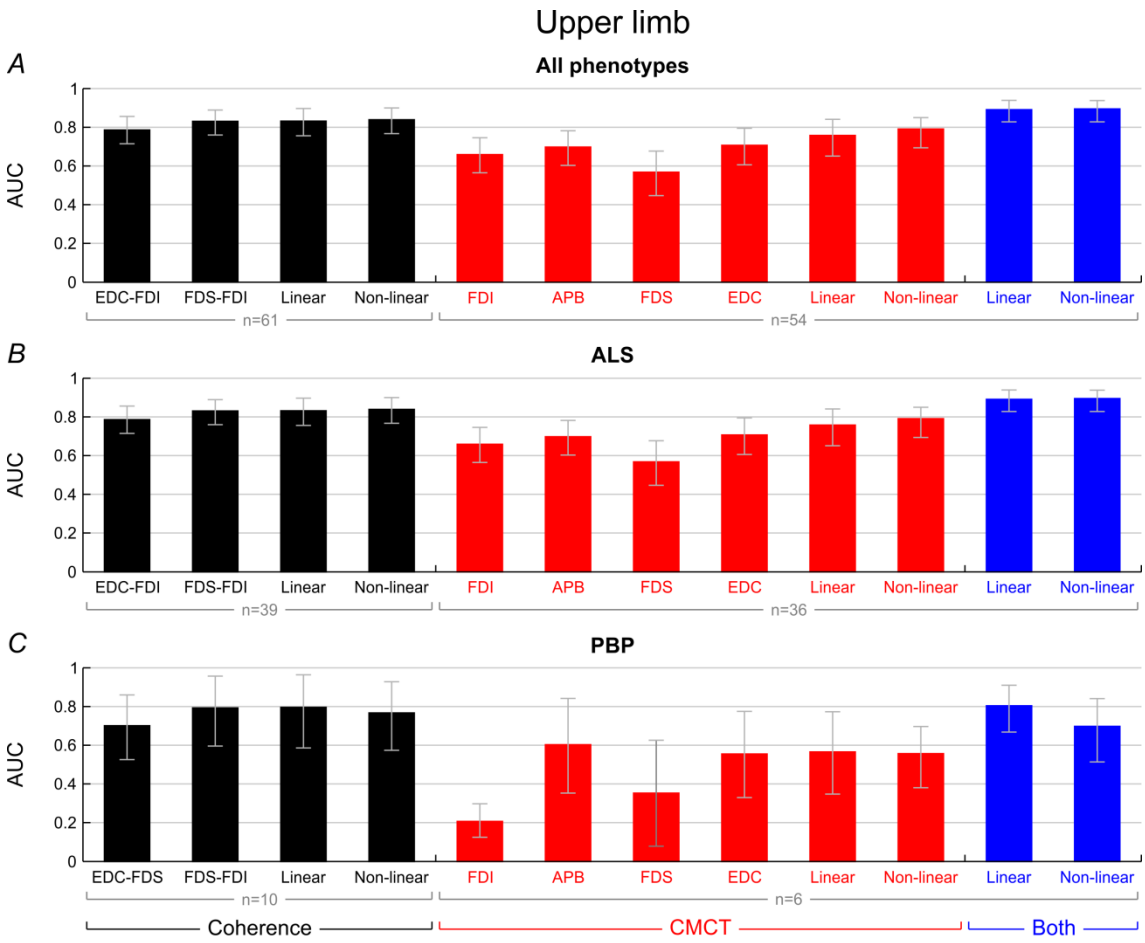
Upper limb
A
All phenotypes
AUC
EDC-FDI
FDS-FDI
Linear
Non-linear
FDI
APB
FDS
EDC
Linear
Non-linear
Linear
Non-linear
n=61
n=54
B
ALS
n=39
n=36
C
PBP
EDC-FDS
n=10
n=6
Coherence
CMCT
Both

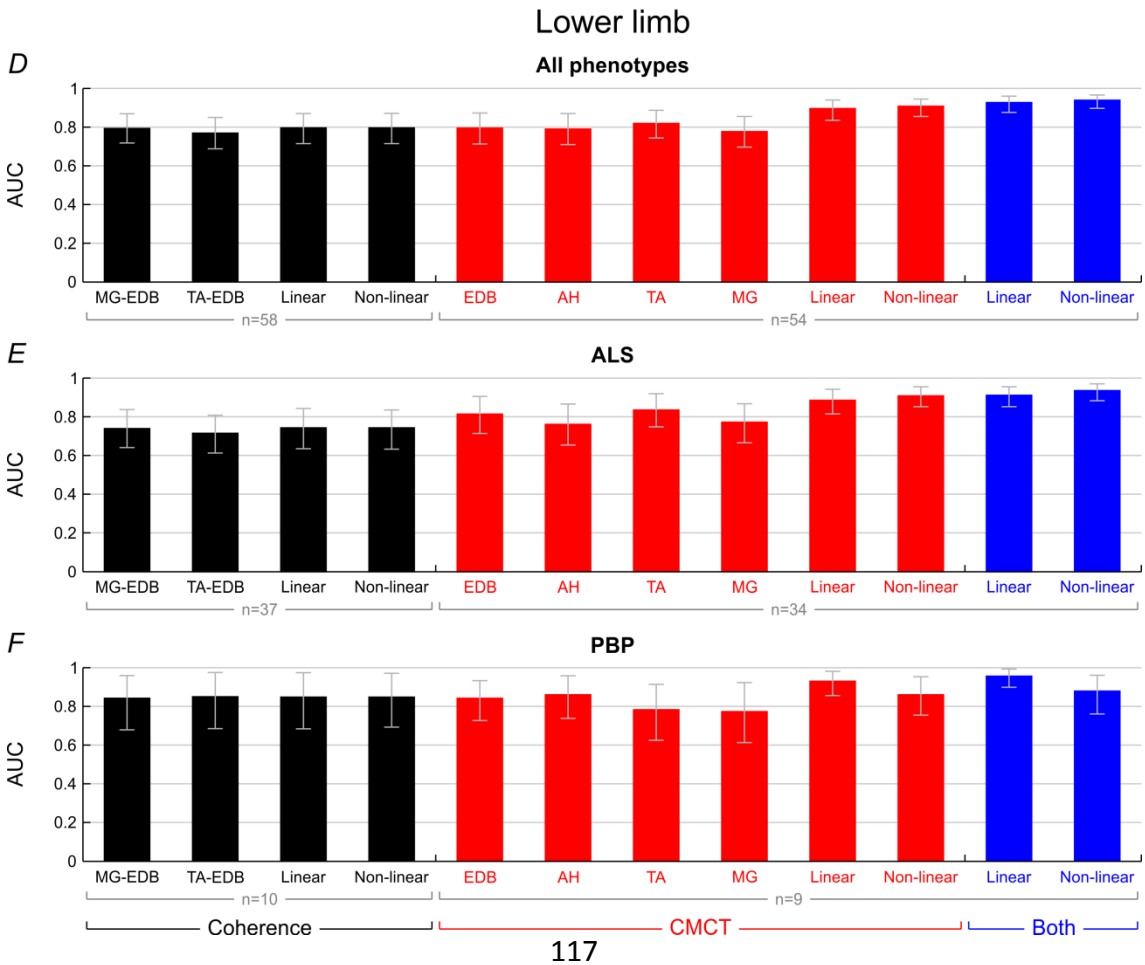
Lower limb
D
All phenotypes
AUC
MG-EDB
TA-EDB
Linear
Non-linear
EDB
AH
TA
MG
Linear
Non-linear
Linear
Non-linear
n=58
n=54
E
ALS
n=37
n=34
F
PBP
n=10
n=9
Coherence
CMCT
Both

Figure 5.10: Area under the ROC curve (AUC) for individual and combined measures of coherence (black), CMCT (red) or both (blue). AUCs are shown for the entire MND cohort ('All phenotypes'; A, D) as well as the ALS (B, E) and PBP (C, F) subgroups. Linear and non-linear combinations were optimised using data from the entire MND cohort and the optimal parameters applied to the subgroups. The number of subjects entering the analysis is given below the relevant markers. Error bars indicate bootstrapped 95% confidence intervals.

5.5 Discussion

The distributions of 15-30Hz IMC and CMCT differed between MND and control groups, suggesting that both types of marker have potential for assessing UMN function in MND.

5.5.1 Analysis

In the previous study from our group, data were plausibly normally distributed as assessed using a Kolmogorov-Smirnov test. The normal model fitted to the data resulted in odds functions with a simple shape and a single maximum (Fisher *et al.*, 2012). The Shapiro-Wilk test used to assess normality in the present study is statistically more powerful than the Kolmogorov-Smirnov test, particularly for small samples; the larger size of the samples gathered here also boosted power (Razali & Wah, 2011). The current data deviated significantly from normality, and a normal model would have poorly fitted the left-hand tails of the distributions (Figure 5.4 A, B, G, H), which define the odds function at the low levels of coherence expected in MND. Whilst a distribution-free variable kernel density model fitted the data well, it often led to odds functions with complex shapes and thus questionable utility.

Therefore, we quantified the performance of individual and combined markers using the area under the ROC curve, which requires no modelling of the population distributions. Furthermore, this approach does not require fixed discrimination thresholds to be specified. Deriving these would require information on costs associated with errors as well as information on disease prevalence (Pepe & Thompson, 2000), and was beyond the scope of this study.

Combinations of markers were optimised using all relevant data. This presents a risk of overfitting, particularly for small subgroups and non-linear combinations with many degrees of freedom, so the reported models might perform less well on a different dataset. The AUCs associated with combined markers should be viewed as exploratory results indicating a ceiling for what may be achieved with optimisation techniques. In the future, the problem of overfitting could be avoided by using cross-validation. This would involve splitting the data into training and validation sets; the former would be used to design the model, with the latter reserved for evaluating performance.

5.5.2 Summary of results

Despite these provisos, analysis of combined markers helped to make several important points. Firstly, IMC in the best muscle pair – FDS-FDI in the upper and MG-EDB in the lower limb – was as good a classifier as any combinations of IMC from both muscle pairs in the respective limb. This implies that only one muscle pair per limb needs to be studied. Secondly, in the upper limb, IMC in the best muscle pair performed better than all CMCT markers, including combinations of CMCT. Thirdly, in the lower limb, the performance of IMC in the best muscle pair was very similar to that of CMCT in individual muscles, but lagged behind combined CMCT markers. Finally, non-linear combinations performed at best marginally better than their linear counterparts, suggesting that linear combinations suffice.

5.5.3 Potential confounders

Transmitter systems involved in the generation of beta-band oscillations and coherence are susceptible to relevant CNS-active drugs. For example, diazepam and propranolol have been reported to alter beta-band oscillations and/or coherence (Baker & Baker, 2003, 2012). We selected control subjects who did not use any neurotropic medication. Since most patients with MND received multiple drugs with potential CNS effects it was not realistic to exclude them. Amongst these patients the numbers of different agents and their combinations were both high, thus precluding subgroup analysis. Importantly, no difference in IMC was previously found between patients on and off riluzole (Fisher *et al.*, 2012), a drug with myriad pharmacological actions used by 57% of patients in our study.

Fatigue is a further factor which can affect coherence. Many previous studies employed tasks involving sustained contractions (Conway *et al.*, 1995; Ohara *et al.*, 2000; Ushiyama *et al.*, 2011b). Whilst such tasks facilitate consistent performance, they would be difficult or impossible to execute for patients with neurological deficits. Therefore, we used a phasic task with minimal or no instrumentation and explicitly allowed subjects to request breaks. Any fatigue which might have occurred despite these measures should have caused coherence to be overestimated (Tecchio *et al.*, 2006; Ushiyama *et al.*, 2011a). With fatigue being more likely in the MND group, the distance between the coherence distributions of MND and control groups would have narrowed, causing the utility of coherence to be underestimated rather than exaggerated.

5.5.4 Pathways probed by IMC

Sensory afferents have been shown to play an important role in the generation of CMC (Baker *et al.*, 2006; Riddle & Baker, 2005; Witham *et al.*, 2011; Witham *et al.*, 2010) and IMC (Kilner *et al.*, 2004; Pohja & Salenius, 2003). It is important to ascertain normal sensory function before coherence can be used to draw inferences about CST integrity. Whilst subclinical sensory abnormalities apparent on nerve conduction studies (NCS) are increasingly recognised in MND (Pugdahl *et al.*, 2007), none were detected in our patient cohort; all underwent NCS, and sensory abnormalities were only detected in two patients with known diabetes mellitus, who were excluded from subsequent analysis. It was previously suggested that somatosensory evoked potentials (SEP) should also be measured (Fisher *et al.*, 2012). However, the association between MND and SEP abnormalities has remained controversial (Hamada *et al.*, 2007), and we did not routinely assess SEP.

We assumed that abnormalities in IMC occurring in the absence of sensory deficits were attributable to CST dysfunction. This assumption is backed by present knowledge of the pathways involved in coherence (Witham *et al.*, 2011; Witham *et al.*, 2010), by the absence of coherence after CST damage through capsular strokes (Farmer *et al.*, 1993), spinal cord lesions (Hansen *et al.*, 2005; Norton *et al.*, 2003) and PLS in humans (Fisher *et al.*, 2012), and by the absence of coherence after selective CST ablation in macaques (Fisher *et al.*, 2012; Nishimura *et al.*, 2009). However, it is difficult to

validate any marker of CST function in MND: at present, there is no gold standard *in vivo* test of CST integrity, and correlating IMC estimates with autopsy findings in a sizeable cohort is not realistic.

It is conceivable that disease outside the CST and sensory pathways might have contributed to abnormalities of IMC, particularly given the widespread nature of MND pathology (Atsuta *et al.*, 2009; Geser *et al.*, 2008). Coherence appeared to be diminished in patients with PMA (Fisher *et al.*, 2012), suggesting that it may be affected by LMN damage. It would be of great interest to determine whether this is the case, as LMN dysfunction would constitute a very common potential confounder in MND.

5.5.5 Outlook

The effect of LMN lesions on coherence requires further study. One approach would involve measuring coherence in patients with acquired neurological conditions causing a LMN deficit (Chapter 6). However, many disorders do not cause pure LMN involvement and/or have low prevalence, making it difficult to recruit an adequately sized cohort. An alternative approach would involve computational simulation of the effects of LMN dysfunction, for example using a model previously developed by our group (Williams & Baker, 2009).

For IMC to be used as a diagnostic biomarker, a classification threshold separating normal from abnormal needs to be specified. This requires an analysis of potential costs. Eventually, any acceleration of the diagnostic process would be subject to a ceiling, as IMC is unlikely to be measured before patients are reviewed by a neurologist yet much of the diagnostic delay occurs prior to this point (Househam & Swash, 2000; Mitchell *et al.*, 2010).

An evaluation of IMC as a prognostic indicator will be possible once more survival data are available for the present cohort. In addition, a longitudinal follow-up study of IMC should be considered, ideally recruiting subjects at a pre-symptomatic stage, for example from kindreds with mutations in superoxide dismutase 1 (SOD1). In the longer

term, a large prospective study will be required to fully delineate the diagnostic utility of IMC.

5.6 Conclusion

We investigated IMC and CMCT as measures of CST integrity in a cohort of patients with MND, assessing performance using the area under the ROC curve. IMC in a single muscle pair per limb performed better than individual or combined CMCT measures in the upper limb, and drew level with individual CMCT measures in the lower limb, where it was only slightly surpassed by combinations of CMCT. Hence, IMC constitutes a simple, fast and acceptable marker of CST function which rivals the performance of CMCT. However, unlike TMS-based measures, it does not require expensive equipment, and could be deployed at minimal cost to existing EMG facilities in clinical neurophysiology departments.

6 Intermuscular coherence in patients with motor neuron disease mimic syndromes

A spectrum of evidence suggests that the corticospinal tract is critical to coherence. By contrast, the role of peripheral motor nerves and muscles is less clear. In this chapter, I probe the role of different parts of the motor system by examining intermuscular coherence in patients with a range of neurological conditions.

6.1 Abstract

Objective: Intermuscular coherence (IMC) was measured in patients with neurological conditions affecting different parts of the motor system in order to elucidate the relative contributions of these parts to IMC generation.

Methods: 12 patients with hereditary spastic paraparesis (HSP), 7 patients with multifocal motor neuropathy (MMN), 8 patients with inclusion body myositis (IBM), and 92 healthy control subjects were included. In the upper limb, IMC was measured between extensor digitorum communis (EDC) and first dorsal interosseous (FDI) as well as between flexor digitorum superficialis (FDS) and FDI. In the lower limb, IMC was estimated between medial gastrocnemius (MG) and extensor digitorum brevis (EDB) as well as between tibialis anterior (TA) and EDB. Individual and combined IMC markers were analysed using population distributions and the area under the receiver-operating characteristic curve (AUC).

Results: In HSP, IMC was usually decreased in the lower limb and near-normal in the upper limb. In MMN, IMC was slightly diminished in the upper limb and more markedly decreased in the lower limb. In IBM, IMC was globally increased.

Conclusion: HSP affects the corticospinal tract (CST) projecting to lower limb muscles, and the results support the suggestion that the CST has an important role in mediating IMC. MMN is typically thought of as a peripheral motor disorder, and therefore the IMC findings are surprising; possible explanations are discussed. The increase in IMC

observed in IBM is probably attributable to the altered electrical properties of muscle fibres which may facilitate the detection of synchronisation between muscles. Computational modelling may help to clarify further how different parts of the motor system contribute to IMC generation.

6.2 Introduction

At present, there is no sensitive and specific marker of upper motor neuron (UMN) function. Clinical signs such as clonus, hyperreflexia and extensor plantar responses have limited sensitivity for corticospinal tract (CST) pathology (Kaufmann *et al.*, 2004), and do not necessarily reflect pathology in the CST alone (Brown, 1994). Markers based on transcranial magnetic stimulation (TMS) have not shown sufficient diagnostic utility to gain widespread acceptance (Mills, 2003). Similarly, approaches using magnetic resonance imaging (MRI) do not currently reach an adequate level of single-subject performance (Filippi *et al.*, 2010) and remain confined to research facilities.

A recently proposed marker of UMN function exploits the role of the CST in the propagation of oscillatory activity (Fisher *et al.*, 2012). 15-30Hz beta-band oscillations can be recorded from the primary motor cortex (Conway *et al.*, 1995; Halliday *et al.*, 1998; Ohara *et al.*, 2000; Pfurtscheller, 1981). They can be shown to be synchronised with beta-band oscillations in contralateral muscles by means of coherence analysis (corticomuscular coherence, CMC; Conway *et al.*, 1995; Halliday *et al.*, 1998; Ohara *et al.*, 2000). Similarly, beta-band oscillations are coherent between co-contracting muscles in a given limb (Farmer *et al.*, 1993), and such intermuscular coherence (IMC) is deemed to reflect a shared cortical drive. IMC is often preferred to CMC for practical reasons and because it is more consistently detectable in normal subjects (Fisher *et al.*, 2012; Ushiyama *et al.*, 2011b).

A range of evidence outlined in Chapter 5 indicates that IMC is mediated by an efferent-afferent feedback loop in which the CST forms a key component. This has prompted the suggestion that, in the absence of a sensory lesion, IMC constitutes a marker of CST function (Fisher *et al.*, 2012). The hypothesis is difficult to test directly as

there is no gold standard *in vivo* marker of CST function and histological correlates from *post mortem* assessment of the spinal cord are rarely available. It remains possible that, in addition to the CST and afferent pathways, peripheral motor nerves are involved in coherence generation.

To help delineate the relative contributions to IMC generation from different parts of the efferent pathways, we examined IMC in a range of neurological disorders, including hereditary spastic paraparesis (HSP), multifocal motor neuropathy (MMN) and inclusion body myositis (IBM). An overview of these conditions is given below.

HSP affects 3-10/100,000 individuals, and the mode of inheritance may be autosomal dominant, autosomal recessive or X-linked recessive (for a review, see Salinas *et al.*, 2008). The condition is characterised clinically by insidiously progressive spasticity and weakness of the lower limbs, and pathologically by retrograde axonal degeneration of the CST. Pure forms of HSP are dominated by involvement of the CST to the lower limbs, though minor bladder dysfunction, muscle wasting or decreases in distal vibration sense may occur in longstanding disease. Complicated forms involve a more extensive neurological and/or non-neurological phenotype, including polyneuropathy, extrapyramidal and cerebellar features, cognitive impairment, epilepsy, retinopathy, optic atrophy, deafness and skin lesions. For this study, we selected patients with autosomal dominant HSP who carried mutations in the SPG4 and SPG31 genes, which are typically associated with a pure phenotype (Finsterer *et al.*, 2012; Salinas *et al.*, 2008).

MMN is an autoimmune motor neuropathy which has a prevalence of 0.6/100,000 and is commoner in men (M:F=2.7:1; for a review, see Vlam *et al.*, 2012). Clinically, it causes slowly progressive, asymmetrical distal limb weakness without sensory loss. The electrophysiological hallmark is conduction block of peripheral motor nerves outside of common entrapment sites in the absence of sensory abnormalities; however, this can be difficult to detect. High titres of anti-GM1 antibodies are found in approximately 50% of patients but are not entirely specific for MMN. The treatment of choice is intravenous immunoglobulin, which typically results in rapid but temporary improvements in clinical and electrophysiological function.

IBM is a condition of unclear cause which affects 0.43-0.93/100,000 individuals, rising to 3.53/100,000 above the age of 50 (for a review, see Dalakas, 2006). It presents with slowly progressive weakness and atrophy of proximal and distal muscles, often with a characteristic predilection for the quadriceps and deep finger flexors. Affected muscles demonstrate a distinctive histopathology comprising a combination of autoimmune and degenerative features. Despite the pronounced inflammatory component, immunosuppression is generally ineffective.

In this study, IMC readings from patients with HSP, MMN and IBM were compared to readings from healthy control subjects. IMC was evaluated as a binary classifier using the approach described in Chapter 5; receiver-operating characteristic (ROC) curves were constructed and summarised by calculating the area under the curve (AUC). In addition to IMC measurements from individual muscle pairs, we explored optimal linear and non-linear combinations of IMC measurements from both muscle pairs in a given limb.

In HSP, IMC measurements were generally lower than normal in the lower limb but near-normal in the upper limb. In MMN, IMC readings were mostly lower than normal in both upper and lower limbs. In IBM, IMC values were typically greater than normal in upper and lower limbs. The somewhat unexpected findings in MMN and IBM raise interesting points about the extent of MMN pathology and the impact of myopathy on IMC.

6.3 Methods

6.3.1 Subjects

Fourteen patients with genetically confirmed HSP were recruited from the neurogenetics service at Newcastle Upon Tyne Hospitals (P. F. Chinnery); all of these had a 'pure' phenotype suggesting isolated involvement of the CST. Similarly, nine patients with an electroclinical diagnosis of MMN and 11 patients with a clinico-pathological diagnosis of IBM were recruited from the local neuromuscular service (J. A. L. Miller). Two patients with HSP were excluded due to a history of spinal surgery and

an intrathecal baclofen pump respectively. All patients with MMN received regular treatment with intravenous immunoglobulin, and the study was timed such that weakness was clinically apparent but did not preclude effective performance of the coherence task. Patients with MMN or IBM all underwent nerve conduction studies; two patients with MMN and three patients with IBM were excluded due to sensory neuropathy. Thus, 12 patients with HSP, seven patients with MMN and eight patients with IBM were included in the analysis. Clinical features including drug histories are summarised in Appendix C.

Control data were obtained from 92 healthy subjects (51 men, 41 women; age range 22-77 years, mean±SD 48.6±17.2). None had any history of neurological disorders or diabetes mellitus, and none took any neurotropic medication.

All subjects provided written informed consent. The studies on patients and control subjects were approved by the National Research Ethics Service (County Durham and Tees Valley Research Ethics Committee, reference number 08/H0908/3) and Newcastle University's Medical Faculty respectively. Both studies conformed to the Declaration of Helsinki.

6.3.2 Recording

Every effort was made to maintain subjects at a constant level of alertness. Subjects were seated in a comfortable chair with their arm resting on a cushion. Surface EMG was recorded from abductor pollicis brevis (APB), first dorsal interosseous (FDI), flexor digitorum superficialis (FDS) and extensor digitorum communis (EDC) in the upper limb, and extensor digitorum brevis (EDB), abductor hallucis (AH), tibialis anterior (TA) and medial gastrocnemius (MG) in the lower limb. Adhesive electrodes (Bio-Logic M0476; Natus Medical, Mundelein, IL) were placed in a belly-tendon montage over the intrinsic muscles of the hand or foot; for the long muscles of the forearm or calf, the electrodes were placed 4cm apart, one third along the muscle from its proximal origin. Signals were amplified, band-pass filtered (30Hz-2kHz; Digitimer D360, Digitimer, Welwyn Garden City, UK) and digitised at 5kHz (Micro1401, Cambridge Electronic Devices, Cambridge, UK).

6.3.3 Experimental procedure

In the upper limb, subjects were asked to perform a repetitive precision grip task. A length of compliant plastic tubing (length 19cm, Portex translucent PVC tubing 800/010/455/800; Smith Medical, Ashford, UK) was attached to the index finger and thumb with Micropore tape (3M Health Care, Neuss, Germany), and subjects were asked to oppose both ends of the tubing when prompted by visual and auditory cues. This auxotonic task – so-called because force increases with displacement in a spring-like fashion – required a minimum force of 1N (Fisher *et al.*, 2012) and was similar to a precision grip task used in our previous studies, albeit without measuring digit displacement (Kilner *et al.*, 2000; Riddle & Baker, 2006). In the lower limb, subjects were asked to dorsiflex ankle and toes in the air while resting the heel on the ground. Subjects produced 4s of contraction alternating with 2s of relaxation, and at least 100 repetitions. Where necessary, the recording was divided into a number of sections separated by rest to prevent fatigue. Visual feedback of raw EMG traces was provided to facilitate consistent task performance.

In each subject, one upper limb and one lower limb were assessed. We studied the most affected upper and lower limb as reported by the subject. If the subject was unable to perform the coherence task using the most affected limb, we assessed the contralateral limb instead. Where both sides were unaffected or equally affected, the limb on the dominant side was assessed. All assessments in control subjects were carried out on the dominant side.

6.3.4 Data analysis

Analysis was performed in Matlab (Mathworks, Natick, MA) using custom scripts.

Raw IMC data were visually inspected and the first 100 adequately performed trials examined further. Analysis focussed on the early hold phase of the contraction where beta-band oscillations are known to be maximal (Baker *et al.*, 1997; Sanes & Donoghue, 1993). EMG signals were full-wave rectified. Starting 0.8s after the cue prompting contraction, two contiguous 0.82s-long sections of data from each trial were subjected to a 4096-point fast Fourier transform (FFT), giving a frequency resolution of 1.22Hz. Many subjects showed a drop-off in EMG activity so the last 1.56s of the 4s active

phase did not enter the analysis. Denoting the Fourier transform of the lth section of the first EMG signal as $F_{1,l}(\lambda)$, the auto-spectrum is given by

$$f_{11}(\lambda) = \frac{1}{L}\sum_{l=1}^{L} F_{1,l}(\lambda)\,\overline{F_{1,l}(\lambda)} \tag{6.1}$$

where λ is the frequency (Hz), L is the total number of sections and where the overbar denotes the complex conjugate. The cross-spectrum for two EMG signals with Fourier transforms $F_{1,l}(\lambda)$ and $F_{2,l}(\lambda)$ was calculated as

$$f_{12}(\lambda) = \frac{1}{L}\sum_{l=1}^{L} F_{1,l}(\lambda)\,\overline{F_{2,l}(\lambda)} \tag{6.2}$$

Coherence was computed as the cross-spectrum normalised by the auto-spectra

$$C(\lambda) = \frac{|f_{12}(\lambda)|^2}{f_{11}(\lambda)f_{22}(\lambda)} \tag{6.3}$$

Coherence was calculated for the muscle pairs EDC-FDI, FDS-FDI, MG-EDB and TA-EDB. The wide anatomical spacing between the paired muscles minimised the risk of volume conduction causing inflated coherence values (Grosse *et al.*, 2002).

Under the null hypothesis of linear independence between the signals, a level of significant coherence was determined as (Rosenberg *et al.*, 1989)

$$Z = 1 - \alpha^{1/(L-1)} \tag{6.4}$$

where the significance level α was set at 0.05.

To provide a group summary, coherence spectra for each muscle pair were averaged across all patients with a given condition and all control subjects respectively. The significance level for averaged coherence was determined using the method described by Evans and Baker (2003).

In each subject, coherence was averaged across the 15-30Hz window. Cumulative distribution functions (CDFs) were constructed from these averages for each muscle pair and group.

In each limb, coherence readings from both muscle pairs were treated as separate markers M_i. The diagnostic accuracy of these markers as tests for a given condition was quantified using the area under the ROC curve. The ROC curve for each marker M_i was defined as the set of points {FPR(d), TPR(d)} where TPR(d) and FPR(d) are the true and false positive rates associated with a discrimination threshold d in the range $(-\infty,0]$. The same positivity criteria were used as had been assigned in the main MND analysis (Chapter 5); since no inversion of the criteria was permitted, AUCs had a range of [0,1].

We calculated linear and non-linear combinations of both coherence markers in a given limb. Each individual coherence marker M_i was transformed to standardised Z-scores. The coefficients α_i were those previously determined in the main MND analysis (Chapter 5). Linear combinations required only a single coefficient α and were calculated as:

$$N(\alpha) = \alpha M_1 + \sqrt{1-\alpha^2} \cdot M_2 \tag{6.5}$$

Non-linear combination involved two coefficients α_1 and α_2. The first coefficient did not require transformation, so $\gamma_1 = \alpha_1$; the second one was transformed according to the formula:

$$\gamma_2 = \alpha_2\sqrt{1-{\alpha_1}^2} \tag{6.6}$$

The non-linear combination was then calculated as:

$$N(\gamma) = \sum_{i=1}^{2} \gamma_i M_i + \sqrt{1-\sum_{i=1}^{2} \gamma_i^2} \cdot M_1 M_2 \tag{6.7}$$

6.4 Results

Single-subject power and coherence for a control subject and a patient with HSP are shown in Figure 6.1. In control subjects, power usually peaked in the 15-30Hz band; the peak in this band was often less distinct or absent in patients, particularly those with HSP and MMN. In control subjects, coherence typically also peaked in the 15-30Hz band; this peak was often exaggerated in patients with IBM, but was diminished or absent in those with HSP or MMN.

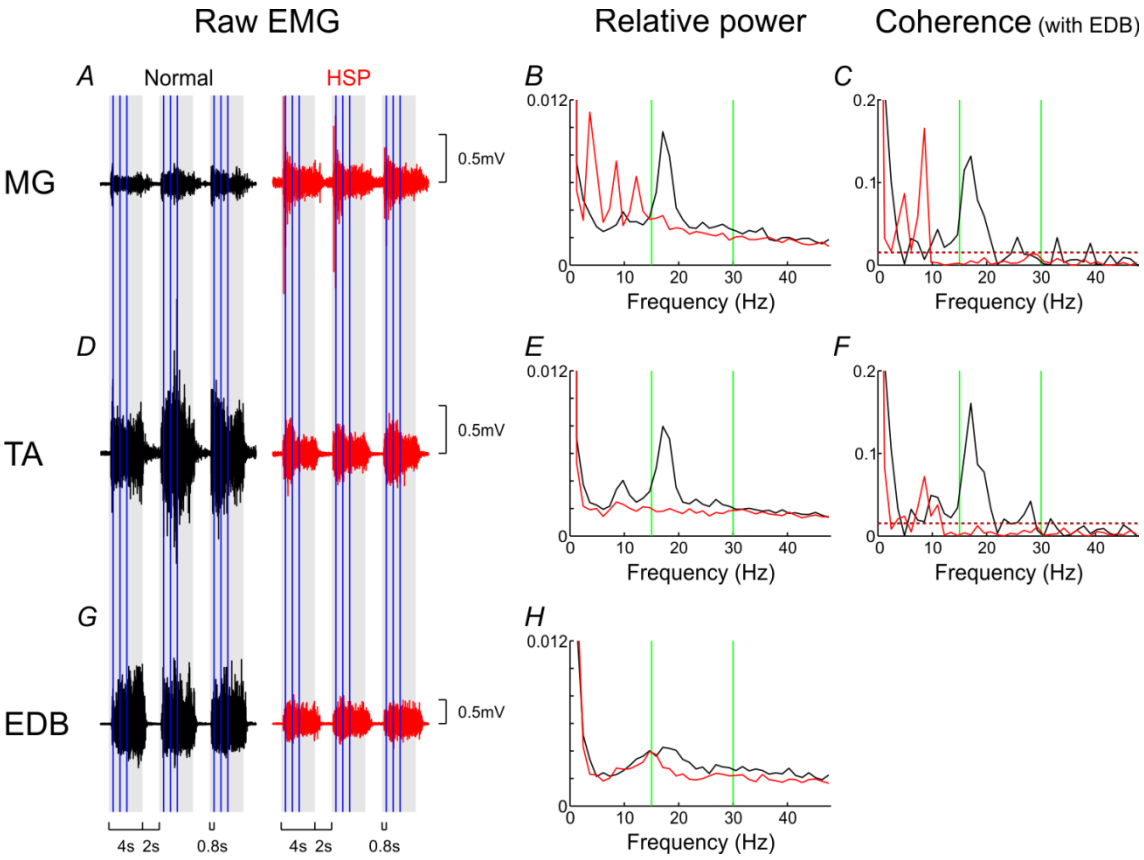

Figure 6.1: Single-subject power and coherence in the lower limb. Raw EMG is shown for three sample trials in a normal control subject (black) and in a patient with hereditary spastic paraparesis (HSP; red; A, D, G). The cued contraction phase of the task is represented by the grey boxes, and the two FFT windows during the hold phase are indicated by the vertical blue lines. Spectra of relative power (B, E, H) and coherence with EDB (C, F) are shown for each subject. The 15-30Hz beta-band is flanked by the green lines, and the dotted horizontal lines indicate the significance level for coherence. In the normal subject, power and coherence spectra show a clear peak in the 15-30Hz band. In the patient with HSP, power peaked at 15Hz in EDB but showed no clear peaks within the 15-30Hz window in MG and TA; coherence was not significant across the 15-30Hz band.

To illustrate these differences in coherence between groups, we calculated group averages (Figure 6.2). In the control group, 15-30Hz coherence was significant in all muscle pairs. In HSP, 15-30Hz coherence was diminished in TA-EDB but was near-normal in other muscle pairs. In MMN, 15-30Hz coherence was near-normal in EDC-FDI, slightly decreased in FDS-FDI, and near the significance level in both muscle pairs in the lower limb. In IBM, 15-30Hz coherence was increased in MG-EDB and EDC-FDI, and near-normal in the remaining muscle pairs.

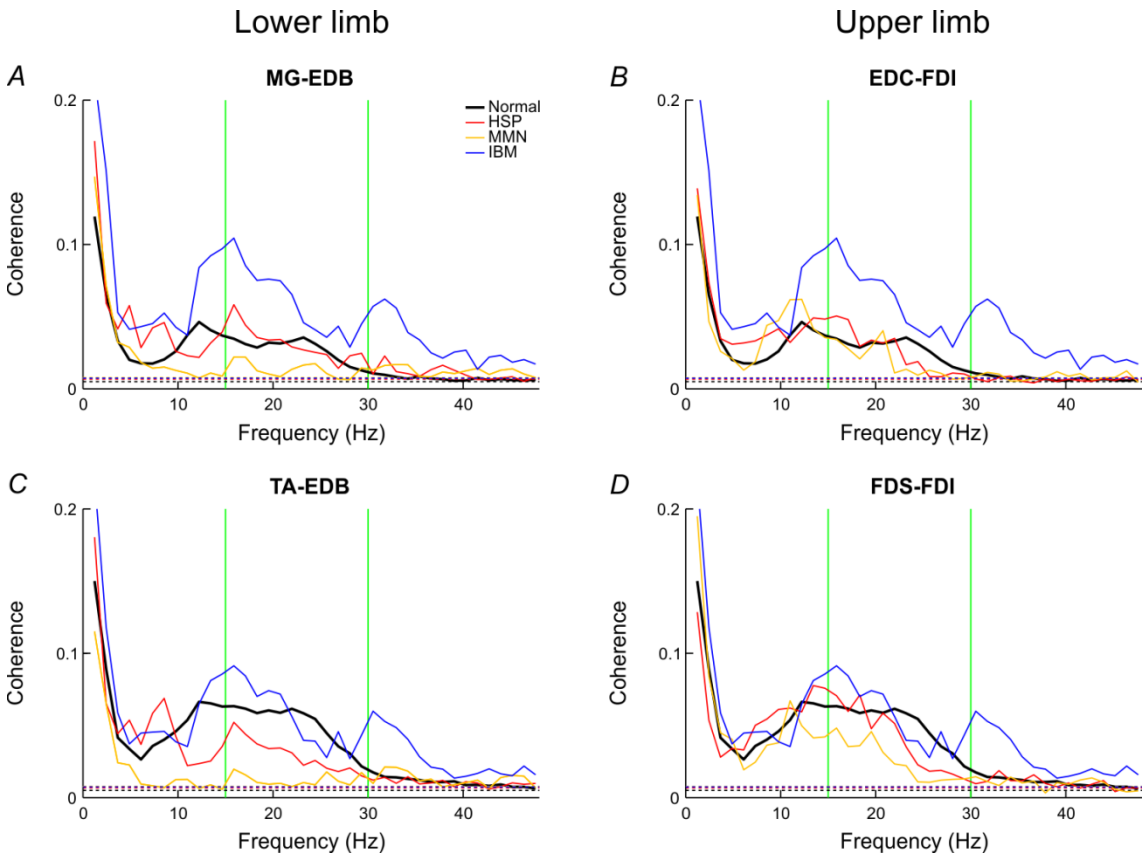

Figure 6.2: Group data for coherence. Average coherence spectra are shown for MG-EDB and TA-EDB in the lower limb (A, C) and for EDC-FDI and FDS-FDI in the upper limb (B, D). The dotted horizontal lines represent the significance level for average coherence, with the vertical green lines indicating the 15-30Hz beta-band. In normal subjects (black), significant average coherence was present in the 15-30Hz band for each muscle pair. In HSP (red), average 15-30Hz coherence was decreased in TA-EDB but at near-normal levels in other muscle pairs. In MMN (orange), average 15-30Hz coherence was near-normal in EDC-FDI, slightly diminished in FDS-FDI, and near the significance level in MG-EDB and TA-EDB. In IBM (blue), average 15-30Hz coherence was increased in MG-EDB and EDC-FDI, and near-normal in the two other muscle pairs.

Although these group averages report general trends, they do not allow us to visualise the variation within each group. To achieve this, we compared the distributions of individual coherence measurements between all groups. Coherence was averaged across the 15-30Hz window in each subject, and the cumulative distributions of the averages plotted on a semi-log scale (Figure 6.3 A, B, E, F). In addition, ROC curves were constructed (Figure 6.3 C, D, G, H), and the area under the ROC curve (AUC) was calculated as a summary measure of performance for coherence in each muscle pair. In HSP, the distribution of coherence in the upper limb was similar to the control group, and the ROC curve ran close to the diagonal; in the lower limb, the distribution was partly shifted to lower coherence values, which was reflected in the ROC curves lying partly above the diagonal. In four patients, IMC readings in the lower limb were relatively high, falling into the upper half of the normal range. However, there were no apparent differences in age, disability or duration of symptoms between this group and other patients with HSP. In MMN, the distribution of coherence in the upper limb was slightly shifted to lower values than controls, and in the lower limb this shift was more pronounced. Accordingly, the ROC curves lay above the diagonal, more so in the lower limbs. In IBM, the distributions in upper and lower limbs were shifted to higher values of coherence relative to controls, reflected by ROC curves running below the diagonal.

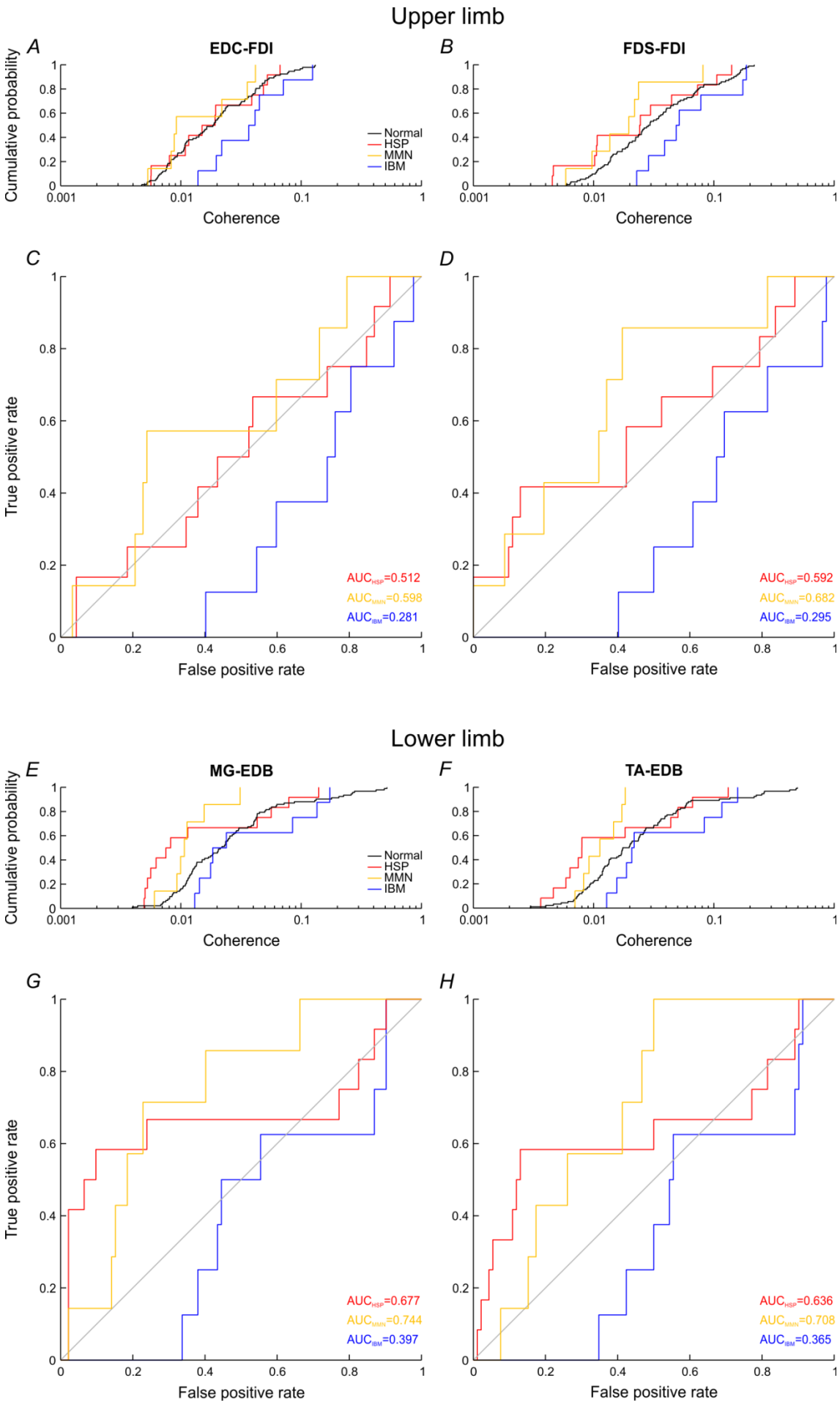
Upper limb
A
EDC-FDI
B
FDS-FDI
Cumulative probability
Coherence
Normal
HSP
MMN
IBM
C
D
True positive rate
False positive rate
AUC_HSP=0.512
AUC_MMN=0.598
AUC_IBM=0.281
AUC_HSP=0.592
AUC_MMN=0.682
AUC_IBM=0.295
Lower limb
E
MG-EDB
F
TA-EDB
G
H
AUC_HSP=0.677
AUC_MMN=0.744
AUC_IBM=0.397
AUC_HSP=0.636
AUC_MMN=0.708
AUC_IBM=0.365

Figure 6.3: Comparison of coherence between normal control subjects (black) and patients with HSP (red), MMN (orange), and IBM (blue). The stairstep curves represent the cumulative probability distribution of average 15-30Hz coherence within each group (A, B, E, F), with the corresponding ROC curves shown below (C, D, G, H). In HSP, coherence was similar to the control group in the upper limb, with the ROC curve running close to the diagonal; in the lower limb, coherence was mostly lower than normal and the ROC curve lay partly above the diagonal. In MMN, upper limb coherence was slightly decreased and lower limb coherence was more prominently decreased compared to controls; this was reflected in ROC curves lying above the diagonal, more markedly so in the lower limbs. In IBM, coherence readings were generally higher than normal, and the ROC curves lay below the diagonal.

The ROC curves in Figure 6.3 reveal differences between patients and healthy controls for coherence calculated from particular muscle pairs. However, it is interesting to see whether even greater differences could occur by combining measures from multiple muscle pairs. This is illustrated in Figure 6.4, where we extended the analysis to linear combinations of coherence from both muscle pairs in a given limb. The required coefficient α had previously been found by optimisation in the MND dataset (Chapter 5) and focussed strongly on FDS-FDI in the upper limb and MG-EDB in the lower limb. Hence, the ROC curves for the combined marker bore close similarity to the ROC curves for these individual muscle pairs. The side panels allow discrimination thresholds to be read off for any chosen TPR or FPR (as previously outlined in Figure 5.5).

AUCs for individual and combined markers are summarised Figure 6.5 and Table 6.1. Combined markers included both linear and non-linear combinations of coherence from both muscle pairs in a given limb. In HSP, AUCs were close to 0.5 in the upper limb (range 0.51-0.59), with slightly higher values (0.64-0.68) being reached in the lower limb. In MMN, AUCs were generally higher than in HSP (upper limb: 0.60-0.68, lower limb: 0.71-0.74). In IBM, AUCs were all below 0.5 (upper limb: 0.28-0.29, lower limb: 0.37-0.40).

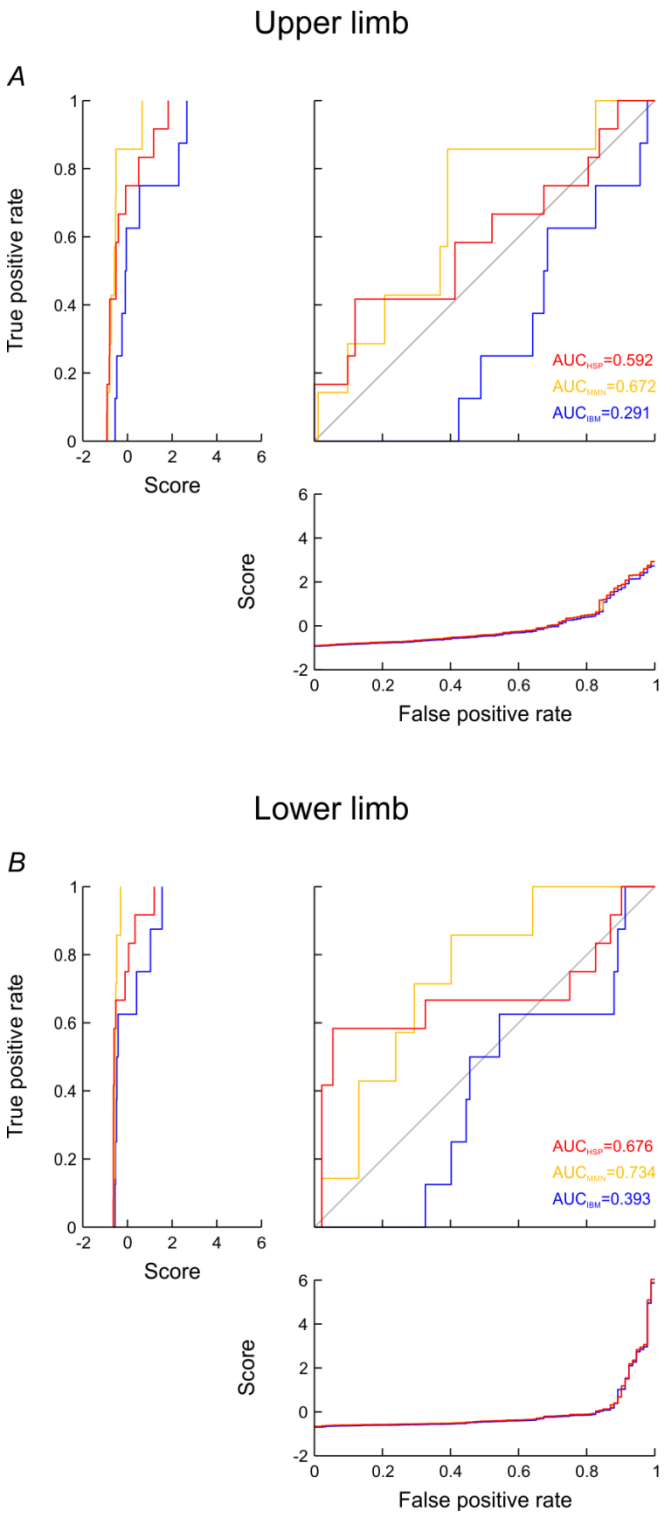

Figure 6.4: Optimal linear combination of coherence data. Standardised coherence readings from both muscle pairs in a given limb were combined using a parameter α, allowing all relative linear combinations. The parameter had been derived previously using the MND dataset (Chapter 5). ROC curves are shown for the combination of both muscle pairs. Since the parameters emphasised coherence in FDS-FDI in the upper limb and coherence in MG-EDB in the lower limb, the combined ROC curves are very similar to the ROC curves in these individual muscle pairs (Figure 6.3). Side panels illustrate the combined measure at a given level of true or false positives.

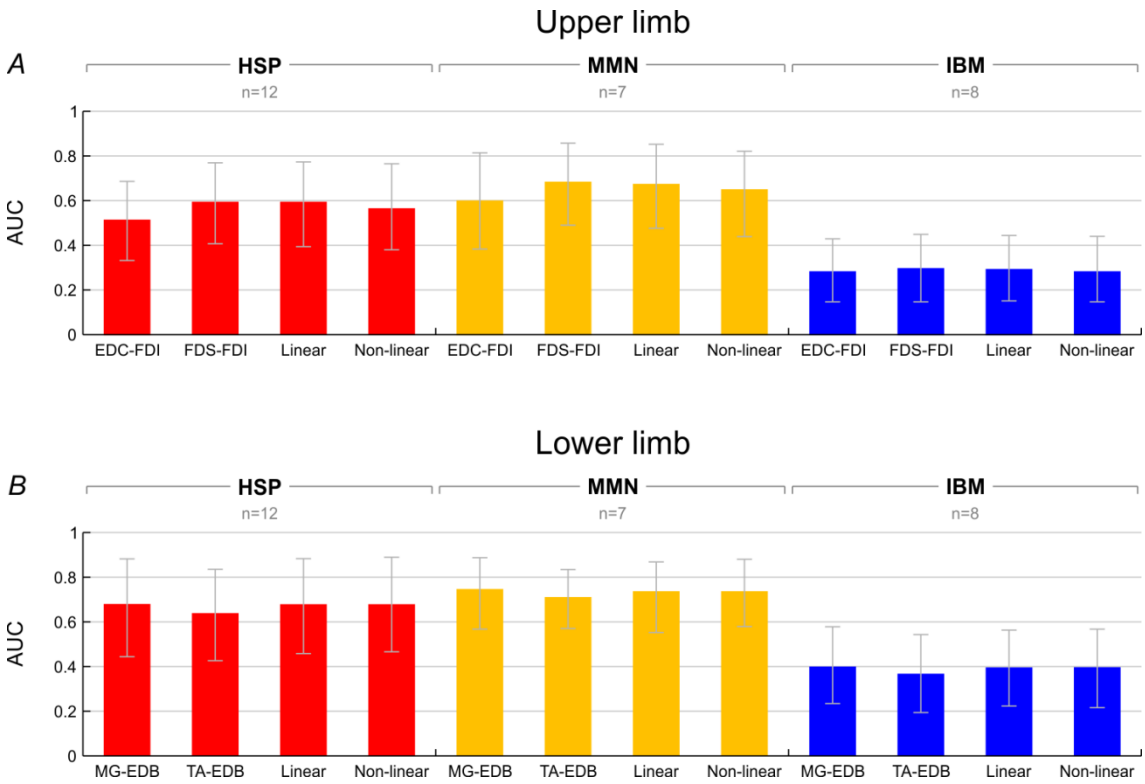

Figure 6.5: Area under the ROC curve (AUC) for individual and combined measures of coherence in HSP (red), MMN (orange), and IBM (blue). Linear and non-linear combinations were calculated using the parameters previously determined in the MND cohort (Chapter 5). Error bars indicate bootstrapped 95% confidence intervals. In HSP, AUCs in the upper limb were near 0.5, whilst those in the lower limb were somewhat higher. In MMN, AUCs were higher than in HSP in both upper and lower limbs. In IBM, AUCs were below 0.5 throughout.

Table 6.1: Area under the receiver-operating characteristic curve (AUC) associated with coherence markers and their linear and non-linear combinations. The coefficients used to calculate the combined markers had been derived previously in the motor neuron disease (MND) cohort (Chapter 5). (comb'n=combination)

	Condition	**AUC**			
		EDC-FDI	FDS-FDI	Linear comb'n	Non-linear comb'n
Upper limb	HSP	0.512	0.592	0.592	0.563
	MMN	0.598	0.682	0.672	0.648
	IBM	0.281	0.295	0.291	0.281
Lower limb	HSP	0.677	0.636	0.676	0.676
	MMN	0.744	0.708	0.734	0.734
	IBM	0.397	0.365	0.393	0.394

6.5 Discussion

6.5.1 Results and their implications

In HSP, IMC was usually decreased in the lower limb but near-normal in the upper limb. As pure HSP should only affect the CST projecting to lower limb muscles, these findings are compatible with the hypothesis that the CST has a pivotal role in mediating IMC. It was surprising that four patients with HSP showed rather high IMC readings in the lower limb without differing from patients with diminished or absent IMC in any obvious manner, including age, duration of symptoms and mutated gene. We did not examine patients clinically as part of this study, so no comparison of clinical signs or scores could be made. Patients with unexpectedly high coherence should be followed up with serial IMC measurements over the coming years.

Patients with MMN showed slightly decreased IMC in the upper limb and more markedly decreased IMC in the lower limb. MMN is conventionally thought to affect peripheral motor nerves only, so this result would suggest that peripheral efferents are involved in mediating IMC. However, there is some evidence that MMN may also cause dysfunction of the CST and/or sensory afferents. In a large series, 8% of cases were noted to display retained or brisk reflexes in an affected limb (Cats *et al.*, 2010), and brisk reflexes in MMN have also been reported elsewhere (Bentes *et al.*, 1999; Oshima *et al.*, 2002; Traynor *et al.*, 2000a). Whilst 'brisk' reflexes were viewed as acceptable, 'pathological' reflexes or other UMN signs were thought to exclude MMN (Cats *et al.*, 2010; Vlam *et al.*, 2012). However, physiologically and pathologically brisk reflexes may not be distinguishable. Furthermore, one study reported two cases with an electroclinical phenotype of MMN and high anti-GM1 titres who exhibited hyperreflexia, an extensor plantar response in one case, and a prolongation of central motor conduction time compared to cases of MMN without UMN signs (Oshima *et al.*, 2002). Hence, it cannot be excluded that the decreases in IMC we observed here were partly attributable to CST dysfunction. There is also clinical, electrophysiological and histological evidence that MMN is associated with mild sensory nerve pathology, particularly in longstanding disease (Cats *et al.*, 2010; Corse *et al.*, 1996). This is less likely to be relevant as patients in our cohort had a shorter duration of disease and showed normal sensory function on NCS.

In IBM, the global increase in IMC is probably attributable to the altered electrical properties of motor units. Normally, voluntary contraction leads to gradual recruitment of units, which respond with well-formed, simply-shaped action potentials. In IBM, recruitment occurs earlier and individual units show unstable, polyphasic discharges; in addition, there are involuntary fibrillation potentials, positive sharp waves and complex repetitive discharges (Kimura, 2001). IMC quantifies synchronisation between discharges in each muscle. It is likely that, at a given force of contraction, synchronisation is more readily detectable in IBM where a larger number of units discharges in a polyphasic manner with multiple spikes, compared to the normal state where a smaller number of units fires simple biphasic action potentials.

Potential confounders discussed in Chapter 5 included neurotropic medication and fatigue during the coherence task. These equally apply to data from patients with HSP, MMN and IBM.

6.5.2 Outlook

HSP and MMN do not necessarily cause a pure lesion in one specific part of the nervous system. This issue, which was most prominent in MMN, markedly complicates the interpretation of results. Studying motor neuropathies other than MMN would not solve the problem as a degree of sensory involvement is almost universal.

Instead, a computational model could be employed to delineate the relative contributions to IMC from different parts of the motor system. Such a model was previously developed in our group (Williams & Baker, 2009) and could be adapted for studying the effects of virtual lesions *in silico*.

6.6 Conclusion

We examined IMC in cohorts of patients with HSP, MMN and IBM in an attempt to clarify efferent pathways involved in IMC generation. The results suggest that IMC is partly sensitive to dysfunction of the CST and of the distal motor units. Although it would be plausible that the proximal motor units – embodied by peripheral motor

nerves – may also be involved if IMC is altered, this point requires further clarification. Neurological conditions including HSP and MMN can be associated with multiple concomitant lesions, some of which may be subclinical, and computational modelling represents an alternative approach which could circumvent this problem.

7 General discussion

7.1 Context

The last few decades have seen the successful development and universal clinical deployment of electrophysiological markers of lower motor neuron (LMN) dysfunction. By contrast, candidate markers of upper motor neuron (UMN) dysfunction have never performed sufficiently well to achieve widespread clinical uptake, and the lack of such markers is perhaps most keenly felt in the diagnosis and follow-up of patients with motor neuron disease (MND). The work presented in this thesis aimed to further the development of biomarkers of UMN function. We investigated a novel biomarker, beta-band intermuscular coherence (IMC), together with central motor conduction time (CMCT), a marker based on transcranial magnetic stimulation (TMS) whose neural substrates are relatively well understood.

7.2 Summary and future directions

We showed that CMCT in healthy individuals was significantly correlated with height in the lower limb but found no significant predictors in the upper limb (Chapter 2). Our regression model can be used to lessen interindividual variability for lower limb CMCT and thus should help to improve diagnostic performance. In addition, a review of the methods used in previous investigations allowed us to reconcile some past discrepancies regarding the correlation of CMCT with age and height. CMCT has now been studied for almost 30 years and major future advances appear unlikely. A recent development is the MATS (magnetic augmented translumbosacral stimulation) coil, which allows direct stimulation of the conus medullaris, thus permitting CMCT to be estimated without a residual peripheral component. However, sensitivity for UMN dysfunction may well remain unchanged, and studies in disease states are still lacking.

Investigating beta-band IMC in the same normal cohort, we found no variation in its amplitude with age (Chapter 3). Hence, IMC appeared to be robust to age-related changes in the nervous system, allowing us to collate IMC data from healthy individuals of all ages into a single normative dataset. The variability of IMC between subjects was considerable, and within a given subject variability was greater between than within recording sessions. Potential contributors include fluctuations in task performance, differences in electrode montage and short-term random variation in coherence. These factors require further exploration and, where possible, minimisation. Investigation of the following two aspects is also required. Firstly, a previous study described that the amplitude and directionality of corticomuscular coupling can change over years within individuals (Witham *et al.*, 2011). The timecourse of these changes and their relationship to the variability of IMC should be characterised. Secondly, there is a disconnect between coherence studies employing a sustained contraction, which is easier to standardise, and those using a phasic task, which exploits the known task specificity of coherence and is easier to perform for disabled subjects. Both types of task should be studied in the same cohort so that the relationship between the corresponding coherence estimates can be clarified.

In keeping with a past report, we found that anodal transcranial direct current stimulation (tDCS) boosted IMC (Chapter 4). These effects were longer-lasting than previously described, and the timecourse of their return to baseline should be mapped out in a future study. The potential use of tDCS as a diagnostic adjunct to IMC is somewhat hampered by the variability of its effects, and it would be interesting to test whether more powerful tDCS protocols elicit more reliable increases in IMC. We were not able to reproduce the classical effects of tDCS on TMS-evoked motor potentials despite using methods which closely paralleled those reported in the literature. Although it is generally assumed that tDCS causes reliable, stable changes in cerebral excitability, even classical studies reported substantial inter- and intrasubject variability. This result highlights that the effects of tDCS are not as robust as is commonly expected.

Our group previously investigated IMC in primary lateral sclerosis and progressive muscular atrophy, and we expanded on this by measuring IMC and CMCT in patients

with all phenotypes of MND (Chapter 5). We studied IMC and CMCT in individual muscles or muscle pairs as well as exploring their linear and non-linear combinations. Instead of specifying cut-off values separating normal from abnormal, which would have required scrutiny of associated costs and disease prevalence, we focussed on the area under the receiver-operating curve (AUC). IMC in a single muscle pair performed as well as combinations of IMC in discriminating between normal and MND groups, thus suggesting an immediate method of simplifying future studies. IMC outperformed CMCT in the upper limb and was comparable to individual CMCT markers in the lower limb, lagging only slightly behind combined CMCT markers. Current evidence indicates that IMC abnormalities are primarily attributable to CST dysfunction, suggesting that IMC constitutes a potential quantitative test of CST integrity.

For the current study, patients were recruited as early as possible after referral to the local MND service. The prognostic value of IMC will be analysed once more survival data are available. Future work should include a longitudinal study to characterise the evolution of IMC throughout the course of MND, ideally following patients from a pre-symptomatic stage, for example in kindreds with familial forms of MND. Further studies and potential clinical uptake of IMC should prove relatively inexpensive since the requisite EMG recording facilities are widely available; in addition, a low-cost, handheld EMG recorder is being developed locally (Brown *et al.*, 2012).

We examined IMC in patients with other neurological conditions to clarify the contribution of different parts of the motor system to IMC generation (Chapter 6). Interestingly, most but not all patients with hereditary spastic paraparesis (HSP) exhibited diminished IMC, and further follow-up of the subgroup retaining normal levels of IMC may prove informative. In multifocal motor neuropathy (MMN), which is typically thought of as a peripheral motor disorder, IMC was diminished. This suggests that dysfunction of peripheral motor nerves may affect IMC and/or that our patients with MMN had subclinical involvement of the corticospinal tract (CST). In inclusion body myositis (IBM), IMC was increased, and a plausible explanation would be that alterations in motor unit discharges caused by IBM make synchronisation more readily detectable. Overall interpretation of results is complicated by HSP and MMN potentially affecting multiple parts of the motor system, and an alternative approach

would be to study the effects of virtual lesions in a computational model of the motor system.

7.3 Conclusion

Thus far, coherence analysis has been predominantly used as a research tool, and it was only recently applied as a marker of CST integrity. Though many questions presently remain unanswered, it is encouraging that, even at this early stage, the performance of IMC appears to match or surpass that of a fully-developed TMS-based marker. Within a few years, the neural substrates of IMC generation will have been clarified and methods of measuring IMC will have seen further optimisation, thus nurturing the hope that IMC could ultimately become a widely used biomarker of CST function.

A Individual beta-band averages for intermuscular coherence in normal subjects

Table A.1: Individual averages of beta-band IMC in normal individuals. Coherence was measured in each individual using the methods described in Chapter 3, and coherence spectra were averaged across the 15-30Hz window for each muscle pair.

	Coherence			
Age	**EDC-FDI**	**FDS-FDI**	**MG-EDB**	**TA-EDB**
22	0.03584	0.02634	0.01173	0.01980
22	0.01879	0.05244	0.02544	0.01202
22	0.00471	0.00589	0.02451	0.02642
23	0.00747	0.01915	0.00998	0.00680
23	0.01343	0.14675	0.04977	0.03167
23	0.01258	0.03766	0.04194	0.04871
23	0.01937	0.02351	0.00926	0.01182
23	0.02262	0.06775	0.04315	0.03156
23	0.01079	0.02239	0.00700	0.01015
23	0.03140	0.02532	0.01115	0.00816
26	0.03421	0.14007	0.20579	0.22506
28	0.04751	0.05635	0.01351	0.01558
28	0.00771	0.00939	0.02352	0.02060
28	0.02011	0.04046	0.01147	0.01335
28	0.00687	0.01981	0.01825	0.02353
29	0.08813	0.11485	0.02048	0.02383
30	0.04754	0.07448	0.01765	0.01127
30	0.00826	0.00731	0.01343	0.01342
30	0.00767	0.00774	0.01118	0.02016
30	0.01896	0.03496	0.02304	0.01751
30	0.03081	0.16687	0.03848	0.03591
31	0.04978	0.07083	0.02041	0.02091
32	0.00778	0.01555	0.17898	0.11097
34	0.02145	0.02848	0.01098	0.00891
35	0.01122	0.02501	0.01502	0.00923
36	0.01100	0.04003	0.05448	0.05268
36	0.01455	0.04611	0.01181	0.01181
36	0.00650	0.01319	0.04499	0.03902
38	0.02049	0.06925	0.04019	0.03426
38	0.00521	0.01071	0.01692	0.01303
38	0.04203	0.03473	0.01311	0.00930
38	0.01587	0.02502	0.03603	0.01712
40	0.02446	0.11101	0.49170	0.48146
40	0.01155	0.01059	0.00681	0.00612
41	0.00760	0.01332	0.02749	0.01741
41	0.02380	0.05039	0.01230	0.01347
41	0.00830	0.00862	0.06277	0.05806
41	0.05002	0.15325	0.26733	0.26086
42	0.01019	0.07663	0.02349	0.02440
45	0.02234	0.01955	0.01237	0.01387
45	0.07707	0.19395	0.01087	0.01092
45	0.00551	0.00647	0.01139	0.01200
46	0.00938	0.01384	0.02895	0.02367
46	0.03181	0.04390	0.26046	0.25017
46	0.07881	0.08268	0.01047	0.00800
49	0.01950	0.01392	0.05084	0.03426
49	0.02085	0.03615	0.08788	0.05944

	Coherence			
Age	**EDC-FDI**	**FDS-FDI**	**MG-EDB**	**TA-EDB**
50	0.00704	0.00638	0.04030	0.03634
50	0.01060	0.01839	0.00809	0.00867
51	0.00818	0.01153	0.01575	0.00759
51	0.00892	0.01734	0.04103	0.02721
51	0.00874	0.01423	0.02356	0.02004
54	0.12905	0.17268	0.01499	0.01723
54	0.01843	0.01943	0.00853	0.00400
55	0.03984	0.04361	0.02850	0.06455
56	0.04164	0.06578	0.00866	0.00717
56	0.02342	0.03158	0.06205	0.05880
57	0.06110	0.16334	0.22525	0.21587
57	0.00642	0.01368	0.00395	0.00695
58	0.03642	0.02950	0.04305	0.04826
59	0.04533	0.07249	0.02673	0.02695
59	0.01085	0.01573	0.00844	0.00743
60	0.06708	0.13309	0.01252	0.01222
61	0.10277	0.16621	0.01263	0.00464
62	0.00618	0.00907	0.01357	0.01710
63	0.05938	0.12506	0.12967	0.13597
63	0.00665	0.01451	0.02196	0.02584
64	0.09815	0.18325	0.01855	0.01620
64	0.00933	0.08226	0.27788	0.26353
64	0.01516	0.03987	0.03035	0.01242
65	0.01556	0.02975	0.00437	0.00298
65	0.00759	0.00974	0.00978	0.01139
67	0.01067	0.01732	0.13317	0.00991
67	0.01641	0.01194	0.02014	0.01180
68	0.04158	0.21654	0.41962	0.42641
68	0.02154	0.02364	0.01291	0.00820
69	0.00526	0.01039	0.01038	0.00947
70	0.05399	0.02224	0.02551	0.02420
70	0.00632	0.02096	0.07212	0.05754
70	0.03386	0.03341	0.03014	0.03930
71	0.05242	0.06781	0.51644	0.49334
71	0.04136	0.04999	0.04223	0.03512
71	0.01641	0.02948	0.02484	0.02628
73	0.03910	0.02756	0.00777	0.00538
73	0.01414	0.01381	0.04040	0.04974
74	0.13105	0.15805	0.05657	0.06124
74	0.02335	0.02569	0.04295	0.04578
75	0.04527	0.05964	0.00712	0.01344
75	0.01050	0.01094	0.01200	0.00729
75	0.01411	0.03814	0.02127	0.04069
76	0.00941	0.02234	0.00750	0.01692
77	0.01079	0.01230	0.00804	0.01094

B Clinical details for patients with motor neuron disease

Table B.1: History for patients with MND. (AF=atrial fibrillation, BFZ=bendroflumethiazide, bilat=bilateral, CABG=coronary artery bypass graft, COPD=chronic obstructive pulmonary disease, DH=drug history, FDR=first degree relative, FH=family history, GTN=glyceryl trinitrate, HT=hypertension, IBS=irritable bowel syndrome, IHD=ischaemic heart disease, inh=inhaler, iPD=idiopathic Parkinson's disease, ISMN=isosorbide mononitrate, L=left, LL=lower limb, MS=multiple sclerosis, NK=not known (hospital file not retrievable), OA=osteoarthritis, PMH=past medical history, R=right, T2DM=type 2 diabetes mellitus, THR=total hip replacement, UL=upper limb)

Patient number	Sex	Age at diagnosis	Duration at diagnosis	Initial presentation	PMH	DH	FH
1	M	52	6m	R UL weakness, wasting, twitching, cramps; then similar symptoms in L UL	Sigmoid colectomy for diverticulosis	Riluzole	Nil
2	F	65	16m	Gradual slurring dysarthria; then dysphagia, bilat LL weakness and falls	Recurrent cystitis, asthma	Cefalexin, fluoxetine, simvastatin, aspirin, trimipramine, salbutamol inh, budesonide and formoterol inh, riluzole	Mother: Lewy body dementia
3	M	70	6m	Neck extensor and UL L>R weakness	T2DM, hypercholesterolaemia	Glicazide, metformin, omeprazole, ibuprofen, rosuvastatin, riluzole	Nil
4	F	70	9m	Weakness of voice and limbs; then gait disturbance, falls, dysphagia	IHD	Baclofen, sertraline, atorvastatin, aspirin, GTN, citalopram	Nil
5	M	55	4m	R hand weakness; then L hand weakness, R LL weakness, dysarthria	Asthma	Mirtazepine, lisinopril, quinine, riluzole	Nil
6	F	80	9m	L hand weakness; then gait disturbance, dysarthria, dysphagia for liquids	Asthma	Salbutamol, oxybutinin, quinine, theophylline	Nil
7	F	72	12m	Dysarthria, dysphagia; then drooling	Nil	Lansoprazole, riluzole	Nil
8	F	41	15m	R LL weakness, cramps, twitching; then falls	Subtotal hysterectomy, bilat oophorectomy, appendicectomy, ulnar nerve decompression at cubital tunnel, OA knees	Nil	Nil
9	F	46	14m	L LL stiffness; then R LL stiffness, weakness, falls, bilat UL stiffness, spastic dysarthria, dysphagia	Nil	Baclofen, citalopram, codeine, paracetamol	Father: MS
10	F	66	24m	R LL weakness; then L LL and R UL weakness, restriction to wheelchair, dysarthria, occasional dysphagia	HT, IHD	Amlodipine, omeprazole, fexofenadine, tolterodine	Nil
11	F	59	30m	Bilat R>L LL weakness and stiffness; then spastic dysarthria	Asthma	Salmeterol and fluticasone inh, baclofen, riluzole	Nil
12	M	46	6m	L hand weakness and wasting; then R LL wasting, weakness	Nil	Riluzole	Nil
13	F	75	10m	Dysphagia, dysarthria	Amiodarone-induced hypothyroidism, paroxysmal AF, THR, hysterectomy	Alendronate, aspirin, bisoprolol, docusate, hyoscine, levothyroxine, paracetamol	Nil
14	M	68	31m	Dysarthria, cough; then fall with ankle fracture, slow to remobilise, new requirement for two sticks	R nephrectomy for malignant tumour 2006	Riluzole	Nil
15	F	62	6m	Dysarthria, dysphagia, L LL cramps and weakness	HT	Quinine, lisinopril, aspirin, baclofen, riluzole	Nil
16	F	58	6m	R UL weakness	Lumbar surgery, mild asthma, vulval dystrophic disease	Budesonide inh	Grandmother: died of problems which allegedly included muscle weakness
17	F	77	8m	Dysarthria; then dysphagia	Breast cancer 2001 (mastectomy, tamoxifen), L ischaemic optic neuropathy 2008, asthma, osteoporosis, HT, hysterectomy	Fluticasone and salmeterol inh, aspirin, amlodipine, risedronate, paroxicam	Nil
18	F	62	7m	R then L LL weakness; subsequently R then L UL weakness; R LL fasciculation, cramping, locking; restriction to rollator/wheelchair	THR, asthma, HT	Ramipril, sertraline, riluzole	Nil
19	F	73	26m	R LL weakness, falls	HT, bilat L4/5 decompression for anterolisthesis 2011	Irbesartan, BFZ, riluzole	Nil
20	F	53	15-18y	R then L UL weakness; subsequently bilat LL weakness	Nil	Codeine, paracetamol	Mother and four maternal uncles: MND
21	M	77	13m	Bilat UL weakness	IHD, myelodysplasia	Clopidogrel, bisoprolol	Mother: dementia
22	M	76	17m	R UL weakness, wasting; then L UL weakness, wasting, bilat LL weakness	IHD, CABG	Amlodipine, ramipril, atenolol, simvastatin, quinine, ISMN, aspirin, riluzole	Nil
23	F	74	10m	Weakness of gait; then dysarthria, cramps	Asthma	Salbutamol inh, riluzole	Nil
24	M	72	16m	R hand weakness	HT, hypercholesterolaemia	Simvastatin, amlodipine, losartan, riluzole	Nil
25	M	63	6m	R hand weakness; subsequently L UL then R LL then L LL weakness	HT, pericarditis, asbestos exposure	Aspirin, codeine, paracetamol, riluzole	Nil
26	M	60	19m	Bilat LL twitching and muscle aches; then spread to all limbs with wasting and weakness	Nil	Ibuprofen, riluzole	Nil

Patient number	Sex	Age at diagnosis	Duration at diagnosis	Initial presentation	PMH	DH	FH
27	F	57	9m	Slurring dysarthria, dysphagia mostly for liquids; then bilat LL cramps, global limb weakness	IBS, anxiety	Amitriptyline, mebeverine, lansoprazole	Nil
28	M	72	14m	R LL weakness, stiffness, falls	HT, hyperlipidaemia	Amlodipine, paracetamol, riluzole	Nil
29	M	67	24m	R hand weakness, wasting; then L hand weakness, wasting	IHD	Omeprazole, aspirin, simvastatin, riluzole	Nil
30	F	74	34m	L then R LL stiffness; subsequently L>R UL stiffness, slurring dysarthria, dysphagia	Pernicious anaemia, HT	Strontium, colecalciferol, aspirin, amlodipine, folate, vitamin B12, baclofen	Nil
31	M	59	23m	L LL giving way	Nil	Baclofen	Nil
32	M	43	22m	Bilat proximal LL weakness	Acne	Oxytetracycline	Maternal grandmother, mother, two maternal uncles, sister: MND
33	M	58	27m	L LL weakness, cramps, falls; then R LL weakness, possible bilat UL weakness	Nil	Quinine, citalopram, omeprazole, dihydrocodeine, diclofenac, riluzole	Three FDRs incl. brother: MND
34	F	66	7-8y	R LL then UL weakness; L limbs unaffected	Breast ductal cancer (local excision)	Solifenacin	Nil
35	F	73	23m	L>R LL weakness; subsequently L then R hand weakness and wasting	L ankle degenerative disease	Amitriptyline, diclofenac, omeprazole, riluzole	Nil
36	F	67	5m	Slurring dysarthria, difficulty chewing, cramping of jaw muscles	T2DM, hiatus hernia	Omeprazole, riluzole	Nil
37	F	71	18m	R>L LL weakness, L UL weakness	Cervical spondylosis, hysterectomy, cholecystectomy	Oxycodone, amitriptyline, chromoglycate	Nil
38	F	48	12m	R hand cramps; subsequently R hand then UL weakness	Asthma, psoriasis	Beclamethasone inh, riluzole	Nil
39	F	59	3m	Dysarthria, dysphagia	Nil	Citalopram, riluzole	Nil
40	F	64	3m	L hand weakness, L foot drop; then slurring dysarthria	Chronic pancreatitis secondary to pancreatic cysts, cholecystectomy, HT	Fluoxetine, lercadipine, atorvastatin, lansoprazole, pancrelipase, dosulepin, paracetamol, ibuprofen	Nil
41	F	37	3m	Bilat LL weakness	Nil	Riluzole	Nil
42	M	61	5-6y	Difficulty walking; subsequently R then L LL weakness, wasting	COPD	Ibuprofen, tramadol, paracetamol, amitriptyline, quinine	Nil
43	M	61	20m	L then R hand weakness; then dysarthria, widespread fasciculation	CABG	Simvastatin, aspirin, lansoprazole, riluzole	Nil
44	F	56	13m	R LL cramps, weakness, falls; then L LL crams	T2DM, HT, IHD, hysterectomy, duodenal ulcer	Amitriptyline, atenolol, BFZ, docusate, doxazosin, losartan, metformin, omeprazole, perindopril, simvastatin, gabapentin	Nil
45	F	66	26m	L hand wasting, weakness, cramping, locking; then spread to rest of L UL	Hypothyroidism	Thyroxine	Nil
46	F	73	21m	R hand cramps/spasms, weakened grip; then similar symptoms in L hand	Glaucoma	Nil	Nil
47	M	68	30m	L>R LL weakness; then L>R hand weakness, slurring dysarthria, minor dysphagia	Hypercholesterolaemia, asthma, IHD, past alcohol excess, surgery for stomach ulcers	Thiamine, salbutamol inh, salmeterol inh, becotide inh, ramipril, paracetamol, lansoprazole, bisoprolol, atorvastatin, baclofen	Nil
48	M	71	15m	Bilat LL weakness; then bilat UL weakness, weak voice	Spondylosis, disc prolapse with symptoms in R LL 1979, diverticulosis, Barrett's oesophagus	Codeine, lanzoprazole, quinine, riluzole	Nil
49	M	56	12m	Bilat UL and LL wasting, weakness; then bilat UL and LL fasciculation	Nil	Quinine, riluzole	Nil
50	M	65	NK	NK	NK	Riluzole	NK
51	M	32	4m	L hand weakness; then L LL weakness, falls, L>R UL weakness	Drug use (cannabis, amphetamines)	Amitriptyline, riluzole	Nil
52	M	55	9m	Slurring dysarthria, dysphagia mostly for liquids	Nil	Temazepam, riluzole	Nil
53	M	32	52m	Tightness in calves, difficulty/inability to play football, falls; then bilat LL wasting	Nil	Baclofen, amitriptyline, riluzole	Nil
54	F	56	9m	L then R UL weakness; subsequently L LL weakness, gait disturbance	L breast cancer 5y ago (wide local excision, chemotherapy, radiotherapy, trastuzumab), HT, hypercholesterolaemia	Irbesartan, lansoprazole, paracetamol, simvastatin, riluzole	Nil
55	F	65	10m	Dysarthria; then dysphagia, drooling, cramps in hands and LLs	COPD, hysterectomy, L Dupuytren's	Seretide inh, simvastatin, quinine, aspirin, carbocisteine	Nil
56	M	53	6m	R LL cramps, weakness; subsequently fasciculation R then L LL, R UL	Fixed facial weakness and R hearing loss from birth	Riluzole	Nil
57	M	52	6m	Dysarthria, dysphagia, mild UL weakness	Nil	Mirtazepine, riluzole	Nil
58	F	55	5m	Bilat LL weakness, twitching, cramps	Nil	Nil	Sister and paternal uncle: MND
59	F	29	15m	Unstable L ankle, falls, foot drop	Cystic fibrosis, pancreatic insufficiency, old L LL sciatica	Azithromycin, flucloxacillin, polymyxin E, salbutamol inh, fluticasone and salmeterol inh, quinine	Nil
60	M	66	13m	Bilat UL stiffness, weakness; then bilat LL weakness, bilat UL and LL wasting	HT, hiatus hernia, Barrett's oesophagus	Amitriptyline, lansoprazole, lisinopril, amlodipine, riluzole	Nil
61	M	83	12m	R hand then UL weakness, knees giving way	T2DM, diverticular disease, primary hyperparathyroidism, hiatus hernia	Atorvastatin, codeine, omeprazole	Sister: iPD
62	M	66	36m	Bilat LL weakness, stiffness; then bilat UL clumsiness, later slurring dysarthria	Depression, ulcerative colitis, alcohol overuse	Mesalazine, omeprazole, simvastatin, fluoxetine, tamsulosin, levodopa, dantrolene, aspirin, codeine	Nil
63	M	69	7m	Bilat proximal UL weakness, axial weakness	T2DM, HT, localised prostatic cancer	Metformin, lisinopril, BFZ, paracetamol, riluzole	Aunt: MS

Table B.2: Examination findings for patients with MND. (MRC=Medical Research Council, N=no/absent, NA=not applicable, NK=not known, Y=yes/present)

	Bulbar						Cervical (right)							Cervical (left)							Lumbosacral (right)							Lumbosacral (left)							
Patient number	Spasticity	Pseudobulbar features	Brisk jaw jerk	Fasciculations	Atrophy	Weakness	Spasticity	Reflexes exaggerated	Hoffman's sign	Fasciculations	Atrophy	Reflex depressed	Weakness	MRC score	Spasticity	Reflexes exaggerated	Hoffman's sign	Fasciculations	Atrophy	Reflexes depressed	Weakness	MRC score	Spasticity	Clonus	Reflexes exaggerated	Babinksi sign	Fasciculations	Atrophy	Reflex depressed	Weakness	MRC score	Spasticity	Clonus	Reflex exaggerated	Babinksi sign	Fasciculations	Atrophy	Reflex depressed	Weakness	MRC score
1	N	N	N	N	N	N	N	Y	N	Y	Y	N	Y	NK	N	Y	N	Y	Y	N	Y	NK	N	N	N	N	Y	N	N	N	NA	N	N	N	N	Y	N	N	N	NA
2	Y	N	Y	Y	Y	Y	N	Y	N	Y	Y	N	Y	4-5	N	Y	N	Y	Y	N	Y	4-5	N	N	Y	N	Y	Y	N	Y	4-5	N	N	Y	N	Y	Y	N	Y	4-5
3	N	N	N	N	N	Y	N	N	N	Y	Y	Y	Y	NK	N	N	N	Y	Y	Y	Y	NK	N	N	N	N	Y	N	N	N	NA	N	N	N	N	Y	N	N	Y	NK
4	Y	Y	Y	N	N	Y	N	Y	NK	N	Y	N	Y	NK	Y	Y	NK	N	N	N	Y	NK	Y	Y	Y	N	N	N	N	Y	NK	Y	Y	Y	N	N	N	N	Y	NK
5	N	N	Y	Y	N	Y	N	Y	NK	Y	Y	N	Y	NK	N	Y	NK	Y	Y	N	Y	NK	N	N	Y	N	Y	N	N	Y	NK	N	N	Y	N	Y	N	N	N	NA
6	N	N	Y	N	N	Y	N	Y	N	N	N	N	N	NA	N	Y	Y	Y	Y	N	Y	NK	N	N	Y	N	Y	N	N	Y	NK	N	N	Y	N	Y	N	N	Y	NK
7	Y	N	NK	Y	Y	Y	N	N	NK	N	N	N	Y	NK	N	N	NK	Y	N	N	Y	NK	N	N	N	N	N	N	N	N	NA	N	N	N	N	N	N	N	N	NA
8	N	N	NK	N	N	N	N	N	NK	N	N	N	N	NA	N	N	NK	N	N	N	N	NA	N	N	Y	Y	Y	N	N	Y	NK	N	N	Y	N	N	N	N	N	NA
9	Y	Y	N	N	N	Y	Y	Y	NK	N	N	N	N	NA	Y	Y	NK	N	N	N	Y	NK	Y	N	Y	Y	N	N	N	Y	NK	Y	N	Y	Y	N	N	N	Y	NK
10	Y	N	NK	N	N	N	Y	Y	NK	N	Y	N	Y	NK	Y	Y	NK	N	Y	N	Y	NK	Y	Y	Y	N	N	N	N	Y	NK	Y	Y	Y	N	N	N	N	Y	NK
11	Y	Y	Y	Y	N	N	N	Y	NK	N	Y	N	Y	NK	N	Y	NK	N	Y	N	Y	NK	Y	Y	Y	N	N	N	N	Y	4-5	Y	Y	Y	N	N	N	N	Y	4-5
12	N	N	NK	N	N	N	N	Y	NK	N	N	N	N	NA	N	Y	NK	Y	Y	N	Y	NK	Y	N	Y	N	Y	N	N	Y	NK	N	N	Y	N	N	N	N	N	NA
13	N	N	N	Y	Y	Y	N	Y	NK	N	Y	N	Y	4-5	N	Y	NK	N	Y	N	Y	4-5	N	N	Y	N	N	N	N	Y	4-5	N	N	Y	N	N	N	N	Y	4-5
14	Y	Y	N	N	N	Y	N	Y	NK	N	N	N	Y	NK	N	Y	NK	N	N	N	Y	NK	Y	N	Y	Y	N	N	N	Y	4-5	Y	Y	Y	Y	N	N	N	Y	4-5
15	Y	N	N	N	N	Y	N	Y	NK	N	N	N	Y	4-5	N	Y	Y	N	N	N	Y	4-5	N	N	Y	N	N	N	N	Y	NK	N	N	Y	N	N	N	N	Y	NK
16	N	N	N	N	N	Y	N	Y	NK	N	Y	N	Y	4-5	N	Y	NK	N	N	N	N	NA	N	N	N	N	N	N	N	N	NA	N	N	N	N	N	N	N	N	NA
17	Y	N	Y	N	N	Y	N	N	NK	Y	N	N	Y	NK	N	Y	NK	Y	N	N	Y	NK	N	N	N	N	N	N	N	N	NA	N	N	N	N	Y	N	N	Y	NA
18	N	N	NK	N	N	N	N	Y	N	Y	Y	N	Y	NK	N	Y	N	Y	Y	N	Y	NK	Y	N	Y	Y	Y	Y	N	Y	NK	Y	Y	Y	Y	Y	Y	N	Y	NK
19	N	N	N	N	N	N	N	N	NK	N	N	N	Y	4-5	N	N	NK	N	N	N	N	NA	N	N	N	N	N	Y	Y	Y	4-5	N	N	N	N	N	Y	Y	Y	4-5
20	N	N	N	N	N	N	N	N	NK	N	Y	Y	Y	0-5	N	N	NK	N	Y	Y	Y	0-5	N	N	N	N	N	Y	Y	Y	4-5	N	N	N	N	N	Y	Y	Y	4-5
21	N	N	NK	N	N	N	N	N	N	Y	Y	Y	Y	4-5	N	N	N	Y	Y	Y	Y	4-5	N	N	N	N	N	N	N	N	NA	N	N	N	N	N	N	N	N	NA
22	N	N	N	N	N	N	N	Y	N	Y	Y	N	Y	NK	N	Y	N	Y	Y	N	Y	NK	N	Y	Y	N	Y	N	Y	N	4-5	N	N	Y	N	N	N	N	Y	4-5
23	Y	N	Y	Y	N	Y	N	N	NK	Y	N	N	Y	NK	N	Y	NK	Y	N	N	Y	NK	N	N	N	N	Y	N	Y	Y	NK	N	N	N	N	Y	N	Y	Y	NK
24	N	N	N	N	N	N	N	Y	Y	Y	Y	N	Y	4-5	N	Y	N	N	N	N	N	NA	N	N	Y	N	N	N	N	N	NA	N	N	Y	N	N	N	N	N	NA
25	Y	N	Y	Y	Y	Y	Y	Y	Y	Y	Y	N	Y	NK	Y	Y	Y	Y	Y	N	Y	NK	N	Y	Y	Y	Y	Y	N	Y	NK	N	Y	Y	N	Y	Y	N	Y	NK
26	N	Y	N	N	N	Y	N	Y	NK	Y	Y	N	Y	NK	N	Y	NK	Y	Y	N	Y	NK	N	N	Y	N	Y	Y	N	Y	4-5	N	N	Y	Y	Y	Y	N	Y	4-5
27	N	N	Y	Y	Y	Y	N	Y	NK	Y	N	N	Y	NK	N	Y	NK	Y	N	N	N	NA	N	N	Y	N	Y	Y	N	N	NA	N	N	Y	N	Y	N	N	N	NA
28	N	N	N	N	N	N	Y	Y	NK	Y	N	N	Y	4-5	N	Y	NK	Y	N	N	Y	4-5	Y	Y	Y	Y	Y	Y	N	Y	0-5	N	N	Y	Y	Y	N	N	N	NA
29	N	N	NK	N	N	N	N	N	NK	Y	Y	N	Y	NK	N	N	NK	Y	Y	N	Y	NK	N	N	N	N	Y	N	N	N	NA	N	N	N	N	Y	N	N	N	NA
30	Y	N	Y	Y	N	Y	N	Y	Y	N	N	N	Y	4-5	N	Y	Y	N	N	N	Y	4-5	Y	N	Y	Y	N	N	N	N	NA	Y	N	Y	Y	N	N	N	N	NA
31	N	N	NK	N	N	N	N	Y	NK	N	N	N	N	NA	N	Y	NK	Y	N	N	N	NA	Y	Y	Y	N	N	N	N	N	NA	Y	Y	Y	N	Y	Y	N	Y	4-5
32	N	N	NK	N	N	N	N	N	NK	N	Y	Y	Y	4-5	N	N	NK	N	Y	Y	Y	4-5	N	N	N	N	Y	N	Y	N	4-5	N	N	Y	N	N	Y	N	Y	4-5
33	N	N	N	N	N	N	N	N	NK	Y	N	N	N	NA	N	N	NK	Y	N	N	Y	NA	N	N	N	N	Y	Y	Y	N	NA	N	N	N	N	Y	Y	Y	Y	4-5
34	N	N	N	N	N	N	Y	Y	NK	N	N	N	Y	NK	N	Y	NK	N	N	N	N	NA	Y	N	Y	Y	N	N	N	Y	NK	Y	N	Y	N	N	N	N	N	NK
35	N	N	N	Y	N	Y	N	Y	N	Y	N	N	Y	NK	N	Y	N	Y	N	N	Y	NK	N	N	Y	N	N	Y	Y	Y	NK	N	N	Y	N	N	Y	Y	Y	NK
36	N	N	NK	Y	Y	Y	N	N	NK	Y	N	N	N	NA	N	N	NK	N	N	N	N	NA	N	N	N	N	Y	N	N	N	NA	N	N	N	N	Y	N	N	N	NA
37	N	N	N	N	N	Y	N	Y	NK	Y	Y	N	Y	NK	N	Y	NK	Y	Y	N	Y	NK	N	N	Y	N	N	Y	Y	Y	NK	N	N	Y	N	N	N	N	Y	NK
38	N	N	NK	N	N	Y	N	Y	NK	Y	Y	N	Y	NK	N	Y	NK	N	N	N	Y	NK	N	Y	Y	N	N	N	N	N	NA	N	N	Y	N	N	N	N	N	NA
39	Y	Y	Y	N	N	Y	N	Y	NK	N	N	N	N	NA	N	Y	NK	N	N	N	N	NA	N	N	Y	N	N	N	N	N	NA	N	N	Y	N	N	N	N	N	NA
40	Y	Y	Y	Y	Y	Y	N	Y	N	N	Y	N	Y	4-5	N	Y	N	N	Y	N	Y	2-5	N	N	N	N	Y	Y	N	Y	4-5	N	N	N	N	N	N	Y	Y	3-5
41	N	N	N	N	N	N	N	N	NK	Y	N	N	Y	NK	N	N	NK	Y	N	N	Y	NK	N	N	N	N	Y	N	N	Y	4-5	N	N	N	N	Y	N	N	Y	4-5
42	N	N	N	N	N	N	N	Y	N	N	N	N	N	NA	N	Y	N	N	N	N	N	NA	N	N	Y	N	N	Y	Y	Y	NK	N	N	Y	N	N	Y	Y	Y	NK
43	Y	Y	NK	Y	Y	Y	N	N	NK	Y	N	N	N	NA	N	Y	NK	Y	Y	N	Y	NK	N	N	N	N	Y	N	N	N	NA	N	N	N	N	Y	N	N	N	NA
44	N	N	NK	N	N	N	N	Y	NK	N	N	N	N	NA	N	Y	NK	N	N	N	N	NA	N	N	Y	N	N	Y	Y	Y	NK	N	N	Y	N	N	N	N	N	NA
45	N	N	N	N	N	Y	N	N	NK	Y	Y	N	Y	4-5	N	N	NK	Y	N	Y	Y	NK	N	N	Y	N	N	N	N	N	NA	Y	N	Y	Y	N	N	N	N	NA
46	N	N	NK	N	N	N	N	N	NK	Y	Y	N	Y	NK	N	N	NK	N	N	N	N	NA	N	N	N	N	N	N	N	N	NA	N	N	N	N	N	N	N	N	NA
47	N	N	NK	Y	N	Y	N	Y	NK	Y	N	N	N	NA	N	Y	NK	N	N	N	Y	NK	Y	Y	Y	N	Y	N	N	Y	NK	Y	Y	Y	N	Y	N	N	Y	NK
48	N	N	N	N	N	Y	N	Y	N	Y	Y	N	Y	NK	N	Y	N	Y	Y	N	Y	NK	N	N	Y	N	Y	N	N	Y	NK	N	N	Y	N	Y	N	N	Y	NK
49	N	N	NK	Y	N	N	N	Y	N	Y	Y	N	Y	4-5	N	Y	N	Y	Y	N	Y	4-5	Y	N	Y	Y	Y	Y	N	Y	4-5	Y	N	Y	N	Y	Y	N	Y	4-5
50	Y	N	Y	Y	Y	NK	N	Y	NK	Y	Y	N	NK	NK	N	Y	NK	Y	Y	N	NK	NK	Y	N	Y	Y	Y	Y	N	NK	NK	Y	N	Y	N	Y	Y	N	NK	NK
51	N	N	NK	N	N	N	N	Y	NK	Y	Y	N	Y	NK	N	Y	NK	Y	Y	N	Y	NK	Y	Y	Y	Y	Y	N	N	N	NA	Y	Y	Y	Y	Y	N	N	N	NA
52	Y	Y	Y	Y	Y	Y	N	Y	NK	Y	N	N	N	NA	N	Y	NK	N	N	N	N	NA	N	N	Y	N	N	N	N	N	NA	N	N	Y	N	N	N	N	N	NA
53	N	N	N	N	N	N	N	Y	N	Y	N	N	Y	NK	N	Y	N	Y	N	N	Y	NK	N	N	Y	N	Y	Y	Y	Y	NK	N	N	Y	N	N	N	N	Y	NK
54	N	N	N	N	N	N	N	Y	NK	Y	Y	N	Y	NK	N	Y	NK	Y	Y	N	Y	NK	Y	Y	Y	N	N	N	N	Y	4-5	Y	Y	Y	N	N	Y	N	Y	4-5
55	Y	N	Y	Y	Y	Y	N	Y	Y	Y	N	N	N	NA	N	Y	Y	Y	N	N	N	NA	N	N	Y	N	Y	N	N	N	NA	N	N	Y	N	Y	N	N	N	NA
56	N	N	N	N	N	N	N	N	N	Y	N	N	N	NA	N	N	N	N	N	N	N	NA	N	N	Y	N	Y	N	N	Y	NK	N	N	Y	N	Y	N	N	N	NA
57	Y	Y	Y	Y	Y	Y	N	N	NK	Y	N	N	Y	NK	N	N	NK	Y	N	N	Y	NK	N	N	N	N	N	N	N	N	NA	N	N	N	N	N	N	N	N	NA
58	N	N	N	N	N	N	N	N	NK	N	N	N	N	NA	N	N	NK	N	N	N	N	NA	N	N	N	N	Y	Y	Y	Y	4-5	N	N	N	N	Y	Y	Y	Y	4-5
59	N	N	NK	N	N	N	N	Y	NK	N	N	N	N	NA	N	Y	NK	N	N	N	N	NA	N	N	Y	N	N	Y	N	Y	0-5	N	N	Y	N	N	Y	N	Y	0-5
60	N	N	NK	N	N	Y	N	N	NK	Y	Y	Y	Y	1-4	N	N	NK	Y	Y	Y	Y	1-4	Y	N	Y	N	Y	Y	N	Y	4-5	Y	N	Y	N	Y	Y	N	Y	4-5
61	N	N	N	N	N	N	N	N	NK	Y	Y	Y	Y	NK	N	N	NK	Y	N	N	N	NA	N	N	N	N	N	N	N	N	NA	N	N	N	N	N	N	N	N	NA
62	Y	N	N	N	N	N	N	Y	N	N	N	N	Y	4-5	Y	Y	Y	N	N	N	Y	4-5	Y	Y	Y	Y	N	N	N	NK	NK	Y	Y	Y	Y	N	N	N	NK	NK
63	N	N	N	N	N	N	N	Y	N	Y	Y	N	Y	4-5	N	Y	N	Y	Y	N	Y	4-5	N	N	N	N	Y	Y	N	N	NA	N	N	N	N	Y	Y	N	N	NA

Table B.3: Blood results for patients with MND. (AChR=acetyl choline receptor, ANCA=anti-neutrophil cytoplasmic antibodies, ESR=erythrocyte sedimentation rate, FBC=full blood count, GAD=glutamic acid decarboxylase, HTLV=human T-lymphotropic virus, MAG=myelin-associated glycoprotein, Microb'y=microbiology, N=normal/negative, SCA=spinocerebellar ataxia, SOD1=superoxide dismutase 1, SPG4=spastic paraplegia 4, TDP-43=transactive response DNA binding protein 43kDa, TSH=thyroid stimulating hormone, VLCFA=very long chain fatty acids)

	Haematology				Biochemistry							Immunology								Microb'y			Genetics
Patient number	FBC	ESR	Vitamin B12	Folate	Copper	Liver function	Thyroid function	Glucose	Creatine kinase (<160)	VLCFA	Hexosaminidase A	Auto-antibody screen	ANCA	Anti-AChR	Anti-GAD	Anti-GM1	Anti-MAG	Anti-neuronal	Serum electrophoresis	Immunoglobulins	Lyme serology	Treponema serology	HTLV serology	
1	N		N	N		N	N	N	845															
2	N					N																		
3	N	N	N	N		N			N			N		N					N	N				
4	N	N		N		N		N																
5	N					N																		
6																								
7	N	N				N	N	N	N			N		N					N	N				
8	N	N	N			N		N	443	N		N							N	N				
9	N		N	N	N	N		N		N		N			N			N						SPG4 N
10	N	N	N	N	N	N	N	N				N						N						
11																								
12	N					N																		
13	N					N			N					N					N	N				
14	N					N	N	N																
15	N					N																		
16	N					N	N																	
17	N		N	N		N		N				N							N	N				
18	N		N	N		N	N																	
19	N		N	N		N	N	N				N							N	N				
20									N			N				N			N	N				SOD1 and TDP-43 N
21	N	N				N		N	N			N				N								
22	N					N																		
23	N					N		N																
24	N	N	N			N	N		N							N			N	N				
25	N	N	N	N		N	N	N	N			N		N					N					
26	N	N	N			N			223			N			N				N	N				
27	N	N	N			N		N	N			N		N					N					
28	N	N				N	N	N	N										N	N				
29	N					N																		
30				N						N														
31	N	N	N	N	N	N	N	N	254			N							N	N				
32	N	N	N			N	N	N	N															
33						N																		SOD1 and TDP-43 N
34	N	N	N			N	N	N	N	N		N							N	N	N	N	N	
35	N	N				N																		
36	N	N	N			N	N		172			N							N	N		N		
37	N	N		N		N	TSH 9.41 (0.3-4.7), thyroxine 11.9 (9.5-21.5)	N	N			N							N	N				
38	N	N	N		N	N	N	N				N							N	N				
39																								
40	N					N												N						
41	N		N	N		N		N	N			N							N	N	N	N		
42	N	N	N			N	N	N	N			N	N						N	N				
43	N					N																		
44	N		N		N	N	N					N	N						N	N				
45	N					N																		
46	N					N										N	N							
47	N	N	N	N		N	N	N				N							N	N			N	
48	N	N				N			323															
49	N	N				N	N	N	564			N							N	N				
50	N					N			209															
51	N	N	N	N	N	N	N			N	N	N	N			N			N			N		
52	N			N		N	N	N	N			N		N										
53	N					N			461															
54	N					N																		
55	N	N				N		N																
56	N					N																		
57	N	N				N	N	N	N			N		N					N	N				
58	N	N				N			N															Heterozygous for familial pathogenic mutation c.229G>T, p.Asp77Tyr in exon 3 of SOD1
59	N	N				N	N	N		N	N	N	N			N	N		N		N	N		
60	N	N	N	N		N	N		N			N							N	N				
61																								
62			N				N															N		Huntingtin N, fragile X and SCA 1/2/3/6/7/17 screen N
63	N	N	N	N		N	TSH 5.16 (0.3-4.7), thyroxine 18.0 (9.5-21.5)	N	1000															

Table B.4: Cerebrospinal fluid (CSF) and MRI findings for patients with MND. (bilat=bilateral, C-spine=cervical spine, CST=corticospinal tract, L=left, L-spine=lumbosacral spine, OCB=oligoclonal bands, R=right, SVD=small vessel disease, T-spine=thoracic spine)

Patient number	CSF (OCB)	MRI brain	MRI C-spine	MRI T-spine	MRI L-spine
1			N		
2		Mild-moderate SVD			
3			Root compression R C4 and bilat C5		
4		Mild atrophy, mild SVD			
5			N		
6					
7	N	N			
8	N				
9	N	N	N		
10	Protein 0.55g/l (absent)	N	N	N	Moderate multilevel degenerative change, potential R L3 and L L5 compression
11		N	N	N	N
12		N	N		
13			N	N	N
14		N	N		
15		N	N		
16					
17		Moderate atrophy, mild SVD			
18					
19	N		Moderate foraminal stenoses L C3/4 and bilat C4/5	Disc protrusions T6/7 and T7/8 distorting but not compressing cord	Previous R L4/5 disc surgery, grade 1 anterolisthesis of L4 on L5
20		Mild SVD			
21	N (absent)		Multiple foraminal stenoses on R, no neural compromise		
22					
23					
24		Mild SVD	Mild-moderate degenerative changes, moderate-severe bilat foraminal stenoses C3/4, moderate bilat foraminal stenoses C6/7		
25					
26					Lateral spinal canal and foraminal stenosis L4/5, no neural compromise
27					
28					Mild degenerative changes, no neural compromise
29			Multilevel degenerative disc disease, foraminal impingement C4/5 and C5/6, worse on R		
30		Bilat linear low signal along posterior motor cortex, moderate atrophy			
31		Mild atrophy, mild SVD			
32					
33					Disc degeneration and retrolisthesis at L5/S1, L S1 root displaced by disc/osteophyte complex
34	N (absent)	Mild SVD	High cord signal C2-6, mild non-compressive disc bulges		
35			Mild-moderate spondylotic changes, mild foraminal stenosis R C5/6		
36		Mild atrophy			
37		Mild atrophy	Multilevel disc-osteophyte complexes C3/4 to C6/7 indenting thecal sac but not compressing cord, bilat foraminal stenosis at these levels but no definite impingement	Posterior disc bulge L4/5, mild impingement L L5	
38			N		
39		Mild SVD			
40		N	N		
41	N (absent)	N	N	N	N
42		Mild SVD	Moderate-severe foraminal stenoses L C4/5, bilat C5/6, R C6/7	N	Mild degenerative changes, most prominent at L4/5 with possible contact on L5 root, more so on R; multiple Tarlov cysts, largest associated with R S1 root
43					
44	N (absent)			Degenerative disc disease, no neural compromise	
45					
46			Mild-moderate foraminal stenosis bilat C5/6		
47	N (absent)				
48					
49					
50					
51	N	Symmetrical high signal in CST	N		
52		N			

Patient number	CSF (OCB)	MRI brain	MRI C-spine	MRI T-spine	MRI L-spine
53					
54		Mild SVD, mild bilat high signal in CST	N	N	N
55		N	Degenerative disease at C5/6 and C6/7, no neural compromise	N	N
56			Moderate Chiari 1 malformation, no syrinx, mild degenerative changes	Impingement R L5	N
57		Moderate atrophy			
58					
59	N (absent)	N			N
60			Mild-moderate spondylotic disease		
61					
62	N		Moderate multilevel degenerative changes, spinal canal stenosis C3/4 but no cord compression, moderate foraminal stenoses bilat C3/4 to C6/7 but no root compression		
63	Protein 0.88g/l				

Table B.5: Phenotype, handedness, affected limbs, limbs studied with TMS and IMC, and exclusion criteria for patients with MND. (F=familial, FA=flail arm, FL=flail leg, R=right, L=left, LL=lower limb, UL=upper limb)

			Affected		TMS				IMC				Exclusion criteria				
Patient number	Phenotype	Handedness	UL	LL	R UL	L UL	R LL	L LL	R UL	L UL	R LL	L LL	Sensory neuropathy on NCS	Bilaterally unable to complete LL coherence task	Declined TMS	No discernible UL root MEP	No discernible LL root MEP
1	ALS/FA	R	R>L	R=L	Y		Y		Y		Y						
2	PBP	R	R=L	L>R	Y		Y		Y		Y					Y	
3	ALS	R	L>R	R=L		Y	Y			Y	Y		Y				
4	PLS	R	L>R	L>R		Y		Y		Y		Y					
5	ALS	R	R=L	R=L	Y		Y		Y		Y						
6	ALS	R	L>R	R=L	Y		Y		Y		Y						
7	PBP	R	Neither	Neither					Y		Y				Y		
8	ALS	R	Neither	R only	Y		Y	Y	Y			Y					
9	PLS	R	L>R	L>R		Y		Y		Y		Y					
10	ALS	R	R>L	R>L	Y		Y		Y		Y						
11	PLS	R	L>R	R>L	Y		Y		Y		Y						
12	ALS	R	L>R	R>L	Y		Y		Y		Y						
13	PBP	R	L>R	L>R		Y		Y		Y		Y					
14	PLS	R	Neither	L>R	Y		Y		Y		Y						
15	PBP	R	L>R	L>R	Y		Y		Y		Y						
16	ALS	R	R>L	Neither	Y		Y		Y		Y						
17	PBP	R	Neither	Neither	Y		Y		Y		Y						
18	ALS	R	R>L	R>L	Y	Y	Y			Y	Y			Y			
19	PMA	R	R>L	R>L	Y		Y	Y	Y			Y					
20	ALS (F)	R	L>R	L>R		Y		Y		Y		Y					
21	PMA	R	R>L	Neither	Y		Y		Y		Y						
22	ALS/FA	R	R>L	R=L		Y	Y			Y	Y						
23	ALS	R	R=L	R>L	Y			Y	Y			Y					
24	ALS/FA	R	R>L	Neither	Y		Y		Y		Y						
25	ALS	R	R>L	R>L		Y		Y		Y		Y					
26	ALS	R	R>L	R>L	Y			Y	Y			Y					
27	PBP	R	R>L	R>L	Y		Y		Y		Y					Y	
28	ALS	R	R=L	R>L	Y		Y		Y		Y						
29	ALS/FA	R	R>L	Neither		Y	Y			Y	Y						
30	PLS	L	L>R	L>R		Y		Y		Y		Y					
31	ALS	R	R=L	L>R	Y			Y	Y			Y					
32	PMA	R	Neither	L>R	Y			Y	Y			Y					
33	ALS (F)	R	L>R	L>R		Y		Y		Y		Y				Y	
34	PLS	R	R>L	R>L		Y	Y			Y				Y			
35	ALS/FA	R	L>R	L>R	Y		Y		Y		Y						
36	PBP	R	Neither	Neither	Y		Y		Y		Y						
37	ALS	R	L>R	R>L	Y			Y	Y			Y					Y
38	ALS/FA	R	R>L	Neither	Y		Y		Y		Y						
39	PBP	R	R>L	R>L	Y		Y		Y		Y						
40	ALS/PBP	L	L>R	L>R	Y		Y		Y		Y						
41	ALS	R	R=L	R=L	Y		Y		Y					Y			
42	ALS	L	R=L	R=L		Y		Y		Y		Y					
43	ALS	R	L>R	R=L		Y		Y		Y		Y					
44	ALS/FL	R	L>R	R>L	Y	Y	Y	Y	Y			Y					
45	ALS/FA	R	L>R	L>R		Y		Y		Y		Y					
46	ALS	R	R>L	Neither	Y		Y		Y		Y						
47	ALS	R	R=L	R=L	Y		Y		Y		Y						
48	ALS	R	R=L	R=L	Y		Y		Y		Y						
49	ALS	R	L>R	L>R	Y		Y		Y		Y						
50	ALS	R	R=L	R=L	Y		Y		Y		Y						
51	ALS	L	L>R	R=L					Y			Y			Y		
52	PBP	R	Neither	Neither	Y		Y		Y		Y					Y	
53	ALS	R	Neither	L>R	Y			Y	Y			Y					
54	ALS	R	L>R	R=L	Y		Y		Y		Y						
55	PBP	L	R>L	R=L	Y			Y	Y			Y					
56	ALS	R	R=L	R>L	Y		Y		Y		Y						
57	PBP/ALS	R	L>R	Neither	Y		Y		Y		Y						
58	ALS (F)	R	R=L	R=L	Y		Y		Y		Y						
59	ALS	R	Neither	L>R	Y		Y	Y	Y		Y						
60	ALS/FA	R	R=L	R=L	Y		Y		Y		Y						
61	ALS/FA	R	R>L	R>L	Y	Y	Y			Y	Y		Y				
62	PLS	R	R>L	L>R	Y			Y	Y			Y					
63	ALS	R	L>R	R=L		Y	Y			Y	Y					Y	Y

C Clinical details for patients with motor neuron disease mimic syndromes

Table C.1: Genetic mutations of patients with HSP. (SPG=spastic paraplegia)

Patient number	Gene	Exon	cDNA change	Consequence
1	SPG4	Exon 4-17	del exon 4-17	Large-scale deletion
2	SPG4	Exon 4-17	del exon 4-17	Large-scale deletion
3	SPG4	Exon 4-17	del exon 4-17	Large-scale deletion
4	SPG4	Exon 4-17	del exon 4-17	Large-scale deletion
5	SPG4	Exon 4-17	del exon 4-17	Large-scale deletion
6	SPG4	Exon 7	c.1091_1093delGGCinsTGT	p.Arg364_Pro365delinsMetSer
7	SPG4	Intron 10	c.1321+2dupT	Splice site disruption
8	SPG4	Exon 11	c.1384A>G	p.Lys462Glu
9	SPG4	Exon 1	del exon 1	Large-scale deletion
10	SPG4	Intron 11	c.1414+1G>A	Splice site disruption
11	SPG31	Exon 5	c.337C>T	p.Arg113X
12	SPG31	Exon 5	c.337C>T	p.Arg113X

Table C.2: Electrophysiological diagnostic category, electrophysiological features, anti-GM1 result and responsiveness to intravenous immunoglobulin (IVIg) for patients with MMN (Olney *et al.*, 2003).

Patient number	Diagnostic category	Demyelinating neuropathy in ≥2 motor nerves	Conduction blocks: definite/probable	Sensory abnormalities	Anti-GM1	IVIg responsiveness
1	Definite MMN with conduction block	Y	3/0	N	N	Y
2	Definite MMN with conduction block	Y	2/0	N	1:400	Y
3	Definite MMN with conduction block	Y	2/0	N	N	Y
4	Definite MMN with conduction block	Y	2/0	N	N	Y
5	MMN (without conduction block)	Y	0/0	N	N	Y
6	MMN (with anti-ganglioside antibodies)	N	0/0	N	1:1600	Y
7	MMN (without conduction block)	Y	0/0	N	N	Y

Table C.3: Clinico-pathological diagnostic category for patients with IBM (ENMC Research Diagnostic Criteria 2011; Rose, 2013).

Patient number	Diagnostic category
1	Clinically-defined
2	Clinically-defined
3	Clinically-defined
4	Clinically-defined
5	Clinically-defined
6	Probable
7	Probable
8	Probable

Table C.4: History for patients with HSP, MMN and IBM. (BFZ=bendroflumethiazide, bilat=bilateral, BPH=benign prostatic hyperplasia, DH=drug history, DHS=dynamic hip screw, DVT=deep vein thrombosis, FH=family history, GORD=gastro-oesophageal reflux disease, HT=hypertension, IHD=ischaemic heart disease, L=left, LL=lower limb, N=normal, NK=not known, NOF=neck of femur fracture, PE=pulmonary embolism, PMH=past medical history, PPM=permanent pacemaker, R=right, SVT=supraventricular tachycardia, THR=total hip replacement, UL=upper limb)

Group	Patient number	Sex	Age at test	Duration at test	Initial presentation	Bladder	Bowel	Sensation	PMH	DH	FH
HSP	1	F	28	16y	Poor running from birth, always last at school, spastic gait noted at age 15	Occasional urgency	Occasional urgency	N	Nil	Baclofen	Mother affected
	2	F	50	40y	Detrusor overactivity, no gait disturbance	Incontinence due to detrusor overactivity	N	N	Nil	Nil	Two of four siblings and daughter affected
	3	M	35	30y	Late walker, increasingly spastic gait	Frequency, urgency	N	N	Nil	Nil	Grandfather in wheelchair from age 14, father with high insteps, both siblings and one of two children affected
	4	F	57	22y	Stiff LLs	Urgency, frequency	N	N	Hysterectomy	Tizanidine, lisinopril, aspirin, simvastatin, BFZ, codeine, paracetamol	Two of four siblings affected
	5	M	62	24y	Progressive stiffness of LLs, gait disturbance, falls	Long-term catheter for neuropathic bladder	N	N	Epilepsy in remission, DVT/PE, complicated sacral sore requiring defunctioning colostomy, HT, peripheral vascular disease, GORD, R NOF/DHS	Phenytoin, phenobarbitone, BFZ, lisinopril, amlodipine, aspirin, tinzaparin, tizanidine, atorvastatin, omeprazole	Paternal grandfather, father, three paternal uncles, two of four sisters affected
	6	F	65	13y	L>R LL stiffness, falls	N	N	N	Polymyalgia rheumatica	Nil	Father and maternal aunt affected
	7	F	72	65y	Tripping over ankles, then progressively spastic LLs	Nocturia, urge and stress incontinence	N	N	Hypothyroidism	Thyroxine, tolterodine, dantrolene, baclofen	Son affected
	8	F	73	5y	Stiff LLs, difficulty walking	Urgency, frequency, nocturia	NK	N	Asthma, anxiety, depression	Chlorpromazine, citalopram, trazodone, temazepam, amitriptyline, paracetamol, oxybutinin, baclofen, tolterodine, codeine, tizanidine, inhalers	Mother and seven of nine siblings affected
	9	M	39	11y	Progressive deterioration in gait after fall	N	N	NK	Nil	NK	Adopted; FH not known
	10	M	49	5y	Dragging toes, catching feet, stiffness around hips	Urge and stress incontinence, nocturia	N	N	Nil	Solifenacin	One of two brothers affected, two children asymptomatic
	11	M	66	63y	Walked at normal age, then balance deteriorated, toe-walking so using callipers throughout teens, clumsiness and wasting of hands from mid-50s	N	N	N	Tendon lengthening in adolescence	Nil	Son and grandson affected
	12	M	43	38y	Slowly progressive spastic gait	Nocturia	N	N	Nil	Nil	Father and one of two children affected
MMN	1	M	59	12y	L>R UL/LL weakness, cramps; subsequently R LL then R UL weakness	NK	NK	N	Asbestos exposure, R malignant epithelioid mesothelioma (talc pleurodesis, palliative chemotherapy, radiotherapy)	Nil (previously on cyclophosphamide for MMN)	Nil
	2	M	61	27y	L UL wasting, weakness, paraesthesia; then R hand wasting and weakness	N	N	N	Past alcohol overuse, HT, BPH, mastoid revision surgery, SVT	Tamsulosin, finasteride, BFZ, metoprolol	Nil
	3	M	51	11y	R UL weakness; subsequently L UL weakness, then bilat LL weakness; marked cramps in all limbs	NK	NK	N	HT	BFZ (previously on cyclophosphamide for MMN)	Nil
	4	F	29	2y	L UL weakness	N	N	N	Eczema	Nil	Nil
	5	M	28	6y	Progressive R hand weakness	NK	NK	N	Asthma	Nil	Nil
	6	M	70	8y	L then R hand weakness	NK	NK	N	HT, R THR, chronic lumbar back pain, nerve root blocks, R L4/5 microdiscectomy	Atenolol, gabapentin, amitriptyline, amlodipine	Nil
	7	M	35	3y	R finger locking/spasms; subsequently R UL weakness, then L ankle weakness	N	N	N	Nil	Nil	Nil

Group	Patient number	Sex	Age at test	Duration at test	Initial presentation	Bladder	Bowel	Sensation	PMH	DH	FH
IBM	1	F	74	39y	Discomfort of muscles hips>shoulders; then difficulty in reaching up and rising from low chairs	NK	NK	NK	Auto-immune hypothyroidism, impaired glucose tolerance, HT, bilat breast cancer (bilat mastectomy, tamoxifen)	Prednisolone, diclofenac, verapamil, thyroxine; previously on methotrexate/azathioprine	Nil
	2	M	78	NK	NK	NK	NK	NK	Cluster headache, HT, obesity, hypercholesterolaemia, depression, airways disease ?type	Carbocisteine, citalopram, inhalers	Nil
	3	F	64	19y	Slowly progressive difficulty climbing stairs, running; then poor L grip, mild dysphagia	N	N	N	IHD, impaired glucose tolerance, hypercholesterolaemia, cholecystectomy, Sjögren's syndrome	BFZ, ezetimibe, atenolol, aspirin	Nil
	4	M	87	10y	Stamping gait L LL, problems climbing stairs; then poor grip and dexterity	NK	NK	N	HT, gout, mitral stenosis, PPM for heart block, B12 deficiency and iron deficiency anaemia, pleural plaques from asbestos exposure	Allopurinol, aspirin	Nil
	5	M	83	7y	Falls related to knees buckling, difficulty climbing stairs	NK	NK	NK	NK	Aspirin, simvastatin, lisinopril	Nil
	6	F	77	12y	Camptocormia, difficulty climbing stairs, unable to stand from low chairs	Urgency	NK	N	Nil	Nil	Nil
	7	M	64	1y	Weakness of L ankle plantarflexion then L hand	N	N	N	Nil	Nil	Nil
	8	F	68	5y	Difficulty rising from squat/climbing and descending stairs; then difficulty with grip and some dysphagia for solids	NK	NK	N	Hypothyroidism, Sjögren's syndrome, vitiligo, hysterectomy, cholecystectomy	Thyroxine, colecalciferol, strontium	Nil

Table C.5: Blood results for patients with HSP, MMN and IBM. (ANA=anti-nuclear antibody, ANCA=anti-neutrophil cytoplasmic antibodies, ESR=erythrocyte sedimentation rate, FBC=full blood count, N=normal/negative, RhF=rheumatoid factor, TSH=thyroid stimulating hormone, VLCFA=very long chain fatty acids)

		Haematology				Biochemistry						Immunology					Microbiology			
Group	Patient number	FBC	ESR	Vitamin B12	Folate	Liver function	Thyroid function	Glucose	Creatine kinase (<160)	VLCFA	White cell enzymes	Auto-antibody screen	ANCA	Anti-tissue transglutaminase	Serum electrophoresis	Immunoglobulins	Treponema serology	Leptospira serology	Brucella serology	Hepatitis serology
HSP	1	N																		
	2																			
	3	N				N		N												
	4																			
	5	N	N			N		N							N	N				
	6	N	N			N	N		N	N		N			N	N				
	7	N		N	N		N		N	N	N	Anti-microsomal >1:6400			N	N	N			
	8	N					N		N											
	9																			
	10	N	N			N		N		N										
	11	N	N	N	N	N	N	N	N	N		N				N				
	12																			
MMN	1	N		N	N	N		N				N			N	N	N	N	N	
	2	N	N	N	N	N	N	N	N			N	N		N	N				
	3	N	N	N	N	N	N	N	N			N			N	N				
	4	N	N	N		N	N					N			N	N				
	5	N	N			N	N		N			N		N	N	N				
	6	N	N	N		N	N	N	N			N	N			N				
	7	N	N			N	N	N	N	N	N	N				N				
IBM	1	N	N	N	N	N	TSH 0.24 (0.3-4.7), thyroxine 26.9 (9.5-21.5)	N	188-603			N			N		N			
	2	N	N	N	N	N	N	N	832			N			N	N				
	3	N		N	N	N	N		361-499						N					N
	4	N	N	N	N	N	N		N					N	N	N				
	5	N	N			N	N		241-270			N			N	N				
	6	N	N	N	N		N	N	N			N								
	7	N							271			N		N	N	N				
	8	N	N			N		N	322-856			ANA, RhF, anti-Ro, anti-La positive			N					

Table C.6: Cerebrospinal fluid (CSF) and MRI findings for patients with HSP, MMN and IBM. (bilat=bilateral, C-spine=cervical spine, L=left, L-spine=lumbosacral spine, OCB=oligoclonal bands, R=right, T-spine=thoracic spine)

Group	Patient number	CSF	MRI brain	MRI C-spine	MRI T-spine	MRI L-spine
HSP	1					
	2					
	3					
	4					Early osteophytes
	5		N			
	6	N	N	N	N	N
	7	N (absent)	N	Degenerative changes C3/4, some compression of L C4 root but no cord compression	N	
	8		Moderate atrophy	Mild foraminal stenoses R C2/3 and L C4/5, moderate-severe foraminal stenoses bilat C5/6, no cord compression	N	Degenerative changes, mild spinal canal stenosis, bilat foraminal stenosis L4/5, grade 1 spondylolisthesis at L5/S1
	9					
	10		N	N	N	N
	11			Mild degenerative changes, most markedly R C3/4, no neural compromise	N	Osteophytes on L, mild lateral recess effacement at several levels, no neural compromise
	12				N	
MMN	1	N (absent)				
	2	N (absent)				
	3	Protein 0.5g/l (absent)	N	Degenerative changes, no root compression on R, moderate-severe foraminal stenoses and root compression at several levels on L		
	4	N	N	N		
	5	N (absent)				
	6	N (absent)		Spondylotic changes between C3/4 and C6/7, foraminal stenosis L C6/7 with compression of C7 root, indentation of theca without cord compression		Multilevel degenerative change, stenosis of L5/S1 foramen, very little fat around L5 nerve root
	7	N	N	Mild foraminal stenosis R C6/7, no neural compromise		
IBM	1					
	2					
	3					
	4					
	5					
	6					
	7					
	8					

References

Abbruzzese G, Schenone A, Scramuzza G, Caponnetto C, Gasparetto B, Adezati L, Abbruzzese M & Viviani GL (1993). Impairment of central motor conduction in diabetic patients. *Electroencephalogr Clin Neurophysiol* **89**, 335-340.

Aggarwal A & Nicholson G (2002). Detection of preclinical motor neurone loss in SOD1 mutation carriers using motor unit number estimation. *J Neurol Neurosurg Psychiatry* **73**, 199-201.

Al-Chalabi A, Jones A, Troakes C, King A, Al-Sarraj S & Van Den Berg LH (2012). The genetics and neuropathology of amyotrophic lateral sclerosis. *Acta Neuropathol* **124**, 339-352.

Allison T, Wood CC & Goff WR (1983). Brain stem auditory, pattern-reversal visual, and short-latency somatosensory evoked potentials: Latencies in relation to age, sex, and brain and body size. *Electroencephalogr Clin Neurophysiol* **55**, 619-636.

Anderson B & Rutledge V (1996). Age and hemisphere effects on dendritic structure. *Brain* **119**, 1983-1990.

Arai T, Hasegawa M, Akiyama H, Ikeda K, Nonaka T, Mori H, Mann D, Tsuchiya K, Yoshida M, Hashizume Y & Oda T (2006). TDP-43 is a component of ubiquitin-positive tau-negative inclusions in frontotemporal lobar degeneration and amyotrophic lateral sclerosis. *Biochem Biophys Res Commun* **351**, 602-611.

Ardolino G, Bossi B, Barbieri S & Priori A (2005). Non-synaptic mechanisms underlie the after-effects of cathodal transcutaneous direct current stimulation of the human brain. *J Physiol* **568**, 653-663.

Atsuta N, Watanabe H, Ito M, Tanaka F, Tamakoshi A, Nakano I, Aoki M, Tsuji S, Yuasa T, Takano H, Hayashi H, Kuzuhara S & Sobue G (2009). Age at onset influences on wide-ranged clinical features of sporadic amyotrophic lateral sclerosis. *J Neurol Sci* **276**, 163-169.

Attarian S, Azulay JP, Lardillier D, Verschueren A & Pouget J (2005). Transcranial magnetic stimulation in lower motor neuron diseases. *Clin Neurophysiol* **116**, 35-42.

Attarian S, Pouget J & Schmied A (2006). Covariation of corticospinal efficiency and silent period in motoneuron diseases. *Muscle Nerve* **34**, 178-188.

Awiszus F (2003). TMS and threshold hunting. *Suppl Clin Neurophysiol* **56**, 13-23.

Baker MR & Baker SN (2003). The effect of diazepam on motor cortical oscillations and corticomuscular coherence studied in man. *J Physiol* **546**, 931-942.

Baker MR & Baker SN (2012). Beta-adrenergic modulation of tremor and corticomuscular coherence in humans. *PLoS ONE* **7**, e49088.

Baker SN, Chiu M & Fetz EE (2006). Afferent encoding of central oscillations in the monkey arm. *J Neurophysiol* **95**, 3904-3910.

Baker SN, Olivier E & Lemon RN (1997). Coherent oscillations in monkey motor cortex and hand muscle EMG show task-dependent modulation. *J Physiol* **501**, 225-241.

Baker SN, Pinches EM & Lemon RN (2003). Synchronization in monkey motor cortex during a precision grip task. II. Effect of oscillatory activity on corticospinal output. *J Neurophysiol* **89**, 1941-1953.

Barker AT (2002). The history and basic principles of magnetic stimulator design. In *Handbook of Transcranial Magnetic Stimulation*, ed. Pastula D, Davey NJ, Rothwell J, Wassermann EM & Puri BK, pp. 3-17. Arnold, London.

Barker AT, Freeston IL, Jalinous R & Jarratt JA (1986). Clinical evaluation of conduction time measurements in central motor pathways using magnetic stimulation of human brain. *Lancet* **1**, 1325-1326.

Barker AT, Freeston IL, Jalinous R & Jarratt JA (1987). Magnetic stimulation of the human brain and peripheral nervous system: An introduction and the results of an initial clinical evaluation. *Neurosurgery* **20**, 100-109.

Barker AT, Jalinous R & Freeston IL (1985). Non-invasive magnetic stimulation of human motor cortex. *Lancet* **1**, 1106-1107.

Bassetti C, Bogousslavsky J, Mattle H & Bernasconi A (1997). Medial medullary stroke: Report of seven patients and review of the literature. *Neurology* **48**, 882-890.

Belsh JM (2000). ALS diagnostic criteria of El Escorial Revisited: Do they meet the needs of clinicians as well as researchers? *Amyotroph Lateral Scler Other Motor Neuron Disord* **1**, S57-60.

Bensimon G, Lacomblez L & Meininger V (1994). A controlled trial of riluzole in amyotrophic lateral sclerosis. *N Engl J Med* **330**, 585-591.

Bentes C, De Carvalho M, Evangelista T & Sales-Luís ML (1999). Multifocal motor neuropathy mimicking motor neuron disease: Nine cases. *J Neurol Sci* **169**, 76-79.

Berardelli A, Abbruzzese G, Chen R, Orth M, Ridding MC, Stinear C, Suppa A, Trompetto C & Thompson PD (2008). Consensus paper on short-interval intracortical

inhibition and other transcranial magnetic stimulation intracortical paradigms in movement disorders. *Brain Stimul* **1**, 183-191.

Berardelli A, Inghilleri M, Cruccu G, Mercuri B & Manfredi M (1991). Electrical and magnetic transcranial stimulation in patients with corticospinal damage due to stroke or motor neurone disease. *Electroencephalogr Clin Neurophysiol* **81**, 389-396.

Bikson M, Datta A & Elwassif M (2009). Establishing safety limits for transcranial direct current stimulation. *Clin Neurophysiol* **120**, 1033-1034.

Bischoff C, Meyer BU, Machetanz J & Conrad B (1993). The value of magnetic stimulation in the diagnosis of radiculopathies. *Muscle Nerve* **16**, 154-161.

Brochier T, Boudreau MJ, Paré M & Smith AM (1999). The effects of muscimol inactivation of small regions of motor and somatosensory cortex on independent finger movements and force control in the precision grip. *Exp Brain Res* **128**, 31-40.

Brooks BR (1994). El Escorial World Federation of Neurology criteria for the diagnosis of amyotrophic lateral sclerosis. *J Neurol Sci* **124**, 96-107.

Brooks BR, Miller RG, Swash M & Munsat TL (2000). El Escorial revisited: Revised criteria for the diagnosis of amyotrophic lateral sclerosis. *Amyotroph Lateral Scler Other Motor Neuron Disord* **1**, 293-299.

Brown K, De Carvalho F, Williams ER, Jackson A, Baker MR & Baker SN (2012). A wearable electronic device for neuroplasticity studies. *Society for Neuroscience*, New Orleans.

Brown P (1994). Pathophysiology of spasticity. *J Neurol Neurosurg Psychiatry* **57**, 773-777.

Bühler R, Magistris MR, Truffert A, Hess CW & Rösler KM (2001). The triple stimulation technique to study central motor conduction to the lower limbs. *Clin Neurophysiol* **112**, 938-949.

Burke D, Hicks R, Stephen J, Woodforth I & Crawford M (1995). Trial-to-trial variability of corticospinal volleys in human subjects. *Electroencephalogr Clin Neurophysiol* **97**, 231-237.

Caramia MD, Bernardi G, Zarola F & Rossini PM (1988). Neurophysiological evaluation of the central nervous impulse propagation in patients with sensorimotor disturbances. *Electroencephalogr Clin Neurophysiol* **70**, 16-25.

Caramia MD, Cicinelli P, Paradiso C, Mariorenzi R, Zarola F, Bernardi G & Rossini PM (1991). 'Excitability' changes of muscular responses to magnetic brain stimulation in patients with central motor disorders. *Electroencephalogr Clin Neurophysiol* **81**, 243-250.

Cats EA, Van Der Pol WL, Piepers S, Franssen H, Jacobs BC, Van Den Berg-Vos RM, Kuks JB, Van Doorn PA, Van Engelen BG, Verschuuren JJ, Wokke JH, Veldink JH & Van Den Berg LH (2010). Correlates of outcome and response to IVIg in 88 patients with multifocal motor neuropathy. *Neurology* **75**, 818-825.

Chancellor AM, Slattery JM, Fraser H, Swingler RJ, Holloway SM & Warlow CP (1993). The prognosis of adult-onset motor neuron disease: A prospective study based on the Scottish Motor Neuron Disease Register. *J Neurol* **240**, 339-346.

Charcot J-M (1874). Amyotrophies spinales deuteropathiques sclerose laterale amyotrophique. In *Oeuvrews Completes*, pp. 234-248. Bureaux du Progres Medical, Paris.

Chen R, Cros D, Curra A, Di Lazzaro V, Lefaucheur JP, Magistris MR, Mills K, Rösler KM, Triggs WJ, Ugawa Y & Ziemann U (2008). The clinical diagnostic utility of transcranial magnetic stimulation: Report of an IFCN committee. *Clin Neurophysiol* **119**, 504-532.

Chokroverty S, Flynn D, Picone MA, Chokroverty M & Belsh J (1993). Magnetic coil stimulation of the human lumbosacral vertebral column: Site of stimulation and clinical application. *Electroencephalogr Clin Neurophysiol* **89**, 54-60.

Chokroverty S, Picone MA & Chokroverty M (1991). Percutaneous magnetic coil stimulation of human cervical vertebral column: Site of stimulation and clinical application. *Electroencephalogr Clin Neurophysiol* **81**, 359-365.

Chu N-S (1986). Somatosensory evoked potentials: Correlations with height. *Electroencephalogr Clin Neurophysiol* **65**, 169-176.

Chu N-S (1989). Motor evoked potentials with magnetic stimulation: Correlations with height. *Electroencephalogr Clin Neurophysiol* **74**, 481-485.

Chu N-S & Hong C-T (1985). Erb's and cervical somatosensory evoked potentials: Correlations with body size. *Electroencephalogr Clin Neurophysiol* **62**, 319-322.

Claus D (1990). Central motor conduction: Method and normal results. *Muscle Nerve* **13**, 1125-1132.

Claus D, Brunholzl C, Kerling FP & Henschel S (1995). Transcranial magnetic stimulation as a diagnostic and prognostic test in amyotrophic lateral sclerosis. *J Neurol Sci* **129**, 30-34.

Conway BA, Halliday DM, Farmer SF, Shahani U, Maas P, Weir AI & Rosenberg JR (1995). Synchronization between motor cortex and spinal motoneuronal pool during the performance of a maintained motor task in man. *J Physiol* **489**, 917-924.

Corse AM, Chaudhry V, Crawford TO, Cornblath DR, Kuncl RW & Griffin JW (1996). Sensory nerve pathology in multifocal motor neuropathy. *Ann Neurol* **39**, 319-325.

Creutzfeldt OD, Fromm GH & Kapp H (1962). Influence of transcortical d-c currents on cortical neuronal activity. *Exp Neurol* **5**, 436-452.

Cros D, Chiappa KH, Gominak S, Fang J, Santamaria J, King PJ & Shahani BT (1990). Cervical magnetic stimulation. *Neurology* **40**, 1751-1756.

Cruz Martinez A, Barrio M, Perez Conde MC & Gutierrez AM (1978). Electrophysiological aspects of sensory conduction velocity in healthy adults. I. Conduction velocity from digit to palm, from palm to wrist, and across the elbow, as a function of age. *J Neurol Neurosurg Psychiatry* **41**, 1092-1096.

Cruz Martínez A & Trejo JM (1999). Transcranial magnetic stimulation in amyotrophic and primary lateral sclerosis. *Electroencephalogr Clin Neurophysiol* **39**, 285-288.

Currà A, Modugno N, Inghilleri M, Manfredi M, Hallett M & Berardelli A (2002). Transcranial magnetic stimulation techniques in clinical investigation. *Neurology* **59**, 1851-1859.

Dalakas MC (2006). Sporadic inclusion body myositis - Diagnosis, pathogenesis and therapeutic strategies. *Nat Clin Pract Neurol* **2**, 437-447.

Datta A, Bansal V, Diaz J, Patel J, Reato D & Bikson M (2009). Gyri-precise head model of transcranial direct current stimulation: Improved spatial focality using a ring electrode versus conventional rectangular pad. *Brain Stimul* **2**, 201-207.

Day BL, Rothwell JC, Thompson PD, Dick JPR, Cowan JMA, Berardelli A & Marsden CD (1987). Motor cortex stimulation in intact man. 2. Multiple descending volleys. *Brain* **110**, 1191-1209.

De Carvalho M, Dengler R, Eisen A, England JD, Kaji R, Kimura J, Mills K, Mitsumoto H, Nodera H, Shefner J & Swash M (2008). Electrodiagnostic criteria for diagnosis of ALS. *Clin Neurophysiol* **119**, 497-503.

De Carvalho M, Evangelista T & Sales-Luís ML (2002). The corticomotor threshold is not dependent on disease duration in amyotrophic lateral sclerosis (ALS). *Amyotroph Lateral Scler Other Motor Neuron Disord* **3**, 39-42.

De Carvalho M, Miranda PC, Luís MLS & Ducla-Soares E (1999). Cortical muscle representation in amyotrophic lateral sclerosis patients: Changes with disease evolution. *Muscle Nerve* **22**, 1684-1692.

De Carvalho M & Swash M (2009). Awaji diagnostic algorithm increases sensitivity of El Escorial criteria for ALS diagnosis. *Amyotroph Lateral Scler* **10**, 53-57.

De Carvalho M, Turkman A & Swash M (2003). Motor responses evoked by transcranial magnetic stimulation and peripheral nerve stimulation in the ulnar innervation in amyotrophic lateral sclerosis: The effect of upper and lower motor neuron lesion. *J Neurol Sci* **210**, 83-90.

Desiato MT & Caramia MD (1997). Towards a neurophysiological marker of amyotrophic lateral sclerosis as revealed by changes in cortical excitability. *Electroencephalogr Clin Neurophysiol* **105**, 1-7.

Di Lazzaro V, Oliviero A, Profice P, Ferrara L, Saturno E, Pilato F & Tonali P (1999). The diagnostic value of motor evoked potentials. *Clin Neurophysiol* **110**, 1297-1307.

Di Lazzaro V, Pilato F, Oliviero A, Saturno E, Dileone M & Tonali PA (2004). Role of motor evoked potentials in diagnosis of cauda equina and lumbosacral cord lesions. *Neurology* **63**, 2266-2271.

Dorfman LJ & Bosley TM (1979). Age-related changes in peripheral and central nerve conduction in man. *Neurology* **29**, 38-44.

Dum RP & Strick PL (1991). The origin of corticospinal projections from the premotor areas in the frontal lobe. *J Neurosci* **11**, 667-689.

Dvorak J, Herdmann J & Theiler R (1990). Magnetic transcranial brain stimulation: Painless evaluation of central motor pathways. Normal values and clinical application in spinal cord diagnostics: Upper extremities. *Spine* **15**, 155-160.

Dvorak J, Herdmann J, Theiler R & Grob D (1991). Magnetic stimulation of motor cortex and motor roots for painless evaluation of central and proximal peripheral motor

pathways: Normal values and clinical application in disorders of the lumbar spine. *Spine* **16**, 955-961.

Efthimiadis KG, Samaras T & Polyzoidis KS (2010). Magnetic stimulation of the spine: The role of tissues and their modelling. *Phys Med Biol* **55**, 2541-2553.

Eisen A, Pant B & Stewart H (1993). Cortical excitability in amyotrophic lateral sclerosis: A clue to pathogenesis. *Can J Neurol Sci* **20**, 11-16.

Eisen A & Shtybel W (1990). AAEM minimonograph #35: Clinical experience with transcranial magnetic stimulation. *Muscle Nerve* **13**, 995-1011.

Eisen A, Shytbel W, Murphy K & Hoirch M (1990). Cortical magnetic stimulation in amyotrophic lateral sclerosis. *Muscle Nerve* **13**, 146-151.

Ellaway PH, Davey NJ, Maskill DW, Rawlinson SR, Lewis HS & Anissimova NP (1998). Variability in the amplitude of skeletal muscle responses to magnetic stimulation of the motor cortex in man. *Electroencephalogr Clin Neurophysiol* **109**, 104-113.

Evans CMB & Baker SN (2003). Task-dependent intermanual coupling of 8-Hz discontinuities during slow finger movements. *Eur J Neurosci* **18**, 453-456.

Eyre JA, Miller S, Clowry GJ, Conway EA & Watts C (2000). Functional corticospinal projections are established prenatally in the human foetus permitting involvement in the development of spinal motor centres. *Brain* **123**, 51-64.

Eyre JA, Miller S & Ramesh V (1991). Constancy of central conduction delays during development in man: Investigation of motor and somatosensory pathways. *J Physiol* **434**, 441-452.

Farmer SF, Bremner FD, Halliday DM, Rosenberg JR & Stephens JA (1993). The frequency content of common synaptic inputs to motoneurones studied during voluntary isometric contraction in man. *J Physiol* **470**, 127-155.

Farmer SF, Gibbs J, Halliday DM, Harrison LM, James LM, Mayston MJ & Stephens JA (2007). Changes in EMG coherence between long and short thumb abductor muscles during human development. *J Physiol* **579**, 389-402.

Filippi M, Agosta F, Abrahams S, Fazekas F, Grosskreutz J, Kalra S, Kassubek J, Silani V, Turner MR & Masdeu JC (2010). EFNS guidelines on the use of neuroimaging in the management of motor neuron diseases. *Eur J Neurol* **17**, 526-533.

Finsterer J, Löscher W, Quasthoff S, Wanschitz J, Auer-Grumbach M & Stevanin G (2012). Hereditary spastic paraplegias with autosomal dominant, recessive, X-linked, or maternal trait of inheritance. *J Neurol Sci* **318**, 1-18.

Fisher KM, Zaaimi B, Williams TL, Baker SN & Baker MR (2012). Beta-band intermuscular coherence: A novel biomarker of upper motor neuron dysfunction in motor neuron disease. *Brain* **135**, 2849-2864.

Fisher RJ, Galea MP, Brown P & Lemon RN (2002). Digital nerve anaesthesia decreases EMG-EMG coherence in a human precision grip task. *Exp Brain Res* **145**, 207-214.

Floyd AG, Yu QP, Piboolnurak P, Tang MX, Fang Y, Smith WA, Yim J, Rowland LP, Mitsumoto H & Pullman SL (2009). Transcranial magnetic stimulation in ALS: Utility of central motor conduction tests. *Neurology* **72**, 498-504.

Fritsch B, Reis J, Martinowich K, Schambra HM, Ji Y, Cohen LG & Lu B (2010). Direct current stimulation promotes BDNF-dependent synaptic plasticity: Potential implications for motor learning. *Neuron* **66**, 198-204.

Furby A, Bourriez JL, Jacquesson JM, Mounier-Vehier F & Guieu JD (1992). Motor evoked potentials to magnetic stimulation: Technical considerations and normative data from 50 subjects. *J Neurol* **239**, 152-156.

Garassus P, Charles N & Mauguere F (1993). Assessment of motor conduction times using magnetic stimulation of brain, spinal cord and peripheral nerves. *Electromyogr Clin Neurophysiol* **33**, 3-10.

Geser F, Brandmeir NJ, Kwong LK, Martinez-Lage M, Elman L, McCluskey L, Xie SX, Lee VMY & Trojanowski JQ (2008). Evidence of multisystem disorder in whole-brain map of pathological TDP-43 in amyotrophic lateral sclerosis. *Arch Neurol* **65**, 636-641.

Gibbs J, Harrison LM & Stephens JA (1997). Cross-correlation analysis of motor unit activity recorded from two separate thumb muscles during development in man. *J Physiol* **499**, 255-266.

Gilbertson T, Lalo E, Doyle L, Di Lazzaro V, Cioni B & Brown P (2005). Existing motor state is favored at the expense of new movement during 13-35 Hz oscillatory synchrony in the human corticospinal system. *J Neurosci* **25**, 7771-7779.

Gooch CL, Kaufmann P & Pullman S (2006). Objective markers of upper and lower motor neuron dysfunction: Electrophysiological studies and neuroimaging techniques. In *Amyotrophic Lateral Sclerosis*, ed. Mitsumoto H, Przedborski S & Gordon PH, pp. 167-200. Taylor & Francis, New York.

Graziadio S, Basu A, Tomasevic L, Zappasodi F, Tecchio F & Eyre JA (2010). Developmental tuning and decay in senescence of oscillations linking the corticospinal system. *J Neurosci* **30**, 3663-3674.

Groppa S, Oliviero A, Eisen A, Quartarone A, Cohen LG, Mall V, Kaelin-Lang A, Mima T, Rossi S, Thickbroom GW, Rossini PM, Ziemann U, Valls-Solé J & Siebner HR (2012). A practical guide to diagnostic transcranial magnetic stimulation: Report of an IFCN committee. *Clin Neurophysiol* **123**, 858-882.

Grosse P, Cassidy MJ & Brown P (2002). EEG-EMG, MEG-EMG and EMG-EMG frequency analysis: Physiological principles and clinical applications. *Clin Neurophysiol* **113**, 1523-1531.

Grosse P, Guerrini R, Parmeggiani L, Bonanni P, Pogosyan A & Brown P (2003). Abnormal corticomuscular and intermuscular coupling in high-frequency rhythmic myoclonus. *Brain* **126**, 326-342.

Gugino LD, Rafael Romero J, Aglio L, Titone D, Ramirez M, Pascual-Leone A, Grimson E, Weisenfeld N, Kikinis R & Shenton ME (2001). Transcranial magnetic stimulation coregistered with MRI: A comparison of a guided versus blind stimulation technique and its effect on evoked compound muscle action potentials. *Clin Neurophysiol* **112**, 1781-1792.

Halliday DM, Conway BA, Farmer SF & Rosenberg JR (1998). Using electroencephalography to study functional coupling between cortical activity and electromyograms during voluntary contractions in humans. *Neurosci Lett* **241**, 5-8.

Hamada M, Hanajima R, Terao Y, Sato F, Okano T, Yuasa K, Furubayashi T, Okabe S, Arai N & Ugawa Y (2007). Median nerve somatosensory evoked potentials and their high-frequency oscillations in amyotrophic lateral sclerosis. *Clin Neurophysiol* **118**, 877-886.

Hanajima R, Ugawa Y, Terao Y, Ogata K & Kanazawa I (1996). Ipsilateral cortico-cortical inhibition of the motor cortex in various neurological disorders. *J Neurol Sci* **140**, 109-116.

Hansen NL, Conway BA, Halliday DM, Hansen S, Pyndt HS, Biering-Sørensen F & Nielsen JB (2005). Reduction of common synaptic drive to ankle dorsiflexor motoneurons during walking in patients with spinal cord lesion. *J Neurophysiol* **94**, 934-942.

Haug H & Eggers R (1991). Morphometry of the human cortex cerebri and corpus striatum during aging. *Neurobiol Aging* **12**, 336-338.

Heffner RS & Masterton RB (1983). The role of the corticospinal tract in the evolution of human digital dexterity. *Brain Behav Evol* **23**, 165-183.

Hepp-Reymond MC, Trouche E & Wiesendanger M (1974). Effects of unilateral and bilateral pyramidotomy on a conditioned rapid precision grip in monkeys (Macaca fascicularis). *Exp Brain Res* **21**, 519-527.

Hess CW, Mills KR & Murray NMF (1986). Magnetic stimulation of the human brain: Facilitation of motor responses by voluntary contraction of ipsilateral and contralateral muscles with additional observations on an amputee. *Neurosci Lett* **71**, 235-240.

Hess CW, Mills KR & Murray NMF (1987). Responses in small hand muscles from magnetic stimulation of the human brain. *J Physiol* **388**, 397-419.

Househam E & Swash M (2000). Diagnostic delay in amyotrophic lateral sclerosis: What scope for improvement? *J Neurol Sci* **180**, 76-81.

Humm AM, Z'Graggen WJ, Von Hornstein NE, Magistris MR & Rösler KM (2004). Assessment of central motor conduction to intrinsic hand muscles using the triple stimulation technique: Normal values and repeatability. *Clin Neurophysiol* **115**, 2558-2566.

Humphrey DR & Corrie WS (1978). Properties of pyramidal tract neuron system within a functionally defined subregion of primate motor cortex. *J Neurophysiol* **41**, 216-243.

Huttenlocher PR (1979). Synaptic density in human frontal cortex: Developmental changes and effects of aging. *Brain Res* **163**, 195-205.

Incel NA, Sezgin M, As I, Cimen OB & Sahin G (2009). The geriatric hand: Correlation of hand-muscle function and activity restriction in elderly. *Int J Rehabil Res* **32**, 213-218.

Iyer MB, Mattu U, Grafman J, Lomarev M, Sato S & Wassermann EM (2005). Safety and cognitive effect of frontal DC brain polarization in healthy individuals. *Neurology* **64**, 872-875.

Jackson A, Spinks RL, Freeman TCB, Wolpert DM & Lemon RN (2002). Rhythm generation in monkey motor cortex explored using pyramidal tract stimulation. *J Physiol* **541**, 685-699.

James LM, Halliday DM, Stephens JA & Farmer SF (2008). On the development of human corticospinal oscillations: Age-related changes in EEG-EMG coherence and cumulant. *Eur J Neurosci* **27**, 3369-3379.

Jane JA, Yashon D, DeMyer W & Bucy PC (1967). The contribution of the precentral gyrus to the pyramidal tract of man. *J Neurosurg* **26**, 244-248.

Jeans AF & Ansorge O (2009). Recent developments in the pathology of motor neurone disease. *Adv Clin Neurosci Rehabil* **9**, 25-26.

Jeffery DT, Norton JA, Roy FD & Gorassini MA (2007). Effects of transcranial direct current stimulation on the excitability of the leg motor cortex. *Exp Brain Res* **182**, 281-287.

Johnston M, Earll L, Mitchell E, Morrison V & Wright S (1996). Communicating the diagnosis of motor neurone disease. *Palliat Med* **10**, 23-34.

Kamp D, Krause V, Butz M, Schnitzler A & Pollok B (2013). Changes of cortico-muscular coherence: An early marker of healthy aging? *Age* **35**, 49-58.

Karandreas N, Papadopoulou M, Kokotis P, Papapostolou A, Tsivgoulis G & Zambelis T (2007). Impaired interhemispheric inhibition in amyotrophic lateral sclerosis. *Amyotroph Lateral Scler* **8**, 112-118.

Kaufmann P, Pullman SL, Shungu DC, Chan S, Hays AP, Del Bene ML, Dover MA, Vukic M, Rowland LP & Mitsumoto H (2004). Objective tests for upper motor neuron involvement in amyotrophic lateral sclerosis (ALS). *Neurology* **62**, 1753-1757.

Keenan KG, Collins JD, Massey WV, Walters TJ & Gruszka HD (2011). Coherence between surface electromyograms is influenced by electrode placement in hand muscles. *J Neurosci Methods* **195**, 10-14.

Kiers L, Cros D, Chiappa KH & Fang J (1993). Variability of motor potentials evoked by transcranial magnetic stimulation. *Electroencephalogr Clin Neurophysiol* **89**, 415-423.

Kilner JM, Baker SN, Salenius S, Hari R & Lemon RN (2000). Human cortical muscle coherence is directly related to specific motor parameters. *J Neurosci* **20**, 8838-8845.

Kilner JM, Baker SN, Salenius S, Jousmäki V, Hari R & Lemon RN (1999). Task-dependent modulation of 15-30 Hz coherence between rectified EMGs from human hand and forearm muscles. *J Physiol* **516**, 559-570.

Kilner JM, Fisher RJ & Lemon RN (2004). Coupling of oscillatory activity between muscles is strikingly reduced in a deafferented subject compared with normal controls. *J Neurophysiol* **92**, 790-796.

Kimura J (2001). *Electrodiagnosis in Diseases of Nerve and Muscle: Principles and Practice*. Oxford University Press, Oxford.

Kloten H, Meyer BU, Britton TC & Benecke R (1992). Normwerte und altersabhängige Veränderungen magnetoelektrisch evozierter Muskelsummenpotentiale [Magnetic stimulation: Standardized determination of normal values for central and peripheral motor latencies regarding age-dependent changes]. *EEG EMG Z Elektroenzephalogr Elektromyogr Verwandte Geb* **23**, 29-36.

Kohara N, Kaji R, Kojima Y & Kimura J (1999). An electrophysiological study of the corticospinal projections in amyotrophic lateral sclerosis. *Clin Neurophysiol* **110**, 1123-1132.

Kong X, Schoenfeld DA, Lesser EA & Gozani SN (2010). Implementation and evaluation of a statistical framework for nerve conduction study reference range calculation. *Comput Methods Programs Biomed* **97**, 1-10.

Krampe RT (2002). Aging, expertise and fine motor movement. *Neurosci Biobehav Rev* **26**, 769-776.

Lacomblez L, Bensimon G, Leigh PN, Guillet P & Meininger V (1996). Dose-ranging study of riluzole in amyotrophic lateral sclerosis. *Lancet* **347**, 1425-1431.

Lang CE, Wagner JM, Edwards DF, Sahrmann SA & Dromerick AW (2006). Recovery of grasp versus reach in people with hemiparesis poststroke. *Neurorehabil Neural Repair* **20**, 444-454.

Lawrence DG & Kuypers HGJM (1968). The functional organization of the motor system in the monkey: I. The effects of bilateral pyramidal lesions. *Brain* **91**, 1-14.

Lemon R (2002). Basic physiology of transcranial magnetic stimulation. In *Handbook of Transcranial Magnetic Stimulation*, ed. Pastula D, Davey NJ, Rothwell JC, Wassermann EM & Puri BK, pp. 61-77. Arnold, London.

Lemon RN (2008). Descending pathways in motor control. *Annu Rev Neurosci* **31**, 195-218.

Lemon RN, Mantel GWH & Muir RB (1986). Corticospinal facilitation of hand muscles during voluntary movements in the conscious monkey. *J Physiol* **381**, 497-527.

Liebetanz D, Koch R, Mayenfels S, König F, Paulus W & Nitsche MA (2009). Safety limits of cathodal transcranial direct current stimulation in rats. *Clin Neurophysiol* **120**, 1161-1167.

Liebetanz D, Nitsche MA, Tergau F & Paulus W (2002). Pharmacological approach to the mechanisms of transcranial DC-stimulation-induced after-effects of human motor cortex excitability. *Brain* **125**, 2238-2247.

Lomen-Hoerth C & Strong MJ (2006). Frontotemporal dysfunction in amyotrophic lateral sclerosis. In *Amyotrophic Lateral Sclerosis*, ed. Mitsumoto H, Przedborski S & Gordon PH, pp. 117-140. Taylor&Francis, New York.

Maccabee PJ (2002). Basic physiology of peripheral and spinal cord magnetic stimulation. In *Handbook of Transcranial Magnetic Stimulation*, ed. Pastula D, Davey NJ, Rothwell JC, Wassermann EM & Puri BK, pp. 78-84. Arnold, London.

Maccabee PJ, Amassian VE, Eberle LP, Rudell AP, Cracco RQ, Lai KS & Somasundarum M (1991). Measurement of the electric field induced into inhomogeneous volume conductors by magnetic coils: Application to human spinal neurogeometry. *Electroencephalogr Clin Neurophysiol* **81**, 224-237.

Maccabee PJ, Lipitz ME, Desudchit T, Golub RW, Nitti VW, Bania JP, Willer JA, Cracco RQ, Cadwell J, Hotson GC, Eberle LP & Amassian VE (1996). A new method using neuromagnetic stimulation to measure conduction time within the cauda equina. *Electroencephalogr Clin Neurophysiol* **101**, 153-166.

Madhavan S & Stinear JW (2010). Focal and bidirectional modulation of lower limb motor cortex using anodal transcranial direct current stimulation. *Brain Stimul* **3**, 42-50.

Magistris MR, Rösler KM, Truffert A, Landis T & Hess CW (1999). A clinical study of motor evoked potentials using a triple stimulation technique. *Brain* **122**, 265-279.

Magistris MR, Rösler KM, Truffert A & Myers JP (1998). Transcranial stimulation excites virtually all motor neurons supplying the target muscle: A demonstration and a method improving the study of motor evoked potentials. *Brain* **121**, 437-450.

Mall V, Berweck S, Fietzek UM, Glocker FX, Oberhuber U, Walther M, Schessl J, Schulte-Mönting J, Korinthenberg R & Helnen F (2004). Low level of intracortical inhibition in children shown by transcranial magnetic stimulation. *Neuropediatrics* **35**, 120-125.

Mano Y, Nakamuro T, Ikoma K, Sugata T, Morimoto S, Takayanagi T & Mayer RF (1992). Central motor conductivity in aged people. *Intern Med* **31**, 1084-1087.

Matsumoto H, Hanajima R, Shirota Y, Hamada M, Terao Y, Ohminami S, Furubayashi T, Nakatani-Enomoto S & Ugawa Y (2010). Cortico-conus motor conduction time (CCCT) for leg muscles. *Clin Neurophysiol* **121**, 1930-1933.

Matsumoto H, Konoma Y, Shimizu T, Okabe S, Shirota Y, Hanajima R, Terao Y & Ugawa Y (2012). Aging influences central motor conduction less than peripheral motor conduction: A transcranial magnetic stimulation study. *Muscle Nerve* **46**, 932-936.

Matsumoto H, Octaviana F, Hanajima R, Terao Y, Yugeta A, Hamada M, Inomata-Terada S, Nakatani-Enomoto S, Tsuji S & Ugawa Y (2009a). Magnetic lumbosacral motor root stimulation with a flat, large round coil. *Clin Neurophysiol* **120**, 770-775.

Matsumoto H, Octaviana F, Terao Y, Hanajima R, Yugeta A, Hamada M, Inomata-Terada S, Nakatani-Enomoto S, Tsuji S & Ugawa Y (2009b). Magnetic stimulation of the cauda equina in the spinal canal with a flat, large round coil. *J Neurol Sci* **284**, 46-51.

Matsuya R, Ushiyama J & Ushiba J (2013). Prolonged reaction time during episodes of elevated β-band corticomuscular coupling and associated oscillatory muscle activity. *J Appl Physiol* **114**, 896-904.

McGuire V & Nelson LM (2006). Epidemiology of ALS. In *Amyotrophic Lateral Sclerosis*, ed. Mitsumoto H, Przedborski S & Gordon PH, pp. 17-42. Taylor & Francis, New York.

Merletti R & Parker PA (2004). *Electromyography: Physiology, Engineering, and Noninvasive Applications*. Wiley, Hoboken.

Miller RG, Jackson CE, Kasarskis EJ, England JD, Forshew D, Johnston W, Kalra S, Katz JS, Mitsumoto H, Rosenfeld J, Shoesmith C, Strong MJ & Woolley SC (2009a). Practice parameter update: The care of the patient with amyotrophic lateral sclerosis: Drug, nutritional, and respiratory therapies (an evidence-based review): Report of the Quality Standards Subcommittee of the American Academy of Neurology. *Neurology* **73**, 1218-1226.

Miller RG, Jackson CE, Kasarskis EJ, England JD, Forshew D, Johnston W, Kalra S, Katz JS, Mitsumoto H, Rosenfeld J, Shoesmith C, Strong MJ & Woolley SC (2009b). Practice parameter update: The care of the patient with amyotrophic lateral

sclerosis: Multidisciplinary care, symptom management, and cognitive/behavioral impairment (an evidence-based review): Report of the Quality Standards Subcommittee of the American Academy of Neurology. *Neurology* **73**, 1227-1233.

Miller RG, Mitchell JD & Moore DH (2012). Riluzole for amyotrophic lateral sclerosis (ALS)/motor neuron disease (MND). *Cochrane Database Syst Rev*, CD001447.

Mills KR (2003). The natural history of central motor abnormalities in amyotrophic lateral sclerosis. *Brain* **126**, 2558-2566.

Mills KR & Murray NMF (1986). Electrical stimulation over the human vertebral column: Which neural elements are excited? *Electroencephalogr Clin Neurophysiol* **63**, 582-589.

Mills KR & Nithi KA (1997a). Corticomotor threshold is reduced in early sporadic amyotrophic lateral sclerosis. *Muscle Nerve* **20**, 1137-1141.

Mills KR & Nithi KA (1997b). Corticomotor threshold to magnetic stimulation: Normal values and repeatability. *Muscle Nerve* **20**, 570-576.

Mills KR & Nithi KA (1998). Peripheral and central motor conduction in amyotrophic lateral sclerosis. *J Neurol Sci* **159**, 82-87.

Mima T & Hallett M (1999). Electroencephalographic analysis of cortico-muscular coherence: Reference effect, volume conduction and generator mechanism. *Clin Neurophysiol* **110**, 1892-1899.

Mima T, Simpkins N, Oluwatimilehin T & Hallett M (1999). Force level modulates human cortical oscillatory activities. *Neurosci Lett* **275**, 77-80.

Miranda PC, Lomarev M & Hallett M (2006). Modeling the current distribution during transcranial direct current stimulation. *Clin Neurophysiol* **117**, 1623-1629.

Miscio G, Pisano F, Mora G & Mazzini L (1999). Motor neuron disease: Usefulness of transcranial magnetic stimulation in improving the diagnosis. *Clin Neurophysiol* **110**, 975-981.

Mitchell JD, Callagher P, Gardham J, Mitchell C, Dixon M, Addison-Jones R, Bennett W & O'Brien MR (2010). Timelines in the diagnostic evaluation of people with suspected amyotrophic lateral sclerosis (ALS)/motor neuron disease (MND) - a 20-year review: Can we do better? *Amyotroph Lateral Scler* **11**, 537-541.

Mitchell WK, Baker MR & Baker SN (2007). Muscle responses to transcranial stimulation in man depend on background oscillatory activity. *J Physiol* **583**, 567-579.

Moscufo N, Guttmann CRG, Meier D, Csapo I, Hildenbrand PG, Healy BC, Schmidt JA & Wolfson L (2011). Brain regional lesion burden and impaired mobility in the elderly. *Neurobiol Aging* **32**, 646-654.

Munneke MAM, Stegeman DF, Hengeveld YA, Rongen JJ, Schelhaas HJ & Zwarts MJ (2011). Transcranial direct current stimulation does not modulate motor cortex excitability in patients with amyotrophic lateral sclerosis. *Muscle Nerve* **44**, 109-114.

Murray EA & Coulter JD (1981). Organization of corticospinal neurons in the monkey. *J Comp Neurol* **195**, 339-365.

Murthy VN & Fetz EE (1992). Coherent 25- to 35-Hz oscillations in the sensorimotor cortex of awake behaving monkeys. *Proc Natl Acad Sci U S A* **89**, 5670-5674.

Murthy VN & Fetz EE (1996). Oscillatory activity in sensorimotor cortex of awake monkeys: Synchronization of local field potentials and relation to behaviour. *J Neurophysiol* **76**, 3949-3967.

Nihei K, McKee AC & Kowall NW (1993). Patterns of neuronal degeneration in the motor cortex of amyotrophic lateral sclerosis patients. *Acta Neuropathol* **86**, 55-64.

Nishimura Y, Morichika Y & Isa T (2009). A subcortical oscillatory network contributes to recovery of hand dexterity after spinal cord injury. *Brain* **132**, 709-721.

Nitsche MA, Cohen LG, Wassermann EM, Priori A, Lang N, Antal A, Paulus W, Hummel F, Boggio PS, Fregni F & Pascual-Leone A (2008). Transcranial direct current stimulation: State of the art 2008. *Brain Stimul* **1**, 206-223.

Nitsche MA, Doemkes S, Karakose T, Antal A, Liebetanz D, Lang N, Tergau F & Paulus W (2007). Shaping the effects of transcranial direct current stimulation of the human motor cortex. *J Neurophysiol* **97**, 3109-3117.

Nitsche MA, Fricke K, Henschke U, Schlitterlau A, Liebetanz D, Lang N, Henning S, Tergau F & Paulus W (2003). Pharmacological modulation of cortical excitability shifts induced by transcranial direct current stimulation in humans. *J Physiol* **553**, 293-301.

Nitsche MA & Paulus W (2000). Excitability changes induced in the human motor cortex by weak transcranial direct current stimulation. *J Physiol* **527**, 633-639.

Nitsche MA & Paulus W (2001). Sustained excitability elevations induced by transcranial DC motor cortex stimulation in humans. *Neurology* **57**, 1899-1901.

Nitsche MA & Paulus W (2011). Transcranial direct current stimulation - update 2011. *Restor Neurol Neurosci* **29**, 463-492.

Norton JA, Wood DE, Marsden JF & Day BL (2003). Spinally generated electromyographic oscillations and spasms in a low-thoracic complete paraplegic. *Mov Disord* **18**, 101-106.

Office for National Statistics (2011). 2011 Census, Key Statistics and Quick Statistics for Wards and Output Areas in England and Wales. Newport.

Ohara S, Nagamine T, Ikeda A, Kunieda T, Matsumoto R, Taki W, Hashimoto N, Baba K, Mihara T, Salenius S & Shibasaki H (2000). Electrocorticogram-electromyogram coherence during isometric contraction of hand muscle in human. *Clin Neurophysiol* **111**, 2014-2024.

Olivier E, Baker SN & Lemon RN (2002). Comparison of direct and indirect measurements of the central motor conduction time in the monkey. *Clin Neurophysiol* **113**, 469-477.

Olney RK, Lewis RA, Putnam TD & Campellone Jr JV (2003). Consensus criteria for the diagnosis of multifocal motor neuropathy. *Muscle Nerve* **27**, 117-121.

Omlor W, Patino L, Hepp-Reymond MC & Kristeva R (2007). Gamma-range corticomuscular coherence during dynamic force output. *NeuroImage* **34**, 1191-1198.

Omlor W, Patino L, Mendez-Balbuena I, Schulte-Mönting J & Kristeva R (2011). Corticospinal beta-range coherence is highly dependent on the pre-stationary motor state. *J Neurosci* **31**, 8037-8045.

Orth M & Rothwell JC (2004). The cortical silent period: Intrinsic variability and relation to the waveform of the transcranial magnetic stimulation pulse. *Clin Neurophysiol* **115**, 1076-1082.

Osei-Lah AD & Mills KR (2004). Optimising the detection of upper motor neuron function dysfunction in amyotrophic lateral sclerosis - a transcranial magnetic stimulation study. *J Neurol* **251**, 1364-1369.

Oshima Y, Mitsui T, Yoshino H, Endo I, Kunishige M, Asano A & Matsumoto T (2002). Central motor conduction in patients with anti-ganglioside antibody associated neuropathy syndromes and hyperreflexia. *J Neurol Neurosurg Psychiatry* **73**, 568-573.

Palmer E & Ashby P (1992). Corticospinal projections to upper limb motoneurones in humans. *J Physiol* **448**, 397-412.

Pauluis Q, Baker SN & Olivier E (1999). Emergent oscillations in a realistic network: The role of inhibition and the effect of the spatiotemporal distribution of the input. *J Comput Neurosci* **6**, 289-310.

Peinemann A, Lehner C, Conrad B & Siebner HR (2001). Age-related decrease in paired-pulse intracortical inhibition in the human primary motor cortex. *Neurosci Lett* **313**, 33-36.

Penfield W & Rasmussen T (1950). *The Cerebral Cortex of Man*. MacMillan, New York.

Pepe MS & Thompson ML (2000). Combining diagnostic test results to increase accuracy. *Biostatistics* **1**, 123-140.

Pfurtscheller G (1981). Central beta rhythm during sensorimotor activities in man. *Electroencephalogr Clin Neurophysiol* **51**, 253-264.

Pfurtscheller G, Stancák Jr A & Neuper C (1996). Post-movement beta synchronization. A correlate of an idling motor area? *Electroencephalogr Clin Neurophysiol* **98**, 281-293.

Pohja M & Salenius S (2003). Modulation of cortex-muscle oscillatory interaction by ischaemia-induced deafferentation. *NeuroReport* **14**, 321-324.

Pohja M, Salenius S & Hari R (2005). Reproducibility of cortex-muscle coherence. *NeuroImage* **26**, 764-770.

Pohl C, Block W, Träber F, Schmidt S, Pels H, Grothe C, Schild HH & Klockgether T (2001). Proton magnetic resonance spectroscopy and transcranial magnetic stimulation for the detection of upper motor neuron degeneration in ALS patients. *J Neurol Sci* **190**, 21-27.

Porter R & Lemon R (1993). *Corticospinal Function and Voluntary Movement*. Oxford University Press, Oxford.

Power HA, Norton JA, Porter CL, Doyle Z, Hui I & Chan KM (2006). Transcranial direct current stimulation of the primary motor cortex affects cortical drive to human musculature as assessed by intermuscular coherence. *J Physiol* **577**, 795-803.

Prout AJ & Eisen AA (1994). The cortical silent period and amyotrophic lateral sclerosis. *Muscle Nerve* **17**, 217-223.

Pugdahl K, Fuglsang-Frederiksen A, De Carvalho M, Johnsen B, Fawcett PRW, Labarre-Vila A, Liguori R, Nix WA & Schofield IS (2007). Generalised sensory system abnormalities in amyotrophic lateral sclerosis: A European multicentre study. *J Neurol Neurosurg Psychiatry* **78**, 746-749.

Quartarone A, Lang N, Rizzo V, Bagnato S, Morgante F, Sant'Angelo A, Crupi D, Battaglia F, Messina C & Girlanda P (2007). Motor cortex abnormalities in amyotrophic lateral sclerosis with transcranial direct-current stimulation. *Muscle Nerve* **35**, 620-624.

Ramón y Cajal S (1893). *Nuevo concepto de la histología de los centros nerviosos*. Henrich.

Raz N & Rodrigue KM (2006). Differential aging of the brain: Patterns, cognitive correlates and modifiers. *Neurosci Biobehav Rev* **30**, 730-748.

Razali NR & Wah YB (2011). Power comparisons of Shapiro-Wilk, Kolmogorov-Smirnov, Lilliefors and Anderson-Darling tests. *J Stat Model Anal* **2**, 21-33.

Riddle CN & Baker SN (2005). Manipulation of peripheral neural feedback loops alters human corticomuscular coherence. *J Physiol* **566**, 625-639.

Riddle CN & Baker SN (2006). Digit displacement, not object compliance, underlies task dependent modulations in human corticomuscular coherence. *NeuroImage* **33**, 618-627.

Riddle CN & Baker SN (2010). Convergence of pyramidal and medial brain stem descending pathways onto macaque cervical spinal interneurons. *J Neurophysiol* **103**, 2821-2832.

Riddle CN, Edgley SA & Baker SN (2009). Direct and indirect connections with upper limb motoneurons from the primate reticulospinal tract. *J Neurosci* **29**, 4993-4999.

Rivner MH, Swift TR & Malik K (2001). Influence of age and height on nerve conduction. *Muscle Nerve* **24**, 1134-1141.

Roche N, Lackmy A, Achache V, Bussel B & Katz R (2011). Effects of anodal transcranial direct current stimulation over the leg motor area on lumbar spinal network excitability in healthy subjects. *J Physiol* **589**, 2813-2826.

Rods MR, Rice CL & Vandervoort AA (1997). Age-related changes in motor unit function. *Muscle Nerve* **20**, 679-690.

Roopun AK, Middleton SJ, Cunningham MO, LeBeau FEH, Bibbig A, Whittington MA & Traub RD (2006). A beta2-frequency (20-30 Hz) oscillation in nonsynaptic networks of somatosensory cortex. *Proc Natl Acad Sci U S A* **103**, 15646-15650.

Rose MR (2013). 188th ENMC International Workshop: Inclusion Body Myositis, 2-4 December 2011, Naarden, The Netherlands. *Neuromuscul Disord*, http://dx.doi.org/10.1016/j.nmd.2013.1008.1007

Rosenberg JR, Amjad AM, Breeze P, Brillinger DR & Halliday DM (1989). The Fourier approach to the identification of functional coupling between neuronal spike trains. *Prog Biophys Mol Biol* **53**, 1-31.

Rosenzweig ES, Brock JH, Culbertson MD, Lu P, Moseanko R, Edgerton VR, Havton LA & Tuszynski MH (2009). Extensive spinal decussation and bilateral termination of cervical corticospinal projections in rhesus monkeys. *J Comp Neurol* **513**, 151-163.

Rossini PM, Barker AT, Berardelli A, Caramia MD, Caruso G, Cracco RQ, Dimitrijevic MR, Hallett M, Katayama Y, Lucking CH, Maertens De Noordhout AL, Marsden CD, Murray NMF, Rothwell JC, Swash M & Tomberg C (1994). Non-invasive electrical and magnetic stimulation of the brain, spinal cord and roots: Basic principles and procedures for routine clinical application. Report of an IFCN committee. *Electroencephalogr Clin Neurophysiol* **91**, 79-92.

Rossini PM, Desiato MT & Caramia MD (1992). Age-related changes of motor evoked potentials in healthy humans: Non-invasive evaluation of central and peripheral motor tracts excitability and conductivity. *Brain Res* **593**, 14-19.

Rossini PM & Pauri F (2002). Central conduction time studies. In *Handbook of Transcranial Magnetic Stimulation*, ed. Pascual-Leone A, Davey NJ, Rothwell J, Wassermann EM & Puri BK, pp. 90-96. Arnold, London.

Rothwell JC, Hallett M, Berardelli A, Eisen A, Rossini P & Paulus W (1999). Magnetic stimulation: Motor evoked potentials. The International Federation of Clinical Neurophysiology. *Electroencephalogr Clin Neurophysiol Suppl* **52**, 97-103.

Russell JR & DeMyer W (1961). The quantitative corticoid origin of pyramidal axons of Macaca rhesus. With some remarks on the slow rate of axolysis. *Neurology* **11**, 96-108.

Salenius S, Portin K, Kajola M, Salmelin R & Hari R (1997). Cortical control of human motoneuron firing during isometric contraction. *J Neurophysiol* **77**, 3401-3405.

Salerno A & Georgesco M (1998). Double magnetic stimulation of the motor cortex in amyotrophic lateral sclerosis. *Electroencephalogr Clin Neurophysiol* **107**, 133-139.

Salinas S, Proukakis C, Crosby A & Warner TT (2008). Hereditary spastic paraplegia: clinical features and pathogenetic mechanisms. *Lancet Neurol* **7**, 1127-1138.

Salmelin R & Hari R (1994). Characterization of spontaneous MEG rhythms in healthy adults. *Electroencephalogr Clin Neurophysiol* **91**, 237-248.

Sandbrink F (2009). The MEP in clinical neurodiagnosis. In *Oxford Handbook of Transcranial Stimulation*, ed. Wassermann EM, Epstein CM, Ziemann U, Walsh V, Tomas P & Lisanby SH, pp. 237-284. Oxford University Press, Oxford.

Sanes JN & Donoghue JP (1993). Oscillations in local field potentials of the primate motor cortex during voluntary movement. *Proc Natl Acad Sci U S A* **90**, 4470-4474.

Schelhaas HJ, Arts I, Overeem S, Houtman C, Janssen H, Kleine B, Munneke M & Zwarts M (2007). Measuring the cortical silent period can increase diagnostic confidence for amyotrophic lateral sclerosis. *Amyotroph Lateral Scler* **8**, 16-19.

Schieber MH (2001). Constraints on somatotopic organization in the primary motor cortex. *J Neurophysiol* **86**, 2125-2143.

Schieber MH & Poliakov AV (1998). Partial inactivation of the primary motor cortex hand area: Effects on individuated finger movements. *J Neurosci* **18**, 9038-9054.

Schriefer TN, Hess CW, Mills KR & Murray NMF (1989). Central motor conduction studies in motor neurone disease using magnetic brain stimulation. *Electroencephalogr Clin Neurophysiol* **74**, 431-437.

Schulte-Mattler WJ, Müller T & Zierz S (1999). Transcranial magnetic stimulation compared with upper motor neuron signs in patients with amyotrophic lateral sclerosis. *J Neurol Sci* **170**, 51-56.

Schwartzman RJ (1978). A behavioral analysis of complete unilateral section of the pyramidal tract at the medullary level in Macaca mulatta. *Ann Neurol* **4**, 234-244.

Seidler RD, Bernard JA, Burutolu TB, Fling BW, Gordon MT, Gwin JT, Kwak Y & Lipps DB (2010). Motor control and aging: Links to age-related brain structural, functional, and biochemical effects. *Neurosci Biobehav Rev* **34**, 721-733.

Semmler JG, Kornatz KW & Enoka RM (2003). Motor-unit coherence during isometric contractions is greater in a hand muscle of older adults. *J Neurophysiol* **90**, 1346-1349.

Shafiq R & Macdonell R (1994). Voluntary contraction and responses to submaximal cervical nerve root stimulation. *Muscle Nerve* **17**, 662-666.

Silverman BW (1986). *Density Estimation for Statistics and Data Analysis*. Chapman&Hall, London.

Sobue G, Hashizume Y, Mitsuma T & Takahashi A (1987). Size-dependent myelinated fiber loss in the corticospinal tract in Shy-Drager syndrome and amyotrophic lateral sclerosis. *Neurology* **37**, 529-532.

Sommer M, Tergau F, Wischer S, Reimers CD, Beuche W & Paulus W (1999). Riluzole does not have an acute effect on motor thresholds and the intracortical excitability in amyotrophic lateral sclerosis. *J Neurol* **246**, 22-26.

Soteropoulos DS, Edgley SA & Baker SN (2011). Lack of evidence for direct corticospinal contributions to control of the ipsilateral forelimb in monkey. *J Neurosci* **31**, 11208-11219.

Stefan K, Kunesch E, Benecke R & Classen J (2001). Effects of riluzole on cortical excitability in patients with amyotrophic lateral sclerosis. *Ann Neurol* **49**, 537-540.

Steriade M, Amzica F & Contreras D (1996). Synchronization of fast (30-40 Hz) spontaneous cortical rhythms during brain activation. *J Neurosci* **16**, 392-417.

Swash M (1998). Early diagnosis of ALS/MND. *J Neurol Sci* **160**, S33-S36.

Talbot K (2009). Motor neuron disease: The bare essentials. *Pract Neurol* **9**, 303-309.

Tanaka S, Hanakawa T, Honda M & Watanabe K (2009). Enhancement of pinch force in the lower leg by anodal transcranial direct current stimulation. *Exp Brain Res* **196**, 459-465.

Tecchio F, Porcaro C, Zappasodi F, Pesenti A, Ercolani M & Rossini PM (2006). Cortical short-term fatigue effects assessed via rhythmic brain-muscle coherence. *Exp Brain Res* **174**, 144-151.

Terao Y, Ugawa Y, Sakai K, Uesaka Y, Kohara N & Kanazawa I (1994). Transcranial stimulation of the leg area of the motor cortex in humans. *Acta Neurol Scand* **89**, 378-383.

Thirugnanasambandam N, Sparing R, Dafotakis M, Meister IG, Paulus W, Nitsche MA & Fink GR (2011). Isometric contraction interferes with transcranial direct current

stimulation (tDCS) induced plasticity - evidence of state-dependent neuromodulation in human motor cortex. *Restor Neurol Neurosci* **29**, 311-320.

Tomberg C (1995). Transcutaneous magnetic stimulation of descending tracts in the cervical spinal cord in humans. *Neurosci Lett* **188**, 199-201.

Tranulis C, Guéguen B, Pham-Scottez A, Vacheron MN, Cabelguen G, Costantini A, Valero G & Galinovski A (2006). Motor threshold in transcranial magnetic stimulation: Comparison of three estimation methods. *Neurophysiol Clin* **36**, 1-7.

Traynor BJ, Codd MB, Corr B, Forde C, Frost E & Hardiman O (2000a). Amyotrophic lateral sclerosis mimic syndromes: A population-based study. *Arch Neurol* **57**, 109-113.

Traynor BJ, Codd MB, Corr B, Forde C, Frost E & Hardiman OM (2000b). Clinical features of amyotrophic lateral sclerosis according to the El Escorial and Airlie House diagnostic criteria: A population-based study. *Arch Neurol* **57**, 1171-1176.

Triggs WJ, Menkes D, Onorato J, Yan RSH, Young MS, Newell K, Sander HW, Soto O, Chiappa KH & Cros D (1999). Transcranial magnetic stimulation identifies upper motor neuron involvement in motor neuron disease. *Neurology* **53**, 605-611.

Truffert A, Rösler KM & Magistris MR (2000). Amyotrophic lateral sclerosis versus cervical spondylotic myelopathy: A study using transcranial magnetic stimulation with recordings from the trapezius and limb muscles. *Clin Neurophysiol* **111**, 1031-1038.

Turner MR, Hardiman O, Benatar M, Brooks BR, Chio A, De Carvalho M, Ince PG, Lin C, Miller RG, Mitsumoto H, Nicholson G, Ravits J, Shaw PJ, Swash M, Talbot K, Traynor BJ, Van Den Berg LH, Veldink JH, Vucic S & Kiernan MC (2013). Controversies and priorities in amyotrophic lateral sclerosis. *Lancet Neurol* **12**, 310-322.

Turner MR, Kiernan MC, Leigh PN & Talbot K (2009). Biomarkers in amyotrophic lateral sclerosis. *Lancet Neurol* **8**, 94-109.

Ugawa Y, Kohara N, Shimpo T & Mannen T (1990). Magneto-electrical stimulation of central motor pathways compared with percutaneous electrical stimulation. *Eur Neurol* **30**, 14-18.

Ugawa Y, Rothwell JC, Day BL, Thompson PD & Marsden CD (1989). Magnetic stimulation over the spinal enlargements. *J Neurol Neurosurg Psychiatry* **52**, 1025-1032.

Uozumi T, Tsuji S & Murai Y (1991). Motor potentials evoked by magnetic stimulation of the motor cortex in normal subjects and patients with motor disorders. *Electroencephalogr Clin Neurophysiol* **81**, 251-256.

Urban PP, Wicht S & Hopf HC (2001). Sensitivity of transcranial magnetic stimulation of cortico-bulbar vs. cortico-spinal tract involvement in Amyotrophic Lateral Sclerosis (ALS). *J Neurol* **248**, 850-855.

Ushiyama J, Katsu M, Masakado Y, Kimura A, Liu M & Ushiba J (2011a). Muscle fatigue-induced enhancement of corticomuscular coherence following sustained submaximal isometric contraction of the tibialis anterior muscle. *J Appl Physiol* **110**, 1233-1240.

Ushiyama J, Suzuki T, Masakado Y, Hase K, Kimura A, Liu M & Ushiba J (2011b). Between-subject variance in the magnitude of corticomuscular coherence during tonic isometric contraction of the tibialis anterior muscle in healthy young adults. *J Neurophysiol* **106**, 1379-1388.

Vlam L, Van Der Pol WL, Cats EA, Straver DC, Piepers S, Franssen H & Van Den Berg LH (2012). Multifocal motor neuropathy: Diagnosis, pathogenesis and treatment strategies. *Nat Rev Neurol* **8**, 48-58.

Vucic S, Cheah BC, Yiannikas C & Kiernan MC (2011). Cortical excitability distinguishes ALS from mimic disorders. *Clin Neurophysiol* **122**, 1860-1866.

Vucic S & Kiernan MC (2006). Novel threshold tracking techniques suggest that cortical hyperexcitability is an early feature of motor neuron disease. *Brain* **129**, 2436-2446.

Vucic S, Nicholson GA & Kiernan MC (2008). Cortical hyperexcitability may precede the onset of familial amyotrophic lateral sclerosis. *Brain* **131**, 1540-1550.

Wang FC, De Pasqua V & Delwaide PJ (1999). Age-related changes in fastest and slowest conducting axons of thenar motor units. *Muscle Nerve* **22**, 1022-1029.

Wassermann EM (2002). Variation in the response to transcranial magnetic brain stimulation in the general population. *Clin Neurophysiol* **113**, 1165-1171.

Weber M, Eisen A, Stewart HG & Andersen PM (2000). Preserved slow conducting corticomotoneuronal projections in amyotrophic lateral sclerosis with autosomal recessive D90A CuZn-superoxide dismutase mutation. *Brain* **123**, 1505-1515.

Wharton S & Ince PG (2003). Pathology of motor neuron disorders. In *Motor Neuron Disorders*, ed. Shaw PJ & Strong MJ, pp. 17-50. Butterworth Heinemann, Philadelphia.

Williams ER & Baker SN (2009). Circuits generating corticomuscular coherence investigated using a biophysically based computational model. I. Descending systems. *J Neurophysiol* **101**, 31-41.

Williams ER, Soteropoulos DS & Baker SN (2010). Spinal interneuron circuits reduce approximately 10-Hz movement discontinuities by phase cancellation. *Proc Natl Acad Sci U S A* **107**, 11098-11103.

Wilson SA, Thickbroom GW & Mastaglia FL (1993). Transcranial magnetic stimulation mapping of the motor cortex in normal subjects. The representation of two intrinsic hand muscles. *J Neurol Sci* **118**, 134-144.

Witham CL, Riddle CN, Baker MR & Baker SN (2011). Contributions of descending and ascending pathways to corticomuscular coherence in humans. *J Physiol* **589**, 3789-3800.

Witham CL, Wang M & Baker S (2010). Corticomuscular coherence between motor cortex, somatosensory areas and forearm muscles in the monkey. *Front Syst Neurosci* **4**.

Witham CL, Wang M & Baker SN (2007). Cells in somatosensory areas show synchrony with beta oscillations in monkey motor cortex. *Eur J Neurosci* **26**, 2677-2686.

Woolsey CN, Settlage PH, Meyer DR, Sencer W, Pinto Hamuy T & Travis AM (1952). Patterns of localization in precentral and "supplementary" motor areas and their relation to the concept of a premotor area. *Res Publ Assoc Res Nerv Ment Dis* **30**, 238-264.

Yokota T, Yoshino A, Inaba A & Saito Y (1996). Double cortical stimulation in amyotrophic lateral sclerosis. *J Neurol Neurosurg Psychiatry* **61**, 596-600.

Z'Graggen WJ, Humm AM, Durisch N, Magistris MR & Rösler KM (2005). Repetitive spinal motor neuron discharges following single transcranial magnetic stimuli: A quantitative study. *Clin Neurophysiol* **116**, 1628-1637.

Zanette G, Tamburin S, Manganotti P, Refatti N, Forgione A & Rizzuto N (2002). Different mechanisms contribute to motor cortex hyperexcitability in amyotrophic lateral sclerosis. *Clin Neurophysiol* **113**, 1688-1697.

Ziemann U, Winter M, Reimers CD, Reimers K, Tergau F & Paulus W (1997). Impaired motor cortex inhibition in patients with amyotrophic lateral sclerosis: Evidence from paired transcranial magnetic stimulation. *Neurology* **49**, 1292-1298.